SYNTHESIS AND CHARACTERISTIC CHEMISTRY OF SIXTEEN-ELECTRON GROUP 6 HYDROCARBYL-CONTAINING NITROSYL COMPLEXES

by

JOHN E. VELTHEER

B.Sc.H., Queen's University at Kingston, 1988

A THESIS SUBMITTED IN PARTIAL FULFILLMENT OF

THE REQUIREMENTS FOR THE DEGREE OF

DOCTOR OF PHILOSOPHY

in

THE FACULTY OF GRADUATE STUDIES

(Department of Chemistry)

We accept this thesis as conforming

to the required standard.

THE UNIVERSITY OF BRITISH COLUMBIA

April 1993

In presenting this thesis in partial fulfilment of the requirements for an advanced degree at the University of British Columbia, I agree that the Library shall make it freely available for reference and study. I further agree that permission for extensive copying of this thesis for scholarly purposes may be granted by the head of my department or by his or her representatives. It is understood that copying or publication of this thesis for financial gain shall not be allowed without my written permission.

(Signature)

Department of Chemistry

The University of British Columbia
Vancouver, Canada

Date 29 April 1993

Abstract

This thesis addresses the non-generality of the previous method used to prepare $CpW(NO)(alkyl)_2$ complexes from their diiodide precursors. The three most significant problems inherent to the original synthetic method were: (a) the reagents being used (i.e. transition-metal dihalide, alkylating agent and solvent), (b) excessive hydrolysis during workup, and (c) thermal decomposition. This work presents a rationalization for, and utilization of, a new general methodology for the preparation of $Cp'M(NO)R_2$ [Cp' = Cp (η^5-C_5H_5), Cp^* (η^5-C_5Me_5); M = Mo, W; R = alkyl, aryl] complexes.

Reactions of $Cp^*M(NO)Cl_2$ with $(aryl)_2Mg{\cdot}X(dioxane)$ [aryl = Ph, *p*-tolyl, *o*-tolyl] in THF provide $Cp^*M(NO)(aryl)_2$ complexes. These 16-electron diaryl complexes irreversibly form 1:1 metal-centered adducts with PMe_3. $CpW(NO)(o\text{-tolyl})_2$ is the only isolable diaryl complex of this type that does not incorporate a Cp^* ligand. Electrochemical and IR studies indicate that these diaryl complexes are more potent Lewis acids than their $Cp'M(NO)(alkyl)_2$ congeners. X-ray crystallographic analyses indicate that these diaryl complexes have more sterically accessible metal centers than related dialkyl complexes. The thermal stability of $Cp'M(NO)R_2$ complexes is Cp^* > Cp, W > Mo and alkyl > aryl. The relative Lewis acidities of this family of nitrosyl complexes mirrors the thermal stability trend.

Reactions of $Cp^*Mo(NO)Cl_2$ with $(alkyl)_2Mg{\cdot}X(dioxane)$ [alkyl = CH_2CMe_3, CH_2CMe_2Ph, CH_2SiMe_3] in THF provide previously inaccessible $Cp^*Mo(NO)(alkyl)Cl$ and $Cp^*Mo(NO)(alkyl)_2$ complexes in a stepwise fashion. $Cp^*Mo(NO)(alkyl)Cl$ species are comparable in Lewis acidity to related $Cp^*Mo(NO)(aryl)_2$ complexes. $Cp^*Mo(NO)(CH_2CMe_3)Cl$ reacts with PMe_3 and pyridine to afford metal-centered 18-electron adducts while CO and $CNCMe_3$ readily insert into its Mo-neopentyl bond. The chloride ligand in $Cp^*Mo(NO)(CH_2CMe_3)Cl$ is easily abstracted by Ag^+ in NCMe to form $[Cp^*Mo(NO)(CH_2CMe_3)(NCMe)]BF_4$. The phosphine complex,

$Cp^*Mo(NO)(CH_2CMe_3)(PMe_3)Cl$, is readily dehydrohalogenated by LDA in THF to afford the novel cyclometallated dialkyl complex $(\eta^5,\eta^1\text{-}C_5Me_4CH_2)Mo(NO)(CH_2CMe_3)(PMe_3)$.

Reactions of $Cp^*Mo(NO)R_2$ complexes with water afford bimetallic complexes of the type, $[Cp^*Mo(NO)R]_2\text{-}(\mu\text{-}O)$, and free hydrocarbon. A kinetic analysis of the reaction between H_2O and $Cp^*Mo(NO)(CH_2SiMe_3)_2$ implicates $Cp^*Mo(NO)(CH_2SiMe_3)(OH)$ as a key intermediate in the formation of $[Cp^*Mo(NO)(CH_2SiMe_3)]_2\text{-}(\mu\text{-}O)$. $Cp'W(NO)(alkyl)_2$ complexes are hydrolytically stable, whereas $Cp'W(NO)(aryl)_2$ complexes react vigorously with water providing $Cp'W(O)_2(aryl)$ complexes.

$CpMo(NO)(CH_2CMe_3)_2$ thermally decomposes via a first-order intramolecular extrusion of neopentane yielding the 16-electron alkylidene complex, $CpMo(NO)(=CHCMe_3)$. A mechanistic analysis of the above-mentioned thermal reaction shows little solvent dependence and suggests a highly ordered transition state. $CpMo(NO)(=CHCMe_3)$ cannot be isolated, but it can be trapped with phosphines or pyridine (L) yielding $CpMo(NO)(=CHCMe_3)L$ complexes. Primary amines and alcohols add their heteroatom-hydrogen bonds across the Mo=C double bond of $CpMo(NO)(=CHCMe_3)$ stereoselectively to give alkyl amide and alkyl alkoxide complexes. $CpMo(NO)(=CHCMe_3)$ reacts with $CpMo(NO)(CH_2CMe_3)_2$ to give $[CpMo(NO)](\mu\text{-}\eta^1\text{:}\eta^2\text{-}NO)(\mu\text{-}CHCMe_3)[CpMo(=CHCMe_3)]$, which contains the first $\mu\text{-}\eta^1\text{:}\eta^2$-nitrosyl ligand.

TABLE OF CONTENTS

List of Figures

List of Tables

List of Schemes

List of Abbreviations

The following list of abbreviations, most of which are commonly used in the chemical literature, have been employed in this thesis.

Å	angstrom, 10^{-10} m
anal.	analysis
atm	atmosphere(s)
bp	boiling point
br	broad (spectral)
°C	degree centigrade
^{13}C	carbon-13
$^{13}C\{^{1}H\}$	proton-decoupled carbon-13 (observe carbon while decoupling proton)
calcd	calculated
C_6D_6	benzene-d_6
$CDCl_3$	chloroform-d_1
CD_2Cl_2	dichloromethane-d_2
cm^{-1}	wavenumbers
COSY	correlation spectroscopy (in NMR spectroscopy)
Cp	η^5-C_5H_5, perhydrocyclopentadienyl
Cp^*	η^5-C_5Me_5, pentamethylcyclopentadienyl
Cp'	both Cp and Cp^*
CV	cyclic voltammogram
δ	chemical shift in ppm referenced to Me_4Si at δ 0
d	doublet (in an NMR spectrum); or day(s)
Δ	heat (in thermolysis)
DCI	direct chemical ionization (in mass spectrometry)
E_a	activation energy

EI	electron-impact (in mass spectrometry)
Et_2O	$(CH_3CH_2)_2O$, ether, diethyl ether
eV	electron volts
FAB	fast-atom bombardment (in mass spectrometry)
Fc	ferrocene, Cp_2Fe
g	gram(s)
$\Delta G^{\ddagger}$	free energy of activation
h	Planck's constant; or hour(s)
^1H	proton
^2H	deuterium
$\Delta H^{\ddagger}$	enthalpy of activation
Hz	Hertz (s^{-1})
iR	(Current) x (resistance)
IR	infrared
J	coupling constant (in NMR spectroscopy)
$^nJ_{AB}$	n-bond coupling constant between atoms A and B
K	degree Kelvin
kJ	kilojoule
k_B	Boltzmann's constant
k_{obs}	observed rate constant
LDA	lithium diisopropylamide
LUMO	lowest unoccupied molecular orbital
m	multiplet (in NMR spectroscopy)
M	Mo and W; or molar; or mega
m/z	mass-to-charge ratio (in mass spectrometry)
Me	CH_3, methyl
mg	milligram(s)
min	minute(s)

mL	milliliter
mmol	millimole
mol	mole
MS	mass spectrum
ν	stretching frequency (in IR spectroscopy); or scan rate (in electrochemistry)
neopentyl	CH_2CMe_3
neophyl	CH_2CMe_2Ph
NMR	nuclear magnetic resonance
ORTEP	Oak Ridge Thermal Ellipsoid Plot
^{31}P	phosphorus-31
$[P]^+$	parent molecular ion (in mass spectrometry)
Ph	C_6H_5, phenyl
ppm	parts per million (in NMR spectroscopy)
pz	pyrazolyl
q	quartet (in an NMR spectrum)
quat	quaternary carbon atom
RT	room temperature
s	singlet (in an NMR spectrum)
$\Delta S^{\ddagger}$	entropy of activation
SCE	standard calomel electrode
t	triplet (in an NMR spectrum)
TBAH	tetrabutylammoniumhexafluorophosphate
tetraglyme	tetraethylene glycol dimethyl ether, $Me(OCH_2CH_2)_4OMe$
o-tolyl	C_6H_4-2-Me, ortho-tolyl
p-tolyl	C_6H_4-4-Me, para-tolyl
THF	C_4H_8O, tetrahydrofuran
THF-d_8	C_4D_8O
UV	ultraviolet (in electronic spectroscopy)

V	volt
vis	visible (in electronic spectroscopy)

Acknowledgements

Many people made the pages that follow an easier accomplishment.

I thank Peter Legzdins for being the bane of mediocrity and for giving me the opportunity to achieve this goal. I also thank him for his support, encouragement, enthusiasm and absolute commitment to excellence. I'm grateful to past and present members of the Legzdins group (P. J. Lundmark, G. B. Richter-Addo, N. H. Dryden, J. D. Debad, K. J. Ross, W. S. McNeil, M. A. Young, E. B. Brouwer, E. C. Phillips, N. J. Christensen, E. G. Vessey, T. C. Chin, S. F. Sayers, M. J. Shaw, R. Reina and K. M. Smith), for their help, humor and friendship. Specific thanks to PJL for continuous moral support and conversation. These four long years weren't so bad. Thanks to GRA for his endless enthusiasm for nitrosyl chemistry. Thanks to NHD for coining "skim the cream". Thanks also to JDD and KJR for numerous mountain biking adventures. Thanks to WSM for proofreading nearly everything I have written.

Thanks to Andrew McKerrow, the true definition of a colleague and friend. Thanks to Dave McConville, the eternal pessimist, for his realistic views of science and research. Thanks to Mike Fryzuk and Brian James for the advice they provided me in numerous hours of discussion. Thanks to Professors R. A. Whitney, M. C. Baird and S. Wolfe who were my biggest influences in pursuing a Ph.D. degree. Thanks to Drs. S. J. Rettig, R. J. Batchelor and F. W. B. Einstein for solving ten crystal structures, and attempting what seems like hundreds more, for me. Thanks to S. Rak, P. Borda, M. Austria, M. Lapawa and L. Darge for their countless hours of work on my behalf. Thanks to Irene Rodway for always having an open door and ear.

I am indebted to my parents, Peter and Gail, for their love and continuing support. I sincerely acknowledge my in-laws, Jim and Emily Taylor, for their love, understanding and interest in my work. I also thank my grandfather, Ed McMahon, and my aunt and late uncle, Pheme and Bill Brown, for always believing in me. Lastly, I owe everything to my wife, Kim Taylor, for her unwavering love, support and companionship. You have made me what I am.

Science is indeed a mirror to nature,
a process of describing the natural
world in increasingly elaborate terms.

Peter Knudtson

To Kim

CHAPTER 1

General Introduction and Scope of This Thesis

1.1 Background

A fundamental principle of transition-metal organometallic chemistry is the 18-valence-electron rule which states that stable organometallic complexes will contain a total of 18 valence electrons.[1] The valence-bond basis of this rule, which is analogous to the octet rule in organic chemistry, is that organometallic complexes generally owe their stability to the filling of the nine valence orbitals of the transition metal with eighteen electrons provided by the metal and the ligands of the complex. In molecular-orbital terms, the rule may be rationalized in terms of the filling of all bonding and nonbonding valence molecular orbitals of the complex by 18 electrons and the existence of a large HOMO-LUMO energy gap. Although the vast majority of known transition-metal organometallic complexes obey this "rule", many compounds have now been isolated that violate it. Particularly interesting among the latter are the complexes that contain 16 valence electrons since such electronically, and often coordinatively, unsaturated organometallic complexes are known to play an important role in catalytic systems.[2]

Like 18-electron species, isolable 16-electron complexes also owe their stability to a large HOMO-LUMO gap, but their LUMOs need not be filled with a pair of electrons in order to attain a stable electronic configuration. Classic examples of sixteen-electron complexes that contain ancillary hydrocarbyl ligands are the square-planar d^8 Group 10 compounds of the type L_2MR_2 [L = two-electron donor; M = Pt or Pd; R = hydrocarbyl][3] and the pseudo-tetrahedral d^0 Group 4 metallocene bis(hydrocarbyl) complexes Cp_2MR_2 [Cp = η^5-C_5H_5; M = Ti, Zr or Hf].[4] More recent examples are the $(PNP)IrR_2$[5] [PNP = $N(SiMe_2CH_2PPh_2)_2$] and $Cp'M(NO)R_2$ [Cp' = Cp or Cp* (η^5-C_5Me_5); M = Mo or W; R = alkyl or aryl] systems,[6] the latter of which form the basis of this thesis. $Cp'M(NO)R_2$ complexes are 16-electron coordinatively and electronically unsaturated pseudo-octahedral molecules whose chemistry our group has been actively investigating since the discovery of $CpW(NO)(CH_2SiMe_3)_2$ in 1985.[7]

These $Cp'M(NO)R_2$ complexes are monomeric and possess 3-legged piano-stool molecular structures in which the M-NO linkages are essentially linear. In this configuration, the nitrosyl group functions as a formal three-electron donor to the metal center and is a strong π-acid ligand, stronger indeed than the well known CO group.[8,9] The M-NO orbital overlaps commonly invoked to account for this synergic bonding are diagrammed in Figure 1.1.

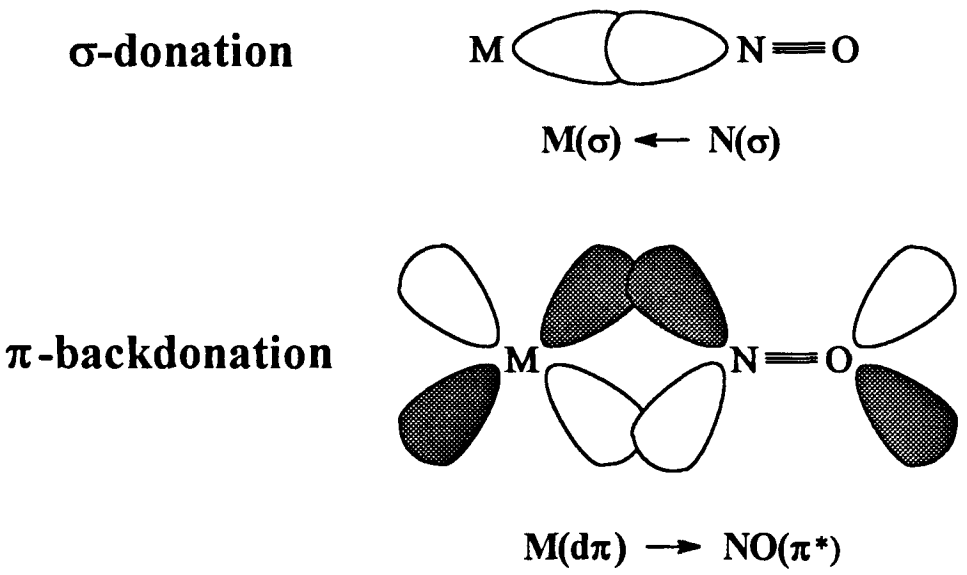

Figure 1.1 Synergic bonding interactions between a transition metal and a linear nitrosyl ligand

The strong π-acidity of the nitrosyl ligand is a key contributor to the molecular-orbital energy levels of the model complex $CpMo(NO)Me_2$ which has the requisite large HOMO-LUMO gap for a stable 16-electron complex. The LUMO of $CpMo(NO)Me_2$ is calculated to be a nonbonding, metal-centered orbital.[7a]

It may be noted at this point that the degree of M(dπ)-NO(π*) backbonding is a direct function of the amount of electron density at the metal center in the compounds studied in this thesis. Transfer of electron density into the NO(π*) antibonding orbital decreases the N-O bond order and thus decreases the nitrosyl stretching frequency (ν_{NO}) as measured in the IR spectrum of the complex. As we shall see later, this sensitive indicator is one of the most useful spectroscopic probes in organometallic nitrosyl chemistry.

1.2 Early Work

It was thought that the bis(hydrocarbyl) derivatives, $Cp'M(NO)R_2$, should be preparable by metathesis reactions from their known dihalide precursors, $Cp'M(NO)X_2$ [X = I, Br, or Cl].[10] The preparations of these latter complexes described in the literature involved treatment of $Cp'M(NO)(CO)_2$ complexes with elemental halogen (eq 1.1).[12,13]

$$Cp'M(NO)(CO)_2 \xrightarrow[-2\ CO]{X_2,\ CH_2Cl_2} Cp'M(NO)X_2 \qquad (1.1)$$

Since solid iodine is the easiest of the halogens to handle stoichiometrically, our work in this area began by using the diiodide complexes as synthetic precursors. In 1985, Luis Sánchez, a Spanish postdoctoral fellow in our group, discovered that treatment of $CpW(NO)I_2$ with two equivalents of the Grignard reagent, Me_3SiCH_2MgCl, in Et_2O at room temperature afforded an unusual 4-coordinate magnesium complex, $\{CpW(NO)(CH_2SiMe_3)_2\}_2MgX_2$, in which the nitrosyl oxygen atoms of the organometallic ligands act as donors to the central Mg (eq 1.2). Hydrolysis of this intermediate isonitrosyl complex (eq 1.3) afforded a high yield of the prototypal

complex, $CpW(NO)(CH_2SiMe_3)_2$, as relatively air-stable and thermally-stable violet crystals.[7a] An X-ray crystallographic analysis established the monomeric nature of the 16-electron complex in the solid state.

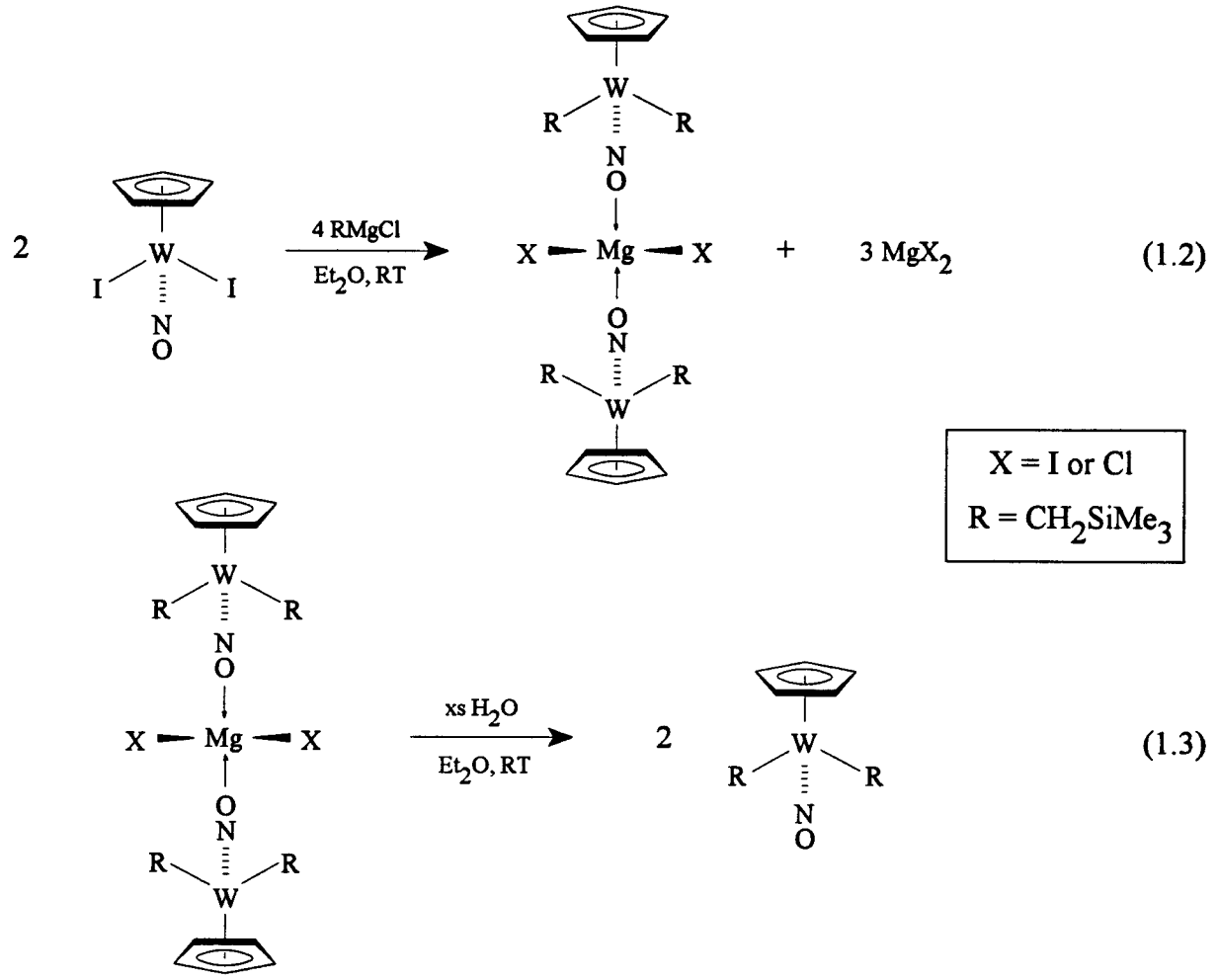

(1.2)

(1.3)

A preliminary survey of the reactivity of this 16-electron dialkyl compound soon showed its chemistry to be dominated by its ability to function as a Lewis acid. In other words, the LUMO of the parent complex is sufficiently low in energy that it can accept electrons from classic Lewis bases. After initial coordination to the metal center, some Lewis bases often underwent subsequent intramolecular insertion reactions involving the alkyl ligands (Scheme 1.1).[7b] In addition to functioning as a Lewis acid at tungsten, the prototypal dialkyl complex also possesses

a good Lewis base site at the nitrosyl oxygen atom (cf. eq 1.2). Hence, the reaction of $CpW(NO)(CH_2SiMe_3)_2$ with $AlMe_3$ provides a monomeric isonitrosyl $AlMe_3$ adduct (Scheme 1.1).

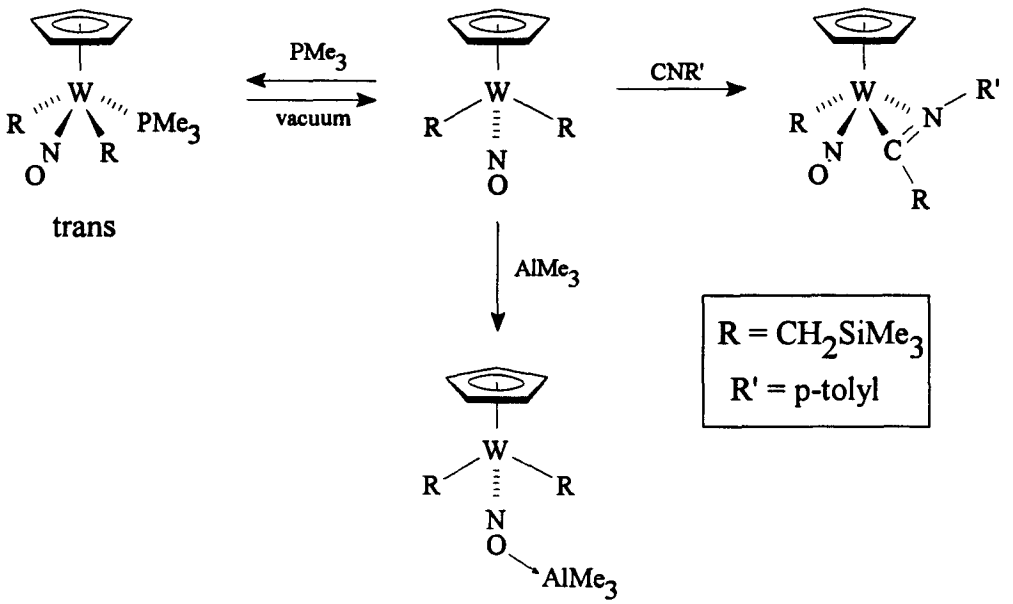

Scheme 1.1 Characteristic reactions of $CpW(NO)(CH_2SiMe_3)_2$

Subsequent work showed that neopentyl (CH_2CMe_3) and neophyl (CH_2CMe_2Ph) analogues of $CpW(NO)(CH_2SiMe_3)_2$ could be prepared in a similar manner to that described above, albeit in lower isolated yields.[7,12b] *On occasion*, $CpMo(NO)(CH_2SiMe_3)_2$ could also be prepared. Since further research efforts showed that reactions 1.2 and 1.3 could be extended no further, a more reliable synthetic route to presumably more reactive complexes was desired. Clearly, room temperature alkylation in diethyl ether was a useful methodology for only a small proportion of our target molecules. The limited set of only Cp'*W*(NO)(*alkyl*)$_2$ complexes precluded a comprehensive investigation of the chemistry of the Cp'M(NO)R_2 family of Lewis acids in general.

1.3 Scope of This Thesis

My thesis addresses the non-generality of the previous method (eq 1.2 - 1.3) and puts forth a new, completely general route to a much larger family of $Cp'M(NO)R_2$ complexes. The three most significant problems inherent to the original synthetic method were:

(a) the reagents being used (i.e. transition-metal dihalide, alkylating agent and solvent),

(b) excessive hydrolysis during workup (eq 1.3)

(c) thermal decomposition

The research in this thesis attempts to rationalize why the original synthetic method was not appropriate for synthesizing most of our desired $Cp'M(NO)R_2$ species. The methodology described in this thesis is now routinely employed in our laboratories and is useful for synthesizing dialkyl, diaryl, alkyl chloro, aryl chloro, mixed dialkyl, mixed diaryl and even mixed alkyl aryl complexes of *both* Mo and W. Under the original reaction conditions (eq 1.2 - 1.3) most $Cp'M(NO)R_2$ species decompose rapidly, although in many cases to isolable, characterizable and often very interesting materials.

Specifically, Chapter 2 of this thesis presents the general synthetic methodology to $Cp'M(NO)R_2$ complexes and applies that method to the preparation of $Cp'M(NO)(aryl)_2$ species. The major chemical conclusion to emanate from the work in this chapter is that $Cp'M(NO)(aryl)_2$ complexes have much more accessible metal centers and are more potent Lewis acids than their $Cp'M(NO)(alkyl)_2$ congeners.[14]

Chapter 3 extends the method put forth in Chapter 2 to previously inaccessible Mo dialkyl and alkyl chloro complexes. The chemical reactivity of $Cp^*Mo(NO)(CH_2CMe_3)Cl$ is examined, as it serves as the prototypal monoalkyl complex. Chapter 3 ties together the concept of relative Lewis acidities of the whole family of $Cp'M(NO)R_2$ complexes using structural, electrochemical, and infrared data. On the basis of such data, we can rank $Cp'M(NO)R_2$ complexes in terms of their relative Lewis acidities (i.e. electron-deficiencies) as Cp > Cp*, Mo > W, and aryl > alkyl. We thus conclude that $CpMo(NO)(aryl)_2$ complexes, if isolable, would be the most electron-deficient of the $Cp'M(NO)R_2$ family of complexes. Conversely, the most easily handled

complexes, namely the $Cp^*W(NO)(alkyl)_2$ species, are also the weakest Lewis acids.[11,14,15] An interesting manifestation of the structure/reactivity relationship developed in Chapter 3 is that sterically or electronically the same conclusions are reached about the relative Lewis acidities of $Cp'M(NO)R_2$ complexes.

Chapter 4 presents the reactions of dialkyl and diaryl complexes of Mo and W with water, a reagent integral to the original synthetic method (eq 1.3). All isolable Mo dialkyl and diaryl compounds are readily hydrolyzed to form bimetallic $[Cp'Mo(NO)R]_2$-(μ-O) complexes and free hydrocarbon.[16] The reaction between H_2O and $Cp^*Mo(NO)(CH_2SiMe_3)_2$ has been subjected to a kinetic analysis in order to gain some insight into the above-mentioned hydrolysis reactions. The *dialkyl* complexes of W are hydrolytically stable, as evidenced by the success of reaction 1.3. However, the diaryl complexes of W are exceedingly moisture-sensitive and are readily converted to dioxo complexes of the type $Cp'W(O)_2R$ upon exposure to water.

The final chapter of this thesis reports the investigation of the characteristic chemistry of $CpMo(NO)(CH_2CMe_3)_2$ and its thermal decomposition product, namely the transient 16-electron alkylidene nitrosyl complex, $CpMo(NO)(=CHCMe_3)$. A detailed kinetic analysis has been performed on the thermolysis of $CpMo(NO)(CD_2CMe_3)_2$, the tetradeutero analogue of $CpMo(NO)(CH_2CMe_3)_2$. The thermal instability of $CpMo(NO)(CH_2CMe_3)_2$ (which is the least thermally stable, yet isolable $Cp'M(NO)R_2$ species) emphasizes the problematic role that temperature played in the original alkylation reactions which were conducted at room temperature. In addition to a variety of new chemical species formed when $CpMo(NO)(=CHCMe_3)$ is trapped with Lewis bases or reacted with heteroatom-hydrogen bonds, the chemistry of $CpMo(NO)(=CHCMe_3)$ led to the discovery of a new bonding mode for coordinated nitric oxide.[17]

1.4 Format of This Thesis

I have organized this thesis in fairly rigorous format in order to facilitate cross-referencing and readability. Allowing X to be the chapter number, Chapters 2 through 5 all have five major sections: **X.1** Introduction, **X.2** Experimental Procedures, **X.3** Results and Discussion, **X.4** Epilogue and Future Work and finally **X.5** References and Notes. Subsections of these major categories are numbered using standard legal outlining procedures, e.g. **X.1.1**, **X.1.1.1** etc. All compounds prepared in each chapter are catalogued numerically, e.g. **X.1**, **X.2** etc. Thus, the conversion of a compound prepared in Chapter 3 to one prepared in Chapter 5 might read "**3.4** was reacted under appropriate conditions to produce **5.11**." Schemes, figures and equations are similarily sequenced. The standard methodologies and experimental procedures outlined in Section 2.2.1 apply to the entire thesis.

1.5 References and Notes

(1) Elschenbroich, C.; Salzer, A. *Organometallics - A Concise Introduction*, 2nd ed.; VCH Publishers: New York, 1992; pp 186, 412.

(2) Collman, J. P.; Hegedus, L. S.; Norton, J. R.; Finke, R. G. *Principles and Applications of Organotransition Metal Chemistry*; University Science Books: Mill Valley, CA, 1987.

(3) Purcell, K. F.; Kotz, J. C. *Inorganic Chemistry*; W. B. Saunders: Toronto, 1977; p 804.

(4) Negishi, E.; Takahashi, T. *Aldrichimica Acta* **1985**, *18*, 31 and references therein.

(5) (a) Fryzuk, M. D.; MacNeil, P. A.; Massey, R. L.; Ball, R. G. *J. Organomet. Chem.* **1989**, *368*, 231. (b) Fryzuk, M. D.; MacNeil, P. A.; Ball, R. G. *J. Am. Chem. Soc.* **1986**, *108*, 6414. (c) Fryzuk, M. D.; MacNeil, P. A.; Rettig, S. J. *J. Am. Chem. Soc.* **1985**, *107*, 6708.

(6) Unless explicitly stated otherwise, throughout this thesis Cp' will always denote *both* η^5-C_5H_5 (Cp) and η^5-C_5Me_5 (Cp^*), M will indicate *both* Mo and W, and R will indicate *both* alkyl and aryl.

(7) (a) Legzdins, P.; Rettig, S. J.; Sánchez, L.; Bursten, B. E.; Gatter, M. G. *J. Am. Chem. Soc.* **1985**, *107*, 1411. (b) Legzdins, P.; Rettig, S. J.; Sánchez, L. *Organometallics* **1988**, *7*, 2394.

(8) Cotton, F. A.; Wilkinson, G. *Advanced Inorganic Chemistry*, 5th ed.; Wiley-Interscience: New York, 1988; Chapter 22.

(9) Richter-Addo, G. B.; Legzdins, P. *Metal Nitrosyls*; Oxford University Press: New York, 1992; Chapter 1.

(10) These complexes possess either monomeric or halide-bridged dimeric molecular structures in the solid state, but in solution they are all formulated as solvated monomers.[11] Hence, they are represented exclusively by their monomeric formulae throughout this thesis.

(11) Dryden, N. H. Ph.D. Dissertation, The University of British Columbia, 1990.

(12) For Cp' = Cp see: (a) Seddon, D.; Kita, W. G.; Bray, J.; McCleverty, J. A. *Inorg. Synth.* **1976**, *16*, 24. (b) Hunter, A. D.; Legzdins, P.; Martin, J. T.; Sánchez, L. *Organomet. Synth.* **1986**, *3*, 66. For Cp' = Cp^* see: (c) Dryden, N. H.; Legzdins, P.; Einstein, F. W. B.; Jones, R. H. *Can. J. Chem.* **1988**, *66*, 2100. (d) Gomez-Sal, P.; de Jesús, E.; Michiels, W.; Royo, P.; de Miguel, A. V.; Martinez-Carrera, S. *J. Chem. Soc., Dalton Trans.* **1990**, 2445.

(13) A more efficient preparation of the dichloride complexes involves the use of PCl_5 as a stoichiometric source of Cl_2. See Dryden, N. H.; Legzdins, P.; Batchelor, R. J.; Einstein, F. W. B. *Organometallics* **1991**, *10*, 2077.

(14) Dryden, N. H.; Legzdins, P.; Rettig, S. J.; Veltheer, J. E. *Organometallics* **1992**, *11*, 2583.

(15) Legzdins, P.; Veltheer, J. E. In *Handbuch der Präparativen Anorganischen Chemie*, 4th ed.; Herrmann, W. A., Ed.; Thieme-Verlag: Stuttgart, Germany, in press.

(16) Legzdins, P.; Lundmark, P. J.; Phillips, E. C.; Rettig, S. J.; Veltheer, J. E. *Organometallics* **1992**, *11*, 2991.

(17) Legzdins, P.; Rettig, S. J.; Veltheer, J. E. *J. Am. Chem. Soc.* **1992**, *114*, 6922.

CHAPTER 2

16-Electron $Cp^*M(NO)(aryl)_2$ [M = Mo or W] Complexes: Their Synthesis, Characterization, and Properties

2.1 Introduction

Previous work in our laboratories resulted in the discovery of a family of 16-electron dialkyl complexes having the general formula, $CpW(NO)R_2$ [R = CH_2SiMe_3, CH_2CMe_3, CH_2CMe_2Ph].[1,2] A surprising property of these electronically and coordinatively unsaturated compounds is their thermal and oxidative stability. For example, under inert atmospheres they are indefinitely thermally stable at room temperature. While they may be handled as solids in air for short periods of time at ambient temperatures with no deleterious effects, exposure to O_2 for several days at 25 °C converts them to the oxo complexes $CpW(O)_2R$.[3] The results of Fenske-Hall MO calculations on the model complexes $CpM(NO)Me_2$ (M = Mo[1] and W[4]) indicate that their LUMOs are metal-centered and non-bonding in nature. As a consequence, many $Cp'M(NO)R_2$ complexes are stable species,[5] despite their formal electron-deficiency.

Originally, the dialkyl nitrosyl complexes were prepared by the sequential treatment of $CpW(NO)I_2$ with RMgCl in Et_2O at room temperature and then hydrolysis of the intermediate

isonitrosyl adducts as summarized in the introductory Chapter of this thesis (Section 1.2: eqs 1.2 and 1.3).[1,2,6]

The methodology described in Section 1.2 is successful for sterically demanding alkyl groups (R) without ß-hydrogens, namely CH_2SiMe_3, CH_2CMe_3 and CH_2CMe_2Ph. However, if R = aryl or the metal is molybdenum (R = alkyl or aryl) the reaction conditions do not give the desired complexes. Therefore, room temperature alkylation in Et_2O was, at the inception of this work, useful for only 1/4 of our target molecules if we desired both dialkyl and diaryl complexes of Mo and W.

Logically, we wished to extend this family of tungsten alkyl nitrosyl compounds to encompass related aryl complexes, as well as molybdenum alkyl and aryl complexes.[7] It was our expectation that the characteristic chemistry exhibited by these new $Cp'M(NO)(aryl)_2$ species would be dependent on the nature of the aryl group. Such ligand dependent behavior has been documented in the related family of 18-electron complexes, $Cp^*Ru(NO)R_2$, for which Bergman and coworkers have established differences in the comparative reactivity of the alkyl- versus aryl-substituted complexes,[8,9] e.g.

$$Cp^*Ru(NO)Me_2 + 2\,PMe_3 \xrightarrow{\Delta} Cp^*Ru(CN)(PMe_3)_2 + H_2O + CH_4 \qquad (2.1)$$

$$Cp^*Ru(NO)Ph_2 + 2\,PMe_3 \xrightarrow{\Delta} Cp^*Ru(NO)(PMe_3)_2 + Ph\text{-}Ph \qquad (2.2)$$

Furthermore, it was probable that the metal centers in the $Cp'M(NO)(aryl)_2$ complexes would be less sterically hindered than in their dialkyl analogues, thereby enhancing the reactivity of the diaryl complexes toward larger, or less reactive Lewis base substrates.

Very early on we discovered that the synthetic methodology employed to prepare the dialkyl complexes (Section 1.2) could not be used to synthesize the analogous diaryl complexes, principally for three reasons. First, the choice of reagents (including the starting material, the alkylating agent and the solvent) was inappropriate. Second, the water needed to hydrolyze the intermediate isonitrosyl adducts was simply disastrous, and third, many of the target complexes

appeared to be very sensitive to thermal decomposition. Indeed, all Cp'M(NO)(aryl)$_2$ complexes synthesized in our laboratories to date react instantaneously with H_2O at ambient temperatures (Chapter 4)[10,11] and thermally decompose in solution at room temperature. Thus, given that the previous synthetic methodology could not be extended to include congeneric diaryl complexes, we had good reason to develop a new set of experimental conditions and reagents to synthesize these compounds.

Development of a general synthetic approach to Cp'M(NO)R_2 [M = Mo *and* W, R = alkyl *and* aryl] complexes began with the Ph.D. research of Neil Dryden and is further elaborated in the present work. A general methodology for the preparation of a wide variety of Cp'M(NO)R_2 complexes has now been established.

2.2 Experimental Procedures

2.2.1 Methods

The methodologies described in this section apply to the entire thesis. All reactions and subsequent manipulations involving organometallic reagents were performed under anhydrous conditions in an atmosphere of prepurified argon or nitrogen. Purification of inert gases was achieved by passing them through a double-walled glass column (10 x 60 cm) containing MnO and activated 4Å molecular sieves. Conventional glovebox and greaseless vacuum line Schlenk techniques were utilized throughout.[12] The specific gloveboxes utilized in this work were Vacuum Atmospheres HE-553-2 and HE-43-2 models. All IR samples were either as THF, Et_2O, hexanes or CH_2Cl_2 solutions in NaCl cells or as Nujol mulls sandwiched between NaCl or CsI plates. IR spectra were recorded on a Nicolet 5DX FT-IR instrument, internally calibrated with a He/Ne laser. All NMR spectra were obtained on Varian Associates XL-300 spectrometer and are reported in parts per million. ^{1}H NMR spectra (299.94 MHz) are referenced to the residual proton signal of C_6D_6 (δ 7.15), CD_2Cl_2 (δ 5.34), $CDCl_3$ (δ 7.24) or THF-d_8 (δ 3.60 and 1.75). ^{31}P{^{1}H} NMR spectra (121.42 MHz) are referenced to external $P(OMe)_3$ set at δ 141.00 ppm

relative to 85% H_3PO_4. $^{13}C\{^1H\}$ NMR spectra (75.43 MHz) are referenced to the natural abundance carbon signals of the solvent employed: C_6D_6 (δ 128.00), $CDCl_3$ (δ 77.00) or CD_2Cl_2 (δ 53.80). Mrs. M. T. Austria, Ms. L. K. Darge, and Dr. S. O. Chan assisted in obtaining the NMR data, as did J. D. Debad. Mass spectra were recorded by Dr. G. K. Eigendorf and the staff of the mass spectroscopy laboratory. Low-resolution mass spectra (EI, 70 eV) were recorded on a Kratos MS50 spectrometer using the direct-insertion method. Fast-atom bombardment (6 kV ion source, 7-8 kV xenon FAB gun) mass spectra were recorded on a AEI MS 9 spectrometer using 3-nitrobenzyl alcohol as matrix. All elemental analyses were performed by Mr. P. Borda of this Department.

2.2.2 Reagents

The organometallic reagents, $Cp'M(NO)Cl_2$ (M = Mo or W), were prepared by established procedures.[13] $Cp'Mo(NO)Cl_2$ complexes were further purified by Soxhlet extraction with CH_2Cl_2, and the $Cp'W(NO)Cl_2$ complexes were stored at -30 °C and used within one month of preparation. PhMgCl, (*p*-tolyl)MgCl and (*o*-tolyl)MgCl (1.0 M in THF) were purchased from Aldrich Chemical Co. and were used as received. Activated magnesium powder was obtained from Baker Scientific. PMe_3 was prepared from $P(OMe)_3$ and MeMgI[14] and was dried over and transferred from sodium/benzophenone. Solvents were freshly distilled from appropriate drying agents under a dinitrogen atmosphere and were either purged for 10 min with argon prior to use or were directly vacuum transferred from the appropriate drying agent. Dioxane, tetrahydrofuran and diethyl ether were distilled from sodium/benzophenone; hexanes, benzene, toluene and pentane were distilled from sodium/benzophenone/tetraglyme; dichloromethane was doubly distilled from P_2O_5.[15] C_6D_6 was dried over activated 4Å molecular sieves and degassed using 3 freeze-thaw-pump cycles.

2.2.3 Electrochemical Measurements

The detailed methodology employed for cyclic voltammetry studies in these laboratories has been outlined elsewhere.[16,17] Potentials were supplied by a BAS CV27 voltammograph, and the resulting cyclic voltammograms were recorded on a Hewlett-Packard Model 7090A Measurement Plotting System in buffered recording mode. All measurements were made at room temperature.

The potentials, $E^{\circ\prime}$, are defined as the average of the cathodic and anodic peak potentials, $(E_{p,c} + E_{p,a})/2$, and are reported versus the aqueous saturated calomel electrode (SCE). In a drybox, solutions were prepared at 0.1 M in the $[n\text{-}Bu_4N]PF_6$ support electrolyte and ~6 x 10^{-4} M in the organometallic complex to be studied. During the course of an electrochemical experiment the solutions were maintained under an atmosphere of argon. The 3-electrode cell consisted of a Pt bead working electrode (~1 mm diameter), a Pt wire auxiliary electrode, and a SCE in a separate holder connected to the cell compartment via a Luggin probe separated by a frit. Compensation for *iR* drop in potential measurements was not employed during this study. Ferrocene (Fc) was used as an internal reference in these studies, with the redox couple Fc/Fc^+, occurring at $E^{\circ\prime}$= 0.54 V versus SCE in THF over the range of scan rates (ν) used (0.10 to 0.80 V s^{-1}). The anodic and cathodic peak separation (ΔE) for this couple increases with increasing scan rate (80 - 240 mV between 0.10 - 0.80 Vs^{-1}), but since the Fc/Fc^+ couple is known to be highly reversible, other redox couples exhibiting similar peak separations and integrations to the internal standard were also considered to be electrochemically reversible, single-electron processes. The ratio of cathodic peak current to anodic peak current, $i_{p,c}/i_{p,a}$, for the oxidation of Fc was unity over all scan rates used, as expected for a chemically reversible process. The linearity of a plot of $i_{p,a}$ vs. $\nu^{1/2}$ was checked for all reduction processes to establish the presence of diffusion control.[17]

2.2.4 General Preparation of $R_2Mg{\cdot}X$(dioxane) (X = 1-2)

A general procedure for the preparation of diarylmagnesium reagents is outlined below; this methodology is a modification of a published procedure for the preparation of unsolvated

dialkylmagnesium complexes.[18] Since Neil Dryden (Ph.D. 1990) conceived the idea of using diaryl magnesium complexes as synthetic reagents to prepare $Cp'M(NO)(aryl)_2$ complexes, he is thankfully acknowledged.[19] The method presented below was utilized to synthesize $(Ph)_2Mg{\cdot}X$(dioxane), (p-tolyl)$_2$Mg·X(dioxane) and (o-tolyl)$_2$Mg·X(dioxane).

A 0.4 M solution of the Grignard reagent in THF was prepared (either from activated Mg powder and aryl chloride or by dilution of purchased RMgCl solution). The solution was then treated with 1,4-dioxane (2.2 equivalents) dropwise from an addition funnel. The resulting white slurry was stirred for 6 - 24 h at room temperature. The supernatant solution containing the desired $R_2Mg{\cdot}X$(dioxane) was isolated by centrifuging portions of the slurry for 20 min at 3500 rpm and then removing the clear supernatant solutions by cannulation. The remaining solids were similarily reextracted with fresh THF. The solvent was removed from the combined supernatant solutions under reduced pressure to obtain tarry residues. These residues were triturated exhaustively with hexanes, the hexanes being carefully removed after each trituration by cannulation. The remaining solid was dried in vacuo (24 h at 25 °C) to obtain the organomagnesium products as dusty white pyrophoric powders. Higher purity diaryl magnesium reagents were prepared by crystallization of these powders from THF/Et_2O. The compositions of the powders or crystals with respect to their active carbanion equivalents were established by hydrolysis of weighed solid samples and titration of the resulting solutions with 0.100 N HCl using phenolphthalein as the indicator.

2.2.5 Preparation of $Cp^*M(NO)(aryl)_2$ [M = Mo, W; aryl = Ph, p-tolyl, o-tolyl] (2.1 - 2.6)

Since the synthetic approach to each of these six complexes is similar, their syntheses are presented in a generalized manner.

Solid $Cp^*M(NO)Cl_2$ (2.00 mmol) and solid $R_2Mg{\cdot}X$(dioxane) (1.98 mmol, slight deficiency) were intimately mixed in a Schlenk tube contained in a glovebox. The tube was removed from the box and was attached to a vacuum line, whereupon THF (25 mL) was vacuum transferred onto the solids at -196 °C. The reaction mixture was then allowed to warm to -50 °C under an

atmosphere of argon. After being stirred for 30 min at -50 °C, the mixture was warmed to 0 °C. The solvent was removed in vacuo *without* further warming of the reaction mixture, and the residues were washed with pentane. The dried blue-to-purple residues were then extracted with cold Et_2O (10 °C) and filtered through Celite (4 x 15 cm) at -20 °C supported on a sintered glass frit.[20] The extracts were concentrated in vacuo until the first signs of crystallization were evident. If brown solids appeared on the sides of the flask during the initial concentration procedure, a second low-temperature filtration was done. Complete crystallization occurred upon storing the concentrated extracts in a freezer overnight. Finally, the desired diaryl complex was isolated by removal of the supernatant solution by cannulation and drying of the remaining crystals in vacuo.

The tungsten complexes, **2.4 - 2.6**, are more robust than the molybdenum complexes, **2.1 - 2.3**, and can therefore be filtered through Florisil (60 -100 mesh) maintained at low temperatures rather than Celite as specified above. However, transfer of the THF by syringe or the use of Grignard reagents in THF as the arylating agents reduce the isolated yields of products by at least 20 - 30%. Occasionally, complete decomposition of the entire reaction mixtures occurs when using commercial Grignard reagents. This observation is attributed to the fact that commercially available aryl Grignard reagents contain residual aryl halide, as well as Wurtz coupling products, which complicate the purification and isolation of the desired organometallic products. The physical properties of **2.1 - 2.6** are collected in Tables 2.1 - 2.3 (Section 2.2.10).

2.2.6 Attempted Syntheses of $CpM(NO)(aryl)_2$ [M = Mo, aryl = Ph, *p*-tolyl, *o*-tolyl; M = W, aryl = Ph, *p*-tolyl]

Efforts to prepare the analogous $CpMo(NO)(aryl)_2$ (aryl = Ph, *o*-tolyl, *p*-tolyl) and $CpW(NO)(aryl)_2$ (aryl = Ph, *p*-tolyl) complexes via methodology similar to that outlined above have so far been unsuccessful. Reaction of $CpM(NO)Cl_2$ complexes with the appropriate diaryl magnesium reagents in THF results in distinctive red-purple to blue solutions. The IR spectra of these reaction solutions show strong bands in the region anticipated for the ν_{NO} of these diaryl complexes, specifically $CpMo(NO)Ph_2$, 1628 cm^{-1}; $CpMo(NO)(p\text{-tolyl})_2$, 1624 cm^{-1};

$CpMo(NO)(o\text{-tolyl})_2$, 1624 cm^{-1}; $CpW(NO)Ph_2$, 1601 cm^{-1}; and $CpW(NO)(p\text{-tolyl})_2$, 1599 cm^{-1}. However, any attempts to isolate these aryl complexes that have involved manipulations above -40 °C resulted in a rapid color change to red-brown and loss of their distinctive IR spectral features.

2.2.7 Synthesis of $CpW(NO)(o\text{-tolyl})_2$ (2.7)

$CpW(NO)(o\text{-tolyl})_2$ is the only isolable diaryl nitrosyl complex that does not incorporate a *pentamethyl*cyclopentadienyl ligand (Cp^*). It is synthesized from $CpW(NO)Cl_2$ and $(o\text{-tolyl})_2Mg{\cdot}X$(dioxane) in a manner analogous to the method used to synthesize complexes **2.1** - **2.6**; filtration through Florisil during work-up, however, is mandatory.[21] Crystallization from diethyl ether provides **2.7** as violet needles in variable yields (10 - 30%).

Anal. calcd for $C_{19}H_{19}NOW$: C, 49.48; H, 4.15; N, 3.04. Found: C, 49.19; H, 4.21; N, 3.05. IR (THF) ν_{NO} 1602 cm^{-1}. IR (Nujol) ν_{NO} 1601 cm^{-1}. ^1H NMR (C_6D_6) δ 7.43 - 7.02 (m, 8H, aryl H), 5.22 (s, 5H, C_5H_5), 2.83 (s, 6H, 2 x $o\text{-}CH_3$). Low-resolution mass spectrum (probe temperature 120 °C): *m/z* 461 (P^+).

2.2.8 Preparation of $Cp^*W(NO)(p\text{-tolyl})_2(PMe_3)$ (2.8)

A sample of $Cp^*W(NO)(p\text{-tolyl})_2$ (35 mg, 0.066 mmol) was dissolved in hexanes (10 mL) at room temperature. PMe_3 (1 atm) was introduced into the Schlenk tube via vacuum transfer from Na/benzophenone whereupon the deep blue solution instantly became yellow. Concentration and cooling of the reaction solution overnight at -30 °C induced the precipitation of a white powder which was collected and washed with cold pentane (5 mL) to obtain analytically pure $Cp^*W(NO)(p\text{-tolyl})_2(PMe_3)$ (32 mg, 80%).

Anal. calcd for $C_{27}H_{38}NOPW$: C, 53.39; H, 6.31; N, 2.31. Found: C, 53.43; H, 6.22; N, 2.30. IR (THF) ν_{NO} 1562 cm^{-1}. IR (Nujol) ν_{NO} 1559 cm^{-1}. ^1H NMR (C_6D_6) δ 7.86 (dm, 2H, 2 of 4 ortho protons, transoidal to PMe_3, J_{HP} not resolved), 7.07 (d, 2H, J_{HH} = 7.1 Hz, 2 of 4 meta protons), 6.99 (d, 2H, J_{HH} = 7.1 Hz, 2 of 4 ortho protons), 6.91 (d, 2H, J_{HH} = 7.1 Hz, 2 of

4 meta protons), 2.23 (s, 6H, 2 x *p*-CH_3), 1.48 (s, 15H, $C_5(CH_3)_5$), 0.59 (d, 9H, J_{HP} = 9.5 Hz, $P(CH_3)_3$). ^{31}P NMR (C_6D_6) δ -21.11 (s, J_{WP} = 320 Hz). Low-resolution mass spectrum (probe temperature 180 °C): *m/z* 531 (P^+-PMe_3). FAB mass spectrum: *m/z* 607 (P^+).

2.2.9 Preparation of $Cp^*W(NO)(o\text{-tolyl})_2(PMe_3)$ (2.9)

A solution of $Cp^*W(NO)(o\text{-tolyl})_2$ was generated from $Cp^*W(NO)Cl_2$ (840 mg, 2.00 mmol) and $(o\text{-tolyl})_2Mg{\cdot}X$(dioxane) (640 mg, 4.00 mmol *o*-tolyl$^-$) in THF (40 mL) at -20 °C. The solvent was removed in vacuo and the residue extracted with CH_2Cl_2/Et_2O (1:1, 50 mL). The extracts were filtered through Florisil (3 x 5 cm). The column was rinsed with CH_2Cl_2 (3 x 25 mL) and the purple filtrate was taken to a purple powder in vacuo. The powder was dissolved in Et_2O (80 mL) and CH_2Cl_2 (3 mL). PMe_3 (1 atm) was introduced into the Schlenk tube containing the solution of $Cp^*W(NO)(o\text{-tolyl})_2$ via vacuum transfer from Na/benzophenone whereupon the violet solution instantly became yellow. The yellow solution was taken to dryness and dried in vacuo for 5 h. The dried extracts were then extracted with CH_2Cl_2 (40 mL) and filtered through alumina I neutral (3 x 4 cm). The column of alumina was rinsed exhaustively with CH_2Cl_2 (150 mL). Removal of solvent from the filtrate, redissolution in a minimum of Et_2O (~50 mL) and crystallization overnight at -30 °C induced the precipitation of $Cp^*W(NO)(o\text{-tolyl})_2(PMe_3)$ (180 mg, 15% based on $Cp^*W(NO)Cl_2$) as an off-white microcrystalline solid.

Anal. calcd for $C_{27}H_{38}NOPW$: C, 53.39; H, 6.31; N, 2.31. Found: C, 53.46; H, 6.29; N, 2.29. IR (Nujol) ν_{NO} 1536 cm^{-1} (br). ^1H NMR (C_6D_6) δ 8.10, 7.45 - 6.91 (m, aryl protons for both cis and trans isomers), 2.86 (s, *o*-CH_3, cis isomer), 2.82 (s, 2 x *o*-CH_3, trans isomer), 2.23 (s, *o*-CH_3, cis isomer), 1.60 (s, $C_5(CH_3)_5$, trans isomer), 1.58 (s, $C_5(CH_3)_5$, cis isomer), 0.87 (d, J_{HP} = 6.3 Hz, $P(CH_3)_3$, trans isomer), 0.81 (d, J_{HP} = 9.0 Hz, $P(CH_3)_3$, cis isomer). ^{31}P NMR (C_6D_6) δ -17.54 (s, trans isomer, J_{WP} = 311 Hz), -20.40 (s, cis isomer J_{WP} = 309 Hz). Low-resolution mass spectrum (probe temperature 100 °C): *m/z* 531 (P^+-PMe_3). FAB mass spectrum: *m/z* 607 (P^+).

2.2.10 Characterization Data for Complexes 2.1 - 2.6

Table 2.1 Numbering Scheme, Color, Yield and Elemental Analysis Data

complex	compd no.	color (yield, %)	elemental analysis found (calcd)		
			C	H	N
Cp*Mo(NO)Ph_2[a]	**2.1**	violet (42)	60.51 (63.61)	5.87 (6.07)	3.19 (3.37)
Cp*Mo(NO)(*p*-tolyl)$_2$	**2.2**	purple (65)	64.83 (65.01)	6.70 (6.59)	2.92 (3.16)
Cp*Mo(NO)(*o*-tolyl)$_2$	**2.3**	purple (32)	65.06 (65.01)	6.57 (6.59)	3.16 (3.16)
Cp*W(NO)Ph_2	**2.4**	blue (55)	52.30 (52.50)	5.00 (5.01)	2.66 (2.78)
Cp*W(NO)(*p*-tolyl)$_2$	**2.5**	blue (81)	53.98 (54.25)	5.52 (5.50)	2.62 (2.63)
Cp*W(NO)(*o*-tolyl)$_2$	**2.6**	violet (40)	55.15 (54.25)	5.89 (5.50)	2.59 (2.63)

[a] The elemental analysis of C, H and N are proportionally low due to a small quantity of residual $MgCl_2$ (approx. 4.9%) which could not be removed without decomposing the organometallic complex.

Table 2.2 Mass Spectral and Infrared Data

compd no.	MS *m/z*[a]	temp[b] (°C)	IR	
			ν_{NO} (THF)	ν_{NO} (Nujol)
2.1	417 [P^+]	90	1615	1592
2.2	445 [P^+] 415 [P^+-NO]	100	1609	1603
2.3	445 [P^+] 415 [P^+-NO]	80	1601	1587
2.4	503 [P^+]	120	1588	1576
2.5	531 [P^+]	100	1582	1576
2.6	531 [P^+] 439 [P^+- C_7H_8]	80	1601	1545

[a] *m/z* values are for the highest intensity peak of the calculated isotopic cluster (^{98}Mo and ^{184}W).

[b] Probe temperatures.

Table 2.3 ^{1}H NMR Data

compd no.	^{1}H NMR (C_6D_6)
2.1	7.81 (dd, 4H, J = 7.2, 1.2 Hz, ortho protons) 7.23 (t, 4H, J = 7.2 Hz, meta protons) 7.12 (t, 2H, J = 7.2 Hz, para protons) 1.59 (s, 15H, $C_5(CH_3)_5$)
2.2	7.77 (d, 4H, J = 6.9 Hz, aryl protons) 6.98 (d, 4H, J = 6.9 Hz, aryl protons) 2.07 (s, 6H, 2 x p-CH_3) 1.59 (s, 15H, $C_5(CH_3)_5$)
2.3	7.25 - 6.94 (m, 8H, aryl protons) 2.20 (s, 6H, 2 x o-CH_3) 1.60 (s, 15H, $C_5(CH_3)_5$)
2.4	7.99 (d, 4H, J = 8.0 Hz, ortho protons) 7.18 (t, 4H, J = 7.4 Hz, meta protons) 7.07 (d, 2H, J = 7.2 Hz, para protons) 1.58 (s, 15H, $C_5(CH_3)_5$)
2.5	8.01 (d, 4H, J = 6.4 Hz, ortho protons) 6.99 (d, 4H, J = 6.4 Hz, meta protons) 2.01 (s, 6H, 2 x p-CH_3) 1.65 (s, 15H, $C_5(CH_3)_5$)
2.6	7.88 - 7.00 (m, 8H, aryl protons) 2.92 (s, 6H, 2 x o-CH_3) 1.62 (s, 15H, $C_5(CH_3)_5$)

2.2.11 Other Characterization Data

Table 2.4 Electrochemical Data for the First and Second Reductions of Complex **2.5**[a]

scan rate (ν, Vs^{-1})	$E^{\circ\prime}{}_1$[b] (V)	ΔE[c]	$i_{p,a}/i_{p,c}$[d]
0.80	-1.21	0.13 (0.14)	1.0
0.40	-1.21	0.10 (0.10)	1.0
0.20	-1.21	0.08 (0.10)	1.0
0.10	-1.21	0.07 (0.08)	1.0

scan rate (ν, Vs^{-1})	$E^{\circ\prime}{}_2$[b] (V)	ΔE[c]	$i_{p,a}/i_{p,c}$[d]
0.80	-2.46	0.12 (0.14)	0.8[e]
0.40	-2.46	0.10 (0.10)	0.8[e]
0.20	-2.46	0.07 (0.10)	0.8[e]
0.10	-2.46	0.06 (0.08)	0.8[e]

[a] In THF containing 0.10 M [n-Bu_4N]PF_6, at a Pt-bead working electrode. Potentials are measured vs SCE.

[b] Defined as the average of the cathodic and anodic peak potentials (± 0.02 V).

[c] Defined as the separation of the cathodic and anodic peak potentials. Values of ΔE given in parentheses are for the Cp_2Fe/Cp_2Fe^+ couple under the same conditions.

[d] Ratio of anodic peak current to cathodic peak current

e Accurate determination of this ratio was not possible since the reduction wave occurred very close to the solvent limit of the THF/TBAH electrolyte system.

2.3 Results and Discussion[22]

2.3.1 A New *General* Synthetic Methodology

A reliable, reproducible synthesis of $Cp'M(NO)R_2$ complexes began, oddly enough, with electrochemistry. Cyclic voltammetry showed that the metathesis reactions forming dialkyl nitrosyl complexes proceeded through isolable radical anion intermediates of the type $[Cp'M(NO)X_2]^{\cdot -}$.[16] This work empirically showed that $[Cp'M(NO)Cl_2]^{\cdot -}$ are the longest lived and most thermally stable dihalo radical anions in this family. Therefore, it was our view that a general synthetic methodology for the preparation of $Cp'M(NO)R_2$ complexes should be designed to maximize the stability of these radical anion intermediates. This requirement implies the use of (a) dichloro nitrosyl starting materials, (b) highly solvating solvents to stabilize ionic intermediates, and (c) low temperatures to avoid possible decomposition pathways of the newly formed organometallics. Obviously, the use of the diiodide complexes at room temperature in diethyl ether did not meet these requirements (Section 1.2). $Cp'M(NO)Cl_2$ complexes are now used exclusively as starting materials in our work since we have previously established that the dichloro complexes, $Cp'M(NO)Cl_2$ (M = Mo or W), are superior to their iodo analogues as synthetic precursors for the preparation of $Cp'M(NO)(alkyl)_2$ complexes.[3,19,22,23,24,25]

Our next step was to overcome the inherent need for water in reaction 1.3. The use of $R_2Mg{\cdot}X$(dioxane) reagents instead of Grignard reagents accomplishes this goal. Equation 2.3 summarizes the synthetic method that was designed to synthesize $Cp^*M(NO)(aryl)_2$ complexes.

$$Cp^*M(NO)Cl_2 + (aryl)_2Mg{\cdot}X(dioxane) \xrightarrow[-50 \text{ to } 0\,^\circ C]{THF,\ argon} Cp^*M(NO)(aryl)_2 + Cl_2Mg{\cdot}(dioxane) \quad (2.3)$$

After metathesis, the dioxane from $R_2Mg{\cdot}X$(dioxane) ligates the $MgCl_2$ formed considerably more efficiently than does the oxygen atom of the nitrosyl ligand of the desired $Cp^*M(NO)R_2$ complexes, thereby removing the need for water to liberate the desired organometallics from isonitrosyl adducts of the type $[Cp^*M(NO)R_2]_2{\cdot}MgCl_2$ (eq 2.1).[26] Additionally, these reagents

are solids and, when properly prepared, are of exact stoichiometries. An additional benefit of reaction 2.3 is that Cl_2Mg·dioxane is very insoluble in even moderately polar solvents thus allowing uncontaminated $Cp^*M(NO)(aryl)_2$ complexes to be extracted from the final reaction mixtures. The desired products of reactions 2.3 range in color from deep indigo-blue to violet and are obtainable as analytically pure, crystalline solids in yields of 32-81%.[27]

2.3.2 Physical Properties

$Cp'M(NO)(aryl)_2$ complexes are thermally stable as solids when analytically pure, but in solution at room temperature decompose over the course of several days or weeks. Overall, these complexes are markedly less stable than their dialkyl analogues since they are prone to decompose autocatalytically, even at low temperatures. The diaryl complexes are soluble in most common organic solvents, but to a noticeably lesser extent than their dialkyl analogues. For instance, $Cp^*W(NO)(p\text{-tolyl})_2$ is the only diaryl complex that is soluble in hexanes, whereas all $Cp'M(NO)(alkyl)_2$ species are pentane soluble. In general, the *p*-tolyl derivatives are more soluble than the *o*-tolyl and phenyl derivatives. Both in solution and in the solid state, $Cp^*M(NO)(aryl)_2$ species decompose rapidly when exposed to the atmosphere.

2.3.3 Spectroscopic Characterization

The spectroscopic properties of the six Cp^* diaryl complexes are consistent with their possessing monomeric, three-legged piano-stool molecular structures having a 16-valence-electron configuration at the metal center. Thus, just as observed previously for related dialkyl complexes, the ^1H NMR spectra of these diaryl complexes (Table 2.3) are not unusual and are fully consistent with their formulations.

The ν_{NO} bands in the IR spectra of the molybdenum diaryl complexes are, on average, some 23 cm^{-1} higher in energy than their tungsten congeners. These ν_{NO} bands are also some 30 - 60 cm^{-1} lower in energy than those exhibited by their parent dichloro complexes, a manifestation of the better electron donation from an aryl ligand than from an electronegative

chloride ligand. However, when the IR spectra of the diaryl complexes are compared to those of the dialkyl complexes, it is obvious than aryl ligands are considerably less electron-donating than alkyl ligands. Both the solution and solid-state IR spectra of the dialkyl derivatives display ν_{NO} values which are 10 - 30 cm^{-1} lower in energy than those of similar diaryl complexes (see Section 1.1 for the conclusions that can be drawn from ν_{NO}). In other words, their IR spectroscopic properties imply that in the $Cp^*M(NO)(aryl)_2$ complexes the metal centers are more electron-deficient than in their alkyl analogues, and this in turn is manifested by the molybdenum and tungsten centers in the aryl species being more Lewis acidic than in related $Cp^*M(NO)(alkyl)_2$ complexes. The topic of relative Lewis acidities is further addressed in Section 3.3.2.

2.3.4 Attempts to Synthesize $CpM(NO)(aryl)_2$ Complexes

Efforts to prepare the Cp-containing members of this class of complexes by reaction 2.3 indicate that the desired diaryl products are indeed formed in solution. This conclusion is supported by the observation of a single ν_{NO} in the IR spectra of the final reaction mixtures (Section 2.2.6) at values consistent with those expected for diaryl nitrosyl complexes. Furthermore, the reaction solutions are a very distinctive blue to purple color which is characteristic of isolable diaryl nitrosyl complexes. However, all attempts to isolate the Cp-containing products from these solutions have been unsuccessful so far, the decomposition of the desired products being indicated by the loss of the characteristic colors of the reaction mixtures upon attempted workup. The only exception to this generalization is that $CpW(NO)(o\text{-tolyl})_2$ is isolable, albeit in fairly low yields (< 35%).[11,32]

Solutions containing in situ generated CpW diaryl complexes can be derivatized (vide infra), but in situ generated $CpMo(NO)(aryl)_2$ complexes have resisted derivatization. For example, a violet THF solution of $CpMo(NO)(p\text{-tolyl})_2$ (1 mmol generated in situ) can be treated with PMe_3 (1 atm) at -50 °C. The product after workup, a yellow solid, gives an amber solution in C_6D_6. A ^1H NMR spectrum of this solution reveals 4,4'-dimethylbiphenyl (δ 7.45, d; 7.03, d; 2.16, s) to be the major product in the mixture. An unidentified Cp peak at δ 5.24 quickly diminishes in

intensity as new spectra are recorded. Within 30 minutes, the peak at δ 5.24 is gone and the walls of the NMR tube are coated with an insoluble dark brown precipitate. The only two identifiable compounds left in solution at this time are PMe_3 and 4,4'-dimethylbiphenyl. Clearly, the aryl ligands of CpMo(NO)(*p*-tolyl)$_2$ are extremely labile.

Our inability to isolate CpW(NO)(aryl)$_2$ complexes other than CpW(NO)(*o*-tolyl)$_2$ was unexpected, since three CpW(NO)(alkyl)$_2$ complexes have been isolated in our laboratories. Since the Cp*-containing analogues are accessible, however, it may be that a planar aromatic ligand in conjunction with the less sterically demanding Cp group does not shield the unsaturated metal center as well as do bulky alkyl and Cp* ligands. Our recent discovery of the thermal instability of CpMo(NO)(CH_2CMe_3)$_2$[25] indicates to us that CpMo(NO)(aryl)$_2$ species are likely to be even more thermally sensitive, particularly since it appears that low activation energy pathways for their decomposition exist (Section 2.2.6). Evidently, the additional steric shielding and greater electron-donating ability of the Cp* ligand versus the Cp ligand provide the necessary factors to render a variety of Cp*M(NO)(aryl)$_2$ complexes stable enough to be isolated. This general stabilizing ability of the Cp* group has also been documented for other systems.[28]

2.3.5 X-ray Crystallographic Analyses of Complexes 2.3 and 2.6

The solid-state molecular structures of both Cp*M(NO)(*o*-tolyl)$_2$ complexes have been established, and their monomeric natures have been confirmed.[29] ORTEP diagrams of these two very similar diaryl complexes are presented in Figure 2.1. The intramolecular geometrical parameters of both molecules resemble those found in CpW(NO)(CH_2SiMe_3)$_2$[2] and CpMo(NO)(CD_2CMe_3)$_2$.[30]

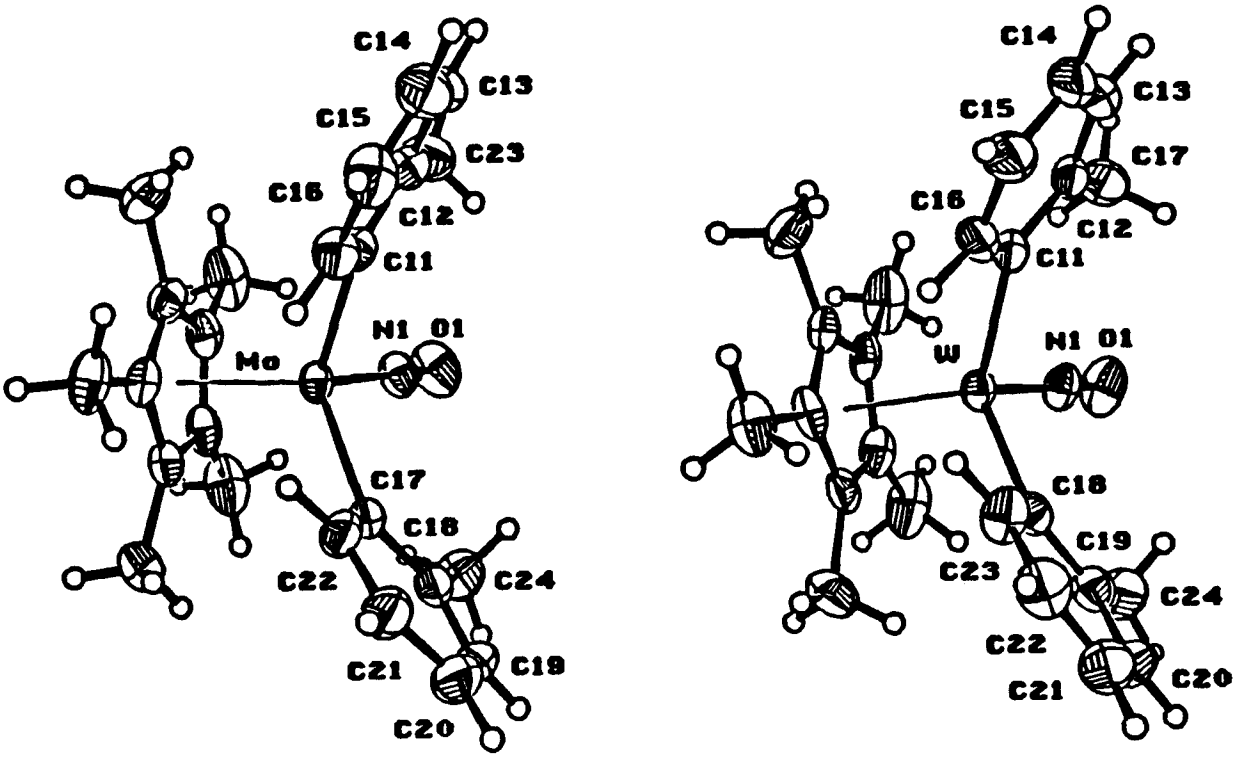

Figure 2.1 Views of the solid-state molecular structures of $Cp^*Mo(NO)(o\text{-tolyl})_2$, **2.3** (on the left) and $Cp^*W(NO)(o\text{-tolyl})_2$, **2.6** (on the right); 33% probability ellipsoids are shown for the non-hydrogen atoms

The solid-state structures of the four crystallographically characterized $Cp'M(NO)R_2$ complexes can be compared. The chemically most interesting metrical parameters of these molecules is the apparent size of the open coordination site at their metal centers. Figure 2.2 shows a triangle with the metal-carbon bond lengths and C-M-C bond angle defining the empty coordination site of each complex. The non-bonded separations between the two carbon atoms directly attached to the central metals are also given.

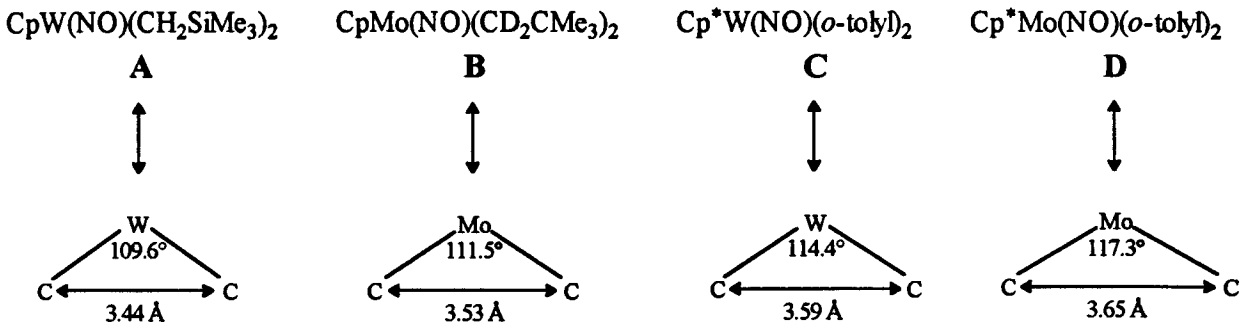

Figure 2.2 Pictorial representations of the open coordination sites at each metal center in representative $Cp'M(NO)R_2$ complexes

For simplicity, allow **A** = $CpW(NO)(CH_2SiMe_3)_2$; **B** = $CpMo(NO)(CH_2CMe_3)_2$; **C** = $Cp^*W(NO)(o\text{-tolyl})_2$; and **D** = $Cp^*Mo(NO)(o\text{-tolyl})_2$. Then, from the series of non-bonded C-C separations it is apparent that aryl complexes have more room at their metal centers than alkyl complexes, i.e. $\mathbf{D}_{CC} > \mathbf{B}_{CC}$ (i.e. 3.65 Å > 3.53 Å) and $\mathbf{C}_{CC} > \mathbf{A}_{CC}$ (i.e. 3.59 Å > 3.44 Å). Additionally, molybdenum complexes have increased accessibility to their metal centers compared to analogous tungsten complexes, thus $\mathbf{B}_{CC} > \mathbf{A}_{CC}$ (i.e. 3.53 Å > 3.44 Å) and $\mathbf{D}_{CC} > \mathbf{C}_{CC}$ (i.e. 3.65 Å > 3.59 Å). Furthermore, it is also evident from the structures of **2.3 (C)** and **2.6 (D)** (Figure 2.1) that the σ-bonded aryl groups are considerably less sterically demanding than are similarly attached bulky alkyl groups. The upshot of the crystallographic analyses is that the diaryl complexes are more *accessible* Lewis acids, this in addition to being more *potent* Lewis acids (Section 2.3.3). Thus, the nonbonded C-C separation, used as a measure of metal accessibility, allows us to conclude that diaryl species are considerably more spatially accessible than their dialkyl analogues. This feature is also manifested by the characteristic chemistry of these complexes which is considered in the next section.

2.3.6 Reactivity Patterns of the Diaryl Complexes

In all cases investigated to date, diaryl complexes react with substrates orders of magnitude faster than analogous dialkyl complexes under similar conditions, e.g. eqs 2.4 and 2.5.

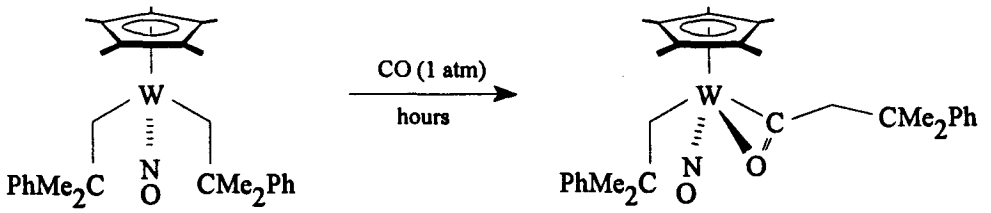

(2.4)

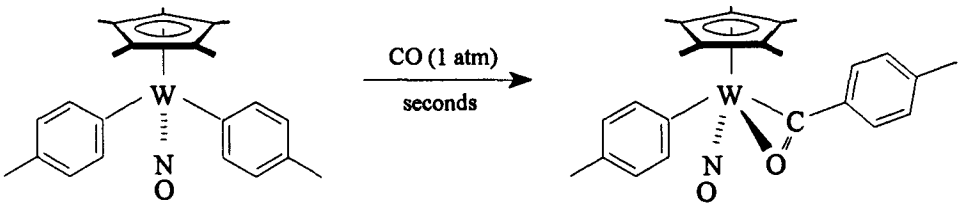

(2.5)

The transformation shown in eq 2.5 involves CO insertion to form an acyl complex. It is very facile, being complete in a matter of seconds under ambient conditions. In comparison, $Cp^*W(NO)(CH_2CMe_2Ph)_2$ reacts with CO to form the analogous monoacyl complex only after 6 h under the same reaction conditions (eq 2.4).[31] In a similar manner, in situ generated $CpW(NO)(p\text{-tolyl})_2$ reacts instantaneously with elemental sulfur in nonpolar solvents at 25 °C to provide $CpW(NO)(S\text{-}p\text{-tolyl})_2$.[32] In contrast, $CpW(NO)(CH_2SiMe_3)_2$ reacts with sulfur in toluene (50 °C) over a period of one day in a sequential manner to form first $CpW(NO)(SCH_2SiMe_3)(CH_2SiMe_3)$, then $CpW(NO)(\eta^2\text{-}S\{S\}CH_2SiMe_3)(CH_2SiMe_3)$, and then finally the analogous bis(thiolate) complex, $CpW(NO)(SCH_2SiMe_3)_2$.[2,33]

$Cp^*M(NO)(aryl)_2$ complexes are also more potent Lewis acids than analogous dialkyl species. Previous work has demonstrated that $CpW(NO)(CH_2SiMe_3)_2$ and PMe_3 establish an equilibrium in toluene at room temperature.[2] Hence, the monophosphine adduct,

$CpW(NO)(CH_2SiMe_3)_2(PMe_3)$, can only be isolated in the presence of an excess of PMe_3, and it loses PMe_3 when exposed to vacuum. In contrast, prolonged exposure of isolated $Cp^*W(NO)(aryl)_2(PMe_3)$ species (**2.8** and **2.9**) to high vacuum for days at room temperature does not regenerate $Cp^*W(NO)(p\text{-tolyl})_2$ (**2.5**) or $Cp^*W(NO)(o\text{-tolyl})_2$ (**2.6**), respectively.

From its spectral data (Table 2.3), complex **2.8** [$Cp^*W(NO)(p\text{-tolyl})_2(PMe_3)$] clearly has equivalent aryl ligands. Thus, the structure in solution must be such that the PMe_3 ligand is trans to the nitrosyl group of the complex (eq 2.6).

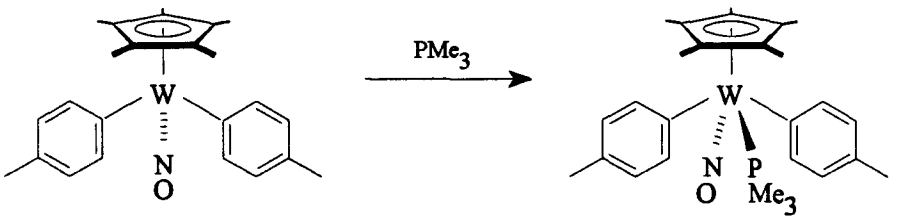

(2.6)

In contrast, complex **2.9**, the *o*-tolyl analog of **2.8**, exists as a 60/40 mixture of cis and trans isomers in C_6D_6. Thus, the ^1H NMR spectrum of **2.9** (Figure 2.3) shows three distinct *o*-Me environments; two for the cis isomer and one for the trans isomer. We can present no rationale for the ability of complex **2.9** to isomerize while **2.8** is configurationally stable, since both are nominally 7-coordinate molecules.

The nitrosyl-stretching frequencies of $Cp^*W(NO)(aryl)_2$ complexes and their 18-electron adduct derivatives can be compared. Adding PMe_3 to $Cp^*W(NO)(p\text{-tolyl})_2$ causes a drop in ν_{NO} of 20 cm^{-1} in THF (16 cm^{-1} in the solid state). Upon going from **2.6** to **2.9**, a drop of 9 cm^{-1} (solid-state) is observed. These observations are consistent with the metal centers in **2.8** and **2.9** being more electron-rich than the parent complexes **2.5** and **2.6**, respectively.

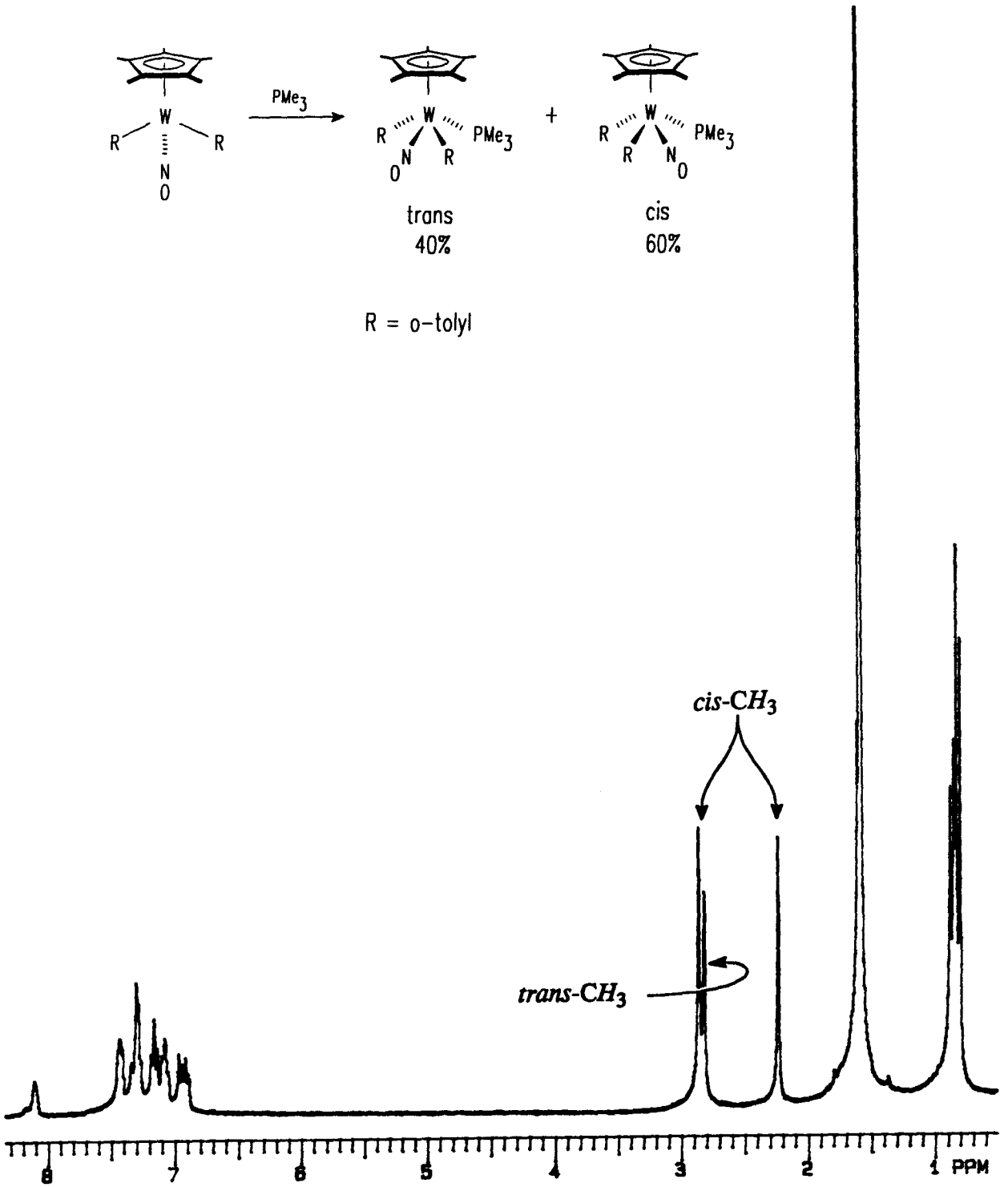

Figure 2.3 300 MHz ^{1}H NMR spectrum of $Cp^*W(NO)(o\text{-tolyl})_2(PMe_3)$ (**2.9**) in C_6D_6

2.3.7 Electrochemical Properties of Complex 2.5

Knowledge of the redox properties of molecules is of fundamental importance to understanding their reactivity behavior and their chemical properties. Hence, $Cp^*W(NO)(p\text{-tolyl})_2$ **(2.5)**, has been investigated by cyclic voltammetry as a representative member of the $Cp^*M(NO)(aryl)_2$ family. The cyclic voltammogram of **2.5** in THF (Figure 2.4) exhibits reduction features consistent with the occurrence of two reversible, one-electron reductions at $E^{\circ\prime}$ values of -1.21 V and -2.46 V. These reductions imply the consecutive formation of $[Cp^*W(NO)(p\text{-tolyl})_2]^{\cdot -}$ and $[Cp^*W(NO)(p\text{-tolyl})_2]^{2-}$ in solution. The cyclic voltammogram of **2.5** is devoid of any oxidation features out to the solvent limit of 0.8 V.

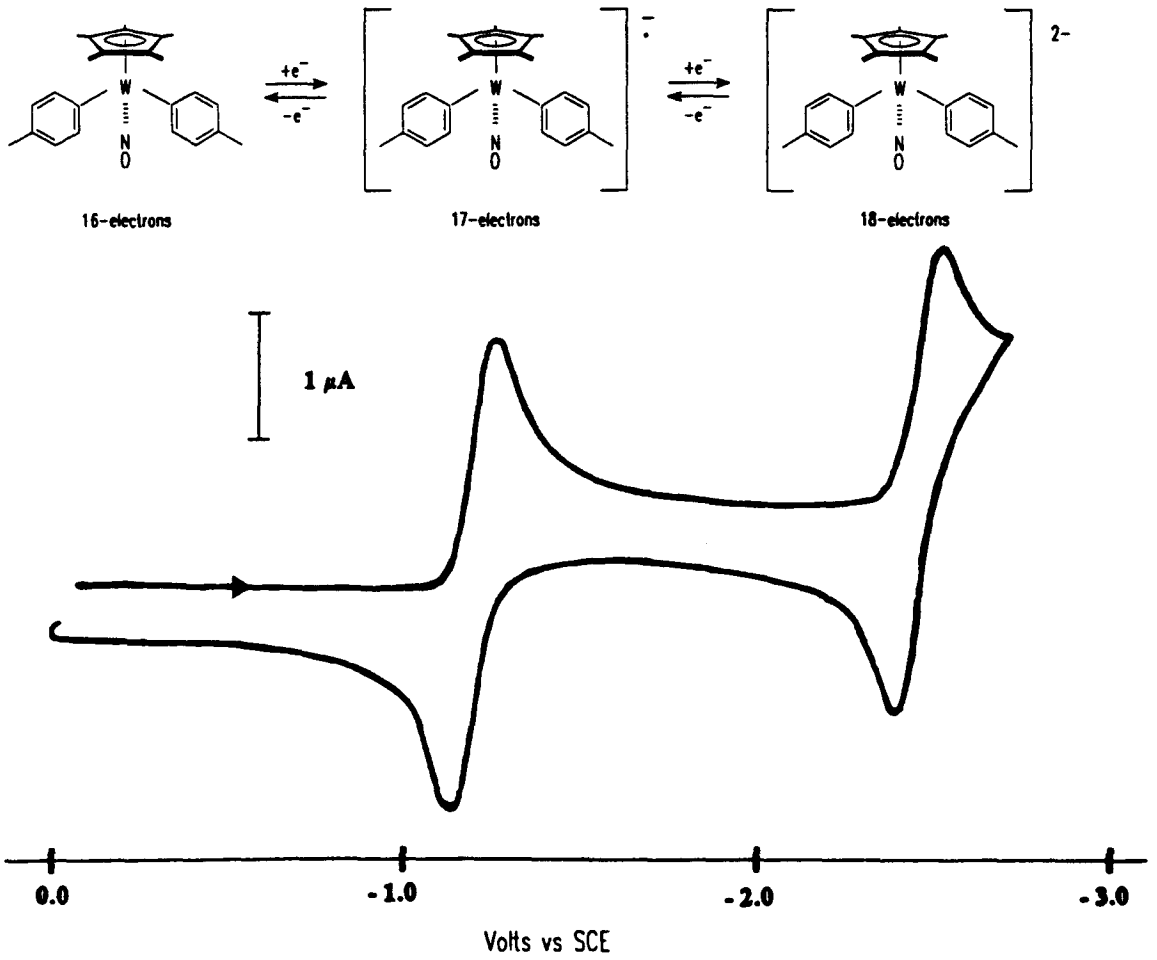

Figure 2.4 Ambient temperature cyclic voltammogram of $Cp^*W(NO)(p\text{-tolyl})_2$ (scan rate = 400 mV s^{-1}) in THF

The linearity of plots of $i_{p,a}$ vs. $\nu^{1/2}$ for these reduction waves shows that the reductions are diffusion controlled. Comparison of the ΔE values for these reductions with the internal Fc/Fc^+ reference indicate that the first reduction is electrochemically reversible. The $i_{p,a}/i_{p,c}$ value for the first reduction is unity over the range of scan speeds used, thereby establishing its chemical reversibility. From Figure 2.4 and the data presented in Table 2.4, it is apparent that an accurate determination of $i_{p,a}/i_{p,c}$ for the second reduction feature is not possible, but the reduction wave *is* electrochemically reversible and in all likelihood is chemically reversible as well. Some of the $[Cp^*W(NO)(p\text{-tolyl})_2]^{2-}$ formed in the second reduction may react with $Cp^*W(NO)(p\text{-tolyl})_2$ to give two molecules of $[Cp^*W(NO)(p\text{-tolyl})_2]^{\cdot-}$ before reoxidizing to $[Cp^*W(NO)(p\text{-tolyl})_2]^{\cdot-}$ electrochemically, a phenomenon that would lower $i_{p,a}/i_{p,c}$ ratios.

$Cp^*W(NO)(p\text{-tolyl})_2$ is easier to reduce by 410 mV than is $Cp^*W(NO)(CH_2CMe_2Ph)_2$ which exhibits a reversible first reduction in THF at -1.62 V.[22] Interestingly, this result is consistent with the diaryl complex containing a more electron-deficient metal center than does the related $Cp^*W(NO)(alkyl)_2$ species. Hence, the aryl ligands of $Cp^*W(NO)(aryl)_2$ evidently provide less electron density to the metal center thus allowing such complexes to accept electrons more easily than analogous $Cp^*W(NO)(alkyl)_2$ complexes. Additionally, $Cp^*W(NO)(p\text{-tolyl})_2$ exhibits a second reduction wave at more negative potential, i.e. -2.46 V. The second reduction of $Cp^*W(NO)(CH_2CMe_2Ph)_2$ in THF apparently occurs beyond the solvent limit of -2.7 V, thereby precluding a comparison of this feature with that exhibited by the $Cp^*W(NO)(p\text{-tolyl})_2$ complex. Thus the formation of $[Cp^*W(NO)(CH_2CMe_2Ph)_2]^{2-}$ occurs at more than 250 mV more negative potential than the second reduction of $Cp^*W(NO)(p\text{-tolyl})_2$.

The electrochemical investigation of $Cp^*W(NO)(p\text{-tolyl})_2$ has established that its reduction behavior is consistent with the Fenske-Hall MO description of $CpMo(NO)Me_2$ (Section 2.1), i.e. the LUMO of $Cp'M(NO)R_2$ complexes is non-bonding and filling of this orbital with electrons is completely reversible and does not disrupt the bonding in these complexes.

Finally, infrared spectral studies of diaryl nitrosyl complexes are also consistent with their being more electron-deficient than comparable dialkyl complexes. Thus, a Nujol mull IR

spectrum of $Cp^*W(NO)(p\text{-tolyl})_2$ shows a strong nitrosyl band at 1576 cm^{-1}, where the more electron-rich $Cp^*W(NO)(CH_2CMe_2Ph)_2$ complex exhibits its ν_{NO} at 1551 cm^{-1} under identical conditions.

2.4 Epilogue and Future Work

In addition to developing a reliable synthetic route to various $Cp^*M(NO)(aryl)_2$ complexes from their $Cp^*M(NO)Cl_2$ precursors, this work has established some fundamental facts about the diaryl species vis-à-vis their better known alkyl analogues. Specifically, the thermal stability of $Cp'M(NO)R_2$ complexes appears to be $Cp^* > Cp$, W > Mo, and alkyl > aryl. Hence, $CpMo(NO)(aryl)_2$ complexes have yet to be isolated. Furthermore, the investigations summarized in this chapter have established that the diaryl complexes are more reactive than their dialkyl counterparts, principally because their metal centers are more electron deficient and sterically more accessible to incoming nucleophilic reactants. In principle it would of great interest to separate the respective magnitudes of steric and electronic contributions to the Lewis acidity of $Cp'M(NO)R_2$ complexes, but it seems unlikely that this will be possible.

Ongoing research in our group includes a study of the reactions of diaryl complexes with organic substrates that do not react with dialkyl complexes. For example, heterocumulenes (CO_2 and isoelectronic analogues) do not react with $Cp'W(NO)(alkyl)_2$ species, but they do react with the highly activated diaryl complexes to give insertion products.[34]

2.5 References and Notes

(1) Legzdins, P.; Rettig, S. J.; Sánchez, L.; Bursten, B. E.; Gatter, M. G. *J. Am. Chem. Soc.* **1985**, *107*, 1411.

(2) Legzdins, P.; Rettig, S. J.; Sánchez, L. *Organometallics* **1988**, *7*, 2394.

(3) Legzdins, P.; Phillips, E. C.; Sánchez, L. *Organometallics* **1989**, *8*, 940.

(4) Bursten, B. E.; Cayton, R. H. *Organometallics* **1987**, *6*, 2004.

(5) In this context, stability of a complex refers to resistance to decomposition, within a reasonable period of time (hours) under "normal" physical conditions (inert atmosphere and ambient temperature) to any intra- or intermolecular chemical processes.

(6) Hunter, A. D.; Legzdins, P.; Martin, J. T.; Sánchez, L. *Organomet. Synth.* **1986**, *3*, 66.

(7) While $Cp'Mo(NO)(CH_2SiMe_3)_2$ were known compounds at the inception of this work neither was synthesizable reproducibly or in greater than 25% yield.[1,3]

(8) Seidler, M. D.; Bergman, R. G. *J. Am. Chem. Soc.* **1984**, *106*, 6110.

(9) Chang, J.; Bergman, R. G. *J. Am. Chem. Soc.* **1987**, *109*, 4298.

(10) Legzdins, P.; Lundmark, P. J.; Phillips, E. C.; Rettig, S. J.; Veltheer, J. E. *Organometallics* **1992**, *11*, 2991.

(11) A particularly interesting example of this reactivity is provided by our discovery of water converting one of these diaryl nitrosyl compounds to its arylimido oxo analogue. Legzdins, P.; Rettig, S. J.; Ross, K. J.; Veltheer, J. E. *J. Am. Chem. Soc.* **1991**, *113*, 4361.

(12) Shriver, D. F.; Drezdzon, M. A. *The Manipulation of Air-Sensitive Compounds*, 2nd ed.; Wiley-Interscience: New York, NY, 1986.

(13) Dryden, N. H.; Legzdins, P.; Batchelor, R. J.; Einstein, F. W. B. *Organometallics* **1991**, *10*, 2077.

(14) Our method of preparing PMe_3 is adapted from Wolfsberger, W.; Schmidbaur, H. *Synth. React. Inorg. Met.-Org. Chem.* **1974**, *4*, 149.

(15) Perrin, D. D.; Armarego, W. L. F.; Perrin, D. R. *Purification of Laboratory Chemicals*, 3rd ed., Pergamon Press: Oxford, 1988.

(16) Herring, F. G.; Legzdins, P.; Richter-Addo, G. B. *Organometallics* **1989**, 8, 1485.

(17) Legzdins, P.; Wassink, B. *Organometallics* **1984**, *3*, 1811.

(18) Anderson, R. A.; Wilkinson, G. *Inorg. Synth.* **1979**, *19*, 262.

(19) Dryden, N. H., Ph.D. Dissertation, The University of British Columbia, 1990.

(20) The requisite low-temperature frit for performing this operation is available from Kimble Science Products under the Kontes trademark (product # 215400; p 157 of the 1988 catalog).

(21) If the filtration is conducted using Celite, the product isolated is the isonitrosyl complex, $[CpW(NO)(o\text{-tolyl})_2]_2 \cdot MgCl_2$ (50 - 70 % yield). Anal. Calcd for $C_{38}H_{38}N_2O_2MgCl_2W_2$: C, 44.85; H, 3.76; N, 2.75. Found: C, 44.52; H, 3.97; N, 2.47. In solution this complex behaves as if it were free $CpW(NO)(o\text{-tolyl})_2$.[32]

(22) The work presented in this chapter has been published, see: Dryden, N. H.; Legzdins, P.; Rettig, S. J.; Veltheer, J. E. *Organometallics* **1992**, *11*, 2583.

(23) Veltheer, J. E.; Legzdins, P. In *Handbuch der Präparativen Anorganischen Chemie*, 4th ed.; Herrmann, W. A., Ed.; in press.

(24) (a) Dryden, N. H.; Legzdins, P.; Phillips, E. C.; Trotter, J.; Yee, V. C. *Organometallics* **1990**, *9*, 882. (b) Legzdins, P.; Jones, R. H.; Phillips, E. C.; Yee, V. C.; Trotter, J.; Einstein, F. W. B. *Organometallics* **1991**, *10*, 986. (c) Dryden, N. H.; Legzdins, P.; Trotter, J.; Yee, V. C. *Organometallics* **1991**, *10*, 2857.

(25) Legzdins, P.; Rettig, S. J.; Veltheer, J. E. *J. Am. Chem. Soc.* **1992**, *114*, 6922.

(26) These adducts are recognizable as red-to-brown Et_2O-insoluble materials.

(27) $Cp^*W(NO)(p\text{-tolyl})_2$ and $Cp^*W(NO)Ph_2$ were first prepared by N. H. Dryden,[19] but the methodology employed in this thesis is considerably more reliable and higher yielding.

(28) Gambarotta, S.; Floriani, C.; Chiesi-Villa, A.; Guastini, C. *Inorg. Chem.* **1984**, *23*, 1739 and references cited therein.

(29) Crystals of **2.3** are monoclinic of space group $P2_1/a$; a = 11.570 (2) Å, b = 10.128 (3) Å, c = 18.439 (4) Å, β = 92.50 (2)°; Z = 4. Crystals of **2.6** are monoclinic of space group $P2_1/a$; a = 11.612 (3) Å, b = 10.168 (5) Å, c = 18.250 (3) Å, β = 91.87 (2)°; Z = 4. Dr. Steve Rettig solved both structures using the Patterson method and full-matrix least-squares refinement procedures to R = 0.030, R_w = 0.033 and R = 0.037, R_w = 0.040, for 3387 and 3019 reflections with $I \geq 3\sigma(I)$, respectively.

(30) The solid-state structure of $CpMo(NO)(CD_2CMe_3)_2$ has been determined, see Chapter 5.

(31) Dryden, N. H.; Legzdins, P.; Lundmark, P. J.; Einstein, F. W. B.; Reisen, A. *Organometallics*, in press.

(32) Legzdins, P.; Ross, K. J. unpublished observations.

(33) Evans, S. V.; Legzdins, P.; Rettig, S. J.; Sánchez, L.; Trotter, J. *Organometallics* **1987**, *6*, 7.

(34) Brouwer, E. B., M.Sc. Dissertation, The University of British Columbia, 1992.

CHAPTER 3

Chemistry of $Cp^*Mo(NO)(R)Cl$ and $Cp'Mo(NO)R_2$ [R = alkyl] Complexes: Synthesis and Reactivity of Some Neutral Nitrosyl Lewis Acids

3.1 Introduction

Systems containing transition-metal-carbon σ bonds, especially those with coordinatively and/or electronically unsaturated metal centers, have received the attention of many workers.[1] This fact is due not only to the synthetic utility of such complexes because of their involvement in a variety of stoichiometric and catalytic transformations,[2] but it is also a reflection of the desire of many researchers to continue elucidating the fundamental chemistry of the transition-metal-carbon bond. Our work has centered on the characteristic chemistry of hydrocarbon ligands attached to the 14-valence electron Cp'M(NO) fragments.

In a recent *Account*,[3] we correlated our current knowledge of the *symmetric* 16-electron complexes $Cp'M(NO)R_2$ [R = alkyl, aryl], much of which is described in Chapters 1 and 2. Chapter 3 focuses mainly on related *unsymmetric* species; specifically, this chapter reports four areas of my research. Firstly, the methodology from Chapter 2 is utilized to synthesize a variety of previously inaccessible $Cp'Mo(NO)(alkyl)_2$ complexes. Secondly, that same method allows

straightforward syntheses of $Cp^*Mo(NO)(alkyl)Cl$ complexes which were previously deemed "unsynthesizable" by past members of our group and are the obvious precursors to unsymmetric hydrocarbyl complexes, $Cp^*Mo(NO)(R)R'$. Thirdly, a complete assessment of the relative Lewis acidities (electron deficiencies) of all known $Cp'M(NO)(R)Cl$ and $Cp'M(NO)R_2$ species is presented. The structure/reactivity relationship amongst all known Cp'M(NO)-containing complexes bearing hydrocarbyl ligands is substantiated by spectroscopic, electrochemical, crystallographic and chemical reactivity data. Lastly, the characteristic reactivity of $Cp^*Mo(NO)(CH_2CMe_3)Cl$ is described in detail. This molecule reacts with Lewis bases of many types, silver (I) salts and alkylating (or arylating) agents.

3.2 Experimental Procedures

3.2.1 Methods

The synthetic methodologies employed throughout this thesis are described in detail in section 2.2.1.

3.2.2 Reagents

The organometallic dihalide complexes $Cp'Mo(NO)Cl_2$,[4] were prepared and handled as described in Section 2.2.2. The $(alkyl)_2Mg{\cdot}X(dioxane)$ reagents [R = CH_2CMe_3, CH_2CMe_2Ph, CH_2SiMe_3] were prepared in manner analogous to that described for $(aryl)_2Mg{\cdot}X(dioxane)$ in Section 2.2.4. PMe_3 was prepared as described in Section 2.2.2 and was vacuum transferred from Na/benzophenone. Me_3SiCH_2MgCl (1.0 M in Et_2O, Aldrich) was used as received. Other reagents such as CO (Matheson), $CNCMe_3$, $AgBF_4$ and LDA (Aldrich) were also used as received. Pyridine and acetonitrile (BDH) were twice distilled from CaH_2. Samples of $Cp^*W(NO)(CH_2CMe_3)Cl$ and $Cp^*W(NO)(CH_2CMe_3)_2$ were provided by Jeff D. Debad. THF-d_8 (Aldrich) was used as received. $CDCl_3$ and CD_2Cl_2 (MSD Isotopes) were dried over P_2O_5 and stored in the dark.

The column chromatography material used during this work was alumina (80 - 200 mesh, Fisher neutral, Brockman activity I). Filtrations were performed through Celite 545 diatomaceous earth (Fisher) that had been oven-dried and cooled in vacuo.

3.2.3 Preparation of $CpMo(NO)R_2$ [R = CH_2CMe_2Ph (3.1), CH_2SiMe_3 (3.2)]

The preparation of $CpMo(NO)(CH_2CMe_2Ph)_2$ is given as a representative example of the method used to synthesize both **3.1** and **3.2**. In a glovebox, $CpMo(NO)Cl_2$ (262 mg, 1.00 mmol) and $(PhMe_2CCH_2)_2Mg{\cdot}X$(dioxane) (409 mg, 1.00 mmol) were weighed into a Schlenk tube. THF (20 mL) was then vacuum transferred onto the solids at -196 °C. The stirred reaction mixture was warmed to room temperature over the course of 10 min. The deep red solution (ν_{NO} 1607 cm^{-1}) was then taken to dryness in vacuo. The oily red residue was suspended in Et_2O (40 mL), and transferred to the top of an alumina I neutral column (2 x 2 cm) supported on a medium-porosity frit. The column was washed with Et_2O (2 x 30 mL) until the filtrate was colorless. The filtrate was then taken to dryness and redissolved in pentane (10 mL). Cooling of the pentane solution of **3.1** for several days at -30 °C induced the formation of red crystals of the product (197 mg, 43% yield).

Complex **3.2** (51% yield) was synthesized similarly except Celite was used in place of alumina during the filtration step.

3.2.4 Preparation of $Cp^*Mo(NO)(R)Cl$ [R = CH_2CMe_3 (3.3), CH_2CMe_2Ph (3.4), CH_2SiMe_3 (3.5)]

The preparation of $Cp^*Mo(NO)(CH_2CMe_3)Cl$ (**3.3**) is given as a representative example. $Cp^*Mo(NO)Cl_2$ (332 mg, 1.00 mmol) and $(Me_3CCH_2)_2Mg{\cdot}X$(dioxane) (165 mg, 0.50 mmol) were weighed into a Schlenk tube and the solids were ground to a fine powder with a spatula. THF (40 mL) was then vacuum transferred onto the solids at -196 °C. The stirred reaction mixture was slowly allowed to warm to -45 °C, whereupon the insoluble orange $Cp^*Mo(NO)Cl_2$ was slowly taken into the increasingly purple solution (ν_{NO} 1618 cm^{-1}). When no solid

$Cp^*Mo(NO)Cl_2$ remained in the bottom of the Schlenk tube (2-6 h at -45 °C), the reaction was deemed complete. The reaction mixture was then warmed to -10 °C and the THF was removed in vacuo. The oily purple residue was suspended in pentane (25 mL), stirred for 5 min at room temperature and then taken to dryness to yield a purple powder. The powder was extracted with pentane/Et_2O (4:1, 30 mL), filtered through Celite (2 x 5 cm) and concentrated in vacuo. Cooling of the solution at -30 °C for several days induced the formation of purple needles of **3.3** (203 mg, 55% yield).

For futher reactivity studies, solutions of $Cp^*Mo(NO)(CH_2CMe_3)Cl$ (ca. 90% yield)[5] were used directly after the Celite filtration described in the previous paragraph.

Complexes **3.4** and **3.5** were prepared in a similar manner but substituting the appropriate R_2Mg reagent where necessary. $Cp^*Mo(NO)(CH_2CMe_2Ph)Cl$ forms maroon crystals from hexanes in 64% yield. $Cp^*Mo(NO)(CH_2SiMe_3)Cl$ is a blue-purple oil and has not yet been crystallized.

3.2.5 Preparation of $Cp^*Mo(NO)R_2$ [R = CH_2CMe_3 (3.6), CH_2CMe_2Ph (3.7)]

The $Cp^*Mo(NO)R_2$ complexes were prepared in a manner analogous to that described for their diaryl congeners (Section 2.2.5). The preparation of **3.6** is given as a representative example of the synthetic procedure.

In a glovebox, $Cp^*Mo(NO)Cl_2$ (332 mg, 1.00 mmol) and $(Me_3CCH_2)_2Mg{\cdot}X$(dioxane) (330 mg, 1.00 mmol) were weighed into a Schlenk tube. THF (15 mL) was vacuum transferred onto the solids at -196 °C. The stirred reaction mixture was slowly allowed to warm to 0 °C whereupon the mixture first turned purple then red (ν_{NO} 1588 cm^{-1}). The red reaction mixture was taken to dryness in vacuo. The residue was suspended in Et_2O (30 mL), treated with 2 drops of water and quickly transferred onto a column of alumina I neutral (2 x 3 cm) supported on a glass frit. The column was washed with Et_2O (30 mL) until the eluate was colorless. The ether was then removed from the filtrate to afford a red powder which was dissolved in a minimum of pentane (5 mL). The pentane solution was cooled at -30 °C overnight in a freezer. Large red

crystals of $Cp^*Mo(NO)(CH_2CMe_3)_2$ (240 mg, 59% yield) formed and were isolated by removing the mother liquor via cannulation. Similarily, $Cp^*Mo(NO)(CH_2CMe_2Ph)_2$ (**3.7**) was isolated as red crystals in 70% yield. However, the addition of H_2O was omitted from the procedure leading to **3.7**.

3.2.6 Preparation of $Cp^*Mo(NO)(CH_2SiMe_3)_2$ (3.8)

The procedure outlined below is a significant improvement of the methodology that we employed previously to synthesize this compound.[6] This procedure provided the bulk quantities of complex **3.8** that were required for the chemistry described in Chapter 4.

To a rapidly stirred, brown suspension of $Cp^*Mo(NO)Cl_2$ (4.58 g, 13.8 mmol) in Et_2O (200 mL), maintained at -60 °C, was added Me_3SiCH_2MgCl (27.4 mL of a 1.0 M Et_2O solution, 27.4 mmol) in a dropwise fashion from an addition funnel under a constant purge of Ar. Immediately, the reaction mixture turned purple, and an off-white precipitate slowly formed. The reaction mixture was stirred while the cold bath was permitted to warm slowly to room temperature over 2 h. The final deep purple reaction mixture (ν_{NO} 1593 cm^{-1}) was taken to dryness in vacuo. Under rigorously anaerobic conditions, the remaining lavender solid was suspended in hexanes (50 mL), and the resulting slurry was filtered through Celite (3 x 3 cm). The Celite plug was then rinsed with hexanes (2 x 15 mL). The combined, deep purple filtrates were taken to dryness and extracted with pentane (3 x 15 mL). Cooling of the pentane extracts for 2 days at -30 °C in a freezer induced the deposition of very large (e.g. 10 mm x 5 mm x 2 mm) violet crystals. These crystals (2.55 g) were collected by filtration. Further concentration of the filtrate and cooling afforded a second crop of crystals (1.08 g). Total yield of **3.8** thus obtained was 3.63 g (60%). $Cp^*Mo(NO)(CH_2SiMe_3)_2$ can also be synthesized using $(Me_3SiCH_2)Mg{\cdot}X$(dioxane) as the alkylating reagent, but there is no significant increase in yield.

3.2.7 Preparation of $Cp^*Mo(NO)(CH_2CMe_3)R$ [R = CH_2SiMe_3 (3.9); R = *p*-tolyl (3.10)]

The preparation of **3.9** is representative of the method used for both unsymmetric complexes. $Cp^*Mo(NO)(CH_2CMe_3)Cl$ (262 mg, 0.71 mmol) and $(Me_3SiCH_2)_2Mg{\cdot}X$(dioxane) (92 mg, 0.35 mmol) were weighed into a Schlenk tube. Et_2O (15 mL) was vacuum transferred onto the solids at -196 °C. The stirred reaction mixture was slowly allowed to warm to 0 °C, and the final burgundy mixture was taken to dryness in vacuo. The residue was extracted with pentane (2 x 10 mL), and the combined extracts were filtered through a pad of Celite (2 x 5 cm). The filtrate was taken to dryness in vacuo to obtain **3.9** (123 mg, 41% yield) as an analytically pure red powder.

Similarily, complex **3.10** was isolated as lumps of maroon crystals in 30% yield by crystallization from Et_2O.

3.2.8 Preparation of $Cp^*Mo(NO)(CH_2CMe_3)(Cl)(PMe_3)$ (3.11)

A solution of $Cp^*Mo(NO)(CH_2CMe_3)Cl$ (**3.3**) in Et_2O (10 mL) was generated from $Cp^*Mo(NO)Cl_2$ (1.00 mmol) as described in Section 3.2.4. The purple solution was treated with PMe_3 (excess) which was vacuum transferred from Na/benzophenone. The resulting orange solution was concentrated and cooled for 1 week in a freezer (-30 °C) to obtain **3.11** as large yellow blocks (197 mg, 49% yield).

3.2.9 Preparation of $Cp^*Mo(NO)(CH_2CMe_3)(Cl)(py)$ (3.12)

A sample of $Cp^*Mo(NO)(CH_2CMe_3)Cl$ (184 mg, 0.500 mmol) in Et_2O (10 mL) was treated with pyridine (0.50 mL, excess) at room temperature with no noticeable change in color. Upon cooling to -30 °C, the purple reaction solution turned orange-red, and the desired product began to crystallize. The reaction mixture was stored in a freezer (-30 °C) overnight to complete the crystallization. **3.12** (192 mg, 86% yield) was isolated as orange lumps which were dried in vacuo at low temperature (-10 °C). Prolonged drying at room temperature caused the complex to lose pyridine and darken to the red-purple characteristic of its $Cp^*Mo(NO)(CH_2CMe_3)Cl$ precursor.

3.2.10 Preparation of $Cp^*Mo(NO)(\eta^2\text{-}C\{O\}CH_2CMe_3)Cl$ (3.13)

A sample of $Cp^*Mo(NO)(CH_2CMe_3)Cl$ (188 mg, 0.511 mmol) contained in a 300-mL heavy-walled reaction vessel was dissolved in Et_2O (25 mL). The solution was frozen (-196 °C) and thoroughly degassed via several freeze-pump-thaw cycles. The vessel was charged with CO (2 atm), sealed, and then warmed to room temperature. The reaction solution changed from purple to brown over the course of 4 h at which time the CO pressure and solvent were removed in vacuo. The brown residue was extracted with hexanes/Et_2O (1:2, 85 mL), and the extracts were filtered through Celite (2 x 2 cm). The filtrate was then concentrated and cooled to -30 °C to induce crystallization. Three days later, amber needles of **3.13** (60 mg, 30%) were isolated by removal of the red mother liquor, which was subsequently discarded, since attempts to obtain more pure product from it were unsuccessful.

3.2.11 Preparation of $Cp^*Mo(NO)(\eta^2\text{-}C\{NCMe_3\}CH_2CMe_3)Cl$ (3.14)

In a drybox, a sample of $Cp^*Mo(NO)(CH_2CMe_3)Cl$ (184 mg, 0.500 mmol) contained in a 100-mL reaction vessel was dissolved in Et_2O (10 mL). To the solution was added $CNCMe_3$ (~100 μL, ~0.9 mmol) via a pipette. The unstirred solution instantly changed color from purple to amber. Within seconds the amber solution began to turn bright yellow and a yellow powder precipitated. The reaction vessel was sealed, removed from the drybox, and reattached to a vacuum line. The solvent and excess isocyanide were removed in vacuo. The yellow residue was then dissolved in a minimum of Et_2O (~80 mL) and placed in a freezer to crystallize. Overnight, the desired product crystallized in nearly quantitative yield (212 mg, 95%) as microcrystalline yellow needles. The mother liquor was removed from the product by cannulation, and the remaining needles were dried in vacuo.

3.2.12 Preparation of $[Cp^*Mo(NO)(CH_2CMe_3)(NCMe)]BF_4$ (3.15)

$Cp^*Mo(NO)(CH_2CMe_3)Cl$ (331 mg, 0.900 mmol) and $AgBF_4$ (175 mg, 0.897 mmol) were combined in a Schlenk tube. The tube was cooled to -60 °C and NCMe (10 mL) was slowly

added with a syringe such that it solidified upon entering the tube. The tube and its contents were then warmed to -20 °C, whereupon a color change from purple to red-brown occurred and a white precipitate formed. The precipitate (presumably AgCl) was removed by filtration of the reaction mixture through Celite (2 x 2 cm). The filtrate was then reduced to a brown oil in vacuo. First Et_2O (50 mL) and then pentane (2 x 30 mL) were used to triturate the oil into a tractable yellow powder which was dried in vacuo for 24 h. The powder was dissolved in a minimum of CH_2Cl_2 (~3 mL), and Et_2O (30 mL) was added to the amber solution. Filtration of this solution through Celite (1 x 4 cm) followed by cooling of the filtrate at -60 °C for several hours induced the deposition of **3.15** as irregular orange-yellow crystals (355 mg, 86% yield).

3.2.13 Reaction of $Cp^*Mo(NO)(CH_2CMe_3)(Cl)(PMe_3)$ (3.11) with LDA: Preparation of $(\eta^5,\eta^1\text{-}C_5Me_4CH_2)Mo(NO)(CH_2CMe_3)(PMe_3)$ (3.16)

$Cp^*Mo(NO)(CH_2CMe_3)(Cl)(PMe_3)$ (900 mg, 2.03 mmol) and LDA (220 mg, 2.06 mmol) were combined in a Schlenk tube. THF (25 mL) was vacuum transferred onto the solids at -196 °C. The rapidly stirred reaction mixture was then warmed to room temperature (15 min), and the solvent was removed in vacuo. The oily brown residue was dried in vacuo for 6 h, then suspended in Et_2O (50 mL), and filtered through a column of neutral alumina I (2 x 3 cm). The alumina column was washed with Et_2O until the amber band had been completely eluted. The ether was removed from the filtrate in vacuo, and the remaining yellow residue was extracted with pentane (50 mL). The pentane extraction was filtered through Celite (1 x 2 cm), concentrated and placed in a freezer to induce crystallization. After 1 week at -30 °C, dark amber crystals of complex **3.16** (530 mg, 64% yield) were isolated by removing the mother liquor via cannulation.

3.2.14 Reaction of $Cp^*Mo(NO)(\eta^2\text{-}C\{O\}CH_2CMe_3)Cl$ (3.13) with PMe_3: Generation of $[Cp^*Mo(NO)(C\{O\}\{PMe_3\}CH_2CMe_3)(PMe_3)]Cl$ (3.17)

An NMR tube was charged with a $CDCl_3$ (0.8 mL) solution of complex **3.13** (15 mg). An initial ^1H NMR spectrum was recorded to verify the integrity of the sample.[7] PMe_3 (excess) was then vacuum transferred into the NMR tube. No visible color change occurred. However, a ^1H NMR spectrum of the reaction mixture revealed that all of complex **3.13** had been consumed to form a single product, formulated as $[Cp^*Mo(NO)(C\{O\}\{PMe_3\}CH_2CMe_3)(PMe_3)]Cl$ (**3.17**).

Spectroscopic data for **3.17**: ^1H NMR ($CDCl_3$): δ 2.15 (dd, 1H, CH_2, $^2J_{HH}$ = 15.0 Hz, $^3J_{HP}$ = 6.9 Hz), 1.84 (s, 15H, Cp^*), 1.76 (dd, 9H, PMe_3, $^2J_{HP}$ = 12.9 Hz, $^3J_{PP}$ < 1 Hz), 1.63 (dd, 1H, CH_2, $^2J_{HH}$ = 15.0 Hz, $^3J_{HP}$ = 28.5 Hz), 1.43 (dd, 9H, PMe_3, $^2J_{HP}$ = 9.9 Hz, $^3J_{PP}$ < 1 Hz), 0.84 (s, 9H, C(CH_3)$_3$).

All attempts to isolate the above-mentioned compound were fruitless. For example, removal of the solvent in vacuo yielded a white powder which did not completely redissolve in $CDCl_3$, CD_2Cl_2 or C_6D_6. A ^1H NMR spectrum of the portion that did dissolve revealed the presence of a multitude of compounds, none of which was **3.13** or **3.17**.

3.2.15 Characterization Data for Complexes 3.1 - 3.16

Table 3.1 Numbering Scheme, Color, Yield, and Elemental Analysis Data

complex	compd no.	color (yield, %)	anal. found (calcd)		
			C	H	N
$CpMo(NO)(CH_2CMe_2Ph)_2$	**3.1**	red (43)	65.89 (65.64)	6.84 (6.83)	3.14 (3.06)
$CpMo(NO)(CH_2SiMe_3)_2$	**3.2**	violet (51)	42.60 (42.73)	7.60 (7.39)	4.01 (3.83)
$Cp^*Mo(NO)(CH_2CMe_3)Cl$	**3.3**	violet (55)	48.97 (48.99)	7.05 (7.13)	3.88 (3.81)
$Cp^*Mo(NO)(CH_2CMe_2Ph)Cl$	**3.4**	maroon (64)	55.69 (55.89)	6.71 (6.57)	3.30 (3.26)
$Cp^*Mo(NO)(CH_2SiMe_3)Cl$	**3.5**	blue-violet[a]	[b]		
$Cp^*Mo(NO)(CH_2CMe_3)_2$	**3.6**	red (59)	59.70 (59.54)	9.35 (9.24)	3.50 (3.47)
$Cp^*Mo(NO)(CH_2CMe_2Ph)_2$	**3.7**	red (70)	65.89 (65.64)	6.84 (6.83)	3.14 (3.06)
$Cp^*Mo(NO)(CH_2SiMe_3)_2$	**3.8**	violet (60)	49.74 (49.63)	8.52 (8.57)	3.44 (3.21)
$Cp^*Mo(NO)(CH_2CMe_3)(CH_2SiMe_3)$	**3.9**	red (41)	54.35 (54.40)	8.91 (8.89)	3.25 (3.34)
$Cp^*Mo(NO)(CH_2CMe_3)(p\text{-tolyl})$	**3.10**	maroon (30)	62.38 (62.40)	7.80 (7.85)	3.50 (3.31)
$Cp^*Mo(NO)(CH_2CMe_3)(Cl)(PMe_3)$	**3.11**	yellow (49)	48.89 (48.71)	7.79 (7.95)	3.25 (3.16)
$Cp^*Mo(NO)(CH_2CMe_3)(Cl)(py)$	**3.12**	orange (86)	53.88 (53.76)	7.06 (6.99)	6.48 (6.27)
$Cp^*Mo(NO)(\eta^2\text{-}C\{O\}CH_2CMe_3)Cl$	**3.13**	amber (30)	48.63 (48.56)	6.56 (6.62)	3.43 (3.54)
$Cp^*Mo(NO)(\eta^2\text{-}C\{NCMe_3\}CH_2CMe_3)Cl$	**3.14**	yellow (95)	53.47 (53.28)	7.80 (7.82)	6.27 (6.21)
$[Cp^*Mo(NO)(CH_2CMe_3)(NCMe)]BF_4$[c]	**3.15**	yellow (86)	43.58 (44.37)	6.27 (6.35)	5.57 (6.09)
$(C_5Me_4CH_2)Mo(NO)(CH_2CMe_3)(PMe_3)$	**3.16**	amber (64)	53.04 (53.07)	8.51 (8.41)	3.37 (3.44)

[a] Due to the viscosity of this oil, the yield can only be approximated (~60%).

[b] Due to oily nature of this material, satisfactory elemental analysis could not be obtained.

[c] The difficulty in obtaining satisfactory combustion analysis may be attributed to the formation of CF_4.

Table 3.2 Mass Spectral and Infrared Data

compd	MS	temp[b]	IR (Nujol mull)	
no.	*m/z*[a]	(°C)	ν_{NO}	other bands
3.1	*c*	———	1575 (vs)	———
3.2	367 [P^+]	100	1587 (vs)	———
3.3	*c*	———	1606 (vs)	———
3.4	*c*	———	1606 (vs)	———
3.5	*c*	———	1628 (vs)	1243 (w, $SiMe_3$)
3.6	405 [P^+]	150	1593 (vs)	1235 (w, CMe_3)
3.7	529 [P^+]	100	1594 (vs)	———
3.8	437 [P^+]	100	1595 (vs)	———
3.9	421 [P^+]	120	1599 (vs)	———
3.10	425 [P^+]	150	1611 (vs)	1234 (w, CMe_3)
3.11	387 [$P^+ - CH_2CMe_3$] 369 [$P^+ - PMe_3$]	DCI[d]	1575 (vs)	1233 (w, CMe_3) 958 (m, PMe_3)
3.12	*c*	———	1600 (sh)[e] 1580 (s) 1561 (s)	1223 (w, CMe_3)
3.13	397 [P^+]	180	1601 (vs)	1246 (w, CMe_3) 1624 (s, CO)
3.14	452 [P^+] 422 [$P^+ - NO$]	180	1574 (vs)	1715 (m, CN) 1231 (w, CMe_3)
3.15	462 [P^+]	+ FAB[f]	1606 (vs)	2316, 2290 (NCMe) 1230 (w, CMe_3) 1063 (br, BF_4)
3.16	409 [P^+]	120	1595 (m) 1544 (br)	952 (m, PMe_3)

[a] *m/z* values are for the highest intensity peak of the calculated isotopic cluster (^{98}Mo and ^{184}W).

[b] Probe temperatures.

[c] Decomposes upon warming.

[d] NH_3 carrier.

[e] Which of these three bands is ν_{NO} could not be determined unambiguously.

[f] FAB-MS (matrix: 3-nitrobenzyl alcohol).

Table 3.3 NMR Data (C_6D_6)

compd no.	^{1}H NMR (δ, ppm)	^{13}C{^{1}H} NMR (δ, ppm)
3.1	7.39 (m, 4H, Ph) 7.30 (m, 4H, Ph) 7.17 (m, 2H, Ph) 5.26 (s, 5H, Cp) 4.18 (d, 2H, CH_2, J_{HH} = 9.6 Hz) 1.53 (s, 6H, C(CH_3)$_2$) 1.33 (s, 6H, C(CH_3)$_2$) -0.52 (d, 2H, CH_2, J_{HH} = 9.6 Hz)	152.26 (C_{ipso}) 137.76 (C_{ortho}) 126.00 (C_{meta}) 125.66 (C_{para}) 101.32 (C_5H_5) 96.28 (CH_2) 46.13 (C(CH$_3$)$_2$) 32.36 (C(CH$_3$)$_2$) 32.23 (C(CH$_3$)$_2$)
3.2	5.18 (s, 5H, Cp) 3.11 (d, 2H, CH_2, J_{HH} = 8.7 Hz) 0.35 (s, Si(CH$_3$)$_3$) -0.24 (d, 2H, CH_2, J_{HH} = 9.6 Hz)	101.36 (C_5H_5) 65.96 (CH_2) 2.37 (Si(CH$_3$)$_3$)
3.3	3.73 (d, 1H, CH_2, J_{HH} = 10.8 Hz) 1.44 (s, 15H, Cp*) 1.20 (s, 9H, C(CH_3)$_3$) -0.06 (d, 1H, CH_2, J_{HH} = 10.8 Hz)	113.69 (CH_2) 110.41 (C_5(CH$_3$)$_5$) 40.12 (C(CH$_3$)$_3$) 32.89 (C(CH$_3$)$_3$) 9.86 (C$_5$(CH$_3$)$_5$)
3.3[a]	3.68 (d, 1H, CH_2, J_{HH} = 11.1 Hz) 1.87 (s, 15H, Cp*) 1.15 (s, 9H, C(CH_3)$_3$) 0.11 (d, 1H, CH_2, J_{HH} = 11.1 Hz)	*b*
3.4	7.19 (d, 2H, Ph) 7.09 (d, 2H, Ph) 7.17 (t, 1H, Ph) 4.01 (d, 1H, CH_2, J_{HH} = 9.0 Hz) 1.71 (s, 3H, C(CH_3)$_2$) 1.64 (s, 3H, C(CH_3)$_2$) 1.41 (s, 15H, Cp*) 0.38 (d, 1H, CH_2, J_{HH} = 9.0 Hz)	151.72 (C_{ipso}) 127.51 (C_{ortho}) 126.19 (C_{meta}) 125.90 (C_{para}) 114.09 (CH_2) 110.50 (C_5(CH$_3$)$_5$) 46.74 (C(CH$_3$)$_2$) 31.79 (C(CH$_3$)$_2$) 30.63 (C(CH$_3$)$_2$) 9.74 (C$_5$(CH$_3$)$_5$
3.5	2.61 (d, 1H, CH_2, J_{HH} = 10.5 Hz) 1.94 (d, 1H, CH_2, J_{HH} = 10.5 Hz) 1.51 (s, 15H, Cp*) 0.32 (s, 9H, Si(CH_3)$_3$)	113.73 (C_5(CH$_3$)$_5$) 70.65 (CH_2) 10.01 (C$_5$(CH$_3$)$_5$) 1.65 (Si(CH$_3$)$_3$)
3.6	3.08 (d, 2H, CH_2, J_{HH} = 12.1 Hz) 1.61 (s, 18H, C(CH_3)$_3$) 1.45 (s, 15H, Cp*) -0.95 (d, 2H, CH_2, J_{HH} = 12.1 Hz)	109.78 (C_5(CH$_3$)$_5$) 97.97 (CH_2) 39.05 (C(CH$_3$)$_3$) 33.85 (C(CH$_3$)$_3$) 9.92 (C$_5$(CH$_3$)$_5$)

3.7	7.43 (m, 4H, Ph) 7.20 (m, 4H, Ph) 7.09 (m, 2H, Ph) 3.21 (d, 2H, CH_2, J_{HH} = 10.2 Hz) 1.55 (s, 6H, C(CH_3)$_2$) 1.37 (s, 6H, C(CH_3)$_2$) 1.21 (s, 15H, Cp*) -0.85 (d, 2H, CH_2, J_{HH} = 10.2 Hz)	152.86 (C_{ipso}) 135.20 (C_{ortho}) 126.05 (C_{meta}) 117.62 (C_{para}) 110.01 (C_5(CH$_3$)$_5$) 101.24 (CH_2) 33.53 (C(CH$_3$)$_2$) 31.62 (C(CH$_3$)$_2$) 31.40 (C(CH_3)$_2$) 9.84 (C_5(CH_3)$_5$)
3.8	2.21 (d, 2H, CH_2, J_{HH} = 10.8 Hz) 1.49 (s, 15H, Cp*) 0.37 (s, 18H, Si(CH_3)$_3$) -1.17 (d, 2H, CH_2, J_{HH} = 10.8 Hz)	110.52 (C_5(CH$_3$)$_5$) 66.54 (CH_2) 9.92 (C_5(CH_3)$_5$) 2.56 (Si(CH$_3$)$_3$)
3.9	3.96 (d, 1H, CH_2CMe$_3$, $^2J_{HH}$ = 10.8 Hz) 1.51 (s, 15H, Cp*) 1.33 (s, 9H, CH$_2$C(CH_3)$_3$) 1.19 (d, 1H, CH_2SiMe$_3$, $^2J_{HH}$ = 12.0 Hz, $^2J_{SiH}$ = 19.8 Hz) 0.37 (s, 9H, CH$_2$Si(CH_3)$_3$) -0.67 (d, 1H, CH_2SiMe$_3$, $^2J_{HH}$ = 12.0 Hz, $^4J_{HH}$ = 1.8 Hz) -2.15 (d, 1H, CH_2CMe$_3$, $^2J_{HH}$ = 10.8 Hz, $^4J_{HH}$ = 1.8 Hz)	118.78 (CH_2CMe$_3$) 110.06 (C_5(CH_3)$_5$) 46.21 (CH_2SiMe$_3$) 40.86 (C(CH$_3$)$_3$) 33.43 (C(CH$_3$)$_3$) 9.96 (C_5(CH_3)$_5$) 2.57 (Si(CH$_3$)$_3$)
3.10	7.71 (d, 2H, H_{aryl}, J_{HH} = 7.8 Hz) 7.14 (d, 2H, H_{aryl}, J_{HH} = 7.8 Hz) 4.67 (d, 1H, CH_2, $^2J_{HH}$ = 9.0 Hz) 2.22 (s, 3H, p-CH_3) 1.57 (s, 15H, Cp*) 1.28 (s, 9H, C(CH_3)$_3$) -1.55 (d, 1H, CH_2, $^2J_{HH}$ = 9.0 Hz)	*b*
3.11[c]	2.30 (dd, 1H, CH transoidal to P, J_{HH} = 9.6 Hz, J_{HP} = 3.3 Hz) 1.79 (s, 9H, C(CH_3)$_3$) 1.69 (s, 15H, Cp*) 1.53 (d, 1H, CH cisoidal to P, J_{HH} = 9.6 Hz) 1.32 (d, 9H, P(CH_3)$_3$, J_{HP} = 9.6 Hz)	109.79 (C_5(CH_3)$_5$) 64.70 (d, CH_2, J_{CP} = 7.3 Hz) 38.50 (C(CH$_3$)$_3$) 35.16 (C(CH$_3$)$_3$) 12.42 (d, P(CH_3)$_3$, J_{CP} = 26.6 Hz) 9.75 (C_5(CH_3)$_5$)
3.12[d]	8.98 (br s, 2H, NC$_5H_5$) 8.04 (br s, 1H, NC$_5H_5$) 7.61 (br s, 2H, NC$_5H_5$) 2.08 (br s, 1H, CH_2) 1.53 (br s, 15H, Cp*) 1.10 (br s, 9H, C(CH_3)$_3$) 0.49 (br s, 1H, CH_2)	*b*
3.13	3.08 (d, 1H, CH_2, J_{HH} = 15.5 Hz) 2.62 (d, 1H, CH_2, J_{HH} = 15.5 Hz) 1.61 (s, 15H, Cp*) 0.91 (s, 9H, C(CH_3)$_3$)	280.66 (CO) 112.97 (C_5(CH_3)$_5$) 54.34 (CH_2) 33.08 (C(CH$_3$)$_3$) 29.64 (C(CH$_3$)$_3$) 10.10 (C_5(CH_3)$_5$)

3.14	3.00 (d, 2H, CH_2, J_{HH} = 18.0 Hz) 2.57 (d, 2H, CH_2, J_{HH} = 18.0 Hz) 1.64 (s, 15H, Cp*) 1.33 (s, 9H, $NC(CH_3)_3$) 1.00 (s, 9H, $CH_2C(CH_3)_3$)	*b*
3.15[f]	2.50 (s, 3H, CH_3CN) 1.80 (s, 15H, Cp*) 1.30 (d, 1H, CH_2, J_{HH} = 10.5 Hz) 1.08 (s, 9H, $C(CH_3)_3$) 0.70 (d, 1H, CH_2, J_{HH} = 10.5 Hz)	CH_3CN not observed 113.67 ($C_5(CH_3)_5$) 66.52 (CH_2) 38.80 ($C(CH_3)_3$) 34.25 ($C(CH_3)_3$) 9.31 ($C_5(CH_3)_5$) 4.29 (CH_3CN)
3.16[c,e]	2.88 (vt, 1H, $C_5Me_4CH_2$, J = 3.0 Hz) 2.72 (dd, 1H, $C_5Me_4CH_2$, J = 3.0, 13.2 Hz) 1.93 (d, 3H, Me, J = 2.4 Hz) 1.73 (d, 3H, Me, J = 3.3 Hz) 1.69 (s, 3H, Me) 1.40 (d, 9H, $P(CH_3)_3$, J_{HP} = 7.8 Hz) 1.17 (d, 3H, Me, J_{HP} = 3.6 Hz) 0.99 (s, 9H, $C(CH_3)_3$) 0.87 (m, 1H, CH_2CMe_3) 0.34 (d, 1H, CH_2CMe_3, J = 12.9 Hz)	131.00 ($C_5Me_4CH_2$) 110.16 ($C_5Me_4CH_2$) 108.36 ($C_5Me_4CH_2$) 107.29 (d, $C_5Me_4CH_2$, J_{CP} = 8.0 Hz) 104.36 ($C_5Me_4CH_2$) 64.85 (d, CH_2CMe_3, J_{CP} = 6.5 Hz) 53.94 ($C_5Me_4CH_2$, J_{CP} = 10.4 Hz) 39.26 (d, CH_2CMe_3, J_{CP} = 14.2 Hz) 35.19 ($C(CH_3)_3$) 16.76 (d, $P(CH_3)_3$, J_{CP} = 25.0 Hz) 12.82 (d, $C_5(CH_3)_4CH_2$, J_{CP} = 26.8 Hz) 11.20 ($C_5(CH_3)_4CH_2$, J_{CP} = 19.5 Hz) 9.92 ($C_5(CH_3)_4CH_2$) 9.02 ($C_5(CH_3)_4CH_2$, J_{CP} = 30.7 Hz)
3.16	2.83 (vt, 1H, $C_5Me_4CH_2$, J = 2.7 Hz) 2.49 (dd, 1H, $C_5Me_4CH_2$, J = 2.7, 13.2 Hz) 1.82 (s, 3H, Me) 1.81 (s, 3H, Me) 1.49 (s, 3H, Me) 1.40 (s, 9H, $C(CH_3)_3$) 1.07 (d, 1H, CH_2CMe_3, J = 12.9 Hz) 0.98 (d, 9H, $P(CH_3)_3$, J_{HP} = 7.8 Hz) 0.95 (d, 3H, Me, J_{HP} = 3.6 Hz) 0.48 (dd, 1H, CH_2CMe_3, J = 12.9, 1.2 Hz)	*b*

[a] In THF-d_8 (provided for comparison to low-temperature spectrum of complex **3.12**).

[b] Not recorded.

[c] ^{31}P NMR (δ, ppm): **3.11** = 6.38 (s); **3.16** = -2.89 (s).

[d] In THF-d_8 at -100 °C.

[e] In $CDCl_3$.

[f] In CD_2Cl_2.

Table 3.4 Electrochemical Data for the First Reductions of $Cp^*M(NO)Cl_2$, $Cp^*M(NO)(CH_2CMe_3)Cl$, and $Cp^*M(NO)(CH_2CMe_3)_2$.[a]

complex	scan rate (ν, Vs^{-1})	$E^{\circ\prime}{}_1$[b] (mV)	ΔE[c]	$i_{p,a}/i_{p,c}$[d]
$Cp^*Mo(NO)Cl_2$	1.0	-350	194 (171)	1.0
	0.6	-350	162 (136)	1.0
	0.2	-350	113 (94)	1.0
$Cp^*Mo(NO)(CH_2CMe_3)Cl$	1.0	-970	207 (230)	1.0
	0.6	-960	172 (188)	1.0
	0.2	-970	125 (132)	0.9
$Cp^*Mo(NO)(CH_2CMe_3)_2$				
	1.0	~ -1590	510 (186)	0.7
$Cp^*W(NO)Cl_2$	1.0	-750	234 (167)	1.0
	0.6	-750	178 (136)	1.0
	0.2	-740	116 (109)	1.0
$Cp^*W(NO)(CH_2CMe_3)Cl$	8.0	~ -1220	550	0.7
	4.0	~ -1220	360	0.6
	1.0	~ -1210	170	0.4
$Cp^*W(NO)(CH_2CMe_3)_2$	1.0	-1720	310 (167)	0.9
	0.6	-1700	250 (136)	0.8
	0.2	-1680	180 (109)	0.8

[a] In THF containing 0.10 M [n-Bu_4N]PF_6, at a Pt-bead working electrode. Potentials are measured vs SCE.

[b] Defined as the average of the cathodic and anodic peak potentials.

[c] Defined as the separation of the cathodic and anodic peak potentials. Values in brackets are for the Cp_2Fe/Cp_2Fe^+ couple under identical experimental conditions.

[d] Ratio of anodic peak current to cathodic peak current.

3.3 Results and Discussion

3.3.1 Alkylations of Cp'Mo(NO)Cl_2 Complexes

Since the methodology described in Chapter 2 was successful for the preparation of Cp'M(NO)(aryl)$_2$ complexes, I decided to extend the scope of the methodology to include three hitherto unknown Cp'Mo(NO)(alkyl)$_2$ complexes. Additionally, the preparations of the known complexes CpMo(NO)(CH_2SiMe_3)$_2$ and Cp*Mo(NO)(CH_2SiMe_3)$_2$ have been markedly improved, both in terms of yields and reproducibility, by employing this methodology. Also as a direct result of this study, three Cp*Mo(NO)(alkyl)Cl complexes, which had previously been thought to be inaccessible, were prepared in a single synthetic procedure. These complexes led in turn to the synthesis and isolation of mixed alkyl and alkyl aryl complexes of Mo.

3.3.1.1 Synthesis of Cp'Mo(NO)(alkyl)$_2$ Complexes

Five complexes of this type have been prepared in a straightforward manner. The Cp'Mo(NO)(CH_2SiMe_3)$_2$ complexes were previously known, but could not be reliably prepared.[6,8] As discussed in Chapter 1, several factors were responsible for this lack of reproducibility. Of these, the major reason was the use of water in the original preparation of these complexes. The use of water is unnecessary with the alkylating agents containing dioxane ligands, and thus the preparation of the moisture-sensitive Mo dialkyl complexes is not problematic. Since Cp*Mo(NO)(CH_2CMe_3)$_2$ reacts slowly with water, small quantities can be used during its synthesis to optimize the yield of this complex. As a group, the Mo dialkyl complexes are extremely air-sensitive, converting to a variety of oxo-containing species when exposed to the atmosphere (Chapter 4).[9] All five complexes are thermally sensitive. As solids they decompose within months of storage under argon at -30 °C. The neopentyl and neophyl complexes (**3.1**, **3.6**, **3.7**) can be chromatographed on neutral alumina I. The trimethylsilylmethyl complexes (**3.2**, **3.8**) are not very stable to alumina. Accordingly, they are best purified by filtration through Celite.

The spectroscopic properties of the dialkyl complexes prepared in this chapter are very similar to those exhibited by their W congeners.[6,8,10,11]

3.3.1.2 Synthesis of Cp*Mo(NO)(alkyl)Cl Complexes

For many years our group had been unable to synthesize the 16-electron Cp'W(NO)(R)X [R = alkyl, aryl; X = I, Cl] complexes from their dihalide precursors. The reason that all previous attempts to prepare Cp'W(NO)(R)X compounds failed is because, under the various reaction conditions employed,[12] any such complexes formed react with the alkylating agent present in solution faster that Cp'W(NO)X_2 (vide infra). Indeed, only recently did we communicate the preparation of Cp*W(NO)(CH_2SiMe_3)Cl from Cp*W(NO)(CH_2SiMe_3)$_2$ (eq 3.1), albeit via a somewhat indirect route.[13]

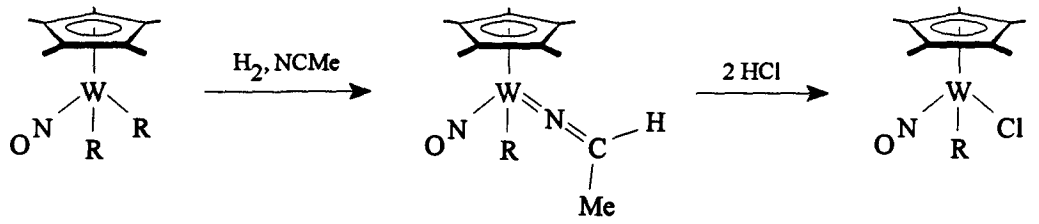

(3.1)

R = CH_2SiMe_3

However, this route is not particularly appealing synthetically, since the overall yield of Cp*W(NO)(CH_2SiMe_3)Cl from Cp*W(NO)Cl_2 suffers from the number of transformations involved (30% overall for 3 steps). Knowing that Cp*W(NO)(CH_2SiMe_3)Cl is inherently stable, I was convinced that it was our previous methodology rather than any intrinsic instability that had thwarted attempts to prepare *mono*(hydrocarbyl) species. Application of the method used to synthesize Cp*M(NO)(aryl)$_2$ complexes (Chapter 2) to their preparation is a much more efficient route to these compounds. The reaction leading to Cp*Mo(NO)(alkyl)Cl is portrayed in eq 3.2.

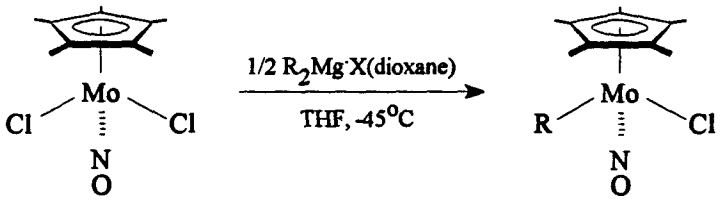

(3.2)

R = CH_2CMe_3 (**3.3**); CH_2CMe_2Ph (**3.4**); CH_2SiMe_3 (**3.5**)

Control of reaction temperature is extremely critical for the success of reaction 3.2. For example, above -45 °C, $Cp^*Mo(NO)(CH_2CMe_3)Cl$ (**3.3**) is reactive with $(Me_3CCH_2)_2Mg{\cdot}X$(dioxane), giving $Cp^*Mo(NO)(CH_2CMe_3)_2$ and unused starting material. Since $Cp^*Mo(NO)Cl_2$ is nearly insoluble in cold THF, extended reaction times in dilute solution (40 mL/mmol) are required to achieve solutions of $Cp^*Mo(NO)(CH_2CMe_3)Cl$ uncontaminated by $Cp^*Mo(NO)(CH_2CMe_3)_2$. It should be noted that it is nearly impossible to isolate pure monoalkylated products from mixtures of the mono- and dialkyl complexes. However, it is easy to perform the reverse separation since the monoalkyl complex is unstable to alumina and the dialkyl complex is chromatographable. Finally, it is also important to note that the $Cp^*Mo(NO)Cl_2$ starting material must be highly purified in order to obtain clean, stoichiometric metathesis.[14]

Since the reactivity of $Cp^*Mo(NO)(CH_2CMe_3)Cl$ (**3.3**) forms a large portion of this chapter, a solution of the complex was often generated in situ, filtered to remove $MgCl_2$·dioxane, and the next solvent or reagent was added directly. Typical yields of solutions of **3.3** generated in this manner are about 90%.[5]

The solid-state structure of $Cp^*W(NO)(CH_2SiMe_3)Cl$ is that of a three-legged, monomeric piano-stool,[13] and there is no reason to believe that any of the Mo monoalkyl complexes (**3.3 - 3.5**) are anything but monomeric. Thus, in solution and the solid-state, they are deep purple, maroon or blue and exhibit strong ν_{NO} bands in their Nujol mull IR spectra (1628 - 1606 cm^{-1}) in the same energy range (1650 - 1550 cm^{-1}) as their monomeric dialkyl and diaryl analogues. The ^1H NMR spectra of **3.3 - 3.5** (Table 3.3) are also consistent with their formulations. The spectra display two doublets attributable to the diastereotopic methylene protons of the alkyl groups at

markedly different chemical shifts indicative of their substantially different magnetic environments in the three-legged piano-stool, i.e. one proton is close to the Cl ligand and the other is close to the nitrosyl ligand. For example, the methylene protons of the **3.3** resonate at δ 3.73 and -0.06 ppm in C_6D_6 ($^2J_{HH}$ = 10.8 Hz) (Figure 3.1(a)).

Complex **3.3** is moderately thermally sensitive (more so than its analogues **3.4** or **3.5**). In the solid state it decomposes uncleanly to a brown oil over the course of several weeks, as evidenced by ^{1}H NMR spectroscopy. However, in benzene, the thermal decomposition (8 h at 100 °C or 6 - 10 weeks at room temperature) is much cleaner (Figure 3.1(b)).

From the spectrum in Figure 3.1(b), it is clear that **3.3** has undergone some sort of isomerization since all resonances from Figure 3.1(a) remain, but are found at different chemical shifts.[15] The structure of the thermolysis product remains a mystery, since the complex can only be described as an oily film that is completely resistant to crystallization from Et_2O, CH_2Cl_2, benzene, toluene or THF or typical combinations of these solvents. Interestingly, the IR spectrum of the complex exhibits no band in the region 2000-1500 cm^{-1} that would be expected for a terminal nitrosyl ligand.

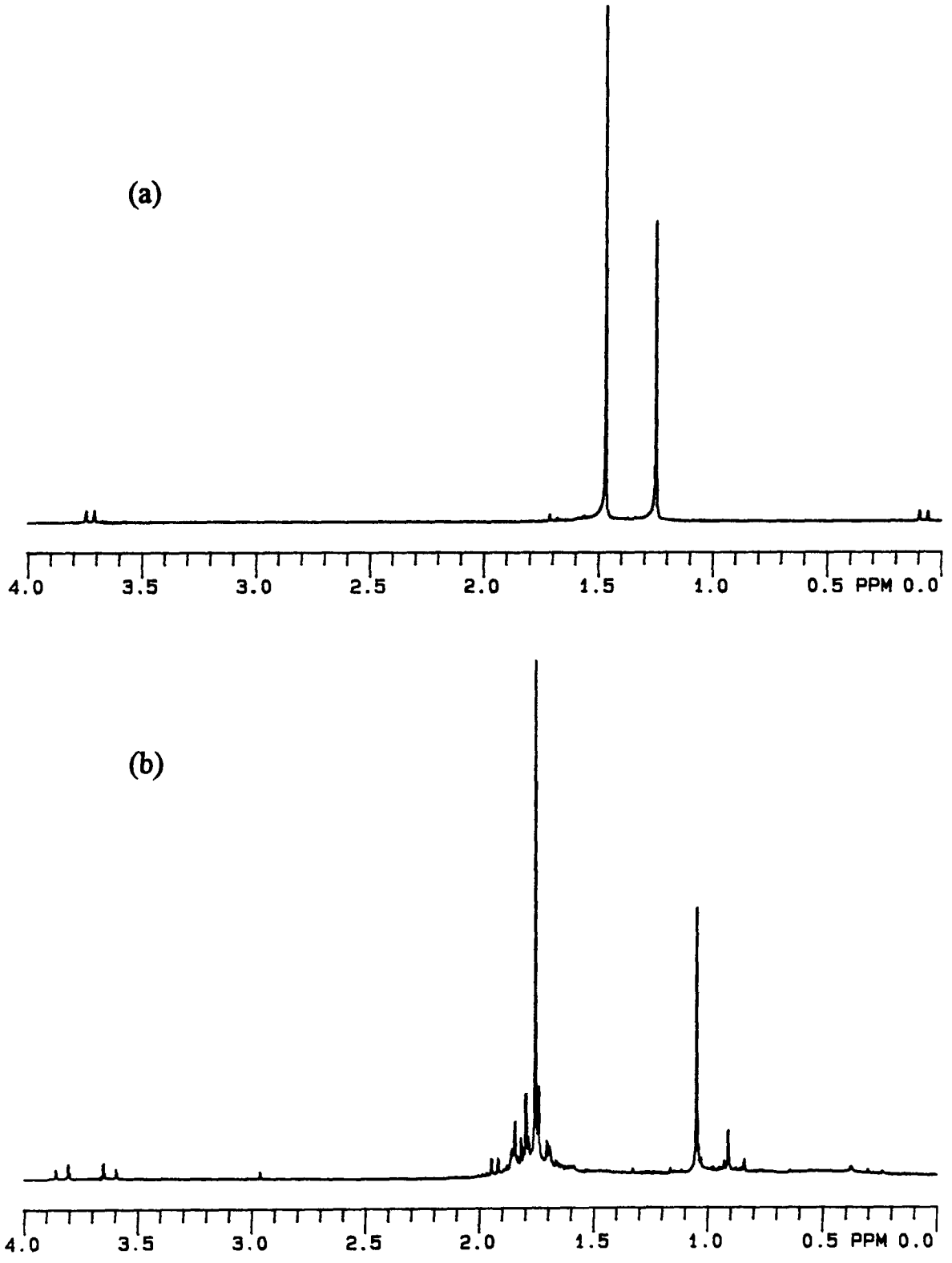

Figure 3.1 300 MHz ^{1}H NMR spectra (C_6D_6) of (a) complex **3.3** at room temperature; (b) complex **3.3** after 8 h at 100 °C

3.3.1.3 Synthesis of $Cp^*Mo(NO)(CH_2CMe_3)R$ Complexes [R = alkyl (3.9), *p*-tolyl (3.10)]

Using the methodology described in this Chapter, Jeff Debad of our group recently synthesized a family of asymmetric bis(hydrocarbyl) complexes of tungsten.[16] Not unexpectedly, analogous Mo complexes can be prepared as well. Using similar methodology to that which provided us with diaryl complexes of Mo and W (Chapter 2), $Cp^*Mo(NO)(CH_2CMe_3)$(alkyl) and $Cp^*Mo(NO)(CH_2CMe_3)$(aryl) complexes are preparable (eq 3.3).

$$Cp^*Mo(NO)(CH_2CMe_3)Cl + 1/2\ R_2Mg \xrightarrow[0\,^oC]{THF} Cp^*Mo(NO)(CH_2CMe_3)R \qquad (3.3)$$

$$R = CH_2SiMe_3\ (\mathbf{3.9}),\ p\text{-tolyl}\ (\mathbf{3.10})$$

As one might expect, the nitrosyl-stretching frequencies of the mixed complexes are essentially the average of their symmetric congeners (vide infra, Section 3.3.2.2). The ^1H NMR spectrum of $Cp^*Mo(NO)(CH_2CMe_3)(CH_2SiMe_3)$ (Figure 3.2) shows some interesting features. First, all four methylene protons of **3.9** are magnetically inequivalent and thus appear as four separate resonances. Two of the resonances (δ 3.96 and -2.15 ppm) show $^2J_{HH}$ couplings of 10.8 Hz and are assigned to CH_2CMe_3. The other two resonances (δ 1.19 and -0.67 ppm) show $^2J_{HH}$ couplings of 12.0 Hz and are assigned to CH_2SiMe_3. Second, one of each of these sets of resonances (δ -0.67 and -2.15 ppm) shows additional $^4J_{HH}$ couplings of 1.8 Hz. The observation of these long-range couplings is attributed to a phenomenon called "W" coupling in organic chemistry.[17] In organic compounds when 4 bonds lie in a plane and align themselves in the conformation of a W, $^4J_{HH}$ couplings can be observed. The arrangement of the two alkyl groups in complex **3.9** must therefore be similar to that shown below.

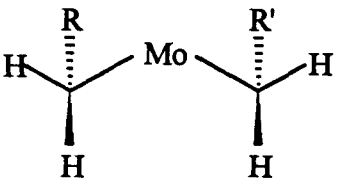

$$R = CMe_3;\ R' = SiMe_3$$

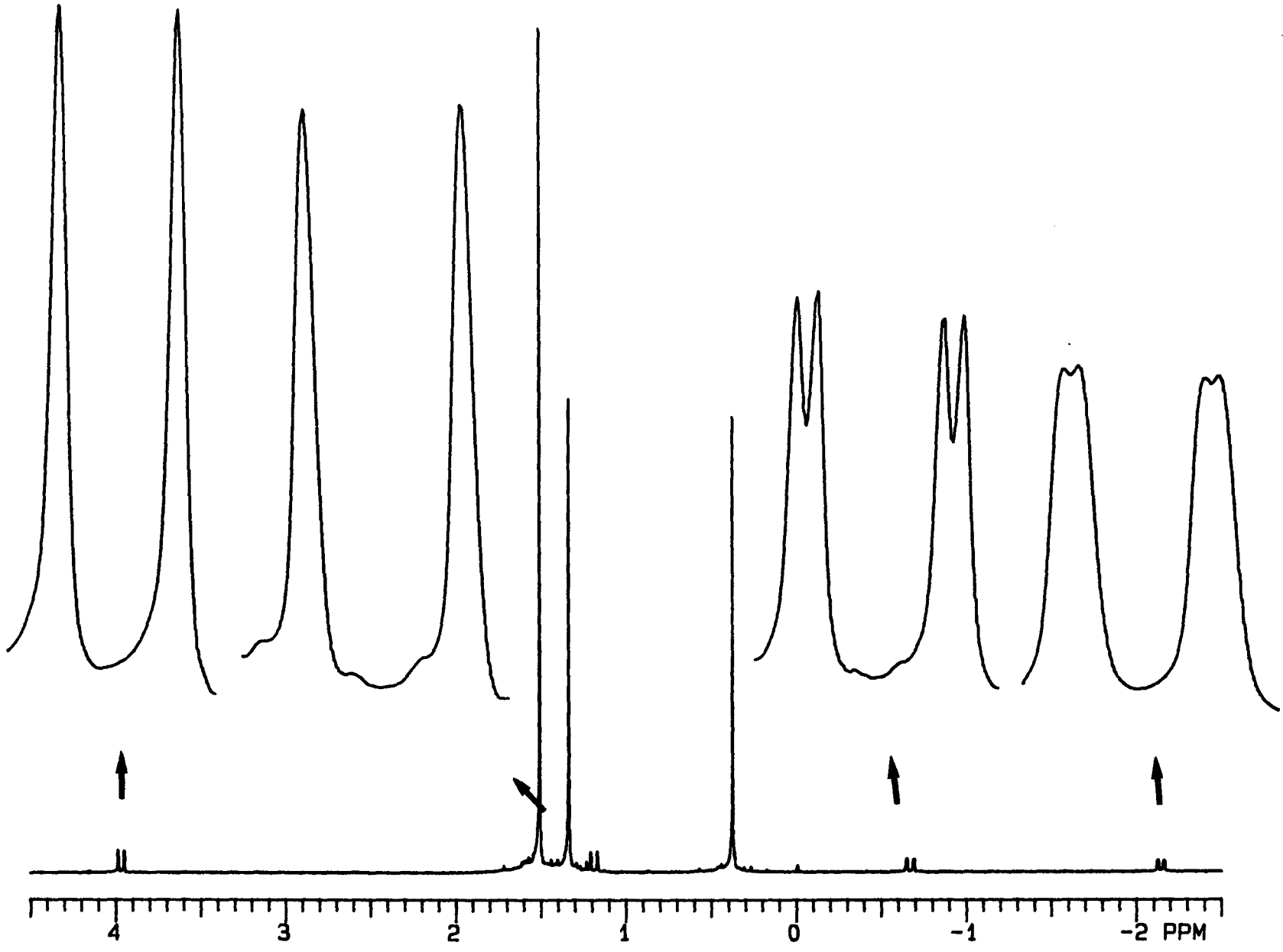

Figure 3.2 300 MHz ^{1}H NMR spectrum of $Cp^*Mo(NO)(CH_2CMe_3)(CH_2SiMe_3)$ **3.9** in C_6D_6

3.3.2 Electrochemical and Infrared Studies: Assessment of Relative Lewis Acidity

The existence of vacant, metal-centered orbitals on 16-electron Cp'M(NO)-containing compounds imparts Lewis-acid characteristics to these materials. In previous work,[3,18,20] it has been found that virtually all $Cp'M(NO)X_2$ [X = I, Br, Cl] and $Cp'M(NO)R_2$ [R = alkyl, aryl] complexes exhibit IR nitrosyl-stretching frequencies which correlate with the relative electron density at the metal centers in these 16-electron species (Section 1.1). Additionally, these complexes exhibit reversible electrochemical reductions in THF or CH_2Cl_2, features attributable to the non-bonding natures of the LUMOs in these species, that are also directly proportional to the electron density at their metal centers. In this section, a correlation of a wide variety of experimental observations is used to establish a structure/reactivity relationship amongst the various Cp'M(NO)-containing compounds prepared in this thesis. Under any criterion used (apparent size of coordination site (Section 2.3.5), nitrosyl-stretching frequency or reduction potential), Cp, Mo and aryl complexes are respectively better Lewis acids than related Cp^*, W and alkyl complexes, without exception.

3.3.2.1 The $Cp^*M(NO)Cl_2$-to-$Cp^*M(NO)(CH_2CMe_3)Cl$-to-$Cp^*M(NO)(CH_2CMe_3)_2$ Series

The Mo and W series of compounds $Cp^*M(NO)Cl_2$, $Cp^*M(NO)(CH_2CMe_3)Cl$ and $Cp^*M(NO)(CH_2CMe_3)_2$ are compared using both IR spectroscopy and electrochemistry in Table 3.5. More detailed electrochemical results are located in Table 3.4 (Section 3.2.15).

Table 3.5 Comparative IR and Electrochemical Data (THF)

compd	ν_{NO} (cm^{-1})	$E^{\circ\prime}_1$ (mV vs SCE at 1.0 V/s)
$Cp^*Mo(NO)Cl_2$	1655	-350[a]
$Cp^*W(NO)Cl_2$	1630	-750[a]
$Cp^*Mo(NO)(CH_2CMe_3)Cl$ (**1**)	1618	-960[a]
$Cp^*W(NO)(CH_2CMe_3)Cl$ (**1'**)	1595	-1210[b]
$Cp^*Mo(NO)(CH_2CMe_3)_2$ (**2**)	1588	-1590[b]
$Cp^*W(NO)(CH_2CMe_3)_2$ (**2'**)	1568	-1700[c]

[a] Reversible.
[b] Quasi-reversible.
[c] Reversible at high scan rates, otherwise quasi-reversible.

As evidenced by the data in Table 3.5, replacement of electronegative chloride ligands with neopentyl groups causes significant shifts in ν_{NO} to lower energy and increases in reduction potential ($E^{\circ\prime}$) to more negative potentials. Consequently, it can be concluded that the metal centers in $Cp^*M(NO)(CH_2CMe_3)_2$ are more electron-rich than their mononeopentyl and dichloride precursors. Additionally, in comparing each of the three pairs of compounds, the W complex *always* exhibits the lower ν_{NO} (average of 23 cm^{-1}) and the more negative reduction potential (by 400, 260 and 110 mV) than its corresponding Mo analogue.

Of the six complexes studied, $Cp^*Mo(NO)(CH_2CMe_3)_2$ and $Cp^*W(NO)(CH_2CMe_3)Cl$ exhibit quasi-reversible reductions in THF. For example, at a scan rate of 1.0 V/s $Cp^*Mo(NO)(CH_2CMe_3)_2$ exhibits a reduction wave ($i_{p,a}/i_{p,c} = 0.7$), having ΔE almost three times that of ferrocene; in contrast, a scan rate of 8.0 V/s is required to achieve a reduction wave with $i_{p,a}/i_{p,c} = 0.7$ for $Cp^*W(NO)(CH_2CMe_3)Cl$. Additionally, $Cp^*W(NO)(CH_2CMe_3)_2$ exhibits a reduction wave that approaches reversibility at high scan rates, but is quasi-reversible at low scan rates (Table 3.4).[19] The other three complexes studied exhibit completely reversible reductions as would be expected on the basis of previous studies[20] and calculations.[21] A representative cyclic voltammogram of $Cp^*Mo(NO)(CH_2CMe_3)Cl$ is shown in Figure 3.3.

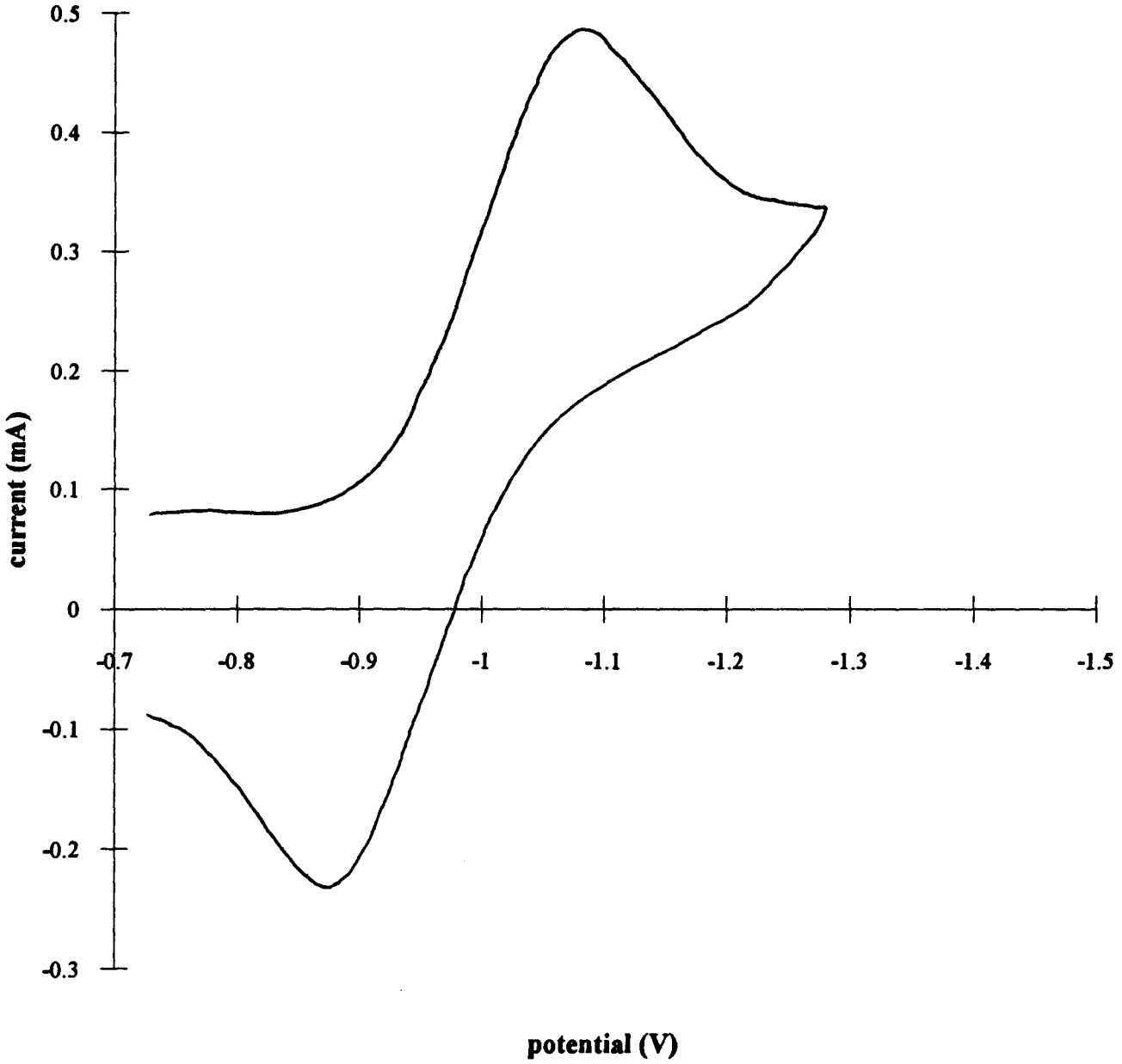

Figure 3.3 Ambient temperature cyclic voltammogram of $Cp^*Mo(NO)(CH_2CMe_3)Cl$ in THF (scan rate = 1 Vs^{-1})

The general conclusion to emanate from the IR data and the electrochemical reduction potentials is that the Mo complexes are more electron-deficient than their W partners. This increased electron-deficiency at the metal is manifested in the higher reactivity of Mo nitrosyl complexes of this type. We have previously determined that $Cp^*M(NO)(aryl)_2$ complexes are better Lewis acids than their $Cp^*M(NO)(alkyl)_2$ congeners due to the increased electron-withdrawing ability of aryl groups (Chapter 2). $Cp^*M(NO)(aryl)_2$ complexes also show a similar trend in reactivity with the more electron-deficient complexes being more reactive.[20] This study indicates that $Cp^*M(NO)(CH_2CMe_3)Cl$ complexes are comparable in electron-deficiency to related $Cp^*M(NO)(aryl)_2$ complexes for both the Mo and W systems. For example, the nitrosyl-stretching frequency of $Cp^*Mo(NO)(Ph)_2$[20] in THF is 1618 cm^{-1}, only 3 wavenumbers higher than that for $Cp^*Mo(NO)(CH_2CMe_3)Cl$. From an electrochemical standpoint, the reduction potential of $Cp^*W(NO)(p\text{-tolyl})_2$[20] in THF is -1210 mV and that of $Cp^*W(NO)(CH_2CMe_3)Cl$ is a comparable -1220 mV.

3.3.2.2 The $Cp^*Mo(NO)(CH_2CMe_3)_2$-to-$Cp^*Mo(NO)(CH_2CMe_3)(p\text{-tolyl})$-to-$Cp^*Mo(NO)(p\text{-tolyl})_2$ Series

$Cp^*Mo(NO)(CH_2CMe_3)(p\text{-tolyl})$ (**3.10**) exhibits a ν_{NO} band at 1600 cm^{-1} in its THF IR spectrum. Similar spectra of **3.10**'s symmetric analogues, $Cp^*Mo(NO)(CH_2CMe_3)_2$ (**3.6**) and $Cp^*Mo(NO)(p\text{-tolyl})_2$ (**2.2**) exhibit ν_{NO} bands at 1609 and 1588 cm^{-1}, respectively, the average of which is 1598.5 cm^{-1} (1.5 cm^{-1} less than that observed for **3.10**). Two other series of nitrosyl-stretching frequencies add to this argument. The mean ν_{NO} value (THF) of $Cp^*Mo(NO)Cl_2$ (1655 cm^{-1}) and $Cp^*Mo(NO)(CH_2CMe_3)_2$ (1588 cm^{-1}) is 1621.5 cm^{-1}. The measured value of ν_{NO} for $Cp^*Mo(NO)(CH_2CMe_3)Cl$ is 1618 cm^{-1}. Similarily, the mean ν_{NO} value of $Cp^*W(NO)Cl_2$ (1630 cm^{-1}) and $Cp^*Mo(NO)(CH_2CMe_3)_2$ (1568 cm^{-1}) is 1599 cm^{-1}, 4 cm^{-1} more than the value of 1595 cm^{-1} observed for $Cp^*W(NO)(CH_2CMe_3)Cl$.

3.3.2.3 Further Comparisons

Scheme 3.1 shows a typical set of related complexes compared to $Cp^*W(NO)(CH_2CMe_3)_2$. Changing the Cp^* ring to Cp causes an increase in ν_{NO} (19 cm^{-1}) and a drop in E° (230 mV). Similarly, changing the metal from W to Mo causes an increase in ν_{NO} (20 cm^{-1}) and a drop in E° (110 mV). Lastly, changing both alkyl groups for aryl ligands also causes an increase in ν_{NO} (14 cm^{-1}) and a drop in E° (490 mV). Clearly, all three complexes in these comparisons are more electron-deficient than $Cp^*W(NO)(CH_2CMe_3)_2$.

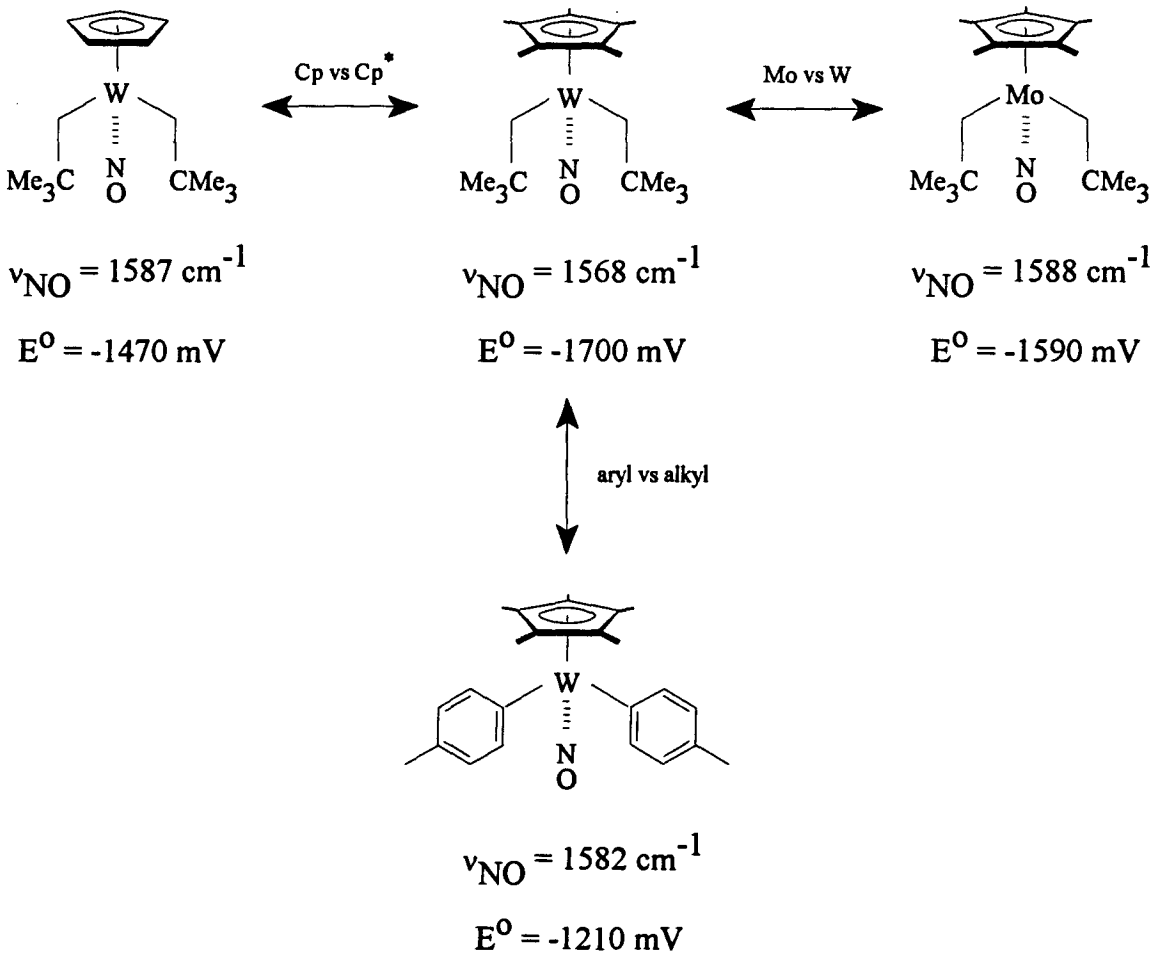

Scheme 3.1 IR and electrochemical comparisons (THF) of pairs of 16-electron organometallic nitrosyl complexes differing only in one component of their respective structures (i.e. Cp vs Cp^*, Mo vs W, aryl vs alkyl)

3.3.3 Reactivity of $Cp^*Mo(NO)(CH_2CMe_3)Cl$

The reactivity of $Cp^*Mo(NO)(CH_2CMe_3)Cl$ (**3.3**), described in this section is part of a companion study of the characteristic chemistry of both the Mo and W chloro neopentyl complexes.[22] Compounds (**3.11 - 3.14, 3.16**) have isostructural tungsten analogues that were prepared by Jeff Debad of our group. As expected, the chloro neopentyl complex **3.3** is more reactive than its W congener.

3.3.3.1 Formation of 1:1 Adducts: Reactions With Pure Lewis Bases

Like related 16-electron bis(hydrocarbyl) nitrosyl complexes, the mononeopentyl complex prepared in this work is very reactive towards Lewis bases.[8,20] The coordinative and electronic unsaturation of the metal center in $Cp^*Mo(NO)(CH_2CMe_3)Cl$ (**3.3**) is satisfied by coordination of a Lewis base. For example, the addition of PMe_3 to a solution of $Cp^*Mo(NO)(CH_2CMe_3)Cl$ causes an immediate color change from purple to yellow and formation of the metal-centered 1:1 adduct (**3.11**) (eq 3.4).

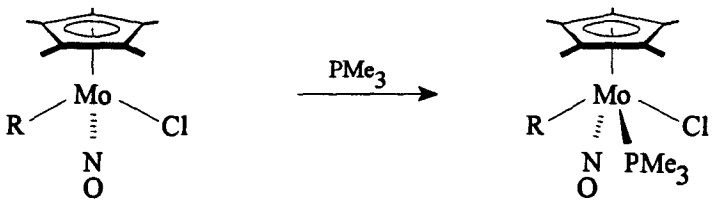

(3.4)

$R = CH_2CMe_3$

The ^1H NMR spectrum (Figure 3.4) of the 18-electron phosphine adduct is diagnostic of a 4-legged piano-stool molecular structure having the PMe_3 ligand trans to the nitrosyl group. A Newman projection of this molecule depicts the stereochemical scenario (Figure 3.4 inset). The methylene protons of the alkyl group are positioned such that H_A is transoidal to the P nucleus ($^3J_{HP}$ = 3.3 Hz) and H_B is cisoidal to the P nucleus ($^3J_{HP}$ = 0 Hz). Since MO calculations and X ray crystallographic analyses have indicated that the vacant coordination site in all 16-electron Cp'M(NO)(Y)(Z) [Y, Z = 1-electron-donor ligand] complexes is trans to the NO ligand it is not

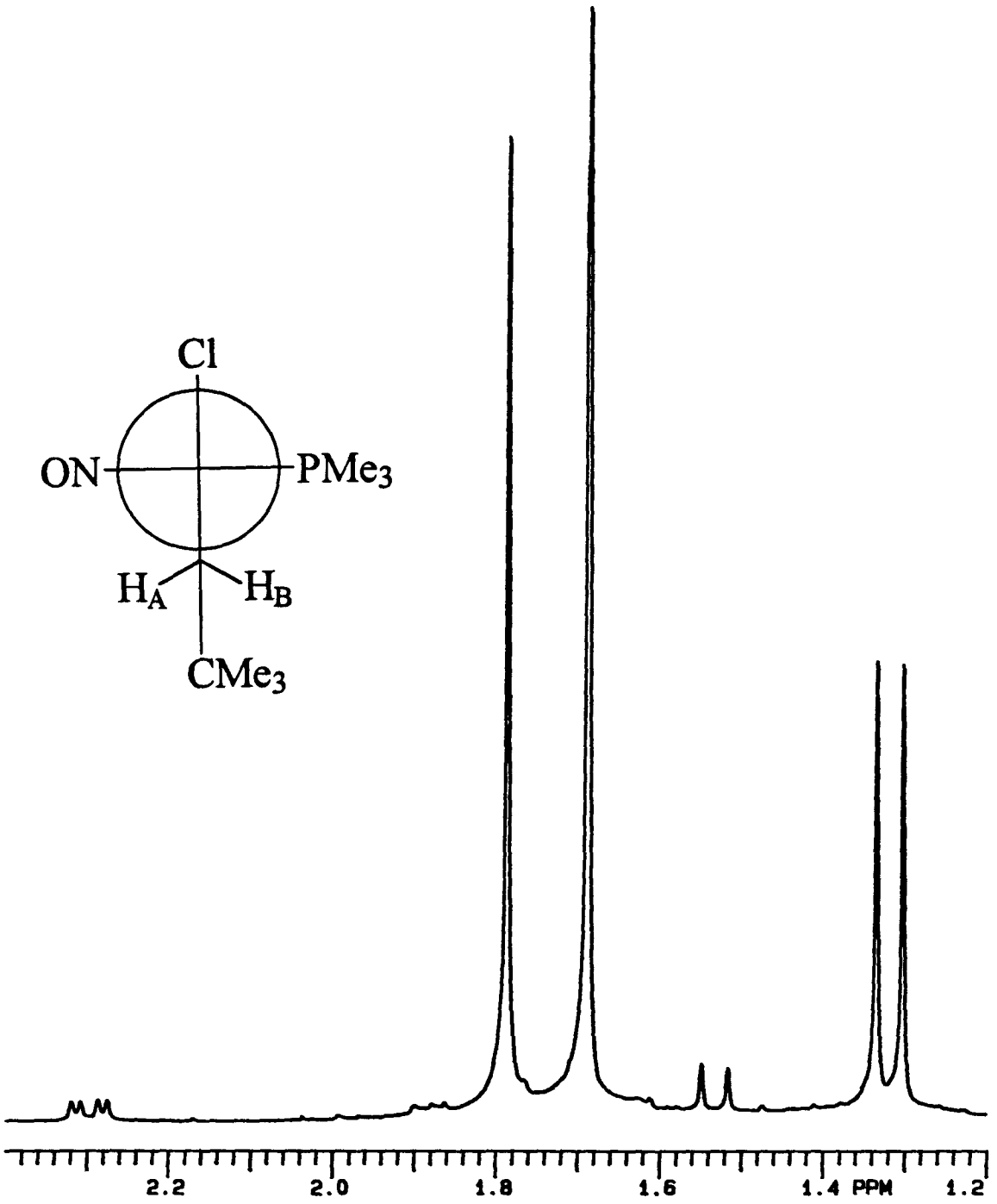

Figure 3.4 300 MHz ^{1}H NMR spectrum of **3.11** in C_6D_6 (inset: Newman projection of $Cp^*Mo(NO)(CH_2CMe_3)(Cl)(PMe_3)$ down the metal-Cp^* centroid axis)

surprising that the PMe_3 enters the metal's coordination sphere at this position.[3] The isolated adduct isomer appears to be the thermodynamically favoured isomer given that no isomerization is observed for this complex. Thermolysis in C_6D_6 leads only to decomposition.

The addition of PMe_3 to **3.3** causes a drop in ν_{NO} of 31 cm^{-1} in the IR spectrum of **3.11**, a feature consistent with the metal center in the adduct becoming markedly more electron-rich. Prolonged exposure of complex **3.11** to high vacuum does not effect the dissociation of the phosphine ligand, as occurs for $CpW(NO)(CH_2SiMe_3)_2(PMe_3)$.[8] Again, this substantiates the conclusion that **3.3** is about as electron-deficient as related diaryl complexes (Section 3.3.2.1) which also bind PMe_3 irreversibly (Section 2.3.6).[20] Interestingly, a bulkier base such as pyridine also coordinates to **3.3**, but in a reversible fashion (eq 3.5).

$$Cp^*Mo(NO)(CH_2CMe_3)Cl \underset{-\ py}{\overset{+\ py}{\rightleftharpoons}} Cp^*Mo(NO)(CH_2CMe_3)(Cl)(py) \qquad (3.5)$$

3.3 **3.12**

At low temperatures, the adduct is stabilized and by virtue of its diminished solubility (compared to **3.3**) will crystallize from Et_2O solutions containing an excess of pyridine. As a solid, the adduct shows a tendency to lose pyridine slowly under vacuum. Dissolution of **3.12** in a coordinating solvent such as THF-d_8 or even a non-coordinating solvent such as C_6D_6 quantitatively liberates pyridine and the starting material as evidenced by ^1H NMR spectroscopy (Figure 3.5a). Consequently, in order to spectroscopically characterize the pyridine adduct, low-temperature (-100 °C) NMR studies in THF-d_8 are required (Figure 3.5b).[23] As a solution of **3.3** and 1 equiv of pyridine is cooled, signals due to the methylene protons of the neopentyl group are the first to coalesce (-30 °C), presumably due to the slowed rotation of the alkyl ligand about its Mo-C bond axis. At lower temperature (-75 °C) signals due to the methyl protons of the Cp^* rings coalesce. At -90 °C, the pyridine in the sample begins to coordinate to the metal, and all signals begin to sharpen. Finally, at -100 °C, only signals attributable to the pyridine complex **3.12** are observable. At this temperature, the sample solution is orange (characteristic of **3.12**) and not purple (characteristic of **3.3**).

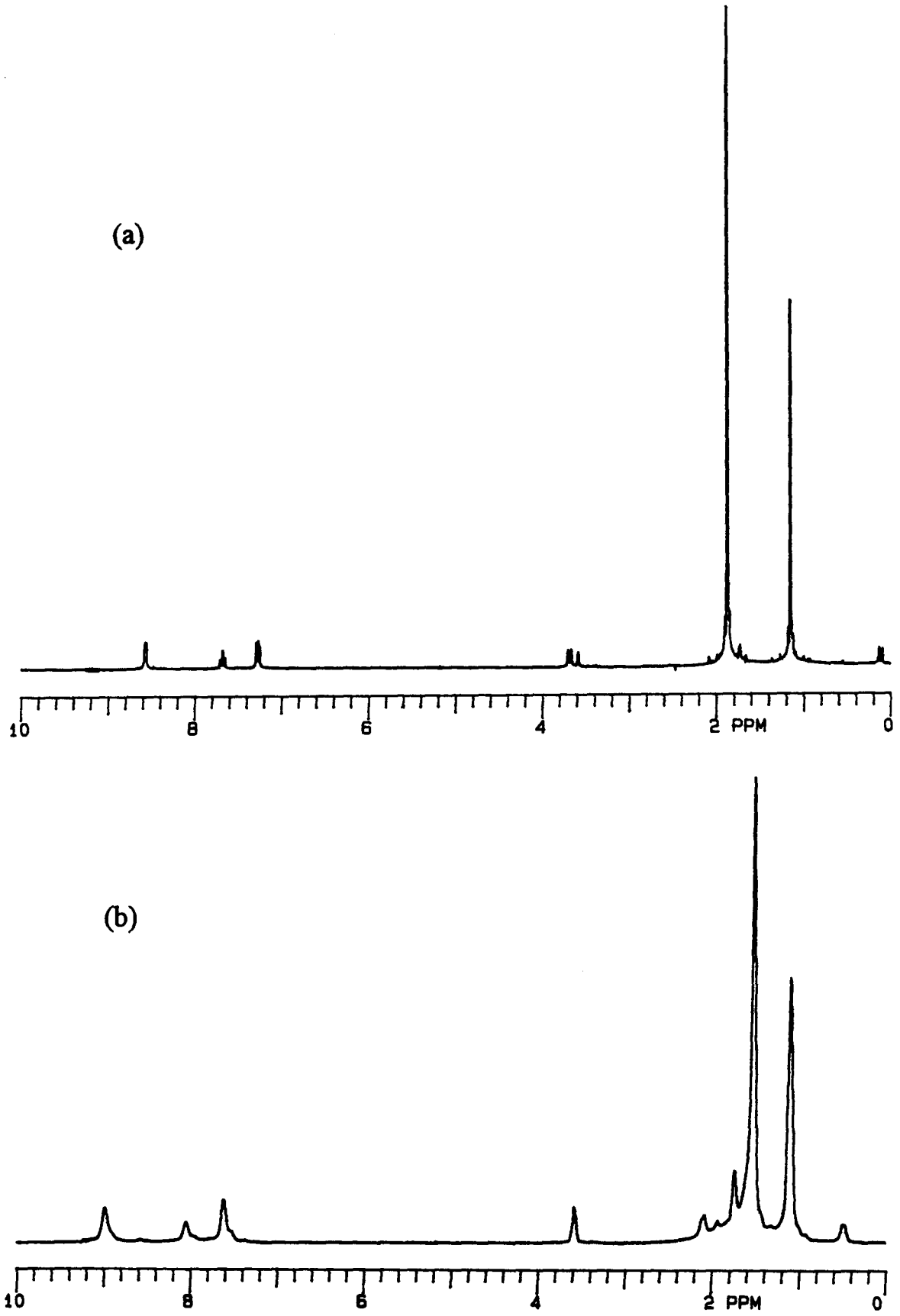

Figure 3.5 300 MHz ^{1}H NMR spectra of **3.12** at (a) room temperature; (b) -100 °C in THF-d_8 (δ 3.60 and 1.75)

3.3.3.2 Formation of Insertion Products: Reactions With Unsaturated Lewis Bases

Lewis-base substrates containing unsaturated linkages also form adducts with $Cp^*Mo(NO)(CH_2CMe_3)Cl$, but once coordinated they undergo facile insertion into the molybdenum-neopentyl bond. Thus, the reactions of $Cp^*Mo(NO)(CH_2CMe_3)Cl$ with CO or $CNCMe_3$ provide the dihapto acyl (**3.13**) and iminoacyl (**3.14**) complexes, respectively (eq 3.6).

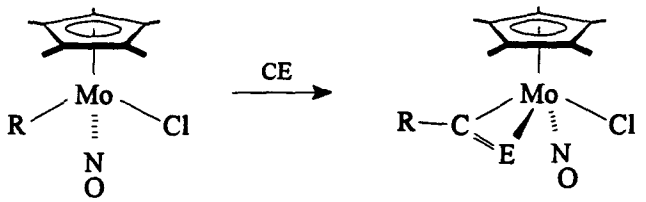

(3.6)

$E = O, NCMe_3$

$R = CH_2CMe_3$

The yield of **3.13** (30%) is substantially lower than the yield of **3.14** (95%) primarily due to the complexity of the CO insertion reaction. After isolation of amber $Cp^*Mo(NO)(\eta^2\text{-}C\{O\}CH_2CMe_3)Cl$ from diethyl ether, the red supernatant solution can be taken to dryness, and the residue can be redissolved in pentane. Crystallization of the pentane solution yields an impure red solid which, by ^1H NMR spectroscopy, exhibits a multitude of signals attributable to Cp^*, CMe_3 and CH_2 protons. Attempts to purify this mixture have not as yet been successful. On the other hand, the tert-butyl isocyanide insertion reaction is facile and very clean. Thus, addition of $CNCMe_3$ to a purple solution of **3.3** causes an immediate color change to amber, presumably due to the adduct $Cp^*Mo(NO)(CH_2CMe_3)(Cl)(CNCMe_3)$, followed by a color change to yellow and precipitation of the inserted species $Cp^*Mo(NO)(\eta^2\text{-}C\{NCMe_3\}CH_2CMe_3)Cl$ (**3.14**).

In accord with other acyl complexes that we have isolated,[8,24] the neopentyl-acyl derivatives prepared in this work exhibit classic η^2-acyl ligands.[25] The IR spectrum of **3.13** as a Nujol mull exhibits two strong bands at 1624 and 1601 cm^{-1} attributable to NO- and CO-stretching frequencies, but unambigous assignment of these bands is not possible without labeling studies.

However, by analogy to related complexes, the 1624 cm^{-1} band can most likely be attributed to ν_{NO}. To confirm the nature of the acyl group in complex **3.13**, it was subjected to an X-ray crystallographic analysis.[26] An ORTEP diagram of the molecular structure of **3.13** is shown in Figure 3.6.

The η^2-acyl ligand is clearly evident in the structure of **3.13**. The two independent molecules of **3.13** that were crystallographically determined exhibit short Mo-O bond lengths of 2.217(2) and 2.226(2) Å and very acute C11-Mo-O2 bond angles of 32.9(1) and 33.3(1)°, respectively (Table 3.6). The differences between the Mo-O2 and Mo-C11 bond lengths of 0.153 and 0.182 Å are characteristic of an η^2-acyl group.[25] A nearly isostructural analogue of complex **3.13** has been reported by Hersh; however, the route to this latter complex does not resemble that in which **3.13** was prepared.[27] This complex, CpMo(NO)(η^2-C{O}*p*-tolyl)(I), exhibits a Δ(Mo-O)-(Mo-C) of 0.163 Å. As of 1988,[25] the known range of Δ[(Mo-O)-(Mo-C)] for structurally characterized η^2-acyl complexes was 0.17 - 0.30 Å. Both the Hersh complex and complex **3.13** are slightly outside of this range. The low values of Δ[(Mo-O)-(Mo-C)] observed for these two complexes are more similar to electron-deficient Group 4 η^2-acyl complexes and are likely a function of the Lewis-acidic metal centers in these compounds.

The IR spectrum of **3.14** is diagnostic for an η^2-iminoacyl moiety. Specifically, a ν_{CN} at 1715 cm^{-1} is characteristic of this ligand type.[25] It is of interest to note that the nitrosyl-stretching frequency for the iminoacyl complex is 50 cm^{-1} lower than that of the acyl complex **3.13**. It can therefore be concluded that an $NCMe_3$ group is a better source of electron density for the Cp^*Mo(NO) fragment than is an oxygen atom from an η^2-acyl group.

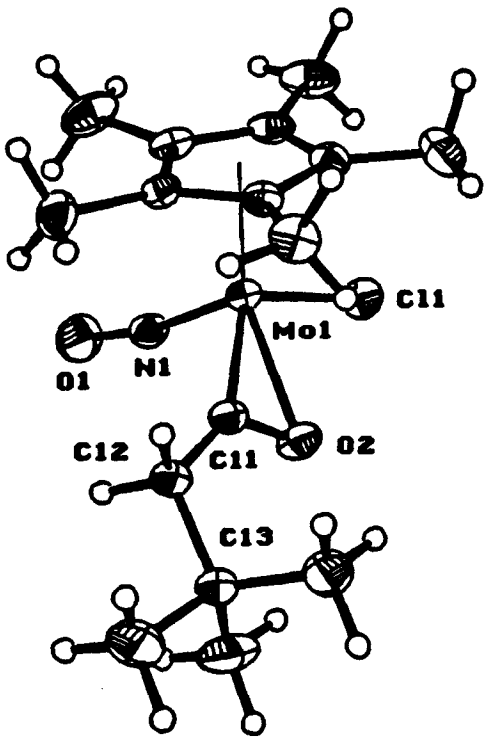

Figure 3.6 ORTEP diagram of **3.13** (only one of the two crystallographically independent molecules is shown). 33% probability ellipsoids are shown for the non-hydrogen atoms.

Table 3.6 Selected bond lengths and angles for complex **3.13**

bond lengths (Å) (esd)			bond angles (°) (esd)		
	molecule A	**molecule B**		**molecule A**	**molecule B**
Mo-O2	2.217(2)	2.226(2)	Mo-C11-O2	80.5(2)	81.5(2)
Mo-C11	2.064(3)	2.044(3)	Mo-O2-C11	66.6(2)	65.3(2)
Mo-Cl	2.4258(8)	2.4204(8)	Mo-N-O1	167.8(2)	168.1(2)
Mo-N	1.763(3)	1.785(3)	C11-Mo-O2	32.9(1)	33.3(1)
			C11-Mo-N	92.8(1)	91.3(1)
			N-Mo-Cl	98.46(9)	98.52(8)
			Cl-Mo-O2	85.79(6)	85.45(6)

3.3.3.3 Halide Abstraction: Reaction with $AgBF_4$

The chloro ligand in **3.3** is very susceptible to abstraction by Ag (I) salts. Treatment of $Cp^*Mo(NO)(CH_2CMe_3)Cl$ with $AgBF_4$ in acetonitrile leads to a good yield of the 16-electron acetonitrile cation $[Cp^*Mo(NO)(CH_2CMe_3)(NCMe)]BF_4$ (**3.15**) (eq 3.7).

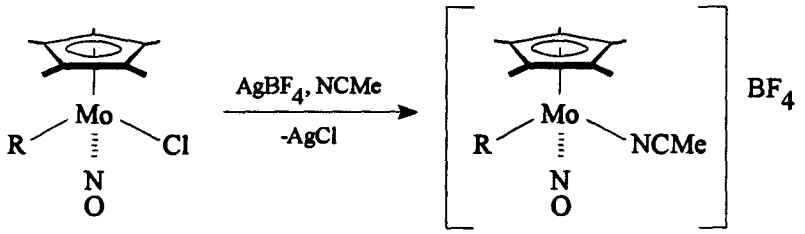

(3.7)

$R = CH_2CMe_3$

Complex **3.15** is related to other Mo and W cations that our group has previously described.[28] However, **3.15** is the first nitrosyl cation of this type to bear a hydrocarbyl ligand. At room temperature, in CD_2Cl_2, **3.15** exhibits only 1 peak for the coordinated nitrile ligand whereas the analogous W cation exhibits two broad singlets attributable to *two* coordinated acetonitrile groups.[22] Evidently, the Mo complex would rather not coordinate a second molecule of acetonitrile for steric or electronic reasons. Why this is so is not clear, since the analogous molybdenum halo *bis*(acetonitrile) cations, $[Cp^*Mo(NO)(X)(NCMe)_2]PF_6$ [X = I, Br, Cl], are known.[28] Possibly the BF_4 anion is weakly coordinated to Mo in **3.15**. Increased energy ν_{CN} (vs free NCMe at 2230 cm^{-1}) at 2316 and 2290 cm^{-1} in the IR spectrum of **3.15** are diagnostic for the presence of an N-bound nitrile ligand;[29] therefore, it is unlikely that the nitrile ligand is π-bound as occurs in the 16-electron acetonitrile cation, $[W(bpy)(PMe_3)_2(Cl)(\eta^2\text{-NCMe})]^+$.[30] Being an ionic species, **3.15** is best crystallized from CH_2Cl_2/Et_2O mixtures, from which it forms irregular orange-yellow crystals. However, upon standing in CD_2Cl_2 for several hours at room temperature, the complex spontaneously decomposes to a mixture of products and free acetonitrile. Clearly, the nitrile ligand in the 16-electron Mo cation is quite labile. Interestingly, a related complex, $[Cp_2Zr(Ph)(NCMe)]BPh_4$, does not persist in the presence of excess acetonitrile, but rather undergoes insertion of NCMe into the Zr-Ph bond. The thermally stable complex thus formed, $[Cp_2Zr(NC\{Me\}Ph)(NCMe)]BPh_4$, contains one NCMe ligand.[31]

Halide abstraction from compound **3.3** in a non-coordinating solvent such as dichloromethane does not lead to tractable products, presumably because the unsolvated 14-electron $[Cp^*Mo(NO)(CH_2CMe_3)]^+$, if formed, would be exceedingly reactive. The scope of ligand types that can be coordinated to the $[Cp^*Mo(NO)(CH_2CMe_3)]^+$ fragment remains to be ascertained. It should be noted that a family of cations isoelectronic with $[Cp^*Mo(NO)(CH_2CMe_3)]^+$ have been extensively studied by Jordan and coworkers.[32] The $[Cp'_2Zr(R)(L)]BX_4$ [R = H, Me, CH_2Ph, Ph; L = NCMe, THF; X = F, Ph] salts mediate a variety of productive insertion processes. Similar reactivity can be envisaged for complexes derived from **3.15**.

3.3.4 Reactions of 18-Electron Derivatives of $Cp^*Mo(NO)(CH_2CMe_3)Cl$

As mentioned in the text, many derivatives of $Cp^*Mo(NO)(CH_2CMe_3)Cl$ (**3.3**) are very reactive and/or decompose readily in solution. This section outlines two reactions that should be a foundation for much future research.

3.3.4.1 Reaction of $Cp^*Mo(NO)(CH_2CMe_3)(Cl)(PMe_3)$ with LDA

Dehydrohalogenation of $Cp^*Mo(NO)(CH_2CMe_3)(PMe_3)Cl$ (**3.11**) with LDA in THF gives moderate yields of the unusual dialkyl complex **3.16** in which the metallated Cp* ring serves as the second alkyl ligand (eq 3.8).

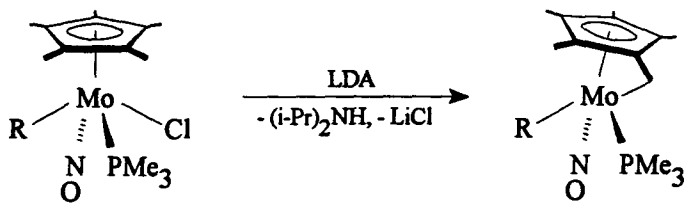

(3.8)

$R = CH_2CMe_3$

Conversion 3.8 probably proceeds via direct deprotonation by LDA of a Me substituent of the Cp* ligand followed by intramolecular metathesis. Alternatively, deprotonation of the

hydrocarbyl ligand would afford a transient alkylidene species that could rearrange to the final product. Bercaw and coworkers have established a precedent for such a rearrangement (eq 3.9).[33]

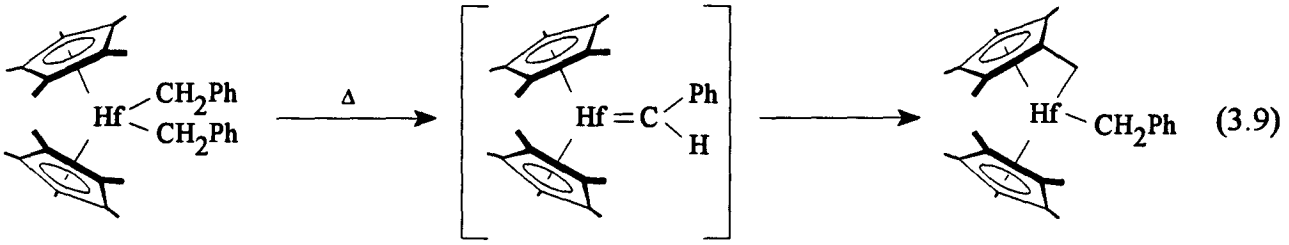

(3.9)

The latter pathway is mechanistically unlikely in the Mo system for two reasons. First, the methylene protons of **3.11** are more sterically protected than the methyl groups of the Cp* ligands and LDA is a hindered base. Secondly, alkylidene complexes of the type, $CpMo(NO)(=CHCMe_3)L$ [L = Lewis base],[34] have been shown to be isolable and thermally stable to at least 150 °C in C_6D_6 (Chapter 5).

The NMR spectra ($CDCl_3$) of **3.16** show four different methylene-proton resonances (^1H NMR) and four inequivalent Cp* methyl-group signals (^1H and $^{13}C\{^1H\}$-APT NMR) in addition to the CMe_3 resonance for the neopentyl ligand. The two sets of methylene protons show markedly different $^2J_{HH}$ couplings characteristic of their chemical environments. Thus, the neopentyl methylene protons are bound to a purely sp^3 methylene carbon and exhibit coupling constants of 12.9 Hz, whereas the methylene protons of the tucked-in Cp* ring are bound to a carbon with considerable sp^2 character and thus are weakly (or geminally) coupled (3.0 Hz).[35] Fortuitously, a single diastereomer is isolated from reaction 3.8.[36] This feature is most clearly evidenced by a single resonance in the ^{31}P NMR spectrum (δ -2.89 ppm) of this material in C_6D_6 (Table 3.3).

The proposed structure of complex **3.16** is based on the solid-state structural analysis of its W congener.[22] Since both Mo and W complexes display nearly identical spectroscopic features, they are very likely isostructural. While other η^5,η^1-Cp*-containing complexes such as

$[Cp^*Ru(\eta^5,\eta^1\text{-}C_5Me_4CH_2)][BF_4]$,[37] $Cp^*Hf(\eta^5,\eta^1\text{-}C_5Me_4CH_2)(CH_2Ph)$,[33] and $Cp^*Zr(\eta^5,\eta^1\text{-}C_5Me_4CH_2)(Ph)$[38] are known, none was prepared by direct deprotonation of a Cp^* ligand.

3.3.4.2 Reaction of $Cp^*Mo(NO)(\eta^2\text{-}C\{O\}CH_2CMe_3)Cl$ with PMe_3

In order to determine if the η^2-acyl ligand in **3.13** could be displaced from its metal center to η^1 coordination, the complex was reacted with PMe_3. Treatment of **3.13** with excess PMe_3 in $CDCl_3$ causes the formation of a single organometallic product that has two different PMe_3 groups. Since the ^1H NMR spectrum of the product reveals that the signals attributable to the methylene protons of the acyl ligand show ^{31}P coupling ($^3J_{HP}$ = 28.5 and 6.9 Hz), in addition to a mutual $^2J_{HH}$ of 15.0 Hz, it seems most likely that one PMe_3 ligand is attached to the acyl carbon and one is attached to the metal, thereby causing the chloro ligand to become a counter anion (eq 3.10).

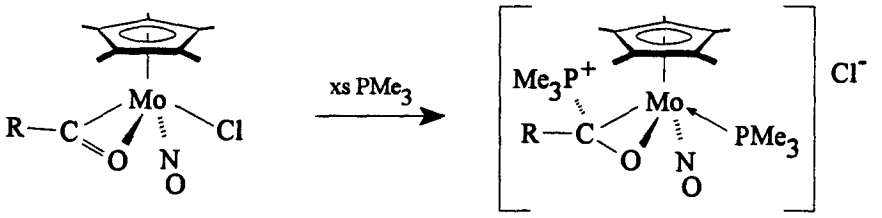

(3.10)

$R = CH_2CMe_3$

The complex, $[Cp^*Mo(NO)(C\{O\}\{PMe_3\}CH_2CMe_3)(PMe_3)]Cl$ (**3.17**) is stable only in solution (in the presence of excess PMe_3) and decomposes readily upon removal of solvent. The insolubility of **3.17** in C_6D_6 is consistent with the ionic formulation of the complex. Nevertheless, without a crystallographic analysis of this salt, the true nature of complex **3.17** remains ambiguous. Anion metathesis may well lead to a more stable derivative of this species.

3.4 Epilogue and Future Work

Two major conclusions about the entire family of Mo alkyl nitrosyl complexes can be made. First, they are synthesizable and are not as unstable as previously speculated. In fact, the alkylations can be conducted in a stepwise fashion, thereby enabling us to prepare asymmetric complexes of the type $Cp^*Mo(NO)(R)(R')$. Future attempts to exploit the chiral nature of these molecules in various asymmetric syntheses should be made. Second, structural, electrochemical and IR studies all lead to the same conclusions about the relative Lewis acidities of the entire Cp'M(NO)(Y)(Z) [Cp' = Cp, Cp^*; M = Mo, W; Y, Z = halide, alkyl, aryl] family of complexes. Namely, Cp-containing complexes have more electron-deficient and more accessible, and thus more reactive, metal centers than their Cp^* congeners. The same statement is true for Mo vs W and aryl vs alkyl. Thus, the most Lewis acidic complex in this series that we can prepare is $CpMo(NO)(aryl)_2$. It is a shame that such species are so thermally sensitive as to defy isolation.

The last part of this chapter describes reactions of $Cp^*Mo(NO)(CH_2CMe_3)Cl$ and some of its derivatives. Clearly, $Cp^*Mo(NO)(CH_2CMe_3)Cl$ is a potent Lewis acid. Its neopentyl group migrates readily to unsaturated substrates and its chloride ligand can be metathesized or abstracted. The reactions of $Cp^*Mo(NO)(CH_2CMe_3)Cl$ (**3.3**) should be extended to other alkyl or aryl complexes since the comparative chemistry of those species would be of interest. Similarily, the chemistry of several reaction products would be of considerable practical interest. For instance, what organic substrates are activated by coordination to $[Cp^*Mo(NO)(CH_2CMe_3)]^+$-containing complexes and what types of bonds can be activated by the strained ring in $(\eta^5,\eta^1\text{-}C_5Me_4CH_2)Mo(NO)(CH_2CMe_3)(PMe_3)$?

3.5 References and Notes

(1) *The Chemistry of the Metal-Carbon Bond*; Hartley, F. R., Ed.; Wiley: New York, 1987; Vol. 4, Part 2.

(2) Collman, J. P.; Hegedus, L. S.; Norton, J. R.; Finke, R. G. *Principles and Applications of Organotransition Metal Chemistry*; University Science Books: Mill Valley, CA, 1987; Chapters 3 and 14.

(3) Legzdins, P.; Veltheer, J. E. *Acc. Chem. Res.* **1993**, *26*, 41.

(4) Dryden, N. H.; Legzdins, P.; Batchelor, R. J.; Einstein, F. W. B. *Organometallics* **1991**, *10*, 2077.

(5) Several reactions mixtures of this type were taken to dryness in tared flasks without crystallization, and the mass of the crude product established by difference. The yields of four separate experiments ranged from 83 - 93%.

(6) Legzdins, P.; Phillips, E. C.; Sánchez, L. *Organometallics* **1989**, *8*, 940.

(7) ^{1}H NMR data for **3.13** in $CDCl_3$: δ 3.45 (d, 1H, CH_2, J_{HH} = 15.9 Hz), 3.06 (d, 1H, CH_2, J_{HH} = 15.9 Hz), 1.95 (s, 15H, $C_5(CH_3)_5$), 1.23 (s, 9H, $C(CH_3)_3$).

(8) Legzdins, P.; Rettig, S. J.; Sánchez, L. *Organometallics* **1988**, *7*, 2394.

(9) Legzdins, P.; Lundmark, P. J.; Phillips, E. C. Rettig, S. J.; Veltheer, J. E. *Organometallics* **1992**, *11*, 2991.

(10) Hunter, A. D.; Legzdins, P.; Martin, J. T.; Sánchez, L. *Organomet. Synth.* **1986**, *3*, 66.

(11) Legzdins, P.; Veltheer, J. E. In *Handbuch der Präparativen Anorganischen Chemie*, 4th ed.; Herrmann, W. A., Ed.; Thieme-Verlag: Stuttgart, Germany, in press.

(12) A commentary of our attempts to synthesize such complexes is provided in a paper describing the chemistry of Cp'M(NO)(η^2-benzyl)Cl complexes (see: Dryden, N. H.; Legzdins, P.; Trotter, J.; Yee, V. C. *Organometallics* **1991**, *10*, 2857). These benzyl complexes are 18-electron species by virtue of their containing 3-electron-donor benzyl groups.

(13) Debad, J. D.; Legzdins, P.; Batchelor, R. J.; Einstein, F. W. B. *Organometallics* **1992**, *11*, 6.

(14) Crude $Cp^*Mo(NO)Cl_2$ prepared from $Cp^*Mo(NO)(CO)_2$ and PCl_5 is best purified by Soxhlet extraction and crystallization from CH_2Cl_2.[4]

(15) ^1H NMR spectral data for this complex (C_6D_6): δ 3.83 (d, 1H, CH_2, J_{HH} = 16.2 Hz), 3.62 (d, 1H, CH_2, J_{HH} = 16.2 Hz), 1.75 (s, 15H, Cp^*), 1.04 (s, 9H, CMe_3).

(16) Debad, J. D.; Legzdins, P.; Batchelor, R. J.; Einstein, F. W. B. *Organometallics*, in press.

(17) Jackman, L. M.; Sternhell, S. *Applications of Nuclear Magnetic Resonance Spectroscopy in Organic Chemistry*; Pergamon Press: Toronto, 1969; 2nd ed., p 334.

(18) Chapter 2 of this thesis.

(19) For moderate charge-transfer rates, quasi-reversible electrochemical behaviour is often observed. The slowness of electron transfer is often ascribed to subtle structural changes that occur upon reduction (or oxidation). For a general description of this phenomenon, see: Geiger, W. E. *Prog. Inorg. Chem.* **1984**, 275. For more detailed descriptions of electrochemical quasi-reversibility, see: (a) Matsuda, H.; Ayabe Y. *Z. Elektrochem.* **1955**, *59*, 494. (b) Bard, A. J.; Faulkner, L. F. *Electrochemical Methods*; John Wiley and Sons: New York, NY, 1980; Chapter 6.

(20) Dryden, N. H.; Legzdins, P.; Rettig, S. J.; Veltheer, J. E. *Organometallics* **1992**, *11*, 2583.

(21) Legzdins, P.; Rettig, S. J.; Sánchez, L.; Bursten, B. E.; Gatter, M. G. *J. Am. Chem. Soc.* **1985**, *107*, 1411.

(22) Debad, J. D.; Legzdins, P.; Rettig, S. J.; Veltheer, J. E. *Organometallics*, submitted for publication.

(23) Initial attempts to obtain a limiting spectrum for this adduct, $Cp^*Mo(NO)(CH_2CMe_3)(Cl)(py)$, in $CHCl_3$ were unsuccessful since the solvent freezes at a temperature higher than that required to form the adduct.

(24) Dryden, N. H.; Legzdins, P.; Lundmark, P. J.; Reisen, A.; Einstein, F. W. B. *Organometallics*, in press.

(25) Durfee, L. D.; Rothwell, I. P. *Chem. Rev.* **1988**, *88*, 1059.

(26) Crystals of **3.13** are monoclinic of space group $P2_1/n$; a = 15.226 (2) Å, b = 12.376 (2) Å, c = 19.641 (2) Å, β = 95.921 (8)°, Z = 8. Dr. Steve Rettig solved the structure using the Patterson method and full-matrix least-squares refinement procedures to $R_F = 0.032$, $R_{wF} = 0.032$ for 7215 reflections with $I \geq 3\sigma(I)$.

(27) Bonnesen, P. V.; Yau, P. K. L.; Hersh, W. H. *Organometallics* **1987**, *6*, 1587.

(28) Chin, T. T.; Legzdins. P.; Trotter, J.; Yee, V. C. *Organometallics* **1992**, *11*, 913.

(29) Nakamoto, K. *Infrared and Raman Spectra of Inorganic and Coordination Compounds*, 4th ed.; Wiley-Interscience: New York, 1986; pp 280-281.

(30) Barrera, J.; Sabat, M.; Harman, W. D. *J. Am. Chem. Soc.* **1991**, *113*, 8178.

(31) Borkowsky, S. L.; Jordan, R. F.; Hinch, G. D. *Organometallics* **1991**, *10*, 1268.

(32) Jordan, R. F.; Bradley, P. K.; LaPointe, R. E.; Taylor, D. F. *New J. Chem.* **1990**, *14*, 505 and references therein.

(33) Bulls, A. R.; Schaefer, W. P; Serfas, M.; Bercaw, J. E. *Organometallics* **1987**, *6*, 1219.

(34) Legzdins, P.; Rettig, S. J.; Veltheer, J. E. *J. Am. Chem. Soc.* **1992**, *114*, 6922.

(35) The exact assignments of the methylene protons were eludicated from a two-dimensional ^{1}H:^{1}H-COSY spectrum of **3.16**.

(36) Based on the X-ray crystallographic analysis of the W analogue of **3.16**, the isolated product has a configuration in which the PMe_3 ligand is trans to the NO ligand, just as in the starting material, $Cp^*Mo(NO)(CH_2CMe_3)(Cl)(PMe_3)$ (**3.11**).

(37) Kreindlin, A. Z.; Petrovskii, P. V.; Rybinskaya, M. I.; Yanovskii, A. I.; Struchkov, Yu. T. *J. Organomet. Chem.* **1987**, *319*, 229.

(38) Schock, L. E.; Brock, C. P.; Marks, T. J. *Organometallics* **1987**, *6*, 232.

CHAPTER 4

Reactions of 16-Electron $Cp'M(NO)R_2$ Complexes of Molybdenum and Tungsten with Water

4.1 Introduction

At present, little is known about the reactions of transition-metal-carbon σ bonds with H_2O.[1] This seems rather anomalous given water's ubiquity and the ease at which most organometallic complexes are hydrolyzed. As outlined in Chapters 2 and 3, the impetus for developing a new synthetic methodology to a range of $Cp'M(NO)R_2$ complexes was necessitated by the propensity of all but the tungsten dialkyl complexes to react rather vigorously with water which was a key reagent in our original preparations of this family of organometallic complexes. This chapter will focus on the products obtained when isolable $Cp'M(NO)R_2$ complexes are treated with water.[2]

A fundamental goal of our research group has been the determination of the distinctive physical and chemical properties that complexes containing 14-valence-electron Cp'M(NO) fragments exhibit. Typically, these properties are dependent upon all three

variables: the metal, the cyclopentadienyl ring, and the ancillary hydrocarbyl ligands. The work described in this chapter provides the clearest illustration of the dependence upon M so far investigated in our laboratories.

In general, the W-C σ-bonds in $Cp'W(NO)(alkyl)_2$ compounds are stable and are not easily hydrolyzed (Chapters 1 and 2). The four isolable $Cp'W(NO)(aryl)_2$ complexes, on the other hand, are converted to their aryl dioxo analogues, $Cp'W(O)_2(aryl)$ when exposed to water. In contrast, the Mo-C σ bonds in *all* (both alkyl and aryl) isolable $Cp^*Mo(NO)R_2$ complexes are readily hydrolyzed to form bimetallic complexes of the type $[Cp^*Mo(NO)R]_2$-(μ-O) and free hydrocarbon. This chapter will focus primarily on these molybdenum systems and present the synthesis, characterization and properties of five such complexes. In light of a preliminary kinetic analysis, a probable mechanism for the formation of these complexes is presented. The chemical relationships between $Cp^*Mo(NO)R_2$ and its oxo derivatives, $[Cp^*Mo(NO)R]_2$-(μ-O), $Cp^*Mo(O)_2R$, and $[Cp^*Mo(O)_2]_2$-(μ-O) are presented. Lastly, the chemistry of the molybdenum systems is contrasted with that of the congeneric tungsten systems.

4.2 Experimental Procedures

4.2.1 Methods

The synthetic methodologies employed throughout this thesis are described in detail in section 2.2.1.

4.2.2 Reagents

The organometallic dihalide complexes, $Cp'M(NO)Cl_2$, were prepared and handled as described in Section 2.2.2. Preparations of $(aryl)_2Mg{\cdot}X(dioxane)$ reagents are outlined in

Section 2.2.4. Other $(alkyl)_2Mg{\cdot}X(dioxane)$ reagents were prepared similarily by substituting the appropriate Grignard reagent. Commercial Grignard reagents were purchased from Aldrich as 1.0 M Et_2O or THF solutions. The $Cp'W(NO)(aryl)_2$ complexes [Cp' = Cp, aryl = *o*-tolyl; Cp' = Cp*, aryl = Ph, *p*-tolyl, *o*-tolyl], were prepared using the methodology outlined in Sections 2.2.5 and 2.2.7. Bulk quantities (1-5 g) of $Cp^*Mo(NO)(CH_2SiMe_3)_2$ were prepared as described in Section 3.2.6. D_2O (MSD Isotopes, 99.8% D) and $^{18}OH_2$ (Aldrich, 97% ^{18}O) were used as received. H_2O_2 (30% aqueous, Fisher) was used as received.

The column chromatography materials used during this work were alumina (80 - 200 mesh, Fisher neutral, Brockman activity I), alumina I deactivated to alumina III with 6% w/w deaerated water, and Florisil (60 - 100 mesh, Fisher). Filtrations were performed through Celite 545 diatomaceous earth (Fisher) that had been oven-dried and cooled in vacuo.

4.2.3 Electrochemical Measurements

The methodology used for electrochemistry was very similar to that described in Section 2.2.3 except that Ag wire was used as the reference electrode. Ferrocene was used as an internal reference during this work, with the redox couple, Cp_2Fe/Cp_2Fe^+, occurring at $E^{\circ\prime}$= 530 mV versus Ag wire in THF over the range of scan rates used (0.10 to 0.80 V s^{-1}).[3]

4.2.4 Kinetic Measurements

The conversion of $Cp^*Mo(NO)(CH_2SiMe_3)_2$ (**3.8**) to $[Cp^*Mo(NO)(CH_2SiMe_3)]_2$-(μ-O) (**4.1**) was studied in order to gain some insight about the mechanism of the hydrolysis reaction. In general, a standard solution of $Cp^*Mo(NO)(CH_2SiMe_3)_2$ was prepared in a drybox in a volumetric flask using THF as

solvent. Aliquots of this standard solution were diluted as required, and 2 mL of the diluted solution was then quickly mixed with 2 mL of a standard solution of water in THF in a 1.00 cm UV-vis spectrophotometric cell equipped with a 4-mm Teflon stopcock. The concentration of the water was sufficiently high such that all runs were effectively conducted under pseudo-first-order conditions. The cell and its contents were shaken, quickly removed from the drybox, and placed in a Hewlett-Packard 8542A diode array spectrometer, which, in conjunction with a Haake W19 temperature bath equipped with a Haake D8 temperature controller, allowed the cell to be maintained at constant temperature (±0.1 °C). The solution was left unstirred and allowed to equilibrate with the spectrometer temperature for 300 s. Spectra were then recorded at regular intervals (usually 150 s), and data were collected for approximately one half-life or until significant deviations from linearity of the monitored parameters occurred. The absorbance values at infinity were determined by calculation, i.e. the correlation coefficients of pseudo-first-order log plots were optimized by empirically varying the values of A_∞.[4] The observed rate constants (k_{obs}) were then calculated from plots of $\ln(A_\infty - A_t)$ versus time (s). Values of $\Delta H^\ddagger$ and $\Delta S^\ddagger$ were determined from Erying plots of $\ln(k_{obs}/T)$ versus 1/T where $\Delta H^\ddagger$ = -R(slope) and $\Delta S^\ddagger$ = R[intercept - $\ln(k_B/h)$] (R, k_B and h are the gas constant, Boltzmann's constant and Planck's constant, respectively).

4.2.5 Preparation of $[Cp^*Mo(NO)(CH_2SiMe_3)]_2$-(μ-O) (4.1)

A solution of $Cp^*Mo(NO)(CH_2SiMe_3)_2$ (**3.8**) generated from $Cp^*Mo(NO)Cl_2$ (1180 mg, 3.55 mmol) and Me_3SiCH_2MgCl (8.0 mL of a 1.0 M Et_2O solution, 8.0 mmol) in Et_2O (150 mL) was prepared at 0 °C. Treatment of the resultant purple solution with deaerated H_2O (0.20 mL) destroyed any excess Grignard reagent and caused the decomposition of $Cp^*Mo(NO)(CH_2SiMe_3)_2$ (ν_{NO} 1593 cm^{-1}) to $[Cp^*Mo(NO)(CH_2SiMe_3)]_2$-(μ-O) ($\nu_{NO}$ 1584 cm^{-1}). The solvent volume was then

reduced to approximately 15 mL by slow evaporation of the Et_2O under reduced pressure. At this point the mixture contained mostly **4.1**, but small quantities of $Cp^*Mo(NO)(CH_2SiMe_3)_2$ persisted in solution. The mixture was then *very slowly* chromatographed on an alumina III column (3 x 8 cm) made up in Et_2O using Et_2O as eluant. As the purple band indicative of the dialkyl starting material passed through the column, it changed color, becoming the red-brown characteristic of **4.1**. The rest of **4.1** eluted from the column next. The combined red-brown eluates were collected, and their volume was reduced in vacuo until the first signs of crystallization became evident. Maintaining the concentrated solution at -20 °C overnight resulted in the deposition of large red-black crystals (650 mg) of $[Cp^*Mo(NO)(CH_2SiMe_3)]_2$-(μ-O) which were collected by filtration. The filtrate was taken to dryness, and the residue was redissolved in hexanes. Crystallization of this second fraction afforded an additional 302 mg of product (75% total yield based on $Cp^*Mo(NO)Cl_2$).

The conversion of $Cp^*Mo(NO)(CH_2SiMe_3)_2$ to $[Cp^*Mo(NO)(CH_2SiMe_3)]_2$-(μ-O) could be conveniently monitored by ^1H NMR spectroscopy which indicated that the yield of the reaction was > 95%. For example, the reaction of $Cp^*Mo(NO)(CH_2SiMe_3)_2$ (38 mg) in C_6D_6 (1.2 mL) with H_2O (10 μL, excess) required approximately 2 min at room temperature to go to completion. The signal due to the 2 equiv of Me_4Si formed in the reaction could be easily detected at δ 0.00 ppm.

4.2.6 Preparation of $[Cp^*Mo(NO)(CH_2CMe_3)]_2$-(μ-O) (4.2)

Solid $Cp^*Mo(NO)Cl_2$ (498 mg, 1.50 mmol) and solid $(Me_3CCH_2)_2Mg{\cdot}X$(dioxane) (510 mg, 3.00 mmol of $Me_3CCH_2^-$) were intimately mixed in a Schlenk tube. The tube was cooled to -80 °C, and THF (20 mL) was added. When the temperature was raised to -20 °C, the solution became orange-red (ν_{NO} 1588 cm^{-1}), a feature indicative of the formation of $Cp^*Mo(NO)(CH_2CMe_3)_2$. The reaction mixture was maintained at

temperatures below 0 °C as the solvent was removed in vacuo. The remaining red solid was then suspended in Et_2O (20 mL). While this suspension was being rapidly stirred, deaerated water (~0.7 mL) was added, thereby producing a red solution and a brown precipitate. After 15 min, the mixture was filtered through a column of alumina I (3 x 3 cm), and the column was rinsed with Et_2O (75 mL). The combined filtrates were taken to dryness. The red solid was dissolved in THF (5 mL), and water (0.5 mL) was added. The mixture was stirred for 6 h, whereupon it was filtered through a column of alumina I (2 x 6 cm) supported on a frit. The filtrate was taken to dryness, and the residue was crystallized from hexanes/Et_2O (5:1) to obtain black crystals of **4.2** (451 mg, 88% yield).

4.2.7 Preparation of $[Cp^*Mo(NO)(CH_2CMe_2Ph)]_2$-(μ-O) (4.3)

Solid $Cp^*Mo(NO)Cl_2$ (664 mg, 2.00 mmol) and solid $(PhMe_2CCH_2)_2Mg{\cdot}X$(dioxane) (398 mg, 3.90 mmol of $PhMe_2CCH_2^-$) were intimately mixed in a Schlenk tube. The tube was cooled to -80 °C, and THF (20 mL) was added. Upon being warmed to -20 °C, the solids dissolved and the solution became red (ν_{NO} 1586 cm^{-1}), thereby indicating the formation of $Cp^*Mo(NO)(CH_2CMe_2Ph)_2$. The solution was warmed to room temperature and stirred for 1 h, and then the solvent was removed in vacuo. The residues were suspended in Et_2O/hexanes (50 mL, 4:1 mixture), the suspension was stirred vigorously, and deaerated water (0.4 mL) was added. The solution quickly became deep red, and an oily beige precipitate formed on the sides of the Schlenk tube. After 10 min, the reaction mixture was filtered through alumina I (2 x 6 cm) supported on a frit. Removal of the solvent from the filtrate left a red oil. This oil was dissolved in pentane and transferred to an alumina I column (2 x 4 cm) supported on a frit. The column was washed with pentane (100 mL), and the washes were discarded. Complex **4.3** was then removed from the column with Et_2O (100 mL). Solvent was removed from the red Et_2O

filtrate, and the residue was dried in vacuo for 48 h at 35 - 40 °C. The red solid thus obtained tended to be somewhat oily, presumably reflecting its contamination with Me_3CPh. Crystallization of this residue from pentane yielded 390 mg (50% yield) of analytically pure **4.3** as dark red needles. Subsequent crops of crystals obtained from the supernatant liquid were too oily to be isolated in analytically pure form.

4.2.8 Preparation of $[Cp^*Mo(NO)(o\text{-tolyl})]_2$-(μ-O) (4.4)

$Cp^*Mo(NO)Cl_2$ (664 mg, 2.00 mmol) was partially dissolved in THF (10 mL) and cooled to -50 °C. A single aliquot of (*o*-tolyl)MgCl (4.2 mL of a 1.0 M THF solution, 4.2 mmol) was added via syringe to the dichloride slurry. The resulting purple solution of $Cp^*Mo(NO)(o\text{-tolyl})_2$ (ν_{NO} 1601 cm^{-1}) was immediately treated with deaerated water (0.1 mL) at -50 °C. The purple solution changed instantly to red-brown. The volume of the solution was reduced to 3 mL in vacuo, and it was transferred to the top of an alumina III column (2 x 5 cm). A brown band was eluted from the column with acetone and collected in a flask. Slow evaporation of the acetone solvent from the eluate in air afforded 512 mg (71% yield) of **4.4** as medium-brown microcrystals which were washed with pentane (10 mL) and dried in vacuo.

4.2.9 Preparation of $[Cp^*Mo(NO)(Ph)]_2$-(μ-O) (4.5)

$Cp^*Mo(NO)Cl_2$ (332 mg, 1.00 mmol) and $Ph_2Mg{\cdot}X$(dioxane) (356 mg, 2.02 mmol of Ph^-) were intimately mixed in a Schlenk tube. The tube and contents were then cooled to -80 °C, and THF (10 mL) was added to the solids by vacuum transfer. The Schlenk tube and its contents were then quickly warmed to room temperature by immersing the tube for 1 min in a warm water bath. The violet solution of $Cp^*Mo(NO)Ph_2$ (ν_{NO} 1615 cm^{-1}) thus produced was taken to dryness, and the residue was redissolved in Et_2O (50 mL) and the solution filtered on Celite (1 x 4 cm). The violet filtrate was cooled to 0 °C and treated

with water (50 μL), whereupon the color of the solution changed to red-brown within 1 min. The ether was removed from the final mixture in vacuo, and the residue was crystallized from CH_2Cl_2/hexanes (1:1) to obtain 269 mg (78% yield) of **4.5** as a dark brown microcrystalline solid.

4.2.10 Preparation of $Cp^*W(O)_2$(aryl) [aryl = Ph (4.6), *p*-tolyl (4.7), and *o*-tolyl (4.8)]

The three pentamethylcyclopentadienyl aryl dioxo complexes were prepared in a similar manner, the synthesis of $Cp^*W(O)_2$(*p*-tolyl) (**4.7**) being presented below as a representative example.

A sample of $Cp^*W(NO)$(*p*-tolyl)$_2$ (200 mg, 0.377 mmol) was dissolved in Et_2O (20 mL). The resulting blue solution was stirred at room temperature, and a single drop of deaerated H_2O was added, whereupon the solution became green immediately. The solution was taken to dryness in vacuo, and the brown residue was extracted with Et_2O (5 x 10 mL). The combined extracts were filtered through Florisil (2 x 3 cm), concentrated under reduced pressure, and placed in a freezer overnight. These operations induced the crystallization of 70 mg (42% yield) of colorless, microcrystalline $Cp^*W(O)_2$(*p*-tolyl) **4.7**, which was collected by filtration.

Similarly, $Cp^*W(O)_2Ph$ (**4.6**) and $Cp^*W(O)_2$(*o*-tolyl) (**4.8**) were obtained in 45 and 80% yield from $Cp^*W(NO)Ph_2$ and $Cp^*W(NO)$(*o*-tolyl)$_2$, respectively. The three aryl dioxo complexes could also be obtained in comparable yields by treatment of their diaryl precursors in the solid state with O_2.

4.2.11 Preparation of $CpW(O)_2$(*o*-tolyl) (4.9)

$CpW(NO)Cl_2$ (1050 mg, 3.00 mmol) and (*o*-tolyl)$_2$Mg·*X*(dioxane) (960 mg, 6.00 mmol of *o*-tolyl$^-$) were intimately mixed in a Schlenk tube. The tube and contents were then cooled to -196 °C, and THF (50 mL) was added by vacuum transfer. The Schlenk tube and its contents were warmed to 10 °C over a period of 2 h. The violet solution of $CpW(NO)$(*o*-tolyl)$_2$ (ν_{NO} 1601 cm^{-1}) thus produced was taken to dryness, and the residue was extracted with Et_2O (5 x 50 mL) and the combined extracts filtered through Celite (3 x 4 cm). The violet filtrate was concentrated to one-half its original volume and treated with 30% aqueous hydrogen peroxide (~0.2 mL), whereupon the color of the solution changed to red-amber within seconds.[5] The reaction mixture was taken to dryness in vacuo and the resulting brown powder extracted with acetone (10 mL). The acetone solution was applied to the top of an alumina I column (2 x 5 cm), and the column was eluted with acetone (100 mL). The eluate was taken to dryness and the residue was extracted with Et_2O (5 x 20 mL). The ether extracts were filtered through Celite (1 x 5 cm), concentrated, and maintained at -30 °C for two weeks. These operations induced the deposition of 583 mg (52% yield) of complex **4.9** as a pale amber, microcrystalline solid.

4.2.12 Reaction of $Cp^*Mo(NO)(CH_2SiMe_3)_2$ with $^{18}OH_2$

$Cp^*Mo(NO)(CH_2SiMe_3)_2$ (24 mg, 0.055 mmol) was dissolved in C_6D_6 (1.2 mL) and was treated with excess $^{18}OH_2$ (10 μL). After being shaken vigorously for 2 min, the sample was filtered through a column of Celite (0.3 x 0.5 cm) into an NMR tube to remove residual $^{18}OH_2$. Approximately 95 % of the signal intensity in the ^{1}H NMR spectrum of the filtrate was attributable to $[Cp^*Mo(NO)(CH_2SiMe_3)]_2$-(μ-^{18}O). A signal at δ 0.00 ppm confirmed the presence of Me_4Si, the byproduct of the hydrolysis reaction.

4.2.13 Reaction of $Cp^*Mo(NO)(CH_2SiMe_3)_2$ with D_2O

$Cp^*Mo(NO)(CH_2SiMe_3)_2$ (20 mg, 0.046 mmol) was dissolved in C_6D_6 (1.2 mL) and treated with excess D_2O (10 μL). After being shaken vigorously for 2 min, the sample was filtered through Celite (0.3 x 0.5 cm) into an NMR tube to remove unused D_2O. The ^1H NMR spectrum of the filtrate revealed the presence of 2 equiv of DH_2CSiMe_3 by its characteristic singlet at δ 0.00 and its 1:1:1 triplet (J_{HD} = 2.1 Hz) at a slightly higher field.

4.2.14 Reaction of 4.1 with O_2

$[Cp^*Mo(NO)(CH_2SiMe_3)]_2$-(μ-O) (100 mg, 0.14 mmol) was dissolved in hexanes (5 mL). The atmosphere in the flask containing the deep red solution was evacuated, and the vessel was then pressurized to 1 atm with O_2. After being stirred at room temperature for 24 h, the resulting amber solution was taken to dryness in vacuo. Extraction of the residue with Et_2O and subsequent crystallization afforded yellow-brown crystals of $[Cp^*Mo(O)_2]_2$-(μ-O) (43 mg, 56% yield).[6] There was no evidence for any $Cp^*Mo(O)_2(CH_2SiMe_3)$ having been formed.

Data determined for $[Cp^*Mo(O)_2]_2$-(μ-O) in this work are as follows: Anal. calcd for $C_{20}H_{30}O_5Mo_2$: C, 44.29; H, 5.58. Found: C, 44.31; H, 5.67. IR (Nujol mull): $\nu_{Mo=O}$ 910 (s), 878 (s) cm^{-1}; $\nu_{Mo-O-Mo}$ 762 (s, br) cm^{-1}. ^1H NMR (C_6D_6): δ 1.78 (s). ^1H NMR (THF-d_8): δ 1.94 (s). Low-resolution mass spectrum (probe temperature 120 °C): *m/z* 526 (P^+-O).

In related experiments, various solutions of complexes **4.2** and **4.5** were allowed to evaporate to dryness in a beaker in the atmosphere. The only organometallic complex detectable in each dried residue by ^1H NMR spectroscopy was $[Cp^*Mo(O)_2]_2$-(μ-O).

4.2.15 Reaction of 4.1 with Excess Water

Treatment of $[Cp^*Mo(NO)(CH_2SiMe_3)]_2$-(μ-O) (28 mg) with an excess of water (25 μL) in THF-d_8 (0.8 mL) for 48 h afforded an amber solution whose ^1H NMR spectrum showed $[Cp^*Mo(O)_2]_2$-(μ-O) (δ 1.94) to constitute > 95 % of the signal intensity. The other principal signals were due to H_2O and Me_4Si.

4.2.16 Characterization Data for Complexes 4.1 - 4.9

Table 4.1 Numbering Scheme, Color, Yield and Elemental Analysis Data

Complex	no.	Color (yield, %)	Anal. Found (Calcd)		
			C	H	N
$[Cp^*Mo(NO)(CH_2SiMe_3)]_2$-(μ-O)	**4.1**	red-black (75)[a]	47.07(47.16)	7.64 (7.35)	3.85 (3.93)
$[Cp^*Mo(NO)(CH_2CMe_3)]_2$-(μ-O)	**4.2**	black (88)[a]	53.00 (52.94)	7.74 (7.70)	3.95 (4.12)
$[Cp^*Mo(NO)(CH_2CMe_2Ph)]_2$-(μ-O)	**4.3**	dark red (50)[a]	59.33 (59.69)	7.15 (7.01)	3.23 (3.48)
$[Cp^*Mo(NO)(o\text{-tolyl})]_2$-(μ-O)	**4.4**	brown (71)[a]	56.68 (56.67)	6.28 (6.15)	3.77 (3.89)
$[Cp^*Mo(NO)(Ph)]_2$-(μ-O)	**4.5**	dark brown (78)[a]	54.73 (55.50)	5.81 (5.82)	4.00 (4.04)
$Cp^*W(O)_2Ph$	**4.6**	colorless (45)[b]	44.93 (44.88)	4.68 (4.71)	0.00 (0.00)
$Cp^*W(O)_2(p\text{-tolyl})$	**4.7**	colorless (42)[b]	46.03 (46.17)	5.05 (5.01)	0.00 (0.00)
$Cp^*W(O)_2(o\text{-tolyl})$	**4.8**	colorless (80)[b]	46.65 (46.17)	5.11 (5.01)	0.00 (0.00)
$CpW(O)_2(o\text{-tolyl})$	**4.9**	colorless (52)[c]	38.80 (38.74)	3.30 (3.25)	0.00 (0.00)

[a] Yield based on $Cp^*Mo(NO)Cl_2$.

[b] Yield based on $Cp^*W(NO)(aryl)_2$ (aryl = Ph, *p*-tolyl, *o*-tolyl).

[c] Yield based on $CpW(NO)Cl_2$.

Table 4.2 Mass Spectral and Infrared Data

no.	MS *m/z*[a]	temp[b] (°C)	IR (Nujol mull) ν_{NO}	ν_{Mo-O}	$\nu_{W=O}$
4.1	716 [P^+], 686 [P^+-NO]	120	1576, 1561	774, 750	———
4.2	680 [P^+], 609 [P^+-CH_2CMe_3]	200	1582, 1566	768	———
4.3	805 [P^+]	100	1578, 1564	774	———
4.4	720 [P^+], 602 [P^+-NO-tolyl]	225	1584, 1576, 1568	771, 743	———
4.5	692 [P^+], 662 [P^+-NO]	100	1589, 1575, 1554	803, 785	———
4.6	428 [P^+]	120	———	———	938, 900
4.7	442 [P^+]	100	———	———	939, 901
4.8	442 [P^+]	100	———	———	940, 899
4.9	372 [P^+], 354 [P^+-O]	120	———	———	951, 910

[a] *m/z* values are for the highest intensity peak of the calculated isotopic cluster.

[b] Probe temperatures.

Table 4.3 ^1H and $^{13}C\{^1H\}$ NMR Spectral Data

no.	^1H NMR (δ, C_6D_6)	$^{13}C\{^1H\}$ NMR (δ, C_6D_6)
4.1	Isomer A (90%) 1.59 (s, 30H, $C_5(CH_3)_5$) 0.84 (d, 2H, J_{HH} = 12.3 Hz, $CH_AH_BSiMe_3$) 0.75 (d, 2H, J_{HH} = 12.3 Hz, $CH_AH_BSiMe_3$) 0.45 (s, 18H, $Si(CH_3)_3$) Isomer B (10%) 1.71 (s, 30H, $C_5(CH_3)_5$) methylene protons not observed 0.42 (s, 18H, $Si(CH_3)_3$)	Isomer A 112.60 ($C_5(CH_3)_5$) 36.50 (CH_2SiMe_3) 9.96 ($C_5(CH_3)_5$) 2.83 ($CH_2Si(CH_3)_3$) Isomer B 113.50 ($C_5(CH_3)_5$) 36.20 (CH_2SiMe_3) 10.26 ($C_5(CH_3)_5$) 3.43 ($CH_2Si(CH_3)_3$)

4.2	Isomer A (100%) 1.80 (d, 2H, J_{HH} = 13.2 Hz, $CH_AH_BCMe_3$) 1.74 (d, 2H, J_{HH} = 13.2 Hz, $CH_AH_BCMe_3$) 1.63 (s, 30H, $C_5(CH_3)_5$) 1.45 (s, 18H, $C(CH_3)_3$)	Isomer A 112.44 ($C_5(CH_3)_5$) 68.06 ($C(CH_3)_3$) 33.89 (CH_2CMe_3) 28.05 ($C(CH_3)_3$) 9.81 ($C_5(CH_3)_5$)
4.3	Isomer A (100 % 7.71 (d, 4H, ortho protons) 7.32 (t, 4H, meta protons) 7.10 (t, 2H, para protons) 2.18 (d, 2H, J_{HH} = 12.4 Hz, $CH_AH_BCMe_2Ph$) 2.04 (d, 2H, J_{HH} = 12.4 Hz, $CH_AH_BCMe_2Ph$) 1.84 (s, 6H, $CH_2C(CH_3)_A(CH_3)_BPh$) 1.78 (s, 6H, $CH_2C(CH_3)_A(CH_3)_BPh$) 1.56 (s, 30H, $C_5(CH_3)_5$)	Isomer A 155.42 (C_{ipso}) 128.40 (C_{phenyl}) 125.91 (C_{phenyl}) 125.34 (C_{phenyl}) 112.83 ($C_5(CH_3)_5$) 69.91 ($CH_2C(CH_3)_2Ph$) 43.78 ($CH_2C(CH_3)_2Ph$) 32.02 $(CH_3)_A$ 30.77 $(CH_3)_B$ 9.76 ($C_5(CH_3)_5$)
4.4	Isomer A (65 %) 7.80 - 7.05 (m, 8H, aryl protons) 2.40 (s, 6H, aryl CH_3) 1.59 (s, 30H, $C_5(CH_3)_5$) Isomer B (35 %) 7.80 - 7.05 (m, 8H, aryl protons) 2.29 (s, 6H, aryl CH_3) 1.62 (s, 30H, $C_5(CH_3)_5$)	*c*
4.5	Isomer A (97%) 7.77 (d, 4H, ortho protons) 7.31 (t, 4H, meta protons) 7.21 (m, 2H, para protons) 1.56 (s, 30H, $C_5(CH_3)_5$) Isomer B (3%) 1.62 (s, 30H, $C_5(CH_3)_5$) other signals not observed	Isomer A 178.10 (C_{ipso}) 135.30 (C_{ortho}) 127.50 (C_{meta}) 127.21 (C_{para}) 114.45 ($C_5(CH_3)_5$) 9.69 ($C_5(CH_3)_5$) Isomer B signals not observed
4.6	7.52 - 7.46 (m, 2H, ortho protons) 7.12 - 6.98 (m, 3H, other aryl protons) 1.66 (s, 15H, $C_5(CH_3)_5$)	*c*
4.7[a]	7.21 (d, 2H, J = 10.1 Hz, aryl protons) 7.11 (d, 2H, J = 10.1 Hz, aryl protons) 2.30 (s, 3H, p-CH_3) 2.01 (s, 15H, $C_5(CH_3)_5$)	C_{ipso} not observed 141.15 (C_{ortho}) 141.01 (C_{para}) 129.69 (C_{meta}) 119.40 ($C_5(CH_3)_5$) 21.52 (p-CH_3) 11.03 ($C_5(CH_3)_5$)

4.8	7.58 (dd, 1H, J = 7.5, 1.5 Hz, ortho proton) 7.20 (d, 1H, J = 7.8 Hz, aryl proton) 7.04 (m, 1H, aryl proton) 6.95 (m, 1H, aryl proton) 2.26 (s, 3H, *o*-CH_3) 1.67 (s, 15H, $C_5(CH_3)_5$)	*c*
4.9[b]	7.80 (m, 1H, aryl proton) 7.12 - 6.98 (m, 3H, aryl protons) 5.68 (s, 5H, C_5H_5) 2.27 (s, 3H, *o*-CH_3)	*c*

[a] Both spectra recorded in CD_2Cl_2.

[b] Relaxation delays of 20 s were used to ensure full integration of Cp proton signals.

[c] Not recorded.

4.2.17 Other Characterization Data

Table 4.4 Electrochemical Data for **3.8** and **4.1**[a]

complex 3.8			
scan rate (ν, Vs^{-1})	$E^{\circ\prime}{}_1$[b] (V)	ΔE[c]	$i_{p,a}/i_{p,c}$[d]
0.80	-1.52	0.69 (0.20)	1.0
0.60	-1.55	0.47 (0.18)	1.0
0.40	-1.54	0.49 (0.15)	1.0
0.20	-1.56	0.36 (0.12)	1.0
0.10	-1.59	0.28 (0.10)	0.9

complex 4.1			
scan rate (ν, Vs^{-1})	$E^{\circ\prime}{}_1$[b] (V)	ΔE[c]	$i_{p,a}/i_{p,c}$[d]
0.80	-1.37	0.19 (0.18)	1.0
0.60	-1.38	0.17 (0.16)	1.0
0.40	-1.38	0.15 (0.14)	1.0
0.20	-1.39	0.12 (0.11)	1.0
0.10	-1.37	0.09 (0.10)	1.0

[a] In THF containing 0.10 M [n-Bu_4N]PF_6, at Pt-bead working electrode. Potentials measured vs Ag wire.

[b] Defined as the average of the cathodic and anodic peak potentials (± 0.02 V).

[c] Defined as the separation of the cathodic and anodic peak potentials. Values of ΔE given in brackets are for the Cp_2Fe/Cp_2Fe^+ couple under the same conditions.

[d] Ratio of anodic peak current to cathodic peak current.

4.2.18 Kinetic Data for the Conversion of 3.8 to 4.1

Table 4.5 Variation of Water Concentration Data (Absorbance at 404 nm vs time)

	water concentration ($\times 10^2$ M)					
time(s)	**0.624**	**1.09**	**1.56**	**3.12**	**4.59**	**6.24**
0	0.0675	0.0560	0.0342	0.0667	0.0529	0.0815
100	0.0781	0.0738	0.0571	0.1012	0.1049	0.1483
200	0.0880	0.0905	0.0786	0.1386	0.1526	0.2038
300	0.0982	0.1068	0.0999	0.1745	0.1966	0.2526
400	0.1080	0.1226	0.1207	0.2083	0.2370	0.2955
500	0.1177	0.1381	0.1411	0.2404	0.2735	0.3330
600	0.1273	0.1532	0.1606	0.2704	0.3069	0.3657
700	0.1369	0.1683	0.1799	0.2991	0.3368	0.3942
800	0.1464	0.1827	0.1986	0.3256	0.3637	0.4191
900	0.1557	0.1970	0.2163	0.3505	0.3881	0.4403
1000	0.1650	0.2113	0.2338	0.3739	0.4099	0.4589
1100	0.1743	0.2250	0.2508	0.3954	0.4295	0.4749
1200	0.1831	0.2384	0.2670	0.4157	0.4468	0.4883
1300	0.1920	0.2517	0.2830	0.4347	0.4627	0.5003
1400	0.2007	0.2644	0.2979	0.4519	0.4768	0.5107
1500	0.2094	0.2770	0.3126	0.4682	0.4894	0.5193
A_∞	0.90	0.86	0.80	0.73	0.61	0.58
k_{obs} ($\times 10^4$ s^{-1})	1.245	2.138	3.020	6.273	10.27	14.10

Table 4.6 Rate Constants (25 °C) for Various Concentrations of **3.8** using H_2O and D_2O

	$[H_2O] = 5.55 \times 10^{-3}$ M	$[D_2O] = 5.55 \times 10^{-3}$ M
[3.15] (M)	k_{obs} (s^{-1})	
2.56×10^{-4}	1.668×10^{-4}	
3.84×10^{-4}	1.844×10^{-4}	3.170×10^{-5}
5.12×10^{-4}	1.821×10^{-4}	3.690×10^{-5}
6.40×10^{-4}	1.798×10^{-4}	3.591×10^{-5}
1.15×10^{-3}	1.446×10^{-4}	
1.58×10^{-3}	1.436×10^{-4}	
2.54×10^{-3}	1.577×10^{-4}	

Table 4.7 Rate Constants as a Function of Temperature Data (Absorbance at 404 nm vs time)

	Temperature (°C)			
time(s)	15.0	20.0	25.0	30.0
0	0.029	0.055	0.070	0.070
300	0.031	0.058	0.073	0.112
600	0.055	0.097	0.127	0.186
900	0.083	0.139	0.181	0.260
1200	0.113	0.182	0.236	0.328
1500	0.145	0.225	0.287	0.391
1800	0.174	0.267	0.337	0.447
2100	0.206	0.308	0.383	0.502
2400	0.237	0.347	0.427	0.549
2700	0.266	0.385	0.468	0.593
3000	0.295	0.421	0.506	0.631
A_∞	1.17	1.17	1.17	1.17
k_{obs} ($\times 10^4$ s^{-1})	0.959	1.438	1.839	2.509

4.3 Results and Discussion

4.3.1 Two Similar Reactions?

This section begins with the comparison of two reactions which, at first glance, would be expected to be quite similar. Previous work in these laboratories[7,8] has established that the preparation of the tungsten dialkyl complexes $Cp'W(NO)(CH_2SiMe_3)_2$ is straightforward via reaction of $Cp'W(NO)I_2$ with 2 equiv of a (trimethylsilyl)methyl Grignard reagent followed by hydrolysis with water, i.e.

$$Cp'W(NO)I_2 \xrightarrow[2)\ \text{excess } H_2O]{1)\ 2\ Me_3SiCH_2MgCl,\ Et_2O} Cp'W(NO)(CH_2SiMe_3)_2 \qquad (4.1)$$

Conversion 4.1 consistently affords the $Cp'W(NO)(CH_2SiMe_3)_2$ complexes in 80% isolated yields.[9] A similar reaction involving one of the congeneric molybdenum diiodide starting materials is not as straightforward. Thus, treating $Cp^*Mo(NO)I_2$ with 2 equiv of an ethereal solution of Me_3SiCH_2MgCl followed by quenching with water leads to the formation of three isolable organometallic products,[2,10] the *minor* one being the expected $Cp^*Mo(NO)(CH_2SiMe_3)_2$ (eq 4.2).

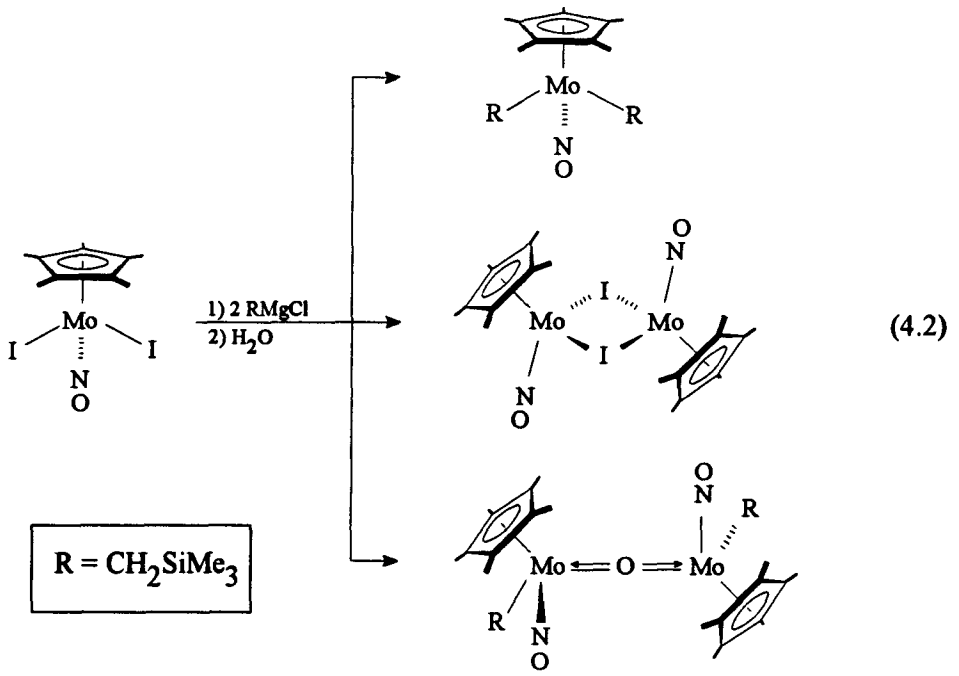

(4.2)

Hence, the desired dialkyl complex is indeed among the final isolated products but in abysmal yield. $[Cp^*Mo(NO)I]_2$ results via the loss of iodide from the $[Cp^*Mo(NO)I_2]^{\cdot-}$ radical anion, which is the first intermediate formed in metathesis reactions of this type.[11,12] However, the key point to emerge from reaction 4.2 is that, unlike its tungsten congener, $Cp^*Mo(NO)(CH_2SiMe_3)_2$ is unstable with respect to hydrolysis.

During efforts to synthesize tungsten diaryl and molybdenum dialkyl and diaryl nitrosyl complexes it was very obvious that these desired compounds were extremely sensitive to moisture, thus prompting me to develop a new synthetic strategy to these complexes (Chapters 2 and 3). Having a set of $Cp'M(NO)R_2$ complexes available, I was then able to conduct a systematic investigation of their reactions with water.

4.3.2 Reactions of $Cp^*Mo(NO)R_2$ Complexes with Water

Five dialkyl and diaryl complexes of molybdenum (**2.1**, **2.3**, **3.6**, **3.7** and **3.8**) have been reacted with water, and it has been found that all five react in a similar manner. Thus, the transformations of $Cp^*Mo(NO)Cl_2$ to $[Cp^*Mo(NO)R]_2$-(μ-O) (R = alkyl or aryl) via $Cp^*Mo(NO)R_2$, as portrayed in eq 4.3, appear to be a general phenomenon.[13]

$$Cp^*Mo(NO)Cl_2 \xrightarrow[\text{or } R_2Mg]{2\ RMgCl} Cp^*Mo(NO)R_2 \xrightarrow{H_2O} 1/2\ [Cp^*Mo(NO)(R)]_2\text{-}(\mu\text{-}O) \quad (4.3)$$

R = alkyl or aryl

As indicated in eq 4.3, both RMgX and R_2Mg reagents may be used to generate the requisite $Cp^*Mo(NO)R_2$ species in situ. Subsequent hydrolysis then affords a variety of bimetallic bridging oxo complexes (**4.1 - 4.5**) whose physical properties are collected in Tables 4.1 - 4.3. The yields of the bimetallic complexes are higher (based on $Cp^*Mo(NO)Cl_2$) if their precursor $Cp^*Mo(NO)R_2$ complexes are generated in situ and not isolated before their reactions with water. For example,

$[Cp^*Mo(NO)(CH_2SiMe_3)]_2$-(μ-O) is best synthesized by generating $Cp^*Mo(NO)(CH_2SiMe_3)_2$ in Et_2O, treating the solution with water, and then chromatographing the final mixture on alumina III with Et_2O as eluant (eq 4.4). Nevertheless, it can also be obtained by treatment of isolated $Cp^*Mo(NO)(CH_2SiMe_3)_2$ with water in benzene or THF (eq 4.5).

$$Cp^*Mo(NO)Cl_2 \xrightarrow[2)\ \text{excess } H_2O]{1)\ 2\ Me_3SiCH_2MgCl,\ Et_2O} [Cp^*Mo(NO)(CH_2SiMe_3)]_2\text{-}(\mu\text{-}O) \qquad (4.4)$$

(75% based on $Cp^*Mo(NO)Cl_2$)

$$Cp^*Mo(NO)(CH_2SiMe_3)_2 \xrightarrow{H_2O} [Cp^*Mo(NO)(CH_2SiMe_3)]_2\text{-}(\mu\text{-}O) \qquad (4.5)$$

(95% based on $Cp^*Mo(NO)(CH_2SiMe_3)_2$)

(57% based on $Cp^*Mo(NO)Cl_2$)

The transformation from $Cp^*Mo(NO)(CH_2SiMe_3)_2$ to **4.1** is clean and chemically straightforward (eq 4.5); however, the highest yield of complex **4.1** is obtained if one does not isolate the dialkyl complex before conducting the hydrolysis reaction.

Several features of these otherwise straightforward conversions (4.3) merit some comment. The relative reactivities of $Cp^*Mo(NO)R_2$ complexes towards water are R = aryl >> CH_2SiMe_3 > CH_2CMe_2Ph >> CH_2CMe_3. Thus, treatment of $Cp^*Mo(NO)(aryl)_2$ complexes with water causes their instantaneous consumption.[14] The (trimethylsilyl)methyl and neophyl derivatives (**4.1** and **4.3**) are formed in about 5-10 min in Et_2O (with which water is immiscible) at ambient temperatures. However, $Cp^*Mo(NO)(CH_2CMe_3)_2$ takes several hours at 20 °C to decompose to **4.2** in THF (with which water is miscible) even in the presence of 30 equiv of water.

The reason other $CpMo(NO)R_2$ complexes prepared in Chapter 3 were not reacted with water is because competitive thermal decomposition pathways complicate these

hydrolysis reactions. This feature is best exemplified by $CpMo(NO)(CH_2CMe_3)_2$ which at room temperature decomposes to $[CpMo(NO)(CHCMe_3)]_2$ (Chapter 5) markedly faster than it reacts with water.[15] Additionally, attempts to synthesize the Cp analogues of **4.4** and **4.5** have been thwarted by the thermal instability of the precursor $CpMo(NO)(aryl)_2$ complexes (Chapter 2).[14]

4.3.3 Physical Properties of $[Cp^*Mo(NO)R]_2$-(μ-O) (R = alkyl, aryl) Complexes

These bimetallic complexes are moderately air-stable as solids, but in solution they are generally air-sensitive and decompose eventually to $[Cp^*Mo(O)_2]_2$-(μ-O). This latter result has been established specifically for complexes **4.1**, **4.2** and **4.5** (vide infra). In contrast, complex **4.4** is sufficiently air-stable to be crystallized in air by slow evaporation of solvent. Perhaps the steric bulk of the *ortho*-methyl groups in $[Cp^*Mo(NO)(o\text{-tolyl})]_2$-(μ-O) provides enough protection for the metal centers to shield them from attack by further water or oxygen. The alkyl derivatives (**4.1** - **4.3**) are dark red-brown to red-black crystalline solids which exhibit high thermal stability. For instance, thermolysis of a sample of **4.1** in benzene in an NMR tube at 80 °C for 2 days results in no detectable change in the NMR spectrum of the sample. The aryl derivatives (**4.4** and **4.5**) are chocolate brown and tend to be less crystalline than their alkyl congeners. The elemental analysis, IR, mass spectral, and NMR data for complexes **4.1** - **4.5** are collected in Tables 4.1 - 4.3.

4.3.4 Spectroscopic Properties of $[Cp^*Mo(NO)R)]_2$-(μ-O) Complexes

Since **4.1** is the prototypal complex in this family, its properties will be considered in some detail. The 300 MHz ^1H NMR spectrum of $[Cp^*Mo(NO)(CH_2SiMe_3)]_2$-(μ-O) in C_6D_6 exhibits an *AB* pattern at 0.84 and 0.75 ppm ($^2J_{HH}$ = 12.3 Hz) for the two pairs of diastereotopic methylene protons and singlet resonances at 1.59 and 0.45 ppm due to the

methyl protons of the Cp^* ligands and the methyl groups attached to the silicon atoms, respectively. In comparison, the two pairs of diastereotopic methylene protons in $Cp^*Mo(NO)(CH_2SiMe_3)_2$ give rise to an *AX* doublet of doublets at 2.21 and -1.17 ppm ($^2J_{HH}$ = 10.8 Hz) while the Cp^* and $SiMe_3$ protons resonate at 1.49 and 0.37 ppm, respectively. The principal feature that differentiates the two spectra is the existence of two small singlets at 1.71 and 0.42 ppm in the proton NMR spectrum of $[Cp^*Mo(NO)(CH_2SiMe_3)]_2$-(μ-O). These latter resonances can be assigned to the Cp^* and $SiMe_3$ protons, respectively, of a minor isomer of **4.1**. However, signals due to the methylene protons of the minor isomer are not observable. The isomers are probably diastereomers, since they do not interconvert thermally (vide supra), and have thus been assigned the molecular structures shown in Figure 4.1.

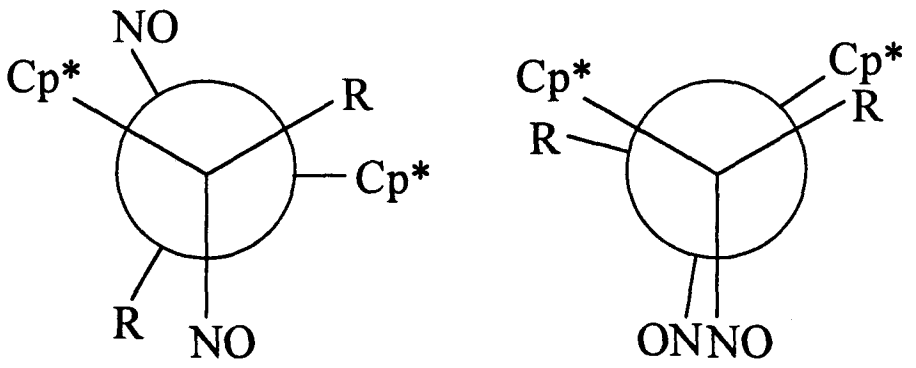

Isomer A (SR) **Isomer B (SS)**

Figure 4.1 Designation of isomers for $[Cp^*Mo(NO)(R)]_2$-(μ-O) complexes. Newman projections are drawn down the Mo-O-Mo axes and are approximate representations.

The solid-state molecular structure of $[Cp^*Mo(NO)(CH_2SiMe_3)]_2$-(μ-O) reveals it to be the *SR* isomer with the two chiral $[Cp^*Mo(NO)(CH_2SiMe_3)]$ units being twisted by 90 ° with respect to each other about the Mo-O-Mo bond.[16] The other diastereomer probably has the same relative configurations at the metal centers, i.e. *RR* or *SS*, the latter

isomer being shown in Figure 4.1. The *SR* isomer is probably the dominant form in solution, as molecular models show that either the *RR* or *SS* isomers possess severe steric interactions between the methyl groups of the Cp^* ligand on one molybdenum with the bulky CH_2SiMe_3 group on the other Mo center. As summarized in Table 4.3, where the major and minor isomers are designated as **A** and **B**, respectively, the ratios of $[Cp^*Mo(NO)R]_2$-(μ-O) isomers are generally dependent on the steric bulk of the ancillary ligands. Consistent with the view that steric factors control the ratio of the two isomers is the fact that for $[Cp^*Mo(NO)(CH_2SiMe_3)]_2$-(μ-O) the ratio major:minor is 9:1 while the less sterically encumbered $[CpMo(NO)(CH_2SiMe_3)]_2$-(μ-O) exhibits an isomer ratio of major:minor = 3:1.[10] The most sterically crowded complex $[Cp^*Mo(NO)(CH_2CMe_3)]_2$-(μ-O) exhibits an isomer ratio of at least 50:1.

The IR spectral features exhibited by these bimetallic μ-oxo complexes (Table 4.2) are different from those displayed by their parent bis(hydrocarbyl) complexes, $Cp^*Mo(NO)R_2$. The IR spectra of $[Cp^*Mo(NO)R]_2$-(μ-O) exhibit strong bands in the region 803 - 743 cm^{-1} which are diagnostic of Mo-O-Mo vibrations.[17] The nitrosyl-stretching frequencies of these bimetallic complexes are some 5-55 cm^{-1} (average = 23 cm^{-1}) lower in energy than the ν_{NO} bands exhibited by their parent bis(hydrocarbyl) complexes. This spectral feature is indicative of there being more electron density available on the molybdenum centers for backbonding into the antibonding orbitals of the nitrosyl ligands in these bridging oxo complexes than in their parent dialkyl and diaryl complexes. Therefore, this would suggest that the bridging oxo ligand is providing each molybdenum center with one electron in the σ Mo-O link and some electron density associated with the lone pairs of electrons in its *p* orbitals. This view is in accord with the X-ray crystallographic analysis of $[Cp^*Mo(NO)(CH_2SiMe_3)]_2$-(μ-O).[16] The oxo bridge between the two molybdenum centers is essentially linear and the two $\{Cp^*Mo(NO)(CH_2SiMe_3)\}$ units are twisted by

approximately 90° with respect to one another. This, taken together with the short Mo-O bond lengths (ca. 1.90 Å) which are intermediate between typical Mo-O and Mo=O bond lengths,[18] suggests that there is a considerable degree of multiple bonding in the central Mo-O-Mo linkage of the bimetallic complex. If the Mo-O-Mo axis is defined as the z axis, the Mo=O=Mo π interaction involves overlap between an empty *d* orbital on each of the {$Cp^*Mo(NO)(CH_2SiMe_3)$} groups with the appropriate filled *p* orbital (i.e. p_x for one group and p_y for the one orthogonal to it) on the bridging oxygen atom. This localized view of the π bonding in the Mo=O=Mo bridge suggests that each Mo center thus achieves the favored 18-valence-electron configuration. Therefore, in these complexes the oxo ligand may be regarded as a formal 6-electron donor, three electrons being donated to each metal center so that the metal can reach electronic saturation. These complexes are very similar to the monomeric 18-electron alkoxyalkyl complexes $Cp^*Mo(NO)(R)(OR)$, in which the alkoxide group also functions as a formal 3-electron donor to the 15-electron $Cp^*Mo(NO)(R)$ fragments.[19]

4.3.5 Related Bridging Oxo Complexes

The bridging oxo complexes presented in this chapter have valence isoelectronic analogues in Group 4. Specifically, $[Cp_2Zr(Me)]_2$-(μ-O),[20] $[Cp_2Hf(Me)]_2$-(μ-O),[21] and $[Cp^*_2Zr(H)]_2$-(μ-O)[22] have been prepared from their Cp'_2MR_2 precursors by reaction with water although systematic study of their formation or chemistry has not been reported in the literature. Non-nitrosyl containing complexes having Mo-O-Mo linkages have been characterized as well. For example, $[(HBpz_3)Mo(O)Cl]_2$-(μ-O)[23] and $[Cp^*Mo(O)Cl]_2$-(μ-O)[24] have been structurally characterized, and both were found to contain nearly linear Mo-O-Mo linkages.

In contrast, $[Ir(PPh_3)(NO)]_2$-(μ-O) (the only other oxo-bridged nitrosyl complex that has been structurally characterized) exhibits an acute Ir-O-Ir angle of 82.3 (3)°, long Ir-O

bond lengths of about 1.94 Å and an Ir-Ir separation of 2.55 Å.[25] The $Ir(PPh_3)(NO)$ fragment seemingly would rather engage in metal-metal bonding to satiate its electronic requirements rather than accepting extra electron density from the oxo ligand. This is probably a function of iridium being a softer Lewis acid than molybdenum.

4.3.6 Electrochemical Studies

During previous investigations, we have found the knowledge of fundamental redox properties of organometallic complexes to be a useful guide in directing our studies of their characteristic chemical properties.[11] It was therefore of interest to determine the electrochemical behavior of $Cp^*Mo(NO)(CH_2SiMe_3)_2$ and $[Cp^*Mo(NO)(CH_2SiMe_3)]_2$-(μ-O) as representative examples of their particular classes of compounds. The cyclic voltammogram of $Cp^*Mo(NO)(CH_2SiMe_3)_2$ in THF reveals that it undergoes a quasi-reversible, one-electron reduction at approximately $E^{\circ\prime}$ = -1.55 V vs Ag wire. While the $i_{p,a}/i_{p,c}$ ratio for this feature indicates reversibility, it is clear from the ΔE values (Table 4.4) that electron transfer in this system occurs at a slower rate than for the ferrocene standard. For example, at 0.8 Vs^{-1} the peak separation is about 700 mV and not the 200 mV observed for Cp_2Fe. Compared to the dialkyl and diaryl complexes in Chapters 2 and 3 this phenomenon of quasi-reversibility, while rare in these systems, is observed.[26] Regardless of the kinetics of the electron-transfer step, the reduction potential of $Cp^*Mo(NO)(CH_2SiMe_3)_2$ is comparable to that exhibited by related dialkyl complexes such as $Cp^*Mo(NO)(CH_2CMe_3)_2$ ($E^{\circ\prime}$ = -1.45 V)[27] and $Cp^*W(NO)(CH_2CMe_2Ph)_2$ ($E^{\circ\prime}$ = -1.62 V).[14] Interestingly, no second reduction of $Cp^*Mo(NO)(CH_2SiMe_3)_2$ occurs out to the solvent limit even though the dianion $[Cp^*Mo(NO)(CH_2SiMe_3)_2]^{2-}$ should exist.[14,28]

The cyclic voltammogram of complex **4.1** in THF indicates that the compound undergoes a reversible, one-electron reduction and a second, irreversible, one-electron

reduction. The first reduction potential for **4.1** occurs at $E^{\circ\prime}$= -1.38 V; the linearity of the plot of $i_{p,c}$ vs $\nu^{1/2}$ establishes that this reduction is diffusion controlled. Furthermore, comparison of the $i_{p,a}/i_{p,c}$ and ΔE values for this reduction with the internal Cp_2Fe/Cp_2Fe^+ reference indicates that it is reversible (Table 4.4). The second reduction of complex **4.1** occurs at -2.18 V but is irreversible, thus implying that the compound is not retaining its structural integrity upon addition of the second electron.

Neither molybdenum complex undergoes any oxidation processes up to the solvent limit of 0.80 V vs Ag wire. Thus, with the information gleaned from this study, it seems that the preparation and isolation of $[Cp^*Mo(NO)(CH_2SiMe_3)_2]^{\bullet-}$ and $\mathbf{4.1}^{\bullet-}$ radical anions should be possible. It is equally clear that $Cp^*Mo(NO)(CH_2SiMe_3)_2$ does not undergo any bond-cleavage processes upon initial electron addition. Hence, it seems unlikely that its reactions with water involve any redox processes (vide infra).

4.3.7 Labeling Studies

A series of experiments was conducted in order to gain some mechanistic insights into the transformation of $Cp^*Mo(NO)(CH_2SiMe_3)_2$ to $[Cp^*Mo(NO)(CH_2SiMe_3)]_2$-(μ-O) by H_2O. The results of these experiments are summarized pictorially in Scheme 4.1. Treatment of $Cp^*Mo(NO)(CH_2SiMe_3)_2$ (**3.8**) with excess water results in its clean conversion to **4.1** (~95% by ^1H NMR spectroscopy) with concomitant formation of 2 equiv of Me_4Si. The ^1H NMR spectrum also contains a small singlet at δ 1.78 ppm attributable to ~2% of $[Cp^*Mo(O)_2]_2$-(μ-O), which results from further hydrolysis of **4.1** (vide infra). Reaction of $Cp^*Mo(NO)(CH_2SiMe_3)_2$ with D_2O results in the synthesis of **4.1**, but with DH_2CSiMe_3 being produced as the byproduct of the reaction. DH_2CSiMe_3 is readily identified by the appearance of a singlet in the ^1H NMR spectrum at δ 0.00 ppm with a smaller 1:1:1 triplet (J_{HD} = 2.1 Hz) at slightly higher field,[29] the latter signal being due to the mono-deuterated methyl group of DH_2CSiMe_3. Finally, treatment of the

bis(trimethylsilyl)methyl complex with $^{18}OH_2$ cleanly converts it to **4.1′**, the ^{18}O labelled analogue of **4.1**. This product may be conveniently characterized by mass spectrometry. The mass spectrum of **4.1′** shows a parent-ion peak at *m/z* 714 (as compared to 712 for unlabeled **4.1** recorded under identical experimental conditions).

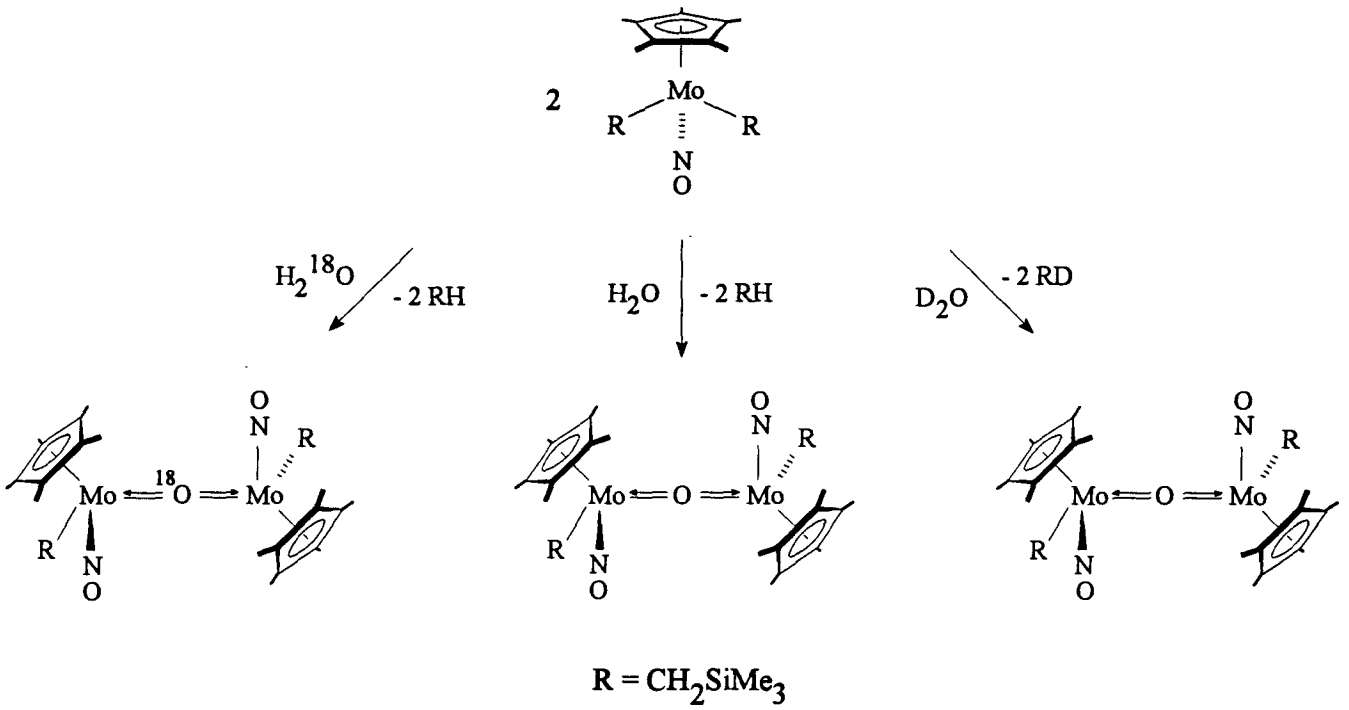

Scheme 4.1 Labelling experiments

Taken together, these experiments clearly demonstrate that the water used to convert 2 moles of $Cp^*Mo(NO)(CH_2SiMe_3)_2$ to 1 mole of complex **4.1** ends up as 2 moles of Me_4Si (RH) and the bridging oxo ligand of complex **4.1**. In other words, the balanced chemical equation for this transformation is as shown in eq 4.6.

$$2\ Cp^*Mo(NO)(CH_2SiMe_3)_2 + H_2O \longrightarrow [Cp^*Mo(NO)(CH_2SiMe_3)]\text{-}(\mu\text{-}O) + 2\ Me_4Si \qquad (4.6)$$

One could propose a number of plausible mechanistic pathways for reaction 4.6. In order to gain some further insight into the mechanism of this reaction, a kinetic analysis of the hydrolysis of $Cp^*Mo(NO)(CH_2SiMe_3)_2$ was undertaken.

4.3.8 Kinetic Studies

4.3.8.1 Monitoring of the Hydrolysis Reaction

The kinetic analysis of reaction 4.6 was hampered by several factors which merit explanation. The first is that the product of reaction 4.6, complex **4.1**, undergoes further reaction with water to produce $[Cp^*Mo(O)_2]_2$-(μ-O) (vide infra). The relative effect of this competitive and undesirable reaction is heightened at low concentrations of the organometallic starting material and under pseudo-first-order conditions where water is in excess. The second factor is the difficulty of monitoring the concentration of $Cp^*Mo(NO)(CH_2SiMe_3)_2$ as conversion 4.6 proceeds. For instance, attempts to probe the kinetics of reaction 4.6 by ^1H NMR spectroscopy were unsuccessful. Since water is immiscible with benzene, it could not be used as a pseudo-first-order reagent in that solvent. In THF (a solvent with which water is miscible), the Cp^* resonances for $Cp^*Mo(NO)(CH_2SiMe_3)_2$ (δ 1.84 ppm) and **4.1** (δ 1.86 ppm) are not sufficiently resolved to be integrated accurately. Furthermore, the signals in the spectral region around δ 0.00 ppm are not sufficiently resolved to permit monitoring of the Me_4Si byproduct. Consequently, I decided to effect the kinetic analysis of reaction 4.6 in THF using UV-vis spectroscopy, since starting material and product exhibit different spectral properties (Table 4.8). The UV-vis spectra of $Cp^*Mo(NO)(CH_2SiMe_3)_2$ and **4.1** in THF are similar except that **4.1** exhibits a strong band at λ_{max} = 404 nm (ε ~14000 $M^{-1}cm^{-1}$) (Figure 4.2).

Table 4.8 UV-vis Data (in THF) for Complexes **3.8** and **4.1**

Complex (conc.)	λ (nm)	A	ε ($M^{-1}cm^{-1}$)
3.8	223	1.613	14038
	300	0.909	7909
(1.149 x 10^{-4} M)	526	0.086	752
4.1	236	3.210	60112
	276	3.102	58089
(5.340 x 10^{-5} M)[a]	404	0.744	13932

[a] Concentration is ½ of **[3.8]** since it requires 2 moles of **3.8** to create 1 mole of **4.1**.

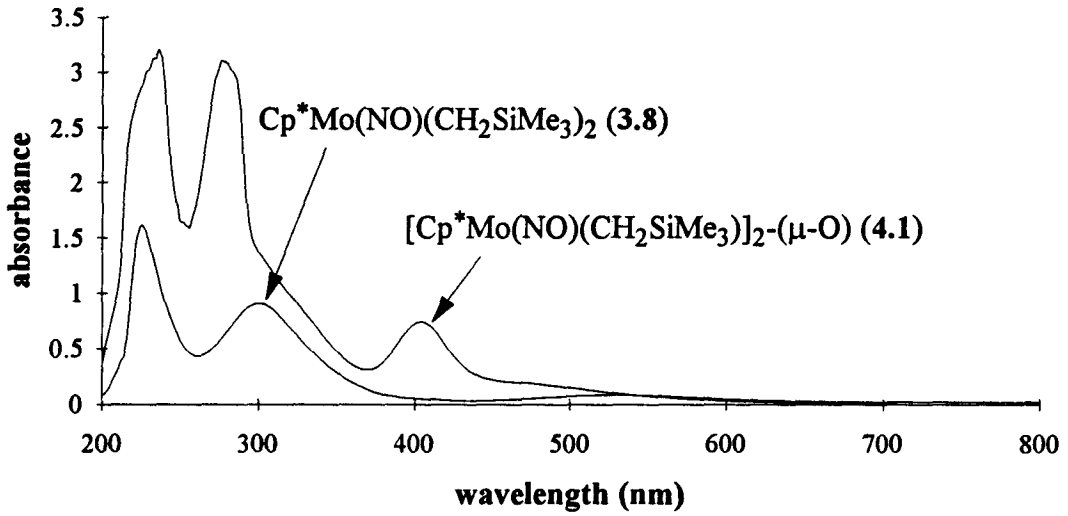

Figure 4.2 Overlaid UV-vis spectra of **3.8** and **4.1** as THF solutions

From the spectral overlay (Figure 4.2) it is clear that monitoring of the disappearance of starting material would be very difficult, since no absorption band of $Cp^*Mo(NO)(CH_2SiMe_3)_2$ is sufficiently resolved from bands of its hydrolysis product **4.1**. However, a Beer's law plot showed the absorptivity of **4.1** at 404 nm to be linear ($r^2 > 0.99$) up to A ~ 1.8, and so this spectral feature was monitored as the hydrolysis reactions

progressed. Reactions were performed under pseudo-first order conditions with an excess of water present. Because complex **4.1** does react further with water to form $[Cp^*Mo(O)_2]_2$-(μ-O), the occurrence of this latter process was minimized by keeping the reactants as concentrated as possible within the linear absorption limits and monitoring only the first half-life or so of each run. For these reasons, the data extracted from the kinetic measurements applies to the initial part of the reaction between water and $Cp^*Mo(NO)(CH_2SiMe_3)_2$.

4.3.8.2 Variation of [3.8], [H_2O] and [D_2O]

Under the experimental conditions employed, the progress of reaction 4.6 in THF is initially first-order in both water and $Cp^*Mo(NO)(CH_2SiMe_3)_2$ since all plots of $\ln (A_\infty - A_t)$ versus time are linear. First, reaction 4.6 was studied by varying the water concentration and keeping the initial concentration of $Cp^*Mo(NO)(CH_2SiMe_3)_2$ constant at 1.116×10^{-3} M. Thus, [H_2O] was varied, but still kept in excess, from 0.62×10^{-2} to 6.24×10^{-2} M in six experiments . The experimental data for these runs are compiled in Table 4.5. Figure 4.3 shows the lowest and highest water-concentration runs. Both lines are nearly linear ($r^2 > 0.999$). As expected, the rates of the hydrolysis runs increase with increasing [H_2O]. The plot of k_{obs} vs [H_2O], confirming that reaction 4.6 is first-order in water, is shown in Figure 4.4 (data taken from Table 4.5).

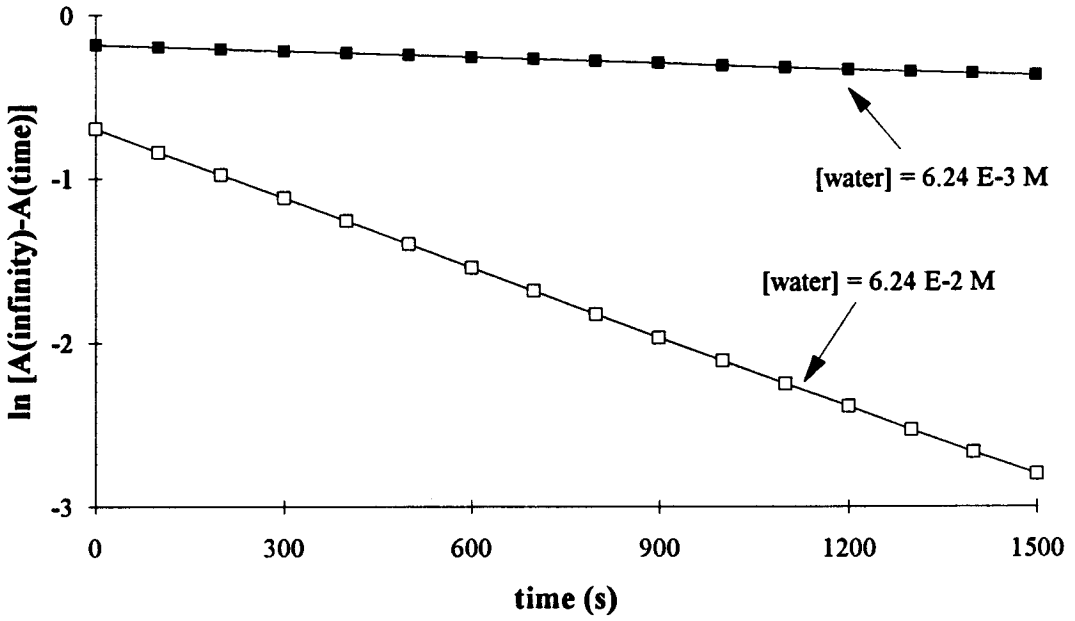

Figure 4.3 Selected first-order plots for the hydrolysis reaction ([**3.8**] = 1.116×10^{-3} M)

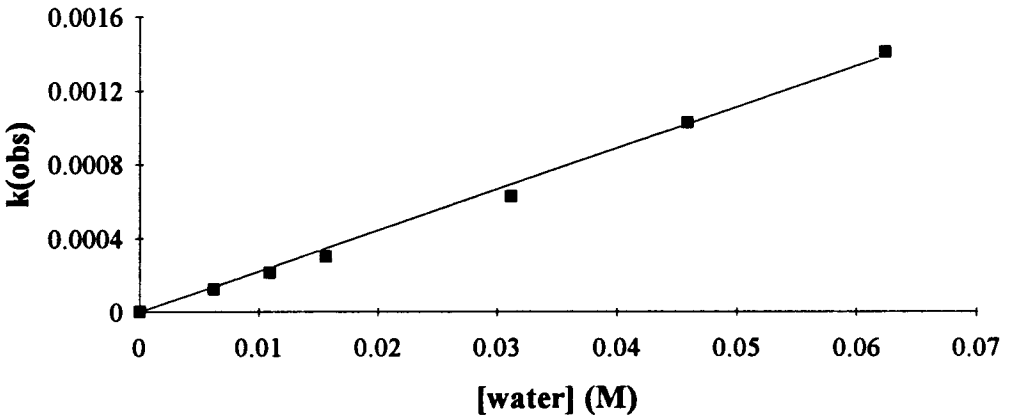

Figure 4.4 Plot of k_{obs} vs [H_2O] for the reaction of $Cp^*Mo(NO)(CH_2SiMe_3)_2$ with H_2O

Additionally, over an order of magnitude change in the concentration of the dialkyl complex ($[\mathbf{3.8}]_0$ = 2.56 x 10^{-4} - 25.39 x 10^{-4} M), reaction 4.6 is also first-order in the metal complex. The concentration of water for the seven experiments defining the concentration range of $Cp^*Mo(NO)(CH_2SiMe_3)_2$ was held constant at 5.55 x 10^{-3} M (pseudo-first-order excess). Values of k_{obs} for these runs are located in Table 4.6. From the plots of ln (A_∞-A_t) versus time, the average value of k_{obs} is 1.66 x 10^{-4} s^{-1} at 25 °C. At very low concentrations of $Cp^*Mo(NO)(CH_2SiMe_3)_2$ (i.e. $[Cp^*Mo(NO)(CH_2SiMe_3)_2]_0$ < 1.0 x 10^{-4} M), plots of ln (A_∞-A_t) versus time are not linear, a feature which probably reflects that the conversion of **4.1** to $[Cp^*Mo(O)_2]_2$-(μ-O) by water becomes much more significant at very low concentrations of the organometallics.

The hydrolysis reaction was also studied using D_2O instead of H_2O in three selected experiments. Values of k_{obs} for these runs are located in Table 4.6. Again, the reaction appears to be first-order with respect to D_2O, the average value of k_{obs} being 3.48 x 10^{-5} s^{-1}. The primary kinetic isotope effect (k_H/k_D) for the hydrolysis reaction is thus 0.000166/0.0000348 = 4.77, thus indicating that the rate of the hydrolysis reaction is slowed substantially by using the heavier isotope. This observation is significant in that it suggests that there is a considerable degree of O-H bond breaking in the transition state, since the maximum kinetic isotope effect, k_H/k_D, expected for breaking an O-H bond is 11.[30]

4.3.8.3 Variation of Temperature: Measurement of Activation Parameters

The kinetics of the hydrolysis reaction were also investigated at five-degree intervals between 15 and 30 °C. The data for these experiments are tabulated in Table 4.7 and graphically depicted in Figure 4.5.

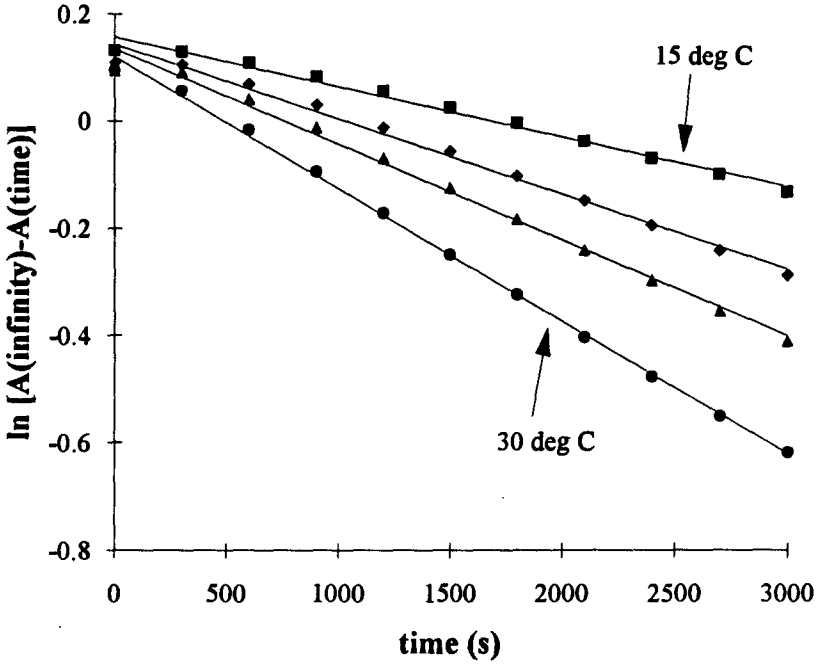

Figure 4.5 Variable temperature first-order rate plots for reactions of $Cp^*Mo(NO)(CH_2SiMe_3)_2$ (**3.8**) with excess H_2O

The data from the four variable-temperature runs afford a straight-line Eyring plot (Figure 4.6) of ln (k_{obs}/T) versus 1/T from which the following activation parameters may be calculated: $\Delta H^{\ddagger} = 43$ kJ mol^{-1}, $\Delta S^{\ddagger} = -41$ eu, $\Delta G^{\ddagger}_{298} = 94$ kJ mol^{-1}.[31] The sign and magnitude of $\Delta S^{\ddagger}$ clearly indicates that the rate-determining step of conversion 4.6 is highly associative in nature. Additionally, an Arrhenius plot of ln k_{obs} vs 1/T yields a straight line from which the activation energy, E_a, is calculated to be 49.0 kJ mol^{-1}.

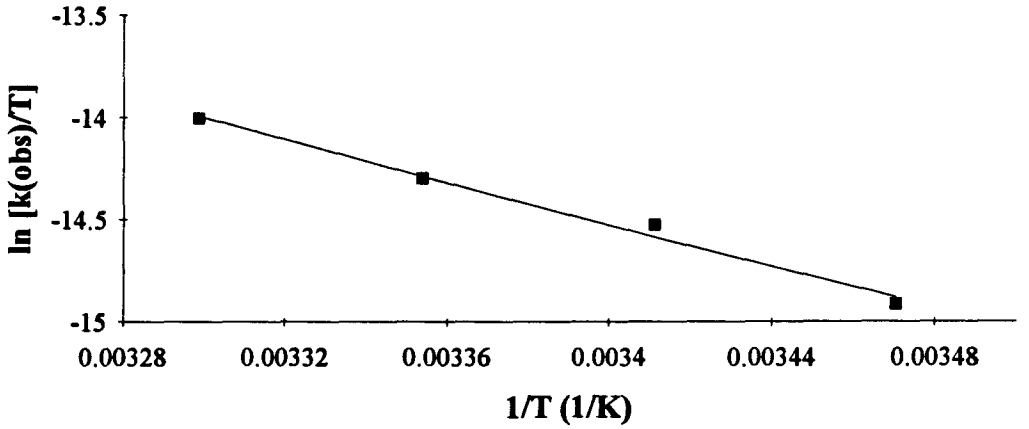

Figure 4.6 Erying plot (15 - 30 °C) for the reaction of $Cp^*Mo(NO)(CH_2SiMe_3)_2$ with H_2O

4.3.8.4 Mechanistic Proposals

The most likely scenario for the mechanistic transformation of $Cp^*Mo(NO)R_2$ to $[Cp^*Mo(NO)R]_2$-(μ-O) is presented in Scheme 4.2.

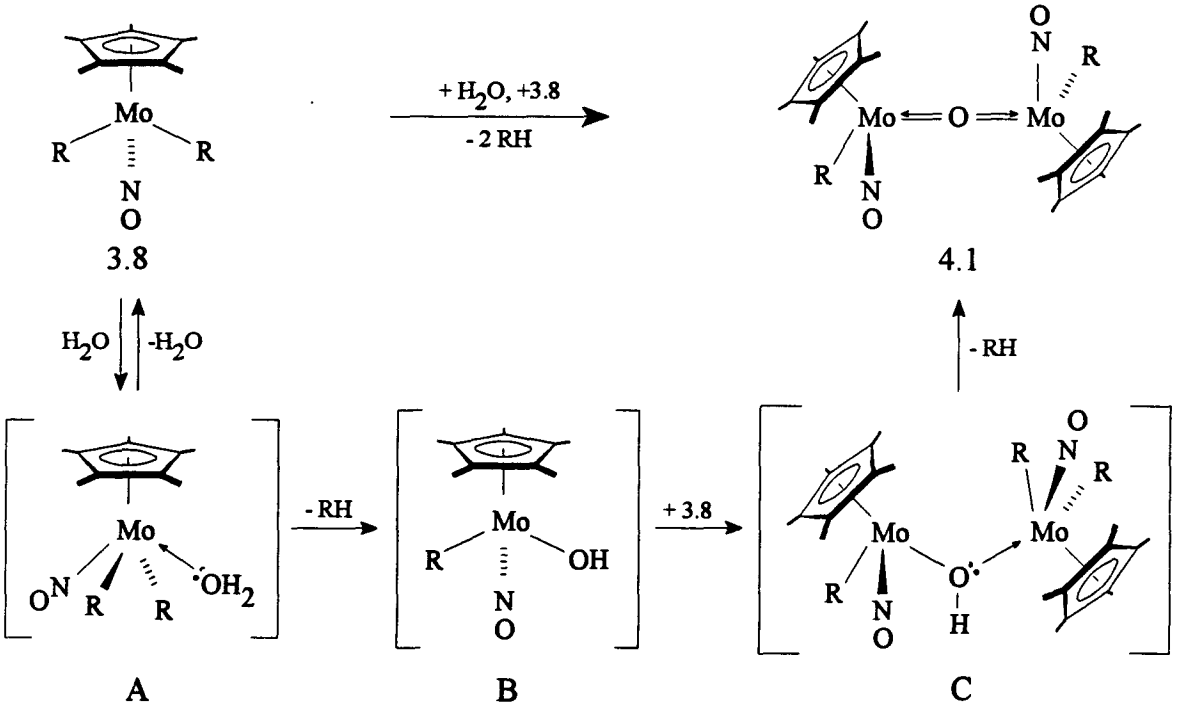

Scheme 4.2 Mechanistic pathway from $Cp^*Mo(NO)R_2$ to $[Cp^*Mo(NO)R]_2$-(μ-O)

Water, a good Lewis base, could form an initial 1:1 adduct (**A**) with the 16-electron dialkyl complex. Intramolecular expulsion of RH would afford the hydroxo alkyl intermediate (**B**)[32] which could function as a Lewis base towards a second molecule of the 16-electron dialkyl Lewis acid to form a bimetallic (μ-OH) complex (**C**). In the final step this latter compound could eliminate RH to form the final bridging oxo product. An alternative mechanism in which two molecules of **B** couple and eliminate water is very remote since the concentration of **B** is never appreciable in the reaction mixture. This claim is substantiated by monitoring of the reaction in THF-d_8 by variable temperature ^{1}H NMR spectroscopy (-80 to +20 °C). Variable temperature NMR spectroscopy failed to detect any signals that could be attributed to anything other than $Cp^*Mo(NO)(CH_2SiMe_3)_2$, either isomer of **4.1**, or Me_4Si. While the mechanism of the hydrolysis reaction is not positively determined, the rate-determining step is highly associative in nature ($\Delta S^{\ddagger} = -41$ eu) and therefore likely involves O-H bond breaking and Mo-O bond formation.

The mechanism put forth in Scheme 4.2 is rewritten in Scheme 4.3 to simplify the rate law determination.

$$\mathbf{3.8} + H_2O \underset{k_{-1}}{\overset{k_1}{\rightleftharpoons}} \mathbf{A}$$

$$\mathbf{A} \xrightarrow[-\,RH]{k_2} \mathbf{B}$$

$$\mathbf{B} + \mathbf{3.8} \xrightarrow{k_3} \mathbf{C}$$

$$\mathbf{C} \xrightarrow[-\,RH]{k_4} \mathbf{4.1}$$

Scheme 4.3 Elementary reaction sequence for the conversion of $Cp^*Mo(NO)R_2$ to $[Cp^*Mo(NO)R]_2$-(μ-O)

A simple analysis of the proposed mechanism for reaction 4.6 must assume a steady-state approximation for the intermediate complexes **A**, **B** and **C**:

- rate = $d[\mathbf{4.1}]/dt = k_4[\mathbf{C}]$
- assume $d[\mathbf{C}]/dt = 0 = k_3[\mathbf{B}][\mathbf{3.8}] - k_4[\mathbf{C}]$

$\therefore$ $k_4[\mathbf{C}] = k_3[\mathbf{B}][\mathbf{3.8}]$ and rate $= k_3[\mathbf{B}][\mathbf{3.8}]$

- assume $d[\mathbf{B}]/dt = 0 = k_2[\mathbf{A}] - k_3[\mathbf{B}][\mathbf{3.8}]$

$\therefore$ $k_3[\mathbf{B}][\mathbf{3.8}] = k_2[\mathbf{A}]$ and rate $= k_2[\mathbf{A}]$

- assume $d[\mathbf{A}]/dt = 0 = k_1[\mathbf{3.8}][H_2O] - k_{-1}[\mathbf{A}] - k_2[\mathbf{A}]$

$\therefore$ $[\mathbf{A}] = (k_1/(k_{-1} + k_2))[\mathbf{3.8}][H_2O]$

$\therefore$ rate $= k_2[\mathbf{A}] = (k_1k_2/(k_{-1} + k_2))[\mathbf{3.8}][H_2O] = k_{obs}[\mathbf{3.8}][H_2O]$

Thus, this mechanism predicts a second-order rate law which exhibits first-order dependence on both reagents. This is indeed the case.

4.3.9 Comparisons of Reactivity

Scheme 4.4 summarizes the reactions of $Cp^*Mo(NO)(CH_2SiMe_3)_2$ and its oxo derivatives with water and oxygen and illustrates the variety of products, both mono- and bimetallic, that may be obtained. To date, three compounds resulting from oxidation or hydrolysis of $Cp^*Mo(NO)(CH_2SiMe_3)_2$ have been isolated. As previously reported, the dialkyl complex reacts with dry O_2 to give the dioxo complex $Cp^*Mo(O)_2(CH_2SiMe_3)$ in moderate yield.[33] This work has shown that $Cp^*Mo(NO)(CH_2SiMe_3)_2$ reacts with H_2O to provide high yields of $[Cp^*Mo(NO)(CH_2SiMe_3)]_2$-($\mu$-O). While $Cp^*Mo(O)_2(CH_2SiMe_3)$ and $[Cp^*Mo(NO)(CH_2SiMe_3)]_2$-($\mu$-O) cannot be interconverted, both species do react with excess water or excess oxygen to form the known

$[Cp^*Mo(O)_2]_2$-(μ-O) complex as the only isolable organometallic product.[34] Exposure of $Cp^*Mo(NO)(CH_2SiMe_3)_2$ to the atmosphere leads to the formation of a mixture of all three oxo derivatives in variable yields depending on the length of exposure and the relative humidity. Thus, sagacious choices of both reagents and reaction conditions are necessary to obtain a particular oxo derivative of $Cp^*Mo(NO)(CH_2SiMe_3)_2$. The reactions of $Cp^*Mo(NO)(CH_2SiMe_3)_2$ outlined in Scheme 4.4 appear to be quite general for the family of $Cp'Mo(NO)R_2$ (R = alkyl, aryl) complexes (vide supra).

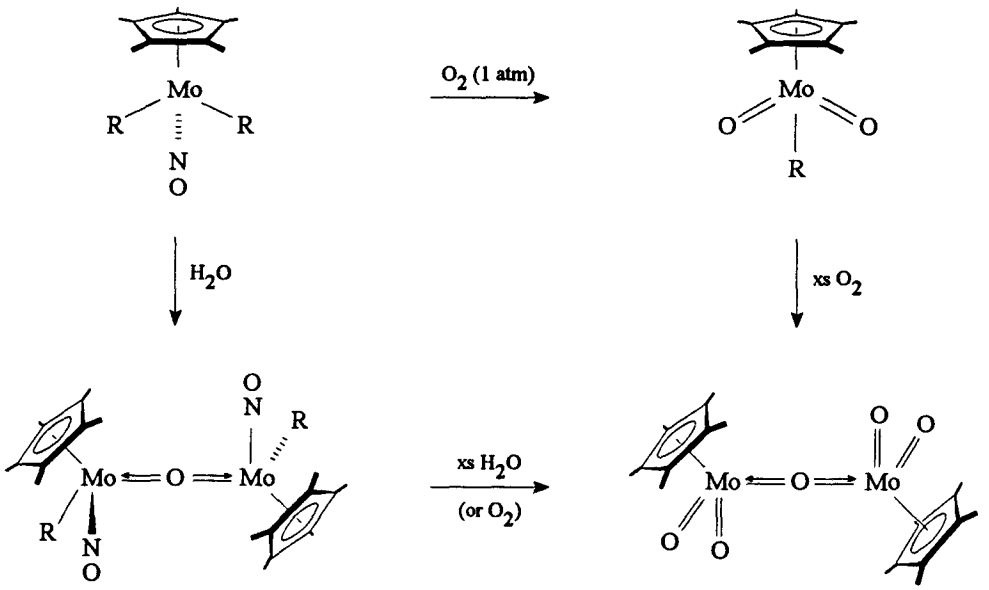

Scheme 4.4 Interrelationships of known oxo derivatives of $Cp^*Mo(NO)(CH_2SiMe_3)_2$

In marked contrast, the reactions of $Cp'W(NO)(alkyl)_2$ species with water and oxygen differ dramatically from those of their $Cp'W(NO)(aryl)_2$ analogues. The $Cp'W(NO)(alkyl)_2$ complexes resist reaction with water, persisting even in the presence of a vast excess of water for prolonged periods of time under ambient conditions. However, all isolable $Cp'W(NO)(aryl)_2$ complexes react instantaneouly with water to form

monometallic aryl dioxo complexes[2] (eq 4.7) which are also the products formed when these diaryl complexes are reacted with molecular oxygen.

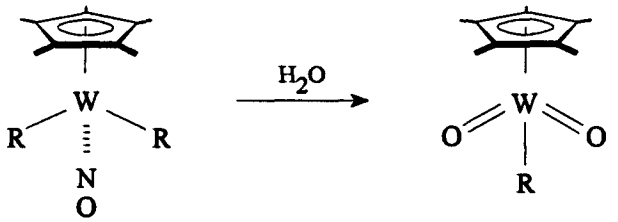

(4.7)

R = aryl

Interestingly, CpW(NO)(*o*-tolyl)$_2$ reacts with water to form two products in an essentially equimolar ratio (eq 4.8).

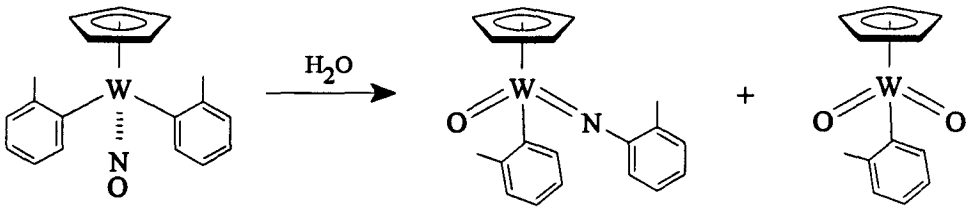

(4.8)

The synthesis of the dioxo complex is more easily accomplished by treatment of CpW(NO)(*o*-tolyl)$_2$ with H_2O_2 (aq). The imido oxo complex,[5] while clearly the more interesting of the two complexes formed by reaction 4.8, is not formed in solutions containing H_2O_2. The characterization data for these Cp'W(O)$_2$(aryl) complexes are collected in Tables 4.1 - 4.3. The spectroscopic features of these latter complexes are similar to those exhibited by their alkyl dioxo analogues.[33] Most notably, they exhibit two strong $\nu_{W=O}$ stretches in their IR spectra. Aryl dioxo complexes tend to be less crystalline and less soluble in common organic solvents than their alkyl congeners, but they are equally air- and moisture-stable.

The fact that the molybdenum and tungsten dialkyl and diaryl species exhibit such different hydrolysis chemistry is unique. Typically, related compounds of the second- and third-row transition metals react in a similar manner, with the third-row compound being the slower to react.[35] Such is indeed the case for the hydrolyses of Cp_2MMe_2 (M = Zr, Hf). Thus, reaction of Cp_2MMe_2 with water in air leads to the formation of isoelectronic analogues of **4.1-4.5**, namely $[Cp_2M(Me)]_2$-(μ-O).[20,21] Clearly, the differences created by changing the metal in related, valence-isoelectronic $Cp'M(NO)R_2$ (M = Mo, W) complexes have a much more pronounced effect on the characteristic chemical behavior of these species.[36]

4.4 Epilogue and Future Work

The work presented in this chapter clarifies the chemical reactivity of the family of $Cp'M(NO)R_2$ complexes with water. Originally, it was thought that these complexes were hydrolytically stable, but this false assumption was based on the reactivity of complexes available at that time, namely the tungsten dialkyl complexes which are very hydrolytically stable. Now that both dialkyl and diaryl complexes of Mo and W are known, such a sweeping generalization no longer holds. The hydrolytic decomposition of the Mo species is general and leads to $[Cp^*Mo(NO)R]_2$-(μ-O) complexes, whereas W diaryl complexes react to form $Cp'W(O)_2$(aryl) species. Presumably, this dependence on metal is reflective of the different mechanisms by which these Mo and W complexes react with water. A preliminary look at the mechanism of the hydrolysis reactions of the Mo species has determined that $Cp^*Mo(NO)R_2$ complexes in all likelihood react with water to form hydroxy complexes {$Cp^*Mo(NO)(R)(OH)$}, which then react further with starting material to yield the $[Cp^*Mo(NO)R]_2$-(μ-O) bridging oxo complexes. In the case of the W systems, such an intermediate does not seem likely, given the outcome of their

hydrolysis reactions. The mechanism of the formation of $Cp'W(O)_2(aryl)$ complexes is yet to be determined.

For future studies in this area, I would suggest an examination of the reactivity of $[Cp^*Mo(NO)(CH_2CMe_3)]_2$-(μ-O) (**4.2**), since it is the easiest to prepare, highest yielding and the most stable of the bridging oxo complexes presented in this chapter. Additionally, complex **4.2** exists as only one diastereomer in solution, thus simplifying spectral interpretations.

4.5 References and Notes

(1) See for example: *The Chemistry of the Metal-Carbon Bond*; Hartley, F. R., Patai, S., Eds.; Wiley: New York, 1985; Vol 2.

(2) The work described in this chapter has been published. See Legzdins, P.; Lundmark, P. J.; Phillips, E. C. Rettig, S. J.; Veltheer, J. E. *Organometallics* **1992**, *11*, 2991.

(3) Nicholson, R. S. *Anal. Chem.* **1966**, *38*, 1406.

(4) Atwood, J. D. *Inorganic and Organometallic Reaction Mechanisms*; Brooks/Cole Publishing Co.: Monterey, CA, 1985.

(5) The reason hydrogen peroxide is used, instead of water, is to maximize the yield of the dioxo complex. If water is reacted with $CpW(NO)(o\text{-tolyl})_2$, two organometallic products are isolable: the dioxo complex $CpW(O)_2(o\text{-tolyl})$ and, more interestingly, CpW(N-*o*-tolyl)(O)(*o*-tolyl) which is a structural isomer of the starting material. See Legzdins, P.; Rettig, S. J.; Ross, K. J.; Veltheer, J. E. *J. Am. Chem. Soc.* **1991**, *113*, 4361.

(6) $[Cp^*Mo(O)_2]_2$-(μ-O) was first synthesized by Faller's group. See Faller, J. W.; Ma, Y. *J. Organomet. Chem.* **1988**, *340*, 59. Later, Rheingold's group published a

detailed crystallographic analysis of all three polymorphs of $[Cp^*Mo(O)_2]_2$-(μ-O), see Rheingold, A. L.; Harper, J. R. *J. Organomet. Chem.* **1991**, *403*, 335.

(7) Legzdins, P.; Rettig, S. J.; Sánchez, L. *Organometallics* **1988**, *7*, 2394.

(8) Hunter, A. D.; Legzdins, P.; Martin, J. T.; Sánchez, L. *Organomet. Synth.* **1986**, *3*, 66.

(9) Even higher yields of $Cp^*W(NO)(CH_2SiMe_3)_2$ are obtained using $Cp^*W(NO)Cl_2$, see Legzdins, P.; Veltheer, J. E. In *Handbuch der Präparativen Anorganischen Chemie*, 4th ed.; Herrmann, W. A., Ed.; Thieme-Verlag: Stuttgart, Germany, in press.

(10) Phillips, E. C. Ph.D. Dissertation, The University of British Columbia, 1989.

(11) Herring, F. G.; Legzdins, P.; Richter-Addo, G. B. *Organometallics* **1989**, *8*, 1485.

(12) Christensen, N. J.; Debad, J. D.; Legzdins, P.; Lundmark, P. J.; Reina, R.; Ross, K. J.; Trotter, J.; Veltheer, J. E.; Yee, V. C., manuscript in preparation.

(13) The only isolable $CpMo(NO)R_2$ complex which reacts faster with water than it thermally decomposes is $CpMo(NO)(CH_2SiMe_3)_2$. Reaction of $CpMo(NO)(CH_2SiMe_3)_2$ with water provides $[CpMo(NO)(CH_2SiMe_3]_2$-(μ-O) in about 60% isolated yield.[2] This reaction was first performed by E. C. Phillips.[10]

(14) Dryden, N. H.; Legzdins, P.; Rettig, S. J.; Veltheer, J. E. *Organometallics* **1992**, *11*, 2583.

(15) Legzdins, P.; Rettig, S. J.; Veltheer, J. E. *J. Am. Chem. Soc.* **1992**, *114*, 6922.

(16) Dr. Steve Rettig solved the structure of $[Cp^*Mo(NO)(CH_2SiMe_3)]_2$-(μ-O).[2,10]

(17) Barraclough, C. G.; Lewis, J.; Nyholm, R. S. *J. Chem. Soc.* **1959**, 3552.

(18) Orpen, A. G.; Brammer, L.; Allen, F. H.; Kennard, O.; Watson, D. G.; Taylor, R. *J. Chem. Soc., Dalton Trans.* **1989**, S1.

(19) Lundmark, P. J. Ph.D. Dissertation, The University of British Columbia, in preparation.

(20) Hunter, W. E.; Hrncir, D. C.; Bynum, R. V.; Pentilla, R. A.; Atwood, J. L. *Organometallics* **1983**, *2*, 750.

(21) Fronzek, F. R.; Baker, E. C.; Sharp, P. R.; Raymond, K. N.; Alt, H. G.; Rausch, M. D. *Inorg. Chem.* **1976**, *15*, 2284.

(22) Hillhouse, G. L.; Bercaw, J. E. *J. Am. Chem. Soc.* **1984**, *106*, 5472.

(23) Lincoln, S.; Koch, S. A. *Inorg. Chem.* **1986**, *25*, 1594.

(24) Umakoshi, K.; Isobe, K. *J. Organomet. Chem.* **1990**, *395*, 47.

(25) Carty, P.; Walker, A.; Mathew, M.; Palenik, G. J. *J. Chem. Soc. D* **1969**, 1374.

(26) See Section 3.3.2.

(27) Chapter 3 of this thesis.

(28) Legzdins, P.; Rettig, S. J.; Sanchez, L.; Bursten, B. E.; Gatter, M. G. *J. Am. Chem. Soc.* **1985**, *107*, 1411.

(29) J_{HD} couplings are typically small ($J_{XH} \sim 6.5\, J_{XD}$).

(30) Moore, J. W.; Pearson, R. G. *Kinetics and Mechanism*, 3rd ed.; Wiley-Interscience: Toronto, 1981, p 369.

(31) Reference 4, p 16.

(32) It may be noted that Bercaw has invoked an analogous hydroxo complex, namely $Cp^*_2Zr(H)(OH)$, as an intermediate species formed when either $Cp^*_2Zr(H)_2$ or $Cp^*_2Zr(N_2)$ reacts with water. The ultimate product in these reactions is $[Cp^*_2Zr(H)]_2$-(μ-O), a valence-isoelectronic analogue of complexes **4.1-4.5**.[22]

(33) Legzdins, P.; Phillips, E. C.; Sánchez, L. *Organometallics* **1989**, *8*, 940.

(34) This ubiquitous complex appears to be the ultimate oxidative decomposition product of a wide variety of $Cp^*Mo(NO)$-containing species. Legzdins, P.; Lundmark, P. J.; Phillips, E. C.; Veltheer, J. E.; Young, M. A., unpublished observations.

(35) "In general, the second and third transition series elements of a given group have similar chemical properties, but show pronounced differences from their light congeners." Cotton, F. A.; Wilkinson, G. *Advanced Inorganic Chemistry*, 5th ed.; Wiley: Toronto, 1988; p 776.

(36) It has been noted that Zr and Hf complexes are more nearly identical than for any other two congeneric elements, mostly due to the lanthanide contraction (see ref 35, chapter 19).

CHAPTER 5

Some Characteristic Chemistry of $CpMo(NO)(CH_2CMe_3)_2$ and its Transient Thermal Decomposition Product, $CpMo(NO)(=CHCMe_3)$

5.1 Introduction

5.1.1 Historical Development

The first compound containing a metal-carbon double bond was prepared in 1964 by E. O. Fischer (eq 5.1).[1] Due to the large volume of work to emanate from the Fischer group, complexes containing M=C(ER)R' groups became inexorably tagged with Fischer's name.

$$W(CO)_6 \xrightarrow[2)\ H^+,\ CH_2N_2]{1)\ PhLi} (CO)_5W{=}C\begin{matrix}\diagup\ OMe\\ \diagdown\ Ph\end{matrix} \qquad (5.1)$$

In general, Fischer carbene complexes contain alkoxy or amido substituents (ER) directly attached to the carbene carbon. Consequently, the thermal stability of Fischer carbenes is often attributed to their having a variety of stabilizing resonance structures. Fischer carbene ligands are almost always derived from metal-bound carbonyl moieties.[2]

The first unstabilized carbene complex (i.e. no α-carbon-heteroatom bond) was prepared nearly a decade later by Schrock during an attempt to prepare $Ta(CH_2CMe_3)_5$ (eq 5.2).[3]

$$Ta(CH_2CMe_3)_3Cl_2 \xrightarrow[-2\,LiCl,\,-CMe_4]{2\,Me_3CCH_2Li} (Me_3CCH_2)_3Ta{=}C\begin{matrix}H\\ \diagup\\ \diagdown\\ CMe_3\end{matrix} \qquad (5.2)$$

This neopentylidene complex had completely different chemical properties than previously studied carbene complexes, and thus constituted a new class of compounds that have since been named Schrock alkylidenes. Typically, Schrock alkylidene complexes are derived via alkane loss from precursors containing *cis*-dialkyl ligands.[4]

In terms of reactivity, Fischer carbenes are typically electrophilic at C_α whereas Schrock alkylidenes are nucleophilic at C_α.[5] The bonding of Fischer carbenes is typically described as M←C(ER)R' dative interactions with substantial M(dπ)→C(pπ*) backbonding.[6] Schrock-type complexes are typically described as containing M=C covalent bonds similar to, but certainly more polar than ethylene.[7]

5.1.2 Relationship to $Cp'M(NO)R_2$ Complexes

As alluded to in the previous chapters of this thesis, many $Cp'M(NO)R_2$ complexes are thermally sensitive. Indeed it is the extreme thermal instability of $CpMo(NO)(aryl)_2$ complexes that has precluded their isolation (Chapter 2). The next most sensitive complexes are the $CpMo(NO)(alkyl)_2$ family (Chapter 3) of which $CpMo(NO)(CH_2CMe_3)_2$ is by far the most thermally sensitive. This chapter describes the characteristic chemistry of this complex and presents the results of a detailed mechanistic study of its thermal decomposition. $CpMo(NO)(CH_2CMe_3)_2$ decomposes via an intramolecular α-hydrogen elimination of neopentane to yield $CpMo(NO)(=CHCMe_3)$. While this 16-electron neopentylidene complex exists only transiently, its reactivity can be, and has been, investigated.[8]

5.2 Experimental Procedures

5.2.1 Methods

The synthetic methodologies employed throughout this thesis are described in detail in section 2.2.1. The flow system for in situ IR spectral monitoring was constructed from a Teflon diaphragm pump (Cole-Parmer 07090-62) and a 0.2 mm NaCl cell (Wilmad 105A10-5).

5.2.2 Reagents

$CpMo(NO)Cl_2$ was prepared and handled as described in Section 2.2.2. The preparation of $(Me_3CCH_2)_2Mg{\cdot}X$(dioxane) is described in Section 3.2.3. $LiAlD_4$ (Aldrich, 98% D) and $P(n\text{-}Bu)_3$, $P(p\text{-tolyl})_3$, PPh_2Me, $CNCMe_3$, $(p\text{-tolyl})NH_2$ (Aldrich) and PPh_3 (Strem) were used as received. $Me_3CC\{O\}Cl$ (Aldrich) was degassed with several freeze-pump-thaw cycles. DMF (BDH) was freshly distilled in vacuo from activated 4Å molecular sieves.[9] Mesitylene (MCB) was dried over $CaCl_2$ and degassed in vacuo. PMe_3 was prepared as described in Section 2.2.2 and was vacuum transferred from Na/benzophenone. Me_3CNH_2 (Aldrich) was vacuum transferred from CaH_2.

The column chromatography material used during this work was alumina (80 - 200 mesh, Fisher neutral, Brockman activity I). Filtrations were performed through Celite 545 diatomaceous earth (Fisher) that had been oven-dried and cooled in vacuo.

5.2.3 Preparation of $CpMo(NO)(CH_2CMe_3)_2$ (5.1)

This complex was prepared in a manner analogous to that described for related complexes found in Chapters 2 and 3, but with a few added precautions. These precautions are required because samples of $CpMo(NO)(CH_2CMe_3)_2$ (**5.1**), when taken to dryness, decompose in a matter of minutes at ambient temperatures. Therefore, in order to isolate spectroscopically pure **5.1**, the following synthetic procedure was used: THF (3 mL) was vacuum transferred onto

$CpMo(NO)Cl_2$ (100 mg, 0.38 mmol) and $(Me_3CCH_2)_2Mg{\cdot}X$(dioxane) (105 mg, 0.75 mmol $Me_3CCH_2^-$) at -196 °C. The reaction mixture was stirred for 1 h as it was warmed to -40 °C, the temperature at which *all* subsequent manipulations were performed. The final red solution (ν_{NO} 1608 cm^{-1}) was taken *almost* to dryness in vacuo. The oily red residue was suspended in Et_2O (10 mL), and the mixture was filtered through alumina I (1 x 2 cm) supported on a medium-porosity glass frit. Solvent was removed from the filtrate to obtain **5.1** as a red solid (~70 mg, ~55% yield). Five different estimates of the yield of similar-scale reactions leading to **5.1** indicated it varied only slightly from 55% (50-59%).

IR (THF) ν_{NO} 1608 cm^{-1}. ^1H NMR (C_6D_6) δ 5.04 (s, 5H, C_5H_5), 4.01 (d, 2H, CH_2, J_{HH} = 12.1 Hz), 1.31 (s, 18H, $C(CH_3)_3$), 0.27 (d, 2H, CH_2, J_{HH} = 12.1 Hz). Due to the thermal instability of $CpMo(NO)(CH_2CMe_3)_2$ as a solid, no elemental analysis or mass spectral data could be obtained for the complex.

5.2.4 Preparation of $(Me_3CCD_2)_2Mg{\cdot}X$(dioxane)[10]

$LiAlD_4$ (3.50 g, 79.1 mmol) was transferred to a 500-mL round-bottom flask in a drybox. The flask, equipped with a large magnetic stirring bar, was removed from the drybox and attached to a vacuum line. A 250-mL pressure-equalized addition funnel was attached to the flask and cooled under a flow of argon. Once cool, the addition funnel was charged with $Me_3CC\{O\}Cl$ (19.1 mL, 155 mmol, 0.98 equiv) diluted with Et_2O (100 mL). Et_2O (300 mL) was added to the solid $LiAlD_4$. The flask was cooled to -78 °C and dropwise addition of the acetyl chloride solution to the $LiAlD_4$ suspension was initiated. After the addition was complete, the reaction mixture was warmed to room temperature and stirred for 4 h. No visible change in the reaction mixture was observed. At that time the flask was cooled to -10 °C, and H_2O (2 mL) was added via a disposable syringe. The contents of the flask were stirred for 5 min, and then NaOH (0.6 g dissolved in 3 mL of water) was added to the flask, thereby causing the contents of the flask to become increasingly viscous. The volatiles were then vacuum transferred from the white solids into a new flask using an oil bath to supply the needed thermal energy. [Attempts to filter

the above reaction mixtures proved to be very difficult and decreased yields substantially.] After thawing, the vacuum-transferred solution was dried overnight on $MgSO_4$. $MgSO_4$ was removed by filtration into a tared 500-mL flask. Removal of the solvent at -25 °C yielded Me_3CCD_2OH (~10 g, 72% yield) as a waxy, white solid. This solid was used directly in the next step.

Me_3CCD_2OH (~10 g, ~111 mmol) was dissolved in DMF (150 mL) in a flask equipped with two addition funnels and a Liebig condenser connected to a 250-mL, one-necked flask. One addition funnel was charged with P(*n*-Bu)$_3$ (42.4 mL, 170 mmol), and the other with Br_2 (8.2 mL, 160 mmol). The P(*n*-Bu)$_3$ was added to the DMF solution over a 5-min period at room temperature. The flask was then immersed in an ice bath, and the bromine addition commenced. After the bromine had been completely added (30 min), the addition funnels were removed from the reaction flask and the orange reaction mixture was stirred at room temperature for 30 min. Distillation of the crude reaction mixture under argon (1 atm) at 140 - 155 °C provided a colorless mixture of DMF and Me_3CCD_2Br. The distillation pot contained a dark red tar which solidified upon cooling.

The following manipulations were executed in air. Addition of H_2O (80 mL) to the DMF/Me_3CCD_2Br mixture caused the solution to separate into two layers. The lower layer of Me_3CCD_2Br was removed using a separatory funnel and was washed with water (20 mL). At this point, the organic product appeared cloudy. Both fractions of water were combined and extracted with Et_2O (50 mL). The ether wash was combined with the crude Me_3CCD_2Br. The resulting Et_2O solution was dried over $CaCl_2$ for 1h, and was filtered into a Schlenk tube, equipped with a 4-mm Kontes Teflon stopcock, containing P_2O_5 (2 g). The contents of the vessel were subjected to 3 freeze-pump-thaw cycles and left to dry in the dark for 3 days. The Me_3CCD_2Br solution was then cannulated onto fresh P_2O_5 (2 g). The residual drying agent was washed with Et_2O (5 mL). After 1 day over P_2O_5, the Me_3CCD_2Br and ether were filtered through Celite (2 x 2 cm) supported on a frit into a new flask. To this were added dibromoethane (1.0 mL) and Et_2O (50 mL). Meanwhile, in a glovebox, a 500-mL flask was charged with Mg powder (5 g, excess). The flask was removed from the glovebox and attached to a vacuum line.

Et_2O (250 mL) was added by syringe to the flask. An addition funnel and a reflux condenser were attached to the flask. The contents of the flask were brought to reflux using an oil bath. The $Me_3CCD_2Br/BrCH_2CH_2Br/Et_2O$ solution was transferred to the addition funnel and dropwise addition of the solution to the refluxing Mg/Et_2O mixture was effected over the course of several hours. The reaction mixture was then refluxed overnight. The resulting yellow mixture was filtered through Celite (3 x 10 cm). The clear yellow filtrate was treated dropwise with 1,4-dioxane (13 mL, 153 mmol, excess). Subsequent workup as described in Section 2.2.4 afforded a pale orange solution of $(Me_3CCD_2)_2Mg{\cdot}X$(dioxane). This solution was used directly in further reactions rather than isolating the organomagnesium species by crystallization, thus minimizing the losses normally associated with crystallization. Hydrolysis of a sample, then titration against standard HCl (0.1000 M) using phenolphthalein as indicator established the carbanion concentration of the stock solution to be 0.12 M.

5.2.5 Preparation of $CpMo(NO)(CD_2CMe_3)_2$ (5.1-d_4)

$CpMo(NO)(CD_2CMe_3)_2$ is markedly more thermally stable than its perhydro analogue. Thus, while its synthesis is similar to that described in Section 5.2.3, the scale of the reaction can be greatly increased with relative ease. THF (50 mL) was vacuum transferred onto $CpMo(NO)Cl_2$ (1048 mg, 4.00 mmol), and $(Me_3CCD_2)_2Mg{\cdot}X$(dioxane) (33.6 mL of a 0.12 M stock solution, 8.1 mmol $Me_3CCD_2^-$) was added dropwise to the stirred dichloride slurry at -78 °C. The reaction temperature was slowly raised to 0 °C, and approximately one-half of the solvent was removed in vacuo. An IR spectrum of the final red solution exhibited a ν_{NO} of 1609 cm^{-1}. Without warming, the reaction mixture was then taken to dryness under reduced pressure. The red residue was suspended in Et_2O (100 mL), and the mixture was filtered through alumina I (2 x 5 cm) supported on a medium-porosity glass frit. The alumina column was washed with ether until the extracts were colorless (~50 mL). The ether was removed in vacuum to leave a red powder which was dissolved in pentane and refiltered through a column of Celite

(2 x 2 cm). Cooling of the pentane solution at -30 °C for several days gave red needles of the desired complex in 39% yield (526 mg).

Anal. Calcd for $C_{15}H_{23}D_4NOMo$: C, 53.41; H, 8.07; N, 4.15. Found: C, 53.60; H, 8.00; N, 4.07. IR (THF) ν_{NO} 1609 cm^{-1}. IR (Nujol) ν_{NO} 1623 cm^{-1}. ^1H NMR ($CDCl_3$) δ 5.67 (s, 5H, C_5H_5), 1.17 (s, 18H, $C(CH_3)_3$). ^1H NMR spectroscopy revealed no detectable methylene proton signals, thus indicating at least 99.5% D incorporation at C_α. ^2H NMR (C_6H_6, 40 MHz) δ 4.00 (s, br, no resolvable couplings), -1.09 (s, br, no resolvable couplings).

5.2.6 Preparation of $[CpMo(NO)(CHCMe_3)]_2$ (5.2)

In a typical experiment, THF (30 mL) was vacuum transferred onto a mixture of $CpMo(NO)Cl_2$ (467 mg, 1.78 mmol) and $(Me_3CCH_2)_2Mg{\cdot}X$(dioxane) (512 mg, 3.66 mmol $Me_3CCH_2^-$) at -78° C. The stirred reaction mixture was allowed to warm to -40° C over 1 h to ensure complete reaction as judged by IR spectroscopy. The final red solution of **5.1** (ν_{NO} 1608 cm^{-1}) was taken *almost* to dryness in vacuo. The oily red residue was redissolved in CH_2Cl_2/hexanes (1:2, 50 mL), and the red reaction mixture was stirred in the dark at room temperature for 2-3 h during which time it became pale orange. Solvent was removed under reduced pressure, and the brown residue was extracted with Et_2O (2 x 50 mL). Filtration of the combined extracts through neutral alumina I (2 x 3 cm) followed by exhaustive washing with Et_2O (200 mL), concentration in vacuo to ~25 mL, and slow cooling of the filtrate to -30° C induced the deposition of pale orange crystals of **5.2** (220 mg, 47% yield) which were collected by filtration.

Anal. Calcd for $C_{20}H_{30}N_2O_2Mo_2$: C, 45.99; H, 5.79; N, 5.36. Found: C, 45.96; H, 5.84; N, 5.34. IR (Nujol) ν_{NO}(terminal) 1595 (vs) cm^{-1}, ν_{NO}(bridging) 1315 (s) cm^{-1}. IR (CH_2Cl_2) ν_{NO} 1594 (vs), 1328 (s) cm^{-1}. ^1H NMR (C_6D_6) δ 12.42 (s, 1H, $CH_{terminal}$), 9.30 (s, 1H, $CH_{bridging}$), 5.20 (s, C_5H_5), 5.16 (s, C_5H_5), 1.28 (s, $C(CH_3)_3$), 1.23 (s, $C(CH_3)_3$). $^{13}C\{^1H\}$ NMR (C_6D_6) δ 301.12 (s, $=CH_{terminal}$), 243.05 (s, $=CH_{bridging}$), 101.64 (s, C_5H_5), 100.83 (s, C_5H_5), 34.99 (s,

$C(CH_3)_3$), 32.23 (s, $C(CH_3)_3$), no resonances for $C(CH_3)_3$ were unambiguously assignable. Low-resolution mass spectrum (probe temperature 120 °C): *m/z* 522 (P^+).

5.2.7 Preparation of CpMo(NO)(=CHCMe$_3$)L [5.3, L = PPh$_2$Me; 5.4, L = PPh$_3$; 5.5, L = P(*p*-tolyl)$_3$)]

All three complexes were synthesized in a similar manner. A solution of $CpMo(NO)(CH_2CMe_3)_2$ was generated from $CpMo(NO)Cl_2$ (2.00 mmol) and $(Me_3CCH_2)_2Mg{\cdot}X$(dioxane) (4.05 mmol $Me_3CCH_2^-$) in THF (30 mL). The solution was taken to dryness in vacuo at -20 °C, extracted with Et_2O (50 mL) and quickly filtered through alumina I (2 x 4 cm) into a Schlenk tube containing the appropriate tertiary phosphine (4.0 mmol, ~4 equiv assuming 50% conversion of $CpMo(NO)Cl_2$ to $CpMo(NO)(CH_2CMe_3)_2$). The reaction mixture was then stirred at room temperature for 3 h in the dark. [Dichloromethane or hexanes were also suitable solvents for these reactions although diethyl ether was the most convenient since the filtration of the dialkyl starting material on alumina *must* be effected using Et_2O as the solvent.] The transformations of $CpMo(NO)(CH_2CMe_3)_2$ to $CpMo(NO)(=CHCMe_3)L$ could be conveniently monitored by IR spectroscopy. For example, an IR spectrum of a solution of $CpMo(NO)(CH_2CMe_3)_2$ and PPh_2Me (4.0 equiv) exhibited a ν_{NO} of 1616 cm^{-1} in Et_2O. Monitoring of this solution by in situ flow-cell IR spectroscopy showed loss of the band at 1616 cm^{-1} and appearance of a new band at 1577 cm^{-1}. After 3 h only the 1577 cm^{-1} band remained, and the reaction was deemed to be complete.

After the reaction was complete, the solvent was removed in vacuo leaving a brown powder. The residue was extracted with Et_2O (**5.3** and **5.5**) or CH_2Cl_2 (**5.4**) and filtered through alumina I (2 x 2 cm). The alumina was washed with the appropriate solvent until the washings were colorless. The filtrate (yellow to amber in color) was taken to dryness and washed with pentane (15 mL) to remove excess phosphine. The remaining residue was crystallized from a minimum of Et_2O. Complex **5.3** and **5.4** were isolated as amber crystals in 57 and 42% yields, respectively.

Complex **5.5** was isolated as a yellow powder in 50% yield. All isolated yields are based on $CpMo(NO)Cl_2$ as the limiting reagent.

Complex 5.3: Anal. Calcd for $C_{23}H_{28}NOPMo$: C, 59.87; H, 6.12; N, 3.04. Found: C, 59.80; H, 5.99; N, 2.94. IR (Nujol) ν_{NO} 1540 (vs) cm^{-1}. ^1H NMR (C_6D_6) δ 13.59 (d, 1H, C*H*, J_{PH} = 3.7 Hz), 7.41 (m, 4H, PPh_2Me), 7.01 (m, 6H, PPh_2Me), 5.26 (s, 5H, C_5H_5), 1.82 (d, 3H, $PPh_2(CH_3)$, J_{PH} = 11.2 Hz), 1.34 (s, 9H, $C(CH_3)_3$). $^{13}C\{^1H\}$ NMR (C_6D_6) δ 316.1 (s, =*C*H), 138.9 (d, C_{ipso} of PPh_2Me, J_{PC} = 42.4 Hz), 137.1 (d, C_{ipso} of PPh_2Me, J_{PC} = 42.1 Hz), 132.5 (d, C_{ortho} of PPh_2Me, J_{PC} = 14.1 Hz), 131.3 (d, C_{ortho} of PPh_2Me, J_{PC} = 14.0 Hz), 130.2 (s, C_{para} of PPh_2Me), 139.7 (s, C_{para} of PPh_2Me), 128.6 (d, C_{meta} of PPh_2Me, J_{PC} = 9.9 Hz), 128.4 (d, C_{meta} of PPh_2Me, J_{PC} = 9.9 Hz), 98.6 (s, C_5H_5), 52.6 (s, $C(CH_3)_3$), 31.3 (s, $C(CH_3)_3$), 17.6 (d, $PPh_2(CH_3)$, J_{PC} = 21.3 Hz). $^{31}P\{^1H\}$ NMR (C_6D_6) δ 36.9 (s). Low-resolution mass spectrum (probe temperature 120 °C): *m/z* 393 (P^+-$CHCMe_3$).

Complex 5.4: Anal. Calcd for $C_{28}H_{30}NOPMo$: C, 64.25; H, 5.78; N, 2.68. Found: C, 64.15; H, 5.74; N, 2.88. IR (Nujol) ν_{NO} 1540 (vs) cm^{-1}. ^1H NMR (C_6D_6) δ 13.80 (d, 1H, C*H*, J_{PH} = 3.6 Hz), 7.77 (m, 6H, PPh_3), 7.15 (m, 9H, PPh_3), 5.40 (s, 5H, C_5H_5), 1.39 (s, 9H,$C(CH_3)_3$). $^{13}C\{^1H\}$ NMR (C_6D_6) δ 319.62 (s, =*C*H), 136.29 (d, C_{ipso} of PPh_3, J_{PC} = 43.2 Hz), 133.70 (d, C_{ortho} of PPh_3, J_{PC} = 12.1 Hz), 130.17 (s, C_{para} of PPh_3), 128.66 (d, C_{meta} of PPh_3, J_{PC} = 9.8 Hz), 98.86 (s, C_5H_5), 53.34 (s, $C(CH_3)_3$), 30.87 (s, $C(CH_3)_3$). $^{31}P\{^1H\}$ NMR (C_6D_6) δ 41.2 (s). Low-resolution mass spectrum (probe temperature 120 °C): *m/z* 525 (P^+).

Complex 5.5: Anal. Calcd for $C_{31}H_{36}NOPMo$: C, 65.84; H, 6.42; N, 2.48. Found: C, 66.11; H, 6.61; N, 2.33. IR (Nujol) ν_{NO} 1553 (vs) cm^{-1}. ^1H NMR (C_6D_6) δ 13.70 (d, 1H, C*H*, J_{PH} = 3.6 Hz), 7.61 (m, 6H, P(*p*-tolyl)$_3$), 6.90 (m, 6H, P(*p*-tolyl)$_3$), 5.34 (s, 5H, C_5H_5), 1.98 (s, 9H, *p*-CH_3), 1.33 (s, 9H, $C(CH_3)_3$). $^{13}C\{^1H\}$ NMR (C_6D_6) δ 316.60 (d, =*C*H, J_{PC} = 13.9 Hz), 176.65 (s, C_{para} of P(*p*-tolyl)$_3$), 133.71 (d, C_{ortho} of P(*p*-tolyl)$_3$, J_{PC} = 12.3 Hz), 129.45 (d, C_{meta} of P(*p*-tolyl)$_3$, J_{PC} = 10.3 Hz), 98.85 (d, C_5H_5, J_{PC} = 7.0 Hz), 53.15 (d, $C(CH_3)_3$, J_{PC} = 6.0 Hz), 30.92 (d, $C(CH_3)_3$, J_{PC} = 5.5 Hz), 21.07 (d, *p*-CH_3, J_{PC} = 6.4 Hz). $^{31}P\{^1H\}$ NMR

(C_6D_6) δ 56.6 (s). Low-resolution mass spectrum (probe temperature 120 °C): *m/z* 567 (P^+), 497 (P^+-$CHCMe_3$).

5.2.8 Reaction of $CpMo(NO)(CD_2CMe_3)_2$ with PPh_2Me

The conversion of $CpMo(NO)(CD_2CMe_3)_2$ to $CpMo(NO)(=CDCMe_3)(PPh_2Me)$ (**5.3-d_1**) could be conveniently monitored by NMR spectroscopy. For example, $CpMo(NO)(CD_2CMe_3)$ (10 mg) and PPh_2Me (10 mg, excess) were dissolved in CD_2Cl_2 (0.6 ml) in an NMR tube and allowed to react overnight. A ^1H NMR spectrum of the reaction mixture revealed $CpMo(NO)(=CDCMe_3)(PPh_2Me)$ to be the only organometallic product. Other resonances were attributable to neopentane-d_3 and residual PPh_2Me.

5.2.9 Preparation of $[(Me_3P)_4Mo(NO)Cl]_2$ (5.6)

A solution of $CpMo(NO)(CH_2CMe_3)_2$ was generated from $CpMo(NO)Cl_2$ (2.00 mmol) and $(Me_3CCH_2)_2Mg{\cdot}X$(dioxane) (4.05 mmol $Me_3CCH_2^-$) in THF (30 mL). The volume of the red solution was reduced to 5 mL, and CH_2Cl_2 (50 mL) was added. The solution was cooled to -50 °C and PMe_3 (1 atm) was vacuum transferred onto the reaction mixture. The reaction mixture was allowed to warm to room temperature was stirred for an additional 5 h. The resulting orange slurry was taken to dryness in vacuo and washed with pentane (20 mL). The residue was extracted with Et_2O/THF (10:1, 4 x 50 mL), and the combined extracts were filtered through alumina I (3 x 3 cm). The orange filtrate was taken to dryness and the reamining solid recrystallized from Et_2O. Over time the Et_2O solution darkened[11] and deposited gold flakes of **5.6** (204 mg, 22% yield).

Anal. Calcd for $C_{12}H_{36}NOP_4ClMo$: C, 30.95; H, 7.79; N, 3.01. Found: C, 31.22; H, 7.77; N, 3.14. IR (Nujol) ν_{NO} 1528 (vs), ν_{PC} 939 (vs) cm^{-1}. ^1H NMR (C_6D_6) δ 1.30 (br t, $P(CH_3)_3$, J = 2.6 Hz). $^{13}C\{^1H\}$ NMR (C_6D_6) δ 19.29 (br s, $P(CH_3)_3$). $^{31}P\{^1H\}$ NMR (C_6D_6) δ -3.03 (s).

5.2.10 Preparation of CpMo(NO)(=CHCMe$_3$)(py) (5.7)

A solution of CpMo(NO)(CH_2CMe_3)$_2$ was generated from CpMo(NO)Cl_2 (1.80 mmol) and (Me_3CCH_2)$_2$Mg·*X*(dioxane) (3.62 mmol $Me_3CCH_2^-$) in THF (30 mL). The solution was taken to dryness in vacuo at -20 °C, extracted with Et_2O (40 mL), and quickly filtered through alumina I (2 × 2 cm) into a reaction vessel containing pyridine (1.0 mL, excess). The contents of the bomb were sealed under vacuum and were stirred overnight in the dark. The amber reaction mixture was then taken to a brown oil in vacuo. Pentane (50 mL) was added to the oil, the resulting solution was stirred rapidly for 1 h, and the pentane was removed in vacuo. Drying under high vacuum for 4 h provided a brown powder which was dissolved in Et_2O (20 mL), filtered through Celite (2 x 2 cm). The filtrate was concentrated in vacuo and placed in a freezer at -30 °C to induce crystallization. Brown crystals of the pyridine adduct were isolated after several days (230 mg, 38% yield). When crushed, the brown crystals became a bright yellow powder.

Anal. Calcd for $C_{15}H_{20}N_2OMo$: C, 52.95; H, 5.92; N, 8.23. Found: C, 52.56; H, 6.02; N, 8.08. IR (Nujol) ν_{NO} 1532 (vs), 1545 (sh) cm^{-1}. ^{1}H NMR (C_6D_6) δ 13.56 (s, 1H, C*H*), 8.28 (d, 2H, pyridine protons, J_{HH} = 1.5 Hz), 6.62 (t, 1H, pyridine proton, J_{HH} = 7.8 Hz), 6.20 (t, 2H, pyridine protons, J_{HH} = 5.7 Hz), 5.52 (s, 5H, C_5H_5), 1.56 (s, 9H, C(CH_3)$_3$). ^{13}C{^{1}H} NMR (C_6D_6) δ 303.51 (s, =*C*H), 155.47, 136.82, 123.93 (s, pyridine carbons), 100.10 (s, C_5H_5), 50.80 (s, *C*(CH_3)$_3$), 32.33 (s, C(*C*H_3)$_3$). Low-resolution mass spectrum (probe temperature 150 °C): *m/z* 540 [(P^+-CHCMe$_3$)]$_2$, 272 (P^+-CHCMe$_3$).

5.2.11 Preparation of CpMo(NO)(=CHCMe$_3$)(PMe$_3$) by Reaction of 5.7 with PMe$_3$

An NMR tube was charged with CpMo(NO)(=CHCMe$_3$)(py) (**5.7**) and C_6D_6 (0.7 mL). The tube and its contents were frozen to -196 °C, then PMe_3 (1.1 equiv) was vacuumed transferred into the tube. The reaction mixture was then warmed to room temperature. Over the course of 30 min the solution darkened to red-brown from amber. A ^{1}H NMR spectrum of the sample revealed that the pyridine adduct had been converted to the PMe_3 adduct and 1 equiv of pyridine had been liberated. The complex, CpMo(NO)(=CHCMe$_3$)(PMe$_3$), was not isolated.

^{1}H NMR (C_6D_6) δ 13.21 (d, 1H, C*H*, J_{PH} = 3.9 Hz), 5.32 (d, 5H, C_5H_5, J_{PH} = 1.2 Hz), 1.43 (s, 9H, $C(CH_3)_3$), 0.92 (d, 9H, PMe_3, J_{PH} = 9.0 Hz).

5.2.12 Attempted Preparations of CpMo(NO)(=CHCMe$_3$)(L) [L = acetone, acetonitrile, thiophene, PhCCH, P(CMe$_3$)$_3$]

All five of these experiments led to the same result. Typically, a solution of $CpMo(NO)(CH_2CMe_3)_2$ was generated in THF then worked-up into CH_2Cl_2 or Et_2O. An excess of the appropriate ligand (5 - 10 eq) was then introduced into the red solution. Stirring of the mixture overnight in the dark at room temperature resulted in a brown solution over copious quantities of a intractable brown powder. Filtration of the reaction mixture through Celite followed by attempts at crystallization provided only more brown powders which were found to consist of many products as judged by ^{1}H NMR spectroscopy. In some cases resonances attributable to small quantities of **5.2** were apparent in the NMR spectra.

5.2.13 Preparation of CpMo(NO)(η^2-C{NCMe$_3$}CH$_2$CMe$_3$)(CH$_2$CMe$_3$) (5.8)

A solution of $CpMo(NO)(CH_2CMe_3)_2$ (from 1 mmol of $CpMo(NO)Cl_2$) in Et_2O (30 mL) was prepared in the usual manner (Section 5.2.7). This solution was cannulated into a reaction vessel containing $CNCMe_3$ (339 μL, 3.00 mmol). As the red solution encountered the isocyanide, it immediately turned yellow. The yellow solution was taken to dryness in vacuo to remove excess $CNCMe_3$. The resulting yellow powder was crystallized from Et_2O in 3 fractions to obtain 200 mg (48% yield) of **5.8**.

Anal. Calcd for $C_{20}H_{36}N_2OMo$: C, 57.68; H, 8.71; N, 6.73. Found: C, 57.89; H, 8.71; N, 6.70. IR (Nujol) ν_{NO} 1549 (vs), ν_{NC} 1680 (m) cm^{-1}. ^{1}H NMR (C_6D_6) δ 5.21 (s, 5H, C_5H_5), 3.17 (d, 1H, CH_2, J_{HH} = 13.5 Hz), 2.68 (d, 1H, CH_2, J_{HH} = 12.0 Hz), 2.25 (d, 1H, CH_2, J_{HH} = 12.0 Hz), 2.20 (d, 1H, CH_2, J_{HH} = 13.5 Hz), 1.51 (s, 9H, $NC(CH_3)_3$), 1.13 (s, 9H, $C(CH_3)_3$), 1.12 (s, 9H, $C(CH_3)_3$). ^{13}C{^{1}H} NMR (C_6D_6) δ 204.86 (s, *C*N), 100.49 (s, C_5H_5), 61.25 (s, $NC(CH_3)_3$), 48.30 (s, CH_2), 37.86 (s, $C(CH_3)_3$), 35.20 (s, $NC(CH_3)_3$), 32.80 (s, $C(CH_3)_3$),

31.87 (s, CH_2), 30.30 (s, $C(CH_3)_3$), 30.25 (s, $C(CH_3)_3$). Low-resolution mass spectrum (probe temperature 180 °C): *m/z* 418 (P^+).

5.2.14 Preparation of CpMo(NO)(CH_2CMe_3)(NHR) [R = CMe_3 (5.9); *p*-tolyl (5.10)]

The reactions leading to **5.9** and **5.10** were conducted in a similar manner. A sample of CpMo(NO)(CH_2CMe_3)$_2$ (from 2 mmol of CpMo(NO)Cl_2) in Et_2O (50 mL) was prepared in the usual manner (Section 5.2.7). The red solution was treated with an excess of amine either as a solid ((*p*-tolyl)NH_2, 600 mg) or by vacuum transfer (Me_3CNH_2, ~1 mL) and stirred for 8 h in the dark at 15 °C. The final reaction mixture (brown for **5.9**, orange for **5.10**) was taken to dryness and the excess amine removed in vacuo. Several hours exposure to dynamic vacuum were necessary to sublime all excess (*p*-tolyl)NH_2 from **5.10**. CpMo(NO)(CH_2CMe_3)($NHCMe_3$) (**5.9**) was recrystallized from pentane as amber needles in 56% yield. Complex **5.10**, CpMo(NO)(CH_2CMe_3)(NH-*p*-tolyl), was recrystallized from Et_2O as orange blocks (33% yield).

Complex 5.9: Anal. Calcd for $C_{14}H_{26}N_2OMo$: C, 50.30; H, 7.84; N, 8.38. Found: C, 50.60; H, 7.79; N, 8.10. IR (Nujol) ν_{NO} 1554 (br, vs) cm^{-1}. ^1H NMR (C_6D_6) δ 8.92 (br s, 1H, N*H*), 5.22 (s, 5H, C_5H_5), 2.16 (d, 1H, CH_2, J_{HH} = 11.8 Hz), 1.61 (d, 1H, CH_2, J_{HH} = 11.8 Hz), 1.30 (s, 18H, 2 x $C(CH_3)_3$). $^{13}C\{^1H\}$ NMR (C_6D_6) δ 102.55 (s, C_5H_5), 68.00 (s, $NHC(CH_3)_3$), 46.16 (s, CH_2), 36.20 (s, $CH_2C(CH_3)_3$), 34.24, 32.75 (s, 2 x $C(CH_3)_3$). Low-resolution mass spectrum (probe temperature 180 °C): *m/z* 335 (P^+-H).

Complex 5.10: Anal. Calcd for $C_{17}H_{24}N_2OMo$: C, 55.44; H, 6.57; N, 7.61. Found: C, 55.25; H, 6.49; N, 7.70. IR (Nujol) ν_{NO} 1548 (s), 1563 (sh) cm^{-1}. ^1H NMR (C_6D_6) δ 10.49, 9.84 (br s, 2H, 2 x N*H*), 7.37, 6.96, 6.81, 6.38 (d, 8H, 2 x H_{ortho} and 2 x H_{meta}, J_{HH} = 7.4 or 9.3 Hz), 5.14, 5.12 (s, 10H, 2 x C_5H_5), 2.26 (2 superimposed doublets, 1H each, CH_{anti}, J_{HH} = 12.9 Hz), 2.08, 2.05 (s, 6H, 2 x *p*-CH_3), 1.82 (d, 1H, CH_{syn}, J_{HH} = 10.8 Hz), 1.67 (d, 1H, CH_{syn}, J_{HH} = 11.1 Hz), 1.32, 1.28 (s, 18H, 2 x $C(CH_3)_3$). ^{13}C NMR (C_6D_6) δ 153.56, 153.15 (2 x C_{ispo}), 133.59, 133.29 (2 x C_{para}), 130.08, 129.42 (2 x C_{ortho}), 119.80, 119.65 (2 x C_{meta}), 103.25, 103.07 (2 x C_5H_5), 57.42, 55.18 (2 x CH_2), 37.52, 36.89 (2 x CMe_3), 34.05, 33.99 (2 x

$C(CH_3)_3$), 20.85 (2 x *p*-CH_3). Low-resolution mass spectrum (probe temperature 200 °C): *m/z* 370 (P^+).

5.2.15 Preparation of CpMo(NO)(CHDCMe$_3$)(NH-*p*-tolyl) (5.10-d_1)

In a drybox, solid CpMo(NO)(CD_2CMe_3)$_2$ (**5.1**-d_4) (100 mg, 0.296 mmol) and solid (*p*-tolyl)NH_2 (100 mg, 0.935 mmol, 3.16 eq) were weighed into a Schlenk tube. Et_2O (10 mL) was vacuum transferred onto the solids to yield a red solution which over the course of 24 h turned dark orange while being stirred. The orange solution was taken to dryness, and excess amine was removed by sublimation at room temperature. The remaining orange solid was extracted with Et_2O (15 mL), filtered through Celite (1 x 2 cm), concentrated, and crystallized over 1 week at -30 °C. Orange crystals of **5.10**-d_1 (74 mg, 68% yield) were isolated by removing the mother liquor with a pipette.

^{1}H NMR (C_6D_6) δ 10.48, 9.83 (br s, 2H, 2 x N*H*), 7.36, 6.97, 6.81, 6.38 (d, 8H, 2 x H_{ortho} and 2 x H_{meta}, J_{HH} = 8.1 Hz), 5.14, 5.12 (s, 10H, 2 x C_5H_5), 2.08, 2.05 (s, 6H, 2 x *p*-CH_3), 1.78, 1.63 (br s, 2H, 2 x C*H*D), 1.32, 1.28 (s, 18H, 2 x $C(CH_3)_3$). ^{2}H NMR (C_6H_6, 40 MHz) δ 2.32 (br s, CH*D*CMe_3). Low-resolution mass spectrum (probe temperature 200 °C): *m/z* 371 (P^+).

5.2.16 Preparation of CpMo(NO)(CH_2CMe_3)(OPh) (5.11)

A solution of CpMo(NO)(CH_2CMe_3)$_2$ (from 1 mmol of CpMo(NO)Cl_2) in Et_2O (25 mL) was prepared in the usual manner (Section 5.2.7). The red solution was cannulated into a bomb containing PhOH (250 mg, 2.5 equiv). The solution was stirred in the dark for 12 h whereupon the solvent and excess phenol were removed in vacuo (8 h at room temperature). The residual red oil was dissolved in hexanes (20 mL) and filtered through Celite (1 x 2 cm). The filtrate was concentrated slightly, and then maintained at -30 °C for 1 week in a freezer. The red oil which settled was separated from the hexanes mother liquor via cannulation. The oil was dried overnight in vacuo (~90 mg, ~25% yield).

Anal. Calcd for $C_{16}H_{21}NO_2Mo$: C, 54.09; H, 5.96; N, 3.94. Found: C, 54.32; H, 6.08; N, 4.00. IR (Nujol) ν_{NO} 1608 - 1588 (v br, vs) cm^{-1}. ^1H NMR (C_6D_6) δ 7.65 - 6.59 (3 br m, 5H, Ph), 5.19 (s, 5H, C_5H_5), 3.51 (d, 1H, CH_2, J_{HH} = 10.2 Hz), 1.41 (d, 1H, CH_2, J_{HH} = 10.2 Hz), 1.15 (s, 9H, $C(CH_3)_3$). $^{13}C\{^1H\}$ NMR (C_6D_6) δ 129.69, 122.39, 117.74, 108.93 (C_{aryl}), 104.58 (s, C_5H_5), 77.08 (s, CH_2), 39.16 (s, $C(CH_3)_3$), 33.28 (s, $C(CH_3)_3$).

5.2.17 Kinetic Measurements

The conversion of $CpMo(NO)(CH_2CMe_3)_2$ (**5.1**) to $CpMo(NO)(=CHCMe_3)$ was studied in order to gain some insight into the mechanism of thermal decomposition operative in this system. All mechanistic studies were performed using the tetradeutero analogue of **5.1**, $CpMo(NO)(CD_2CMe_3)_2$ (**5.1**-d_4). Solid $CpMo(NO)(CD_2CMe_3)_2$ and the appropriate trapping ligand were weighed into a volumetric flask in a drybox. Dissolution with the appropriate solvent was quickly executed. The volumetric flask was shaken and an aliquot was transferred to a 1.00-cm UV-vis spectrophotometer cell equipped with a 4-mm Teflon stopcock. The concentration of the trapping ligand was sufficiently high such that all runs were effectively conducted under pseudo-first-order conditions. The cell was quickly removed from the drybox, and placed in a Hewlett-Packard 8542A diode array spectrometer, which in conjunction with a Haake W19 temperature bath equipped with a Haake D8 temperature controller allowed the cell to be maintained at constant temperature (±0.1 °C). The solution was left unstirred and allowed to equilibrate with the spectrometer temperature for 300 s. Spectra were then recorded at regular intervals and data were collected for at least 3 half-lives. The absorbance values at infinity were determined experimentally by allowing certain runs to proceed for at least 10 half-lives. The measured infinity values were always within 0.1 of computer-optimized infinity values. For example, the infinity value for run 4 was measured and found to be 0.130, while the calculated value for A_∞ was optimized to 0.1299. The observed rate constants (k_{obs}) were then calculated from plots of $\ln(A_\infty - A_t)$ versus time (in seconds). Values of $\Delta H^\ddagger$ and $\Delta S^\ddagger$ were determined from

Erying plots of $\ln(k_{obs}/T)$ versus 1/T where $\Delta H^{\ddagger} = -R(\text{slope})$ and $\Delta S^{\ddagger} = R[\text{intercept} - \ln(k_B/h)]$ (R, k_B and h are the gas constant, Boltzmann's constant and Planck's constant, respectively).

5.3 Results and Discussion

In accord with the theme of this thesis it seemed appropriate to investigate the thermal behaviour of $Cp'M(NO)R_2$ complexes. Since the original method to bis(hydrocarbyl) complexes of this type involved their preparation at room temperature, it was of interest to determine if the reason that many such complexes could not be prepared was due to their thermal instability. In general, 16-electron $Cp'M(NO)R_2$ complexes are thermally stable at 20 °C when isolated in analytically pure form.[12] This stability reflects both the non-bonding nature of the metal-centered LUMO of these complexes and their kinetic inertness toward decomposition.[13] However, as the electron deficiency of these complexes increases, so too does their thermal sensitivity (Chapter 2). Since we were unable to isolate the most thermally sensitive compounds in this class, namely the $CpMo(NO)(aryl)_2$ species, we were not able to effect a systematic study of their thermal decomposition. The next most thermally sensitive class of these nitrosyl complexes involves the related Mo dialkyl complexes, $CpMo(NO)(alkyl)_2$. A representative member of this class, namely $CpMo(NO)(CH_2CMe_3)_2$, was purposely left out of Chapter 3 since the chemistry of this very thermally sensitive compound is sufficient to warrant an entire chapter in this thesis. As it turns out, the most thermally sensitive, yet isolable, $Cp'M(NO)R_2$ complex is the one that decomposes the most cleanly. It has been observed in our group that most $Cp'M(NO)R_2$ complexes do not decompose along one pathway, rather a multitude of thermal decomposition products are formed.[14]

5.3.1 Synthesis and Characterization of $CpMo(NO)(neopentyl)_2$ (5.1 and 5.1-d_4)

$CpMo(NO)(CH_2CMe_3)_2$ and its deuterated analogue $CpMo(NO)(CD_2CMe_3)_2$ are prepared by the methodology developed in Chapters 2 and 3 (eq 5.3).

$$CpMo(NO)Cl_2 \xrightarrow[THF,\ -40\ ^\circ C]{(Me_3CCX_2)Mg\cdot dioxane} CpMo(NO)(CX_2CMe_3)_2 \qquad (5.3)$$

X = H (**5.1**), D (**5.1-d_4**)

Complex **5.1** must be prepared at low temperatures (yield ca. 55%) and used immediately in further derivatization reactions. On the other hand, **5.1-d_4** can be crystallized from pentane in about 40% yield, but must be stored at -30 °C. Both complexes are exceptionally thermally and air-sensitive. They are, however, not particularily sensitive to deaerated water (Chapter 4).

The spectral properties of both complexes are consistent with their formulation as monomeric species. Interestingly, the ^{1}H NMR spectrum of **5.1-d_4** shows no signals attributable to methylene protons, thus implying nearly 100% deuteration at C_α. A possible explanation for this observation is that any α-protio-containing complexes decompose, and are removed, under the conditions in which **5.1-d_4** is handled during workup. The ^{2}H NMR spectrum of **5.1-d_4** exhibits two broad singlets at approximately the same chemical shifts as the two doublets ($^2J_{HH}$ = 12.1 Hz) in the ^{1}H NMR spectrum of **5.1** attributed to the methylene protons of the complex; however, no D-D coupling constants could be extracted from the ^{2}H NMR spectrum.

5.3.1.1 Solid-State Molecular Structure of $CpMo(NO)(CD_2CMe_3)_2$

When carefully prepared, complex **5.1-d_4** forms high quality red crystals suitable for an X-ray crystallographic analysis.[15] The molecular structure is shown in Figure 5.1. The analysis was performed at low temperature (170 K) since the complex, even in highly crystalline form, decomposes completely in under 12 h in the solid state at room temperature.[16] No anomalously close contacts were found to exist between the alkyl residues or between the metal and the CD_2 groups. The refined positions of the methylene deuterons do not suggest any agostic-type C-D-Mo interactions which might be expected for a coordinatively unsaturated 16-electron complex. We found this somewhat surprising given the abnormally high thermal sensitivity of this complex. The intramolecular dimensions about Mo (Table 5.1) are also completely as expected and consistent with this species being a potent Lewis acid (for a full discussion of the structure/Lewis

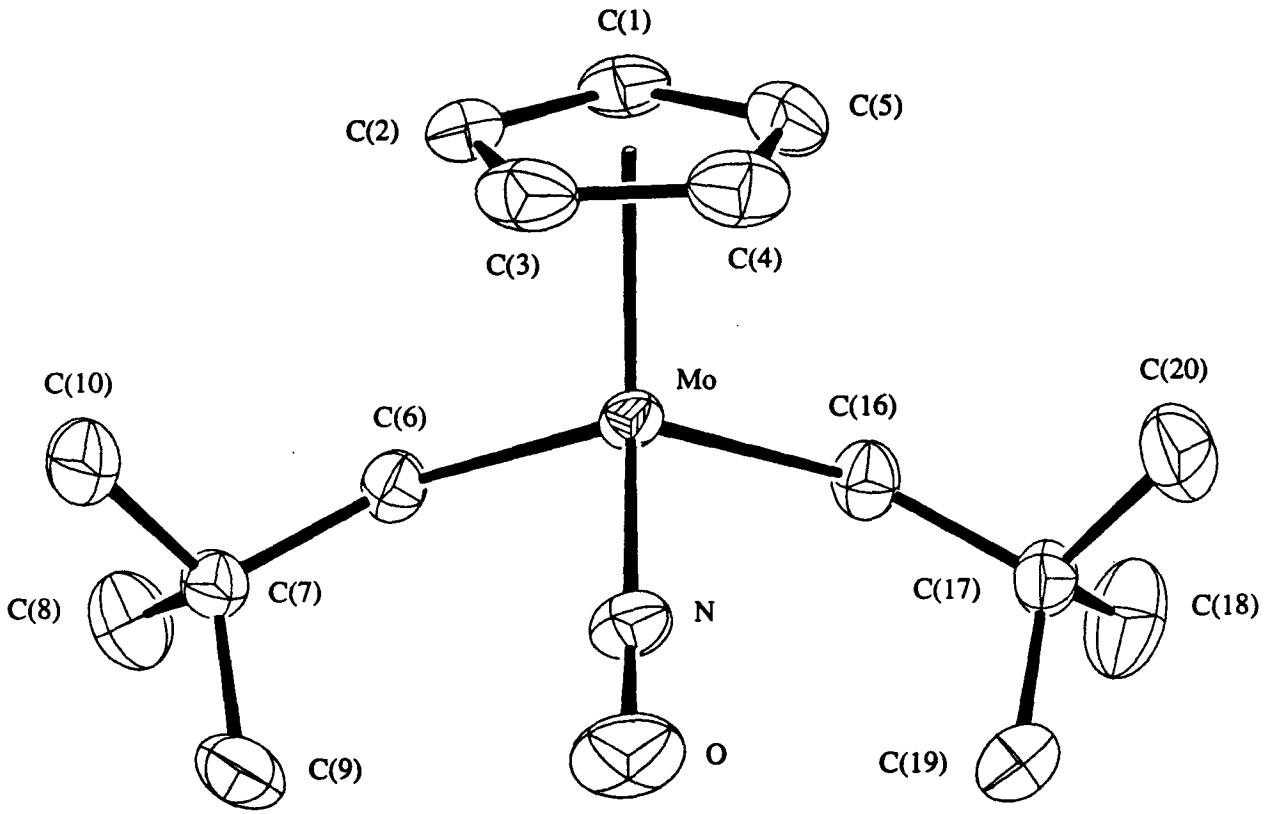

Figure 5.1 ORTEP diagram of **5.1**-d_4. 50% probability ellipsoids are shown for the non-hydrogen atoms

Table 5.1 Representative bond lengths and angles for complex **5.1**-d_4

bond lengths (Å) (esd)		bond angles (°) (esd)	
Mo-N	1.766(3)	C6-Mo-C16	111.52(11)
N-O	1.213(3)	C16-Mo-N	98.27(11)
Mo-C6	2.143(3)	N-Mo-C6	97.51(11)
Mo-C16	2.129(3)	Mo-N-O	168.5(3)

acidity relationship, see Chapter 3). The only intermolecular separations significantly less than the sums of the appropriate pairs of van der Waals radii are O--C(1)' (3.148(4) Å) and O--C(5)' (3.083(4) Å) where the primes indicate the operation -1/2+x, 1/2-y, 1/2+z (space group: $P2_1/n$).

5.3.2 Synthesis and Characterization of $[CpMo(NO)(CHCMe_3)]_2$

To demonstrate the thermal instability of $CpMo(NO)(CH_2CMe_3)_2$, a deep red solution of the complex in dichloromethane (ν_{NO} 1609 cm^{-1}) is stirred at room temperature for several hours. The color of the solution fades with time such that the final solution is pale orange and exhibits a broad band at 1594 cm^{-1} in its IR spectrum. Removal of the solvent, followed by exhaustive extraction with Et_2O affords an amber solution. Attempts to crystallize product from this solution yield an impure brown powder. Additionally, the color of the solution continues to darken with time, thereby implying that reactions are still occurring. Chromatography, however, simplfies the isolation of a pure product. Filtration of the above-mentioned ether solution through alumina I neutral and crystallization of the eluted complex from Et_2O yields pale orange crystals of **5.2**. To date, the highest isolated yield of the complex is 47%. ^1H NMR spectroscopic monitoring of the above reaction shows that the yield is variable (30 - 60%).

Complex **5.2** exhibits very unusual spectral properties which are not easily interpretable. For example, its IR spectra (solution or Nujol mull (Figure 5.2a)) exhibit two strong bands at 1595 and 1315 cm^{-1}, and its ^1H (Figure 5.2b) and ^{13}C NMR spectra exhibit two sets of equal intensity C_5H_5, CH and CMe_3 resonances, and no resonances characteristic of methylene-type protons.

By elemental analysis, the formula of the isolated compound is $CpMo(NO)(CHCMe_3)$, but a mass-spectral parent ion having *m/z* 526 implies that the complex is dimeric.

$$2\ CpMo(NO)(CH_2CMe_3)_2 \xrightarrow{\Delta} [CpMo(NO)(CHCMe_3)]_2 \qquad (5.4)$$

5.1 **5.2**

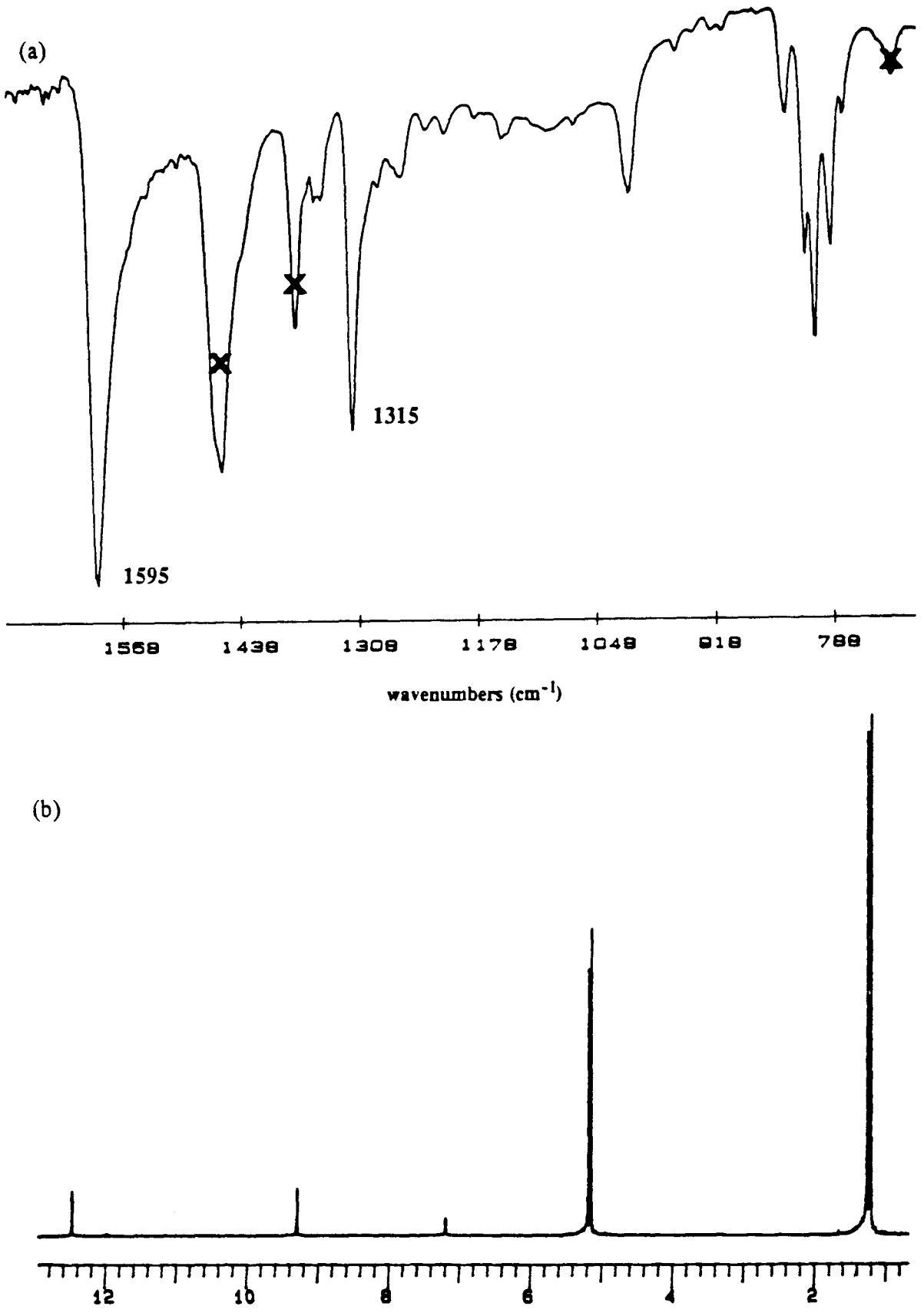

Figure 5.2 Spectroscopic characterization of **5.2**: (a) partial Nujol (marked by **X**) mull infrared spectrum (1700 - 700 cm^{-1}); (b) 300 MHz ^1H NMR spectrum in C_6D_6

But, somehow, the two halves of the dimer are inequivalent. Thus, to resolve any ambiguity as to the molecular structure of complex **5.2**, an X-ray crystallographic analysis was performed on a suitable crystal of the complex.

5.3.2.1 X-ray Crystallographic Analysis of $[CpMo(NO)(CHCMe_3)]_2$

An X-ray analysis of **5.2**[17] establishes that the molecular unit is a dimer of $CpMo(NO)(CHCMe_3)$ whose structure is unique for two significant reasons; (1) the $CpMo(NO)(CHCMe_3)$ units are associated very asymmetrically through bridging nitrosyl and alkylidene groups even though there are no apparent factors prohibiting symmetric association;[18] (2) a μ-η^1:η^2-NO group has never before been observed.[21] An ORTEP diagram of the solid-state molecular structure of **5.2** is shown in Figure 5.3.

The bonding of the bridging nitrosyl group in **5.2** (Figure 5.3) is clearly η^1 to Mo(1) and η^2 to Mo(2). The bonding is best described as the bridging NO ligand acting as a 3-electron donor to Mo(1) and a 2-electron donor to Mo(2) (Figure 5.4). Thus, the intramolecular dimensions (Table 5.2) of the Mo(μ-η^1:η^2-NO)Mo entity involve an elongated N-O linkage (1.296 (3) Å)[19] which is essentially linear with respect to Mo(1) [Mo(1)-N(1)-O(1) = 165.5 (2)°] and is symmetrically disposed with respect to Mo(2) [Mo(2)-N(1) = 2.187 (3) and Mo(2)-O(1) = 2.149 (2) Å].

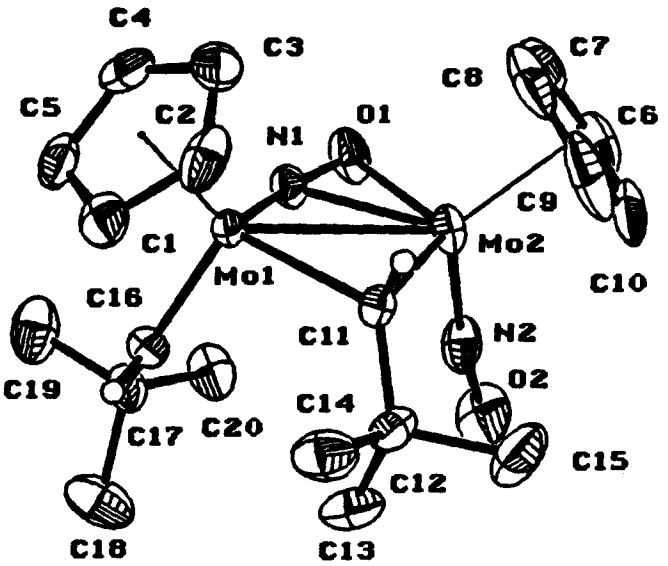

Figure 5.3 ORTEP diagram of [CpMo(NO)](μ-η^1:η^2-NO)(μ-CHCMe$_3$)[CpMo(=CHCMe$_3$)] (**5.2**). 33% probability ellipsoids are shown for the non-hydrogen atoms

Table 5.2 Representative bond lengths and angles for complex **5.2**

bond lengths (Å) (esd)		bond angles (°) (esd)	
Mo1-Mo2	2.9607 (5)	Mo1-N1-O1	165.5 (2)
Mo1-N1	1.784 (3)	Mo2-N2-O2	171.0 (3)
Mo2-N2	1.763 (3)	Mo2-N1-O1	71.0 (2)
N1-O1	1.296 (3)	Mo1-C11-Mo2	85.1 (1)
N2-O2	1.216 (4)	Mo1-C16-C17	137.1 (2)
Mo2-N1	2.187 (3)	Mo1-N1-Mo2	95.9 (1)
Mo2-O1	2.149 (2)	Mo1-C11-C12	127.4 (2)
Mo1-C16	1.940 (3)	Mo2-C11-C12	125.7 (2)
Mo1-C11	2.186 (3)		
Mo2-C11	2.192 (3)		

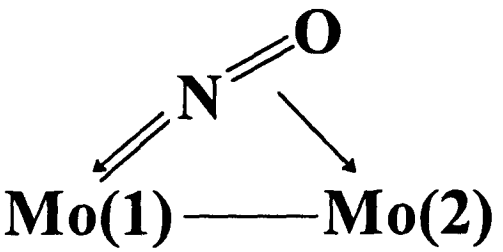

Figure 5.4 Valence-bond representation of a μ_2-η^1:η^2-NO ligand serving as a 5-electron donor to two Mo centers.

The Mo-Mo separation of 2.9607 (5) Å in complex **5.2** is consistent with the existence of a single metal-metal bond which may be invoked to account for the compound's diamagnetism and to provide each metal center with an 18-valence-electron configuration.[20] The spectroscopic properties of **5.2** confirm that the solid-state molecular structure persists in solution (vide supra).

5.3.2.2 Known Nitrosyl Bonding Modes

At the inception of this work there were eight known bonding modes for coordinated nitric oxide reported in the literature (Figure 5.5).[21] Monomeric complexes can have linear (**A**) or bent (**B**) terminal nitrosyl ligands, although structurally characterized bent nitrosyl groups are quite rare.[22] Three types of nitrosyl ligands can be found for bimetallic complexes. Two of these are η^1 bound through nitrogen and can be symmetrically (**C**) or asymmetrically (**D**) bound to the two metal centers. Isonitrosyl complexes (**E**), on the other hand are bound through nitrogen to one metal and oxygen to another metal. Three cluster complexes fill out the eight known bonding modes of NO. These complexes contain NO ligands that are μ_3-η^1 bound (**F**) and two variants on μ_4-η^2 coordination (**G**, **H**).

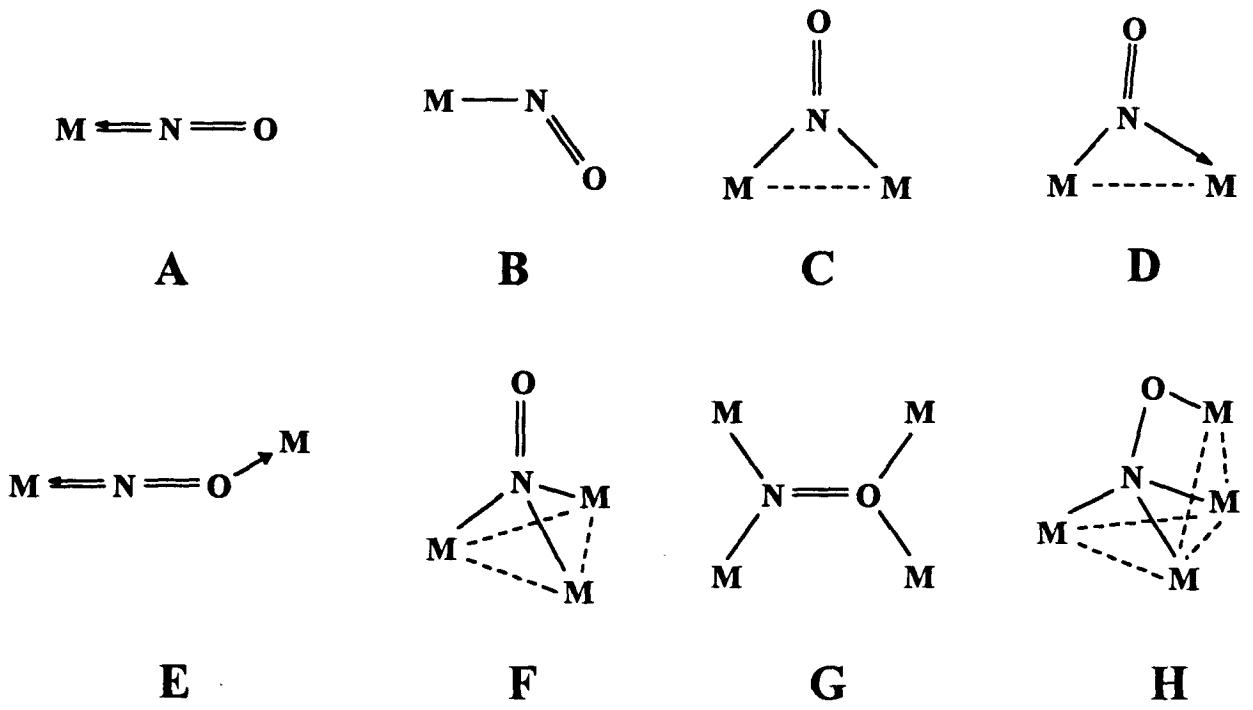

Figure 5.5 Known nitrosyl bonding modes (dashed lines indicate that a bonding interaction may or may not be present).

Clearly, the μ-η^1:η^2-NO ligand in complex **5.2** constitutes the ninth type of nitrosyl ligand to be structurally characterized. It might be noted that a few examples of μ-η^1:η^2-CO ligands can be found in the literature.[23] A theoretical study of μ-η^1:η^2-CO bonding has been presented by Hall and Simpson.[24] Their conclusion was that such CO ligands are a consequence of steric crowding.

5.3.3 Trapping Reactions

While the transformation of **5.1** into **5.2** is interesting and unusual, it also appears to be quite complex. Compound **5.2** is the major product of numerous ones resulting from reaction 5.4, as evidenced by NMR spectroscopic monitoring. In order to gain some chemical evidence for the transient formation of $CpMo(NO)(=CHCMe_3)$ from **5.1**, the dialkyl complex (**5.1**) was allowed to decompose in the presence of potential trapping ligands such as phosphines.

5.3.3.1 Synthesis and Characterization of CpMo(NO)(=CHCMe$_3$)(L) Complexes [L = Lewis base]

Stirring a solution of **5.1** in the presence of excess tertiary phosphines or pyridine, L, produces the adducts CpMo(NO)(=CHCMe$_3$)(L) [**5.3**, L = PPh$_2$Me; **5.4**, L = PPh$_3$; **5.5**, L = P(*p*-tolyl)$_3$; **5.7**, L = py] in good yields in a matter of hours at room temperature (eq 5.5).

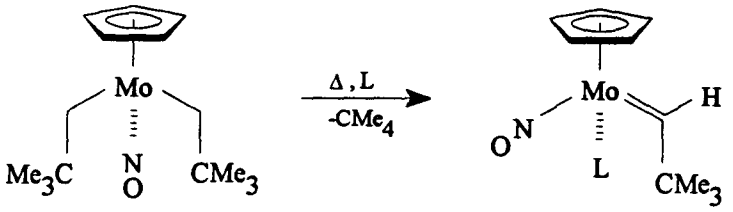

(5.5)

The above-mentioned alkylidene complexes are thermally stable, 18-electron species that can be handled as solids in air for short periods of time. These complexes (**5.3** - **5.5**, **5.7**) are the first monomeric Group 6 mononitrosyl Schrock-type alkylidene compounds to have been isolated. However, a few Fischer-type complexes are known. These are the chromium diphenyl[25] carbene complex, CpCr(NO)(CO)(=CPh$_2$)[26] prepared by Herrmann's group and the three CpM(NO)(CO)(=C(OMe)(Ph)) [M = Cr, Mo, W] complexes prepared by Fischer.[27] As expected, all four of these complexes originate from their dicarbonyl nitrosyl precursors.

While the yields of the phosphine adducts are about 50% based on CpMo(NO)Cl$_2$, this is more a function of the CpMo(NO)Cl$_2$ to CpMo(NO)(CH$_2$CMe$_3$)$_2$ step (~55%) rather than the trapping step (Section 5.2.3). The cleanness of the trapping step can be demonstrated by NMR spectroscopy. For example, an NMR-tube experiment in CD$_2$Cl$_2$ of the reaction of **5.1**-d_4 and excess PPh$_2$Me gives CpMo(NO)(=CDCMe$_3$)(PPh$_2$Me) (**5.3**-d_1) in quantitative yield (Section 5.2.8).

Since the nitrosyl-stretching frequencies (in Et$_2$O) of the starting material (1616 cm^{-1}) and product (1577 cm^{-1}) are so different, the progress of this trapping reaction can be easily monitored by IR spectroscopy (Figure 5.6). The isosbestic point at 1602 cm^{-1} is not as clear as in the UV-vis spectral monitoring (vide infra) of this same reaction, primarily due to the fact that our

IR flow cell system is not perfectly sealed and thus some evaporation of solvent occurs over the course of the reaction.

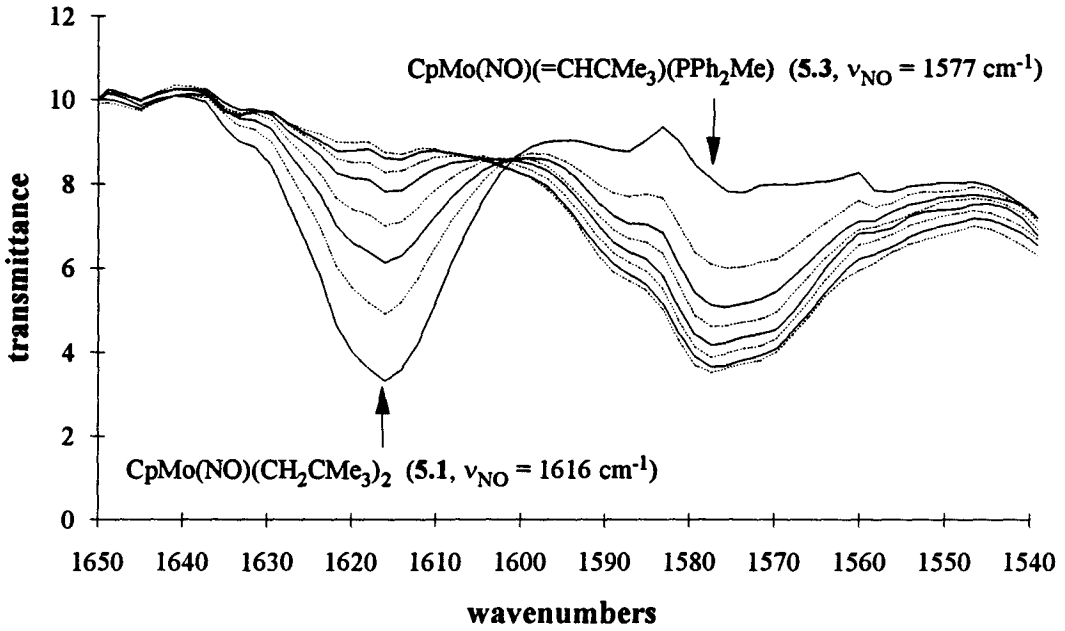

Figure 5.6 IR spectral monitoring (1650 to 1540 cm^{-1}) of the formation of $CpMo(NO)(=CHCMe_3)(PPh_2Me)$ (**5.3**) from **5.1** and excess PPh_2Me in Et_2O. Scans are taken at room temperature in 30-min intervals

$CpMo(NO)(=CHCMe_3)(L)$ complexes exhibit classic neopentylidene resonances in their NMR spectra.[28] For example, complex **5.4** exhibits a very low-field doublet (δ 13.80 ppm, $^3J_{PH}$ = 3.6 Hz) in its ^1H NMR spectrum (Figure 5.7 inset). The doublet arises from the coupling of the alkylidene proton to the ^{31}P nucleus of the phosphine ligand.

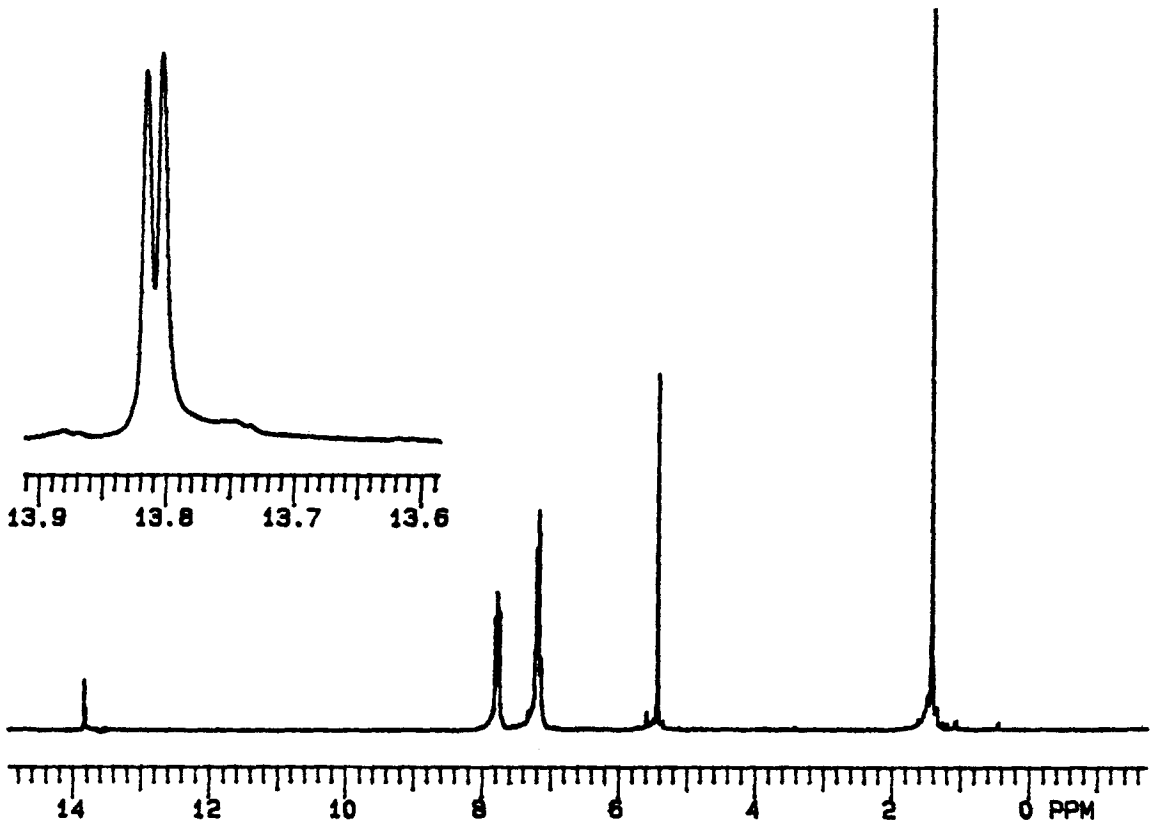

Figure 5.7 300 MHz ^{1}H NMR spectrum of CpMo(NO)(=CHCMe$_3$)(PPh$_3$) (**5.4**) in C_6D_6

The ^{1}H NMR spectrum of the pyridine adduct (**5.7**) shows 3 sets of clearly resolved resonances for the pyridine ring protons implying that the pyridine ring rotates quickly about the Mo-N axis, on the NMR timescale, at 25 °C.

5.3.3.2 X-ray Crystallographic Analysis of CpMo(NO)(=CHCMe$_3$)(PPh$_2$Me) (5.3)

The solid-state structure of CpMo(NO)(=CHCMe$_3$)(PPh$_2$Me)[29] (Figure 5.8) additionally confirms the monomeric nature of this and related neopentylidene nitrosyl complexes prepared in this work. The intramolecular dimensions of **5.3**, as established by X-ray diffraction, resemble those exhibited by the related [CpRe(NO)(=CHPh)(PPh$_3$)]$^+$ cation.[30]

Typically, high-valent alkylidene complexes exhibit M-C$_\alpha${H}-C bond angle distortions and complex **5.3** is no exception.[31] However, the distortion from idealized sp^2 geometry for complex

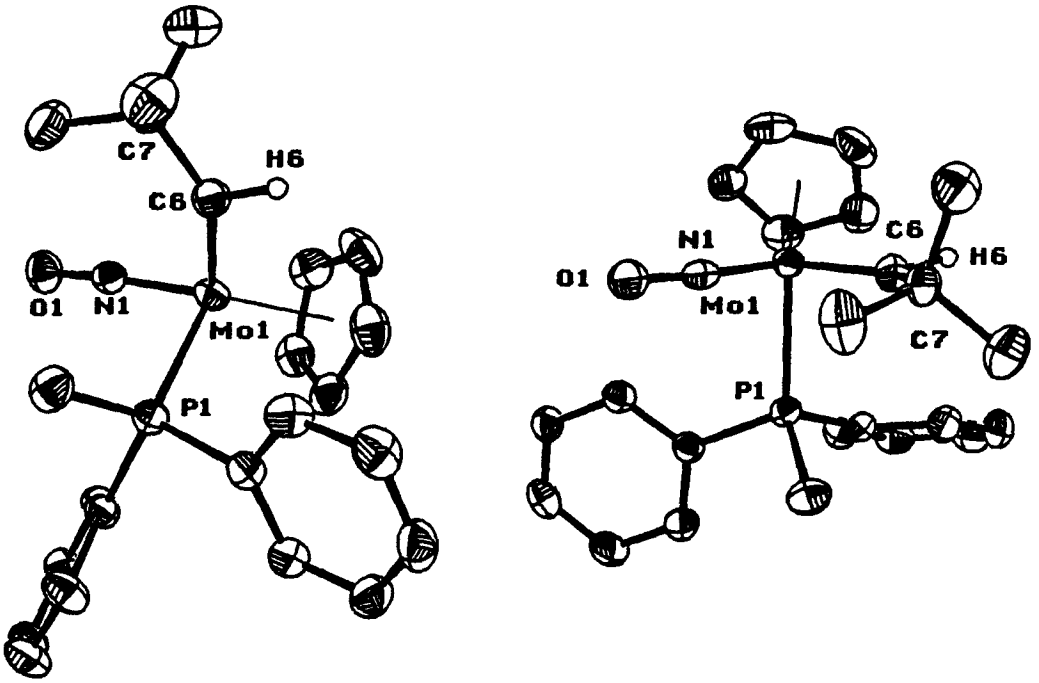

Figure 5.8 ORTEP diagrams of $CpMo(NO)(=CHCMe_3)(PPh_2Me)$ (**5.3**): (a) view perpendicular to alkylidene plane; (b) view parallel to alkylidene plane. 50% probability ellipsoids are shown for the non-hydrogen atoms. Labels for most carbons are omitted for clarity

Table 5.3 Representative bond lengths and angles about Mo in **5.3**

bond lengths (Å) (esd)		bond angles (°) (esd)	
Mo-P	2.451 (1)	P-Mo-N	92.94 (8)
Mo-N	1.757 (3)	P-Mo-C6	94.3 (1)
Mo-C6	1.950 (3)	N-Mo-C6	100.8 (1)
O-N	1.233 (3)	Mo-N-O	172.7 (2)
C6-C7	1.521 (5)	Mo-C6-C7	140.8 (3)
C6-H6	1.01 (4)	Mo-C6-H6	113 (2)
		C7-C6-H6	105 (2)

5.3 is not severe. Typically, an $M=C_\alpha$-C bond angle of 150° implies a significant M=C-H agostic interaction.[4,32] $CpMo(NO)(=CHCMe_3)(PPh_2Me)$, formally a Mo(II) species, exhibits a smaller angle at C_α of 140.8(3) Å. $M=C_\alpha$ bond lengths vary from 1.83 to 2.14 Å, with the shorter bond lengths being found in increasingly electron-deficient complexes. Structurally characterized Mo alkylidene complexes show very little variance of $Mo=C_\alpha$ bond length even though many "oxidation states"[33] have been characterized. The $Mo=C_\alpha$ bond length of 1.950(3) Å in **5.3** is in the middle of the known range (1.917 to 1.989 Å).[34]

5.3.3.3 Attempted Preparation of $CpMo(NO)(=CHCMe_3)(PMe_3)$

When a dichloromethane solution of **5.1** is treated with PMe_3, the expected $CpMo(NO)(=CHCMe_3)(PMe_3)$ complex is not obtained. Instead, $[(Me_3P)_4Mo(NO)Cl]_2$ (**5.6**) is the only isolable product. Evidently the Cp ligand can be removed from the coordination sphere of **5.1** by the potent base PMe_3, whereas weaker and bulkier nucleophiles cannot access the Mo center until the thermally induced loss of neopentane has occurred. The chloride ligand in the ultimate product must arise from the solvent. The dimeric structure of $[(Me_3P)_4Mo(NO)Cl]_2$ has been established by a partial X-ray crystallographic analysis of the complex, but the structure did not refine due to severe disorder amongst the ligands. ^1H, ^{13}C and ^{31}P NMR spectra of complex **5.7** exhibit only broad singlets at room temperature thereby implying that fast chemical exchange of the PMe_3 ligands occurs in solution. The related iodide complexes, $[(Me_3P)_4M(NO)I]_x$ [M = Mo, W; x is unknown], can be prepared by treating $CpM(NO)I_2$ with excess PMe_3.[35]

5.3.3.4 Preparation of $CpMo(NO)(=CHCMe_3)(PMe_3)$

While the reaction of $CpMo(NO)(CH_2CMe_3)_2$ with PMe_3 does not afford a PMe_3 adduct of $CpMo(NO)(=CHCMe_3)$, the complex can be prepared by a different route. Treatment of the pyridine complex (**5.7**) with 1 equiv of PMe_3 in benzene cleanly forms the PMe_3 complex and free pyridine (eq 5.6).

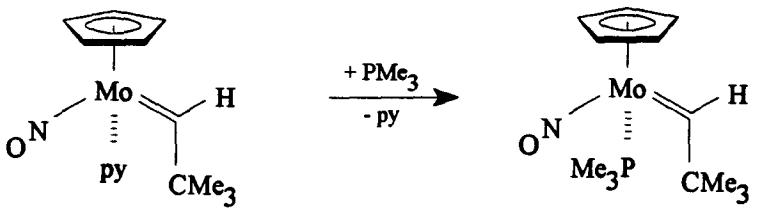

(5.6)

With the success of reaction 5.6 it is clear that the pyridine ligand in complex **5.7** is very labile. It is anticipated that CpMo(NO)(=CHCMe$_3$)(py) can be used as a stable (storable) source of CpMo(NO)(=CHCMe$_3$) in further reactivity studies.

5.3.3.5 Thermal Stability of Adduct Complexes

The three phosphine adducts (**5.3** -**5.5**) are thermally robust species that are unreactive to other Lewis bases. Thermolysis of any of these complexes results only in equilibration of the two possible alkylidene rotamers. The pyridine adduct **5.7**, however, is quite thermally sensitive due to the lability of the pyridine ligand in solution. Over the course of several months at room temperature in C_6D_6 the pyridine complex decomposes to yield (~90%) the asymmetric dimer **5.2** (eq 5.7).

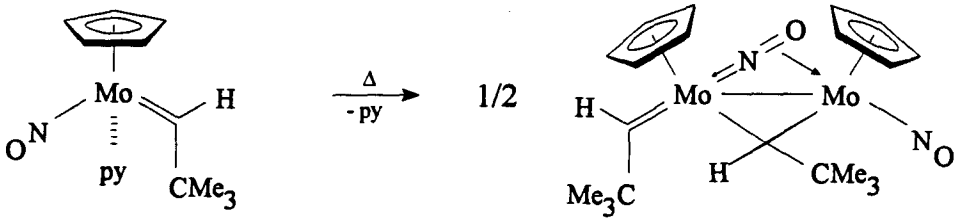

(5.7)

5.3.3.6 Attempted Preparation of CpMo(NO)(=CHCMe$_3$)(CNCMe$_3$): Synthesis of an Insertion Product

CNCMe$_3$ is very reactive towards CpMo(NO)(CH$_2$CMe$_3$)$_2$. Unlike other trapping ligands which cannot access the Mo center of this complex, *t*-butyl isocyanide reacts instantly at room temperature to give an air-stable iminoacyl complex, CpMo(NO)(η^2-C{NCMe$_3$}CH$_2$CMe$_3$)(CH$_2$CMe$_3$) (**5.8**) (eq 5.8).

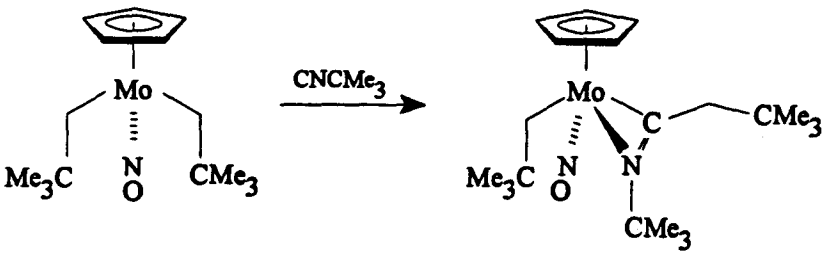

(5.8)

$CpMo(NO)(CH_2CMe_3)_2$ is a potent 16-electron Lewis acid (ν_{NO} 1623 cm^{-1}) and insertion of $CNCMe_3$ into one of the Mo-neopentyl bonds causes a dramatic drop in ν_{NO} by 74 cm^{-1} to that observed for **5.8** (ν_{NO} 1549 cm^{-1}). The η^2 nature of the iminoacyl group is best characterized by a ν_{CN} band at 1680 cm^{-1} in the IR spectrum of the product. This low-energy stretch is typical of other η^2-iminoacyl ligands.[36] As shown in Figure 5.9, the ^1H NMR spectrum of complex **5.8** displays 4 resonances due to the diastereotopic methylene protons of the complex. Signals due to the three inequivalent butyl groups are also apparent at δ 1.51, 1.13 and 1.12 ppm.

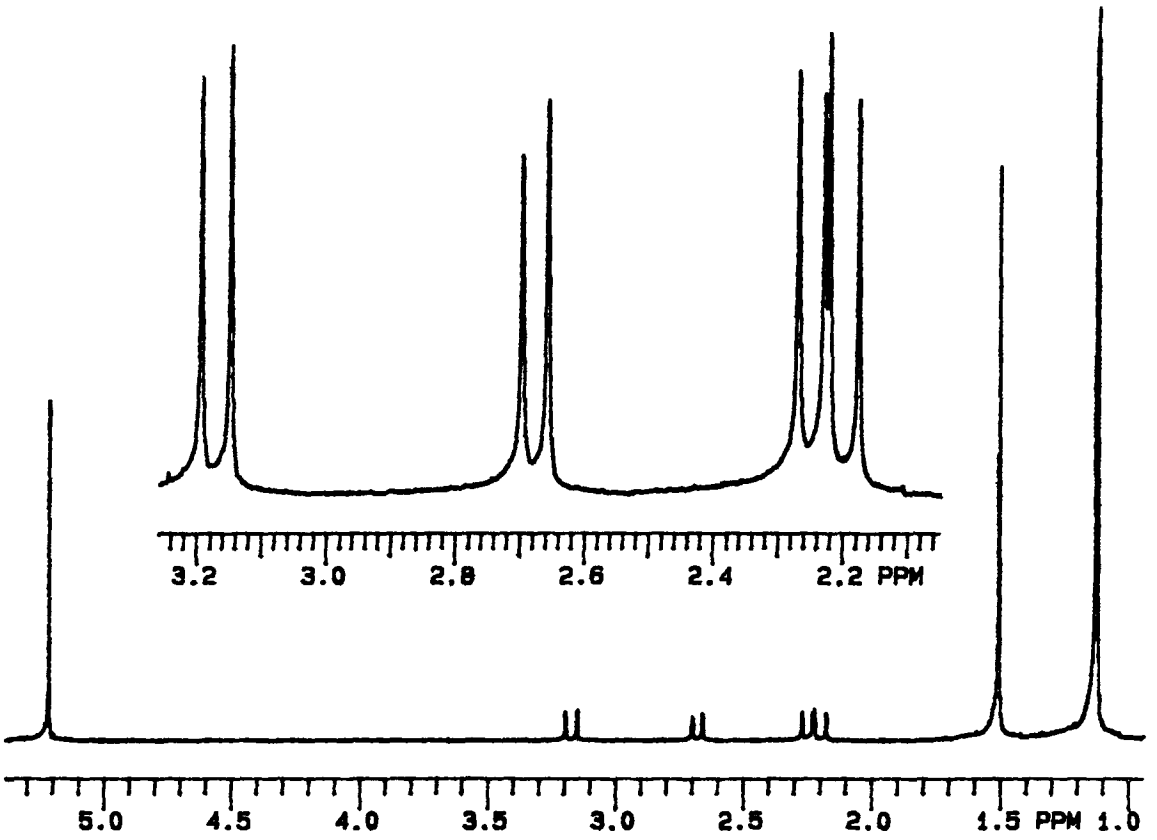

Figure 5.9 ^1H NMR spectrum of complex **5.8** in C_6D_6

Since $CNCMe_3$ is sufficiently small to access the Mo atom in $CpMo(NO)(CH_2CMe_3)_2$, no attempts to trap $CpMo(NO)(=CHCMe_3)$ with small Lewis bases such as CO or H_2 were effected since it was obvious that they would preferentially react with the starting material, $CpMo(NO)(CH_2CMe_3)_2$.

Many trapping reactions are not successful (Section 5.2.11). For example, acetone, acetonitrile, thiophene, PhCCH and $P(CMe_3)_3$ are not appropriate ligands for the formation of $CpMo(NO)(=CHCMe_3)L$ species. Thus, when complex **5.1** is allowed to thermally decompose in the presence of these ligands, total decomposition of the reaction mixture is observed.

5.3.4 Kinetic Studies

With substantial chemical evidence for the transient existence of $CpMo(NO)(=CHCMe_3)$, a kinetic investigation of the trapping reactions (Section 5.3.3.1) seemed in order. Since the transformation leading to the asymmetric alkylidene dimer was not clean, and the reactions leading to the phosphine-trapped alkylidene monomers were very clean as evidenced by both NMR and IR spectroscopies, a detailed analysis of the reactions of $CpMo(NO)(CH_2CMe_3)_2$ with phosphines was conducted. However, the thermal instability of $CpMo(NO)(CH_2CMe_3)_2$ makes a kinetic analysis of its thermal decomposition rather difficult. For example, the complex decomposes in air within seconds of exposure. Also, in the time it takes to get a sample into the drybox, it has thermally decomposed quite substantially.[37] Thus, it seemed that the logical next step was to use the tetra-α-deutero analogue, namely $CpMo(NO)(CD_2CMe_3)_2$, since it was our view that if α-H abstraction was a mechanistic path to the transient alkylidene, it would show a substantial kinetic isotope effect. As it turns out, **5.1**-d_4 is markedly more thermally stable than its perhydro congener and thus was used in all kinetic investigations (vide infra). The increased thermal stability of **5.1**-d_4 is also consistent with the view that its primary pathway for thermal decomposition involves α-H(D) elimination as the rate-determining step. Since the dialkyl complex, $CpMo(NO)(CD_2CMe_3)_2$, is red and most of its derivatives are markedly less colored, this study was conducted using UV-vis spectroscopy to monitor reaction progress.

$CpMo(NO)(CD_2CMe_3)_2$ exhibits a band at ~470-490 nm in its UV-vis spectra, (Table 5.4) whereas the phosphine adducts (**5.3-5.5**) show no features in their UV-vis spectra above 400 nm.

Table 5.4 Monitored Peak UV-vis Data for $CpMo(NO)(CD_2CMe_3)_2$ in Various Solvents

solvent	λ (nm)	ε ($M^{-1}cm^{-1}$)
CH_2Cl_2	472	390
Et_2O	484	391
hexanes	490	391
THF	482	393
mesitylene	486	380

I quickly discovered that the generation of the transient alkylidene complex, $CpMo(NO)(=CDCMe_3)$, was first-order in its dialkyl precursor and independent of the nature of the trapping ligand or its concentration.

5.3.4.1 Variation of Ligand and Ligand Concentration

The rate-determining formation of $CpMo(NO)(=CHCMe_3)$ from **5.1** is supported by kinetic data. Thermolysis of $CpMo(NO)(CD_2CMe_3)_2$ (**5.1-d_4**) in the presence of trapping ligands, L, is cleanly first-order in the complex and zero-order in L (eq 5.5). The decomposition of 1.684×10^{-3} M solutions of **5.1-d_4** in CH_2Cl_2 at 40 °C in the presence of 3.56, 5.24, 10.17 or 13.64 equiv of PPh_2Me, 6.49 equiv of PPh_3 or 9.00 equiv of P(*p*-tolyl)$_3$ affords k_{obs} values of $2.83 \pm 0.16 \times 10^{-4}$ s^{-1} (all 6 experiments are tabulated in Table 5.5). Typical plots are shown for run 5 in Figures 5.10 and 5.11.

Table 5.5 Thermal Decomposition Reactions of **5.1**-d_4 in the Presence of Phosphines in CH_2Cl_2

$[CpMo(NO)(CD_2CMe_3)_2] = 1.684 \times 10^{-3}$ M				
run	**trapping ligand**	**[ligand] (M)**	**equiv of ligand**	**k_{obs} (s^{-1})**
1	PPh_2Me	5.994×10^{-3}	3.56	2.785×10^{-4}
2	PPh_2Me	8.831×10^{-3}	5.24	2.514×10^{-4}
3	PPh_2Me	1.712×10^{-2}	10.17	2.891×10^{-4}
4	PPh_2Me	2.298×10^{-2}	13.64	2.898×10^{-4}
5	PPh_3	1.093×10^{-2}	6.49	2.930×10^{-4}
6	P(*p*-tolyl)$_3$	1.456×10^{-2}	9.00	2.935×10^{-4}

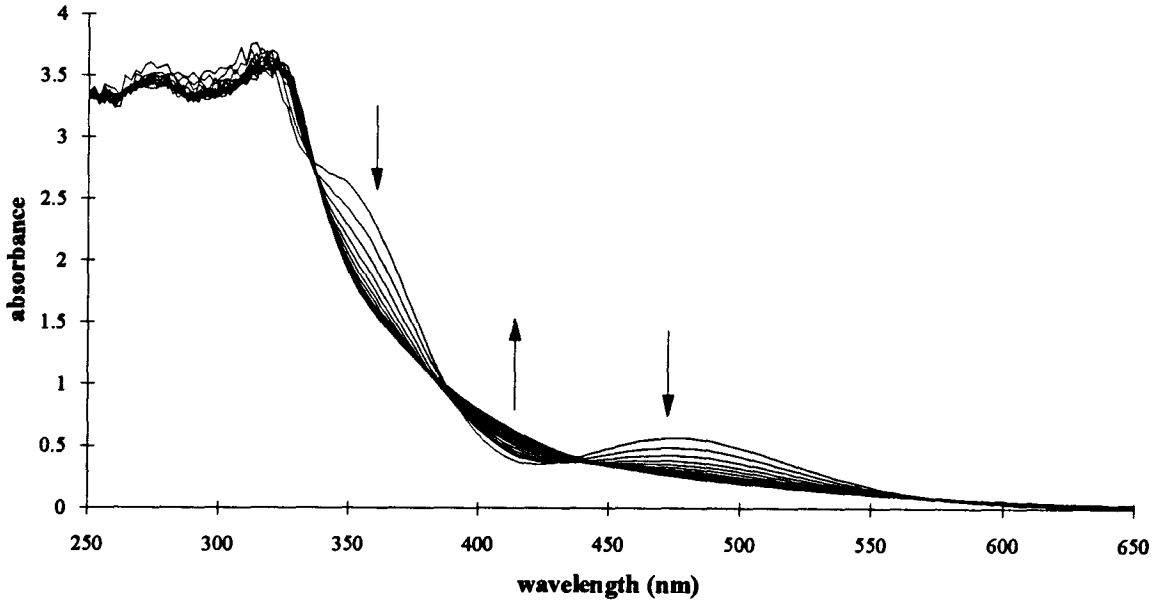

Figure 5.10 Absorption spectral changes for the thermolysis of $CpMo(NO)(CD_2CMe_3)_2$ in CH_2Cl_2 in the presence of 6.49 equiv PPh_3 (run 5)

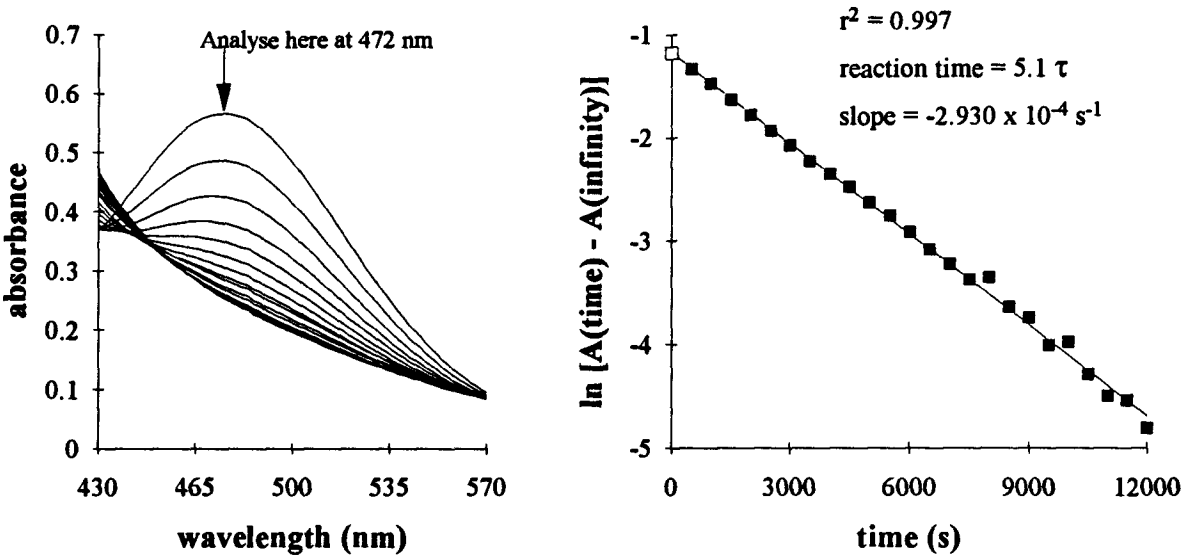

Figure 5.11 Spectral expansion of region around 472 nm and first-order log plot of data (run 5)

Since the reaction to form adducts of $CpMo(NO)(=CHCMe_3)$ is independent of the nature or concentration of the trapping ligand an *intramolecular* elimination of neopentane via an α-H abstraction reaction as the rate-determining step is strongly inferred as the mechanistic path to the key neopentylidene nitrosyl intermediate (eq 5.9).

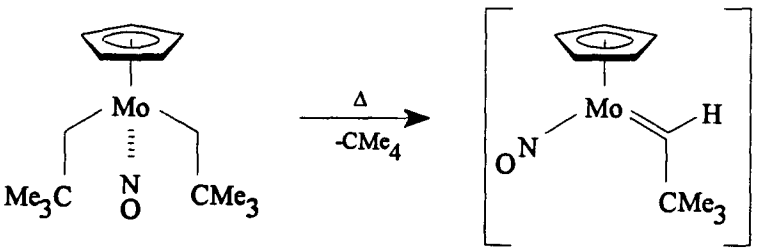

(5.9)

The transient neopentylidene complex has a very short lifetime and in solution is quickly trapped by phosphine. This conclusion is substantiated by the observation of an isosbestic point in both IR and UV-vis spectral monitoring of these thermolysis reactions.[38]

5.3.4.2 Variation of Temperature

To gain some insight into the nature of the transition state during the generation of $CpMo(NO)(=CDCMe_3)$ a kinetic analysis at various temperatures was conducted. Measurements were carried out in five solvents under identical chemical conditions. In all 27 runs (Table 5.6) the concentration of **5.1**-d_4 was maintained at 3.558×10^{-3} M (30.0 mg in 25 mL). The trapping ligand used was PPh_2Me (concentration = 2.490×10^{-2} M: 124.7 mg in 25 mL, 7.000 equiv).

Comparing rates at one temperature (25 °C), the reaction is fastest in dichloromethane. The other four solvents shows very similar rate constants. Thus, if we set $k_{obs}(THF) = 100$ then the rate increases THF (100) < mesitylene (111) < Et_2O (117) < hexanes (121) < CH_2Cl_2 (235) at 25 °C. At 40 °C, the order changes slightly to THF (100) < Et_2O (108) < hexanes (114) < mesitylene (115) < CH_2Cl_2 (207). Thus, within the errors of the measurements, dichloromethane seems to double reaction rates for reaction 5.9 but the rates are nearly independent of all other solvents used in this study. These results stand in marked constrast to those observed by Schrock in related studies of some Ta systems where he found rate constants at room temperature to increase as Et_2O (100) < pentane (200) < benzene (400) < $CHCl_3$ and CH_2Cl_2 (1500).[39] In both systems halogenated solvents seem to be promoters of α-H abstraction reactions, but the role the solvent plays is still ambiguous.

Kinetic measurements were also attempted in $CHCl_3$, benzene and toluene, but it appears that these solvents are reactive towards $CpMo(NO)(=CDCMe_3)$. It might be speculated that C-H activation of solvent molecules is competitive with phosphine trapping. In the case of benzene activation, the product would be $CpMo(NO)(CH_2CMe_3)Ph$ which is expected to be far more thermally unstable than complex **5.1** and would quickly decompose under the conditions in which it would be formed.

Conversion of selected data in Table 5.6 to Eyring plots is shown in Figure 5.12, and the respective activation parameters for all solvents are compiled in Table 5.7.

Table 5.6 Rate Constants as a Function of Temperature in Various Solvents

run	solvent	temp. (°C)	k_{obs} (s^{-1})	ln (k_{obs}/T)
7	CH_2Cl_2	15.0	1.964×10^{-5}	-16.50
8		20.0	3.453×10^{-5}	-15.95
9		25.0	5.856×10^{-5}	-15.44
10		30.0	9.523×10^{-5}	-14.97
11		35.0	1.824×10^{-4}	-14.34
12		40.0	2.912×10^{-4}	-13.89
13		45.0	4.834×10^{-4}	-13.40
14	Et_2O	25.0	2.920×10^{-5}	-16.14
15		30.0	4.779×10^{-5}	-15.66
16		32.5	6.632×10^{-5}	-15.34
17		37.5	1.052×10^{-4}	-14.90
18		40.0	1.515×10^{-4}	-14.54
19	hexanes	25.0	3.010×10^{-5}	-16.11
20		32.5	6.387×10^{-5}	-15.38
21		40.0	1.610×10^{-4}	-14.48
22		47.5	2.819×10^{-4}	-13.94
23		55.0	6.014×10^{-4}	-13.21
24	THF	25.0	2.491×10^{-5}	-16.30
25		32.5	5.674×10^{-5}	-15.50
26		40.0	1.409×10^{-4}	-14.61
27		45.0	2.016×10^{-4}	-14.27
28		60.0	7.893×10^{-4}	-12.95
29	mesitylene	25.0	2.757×10^{-5}	-16.20
30		32.5	6.956×10^{-5}	-15.30
31		40.0	1.619×10^{-4}	-14.48
32		45.0	2.268×10^{-4}	-14.15
33		65.0	1.103×10^{-3}	-12.63

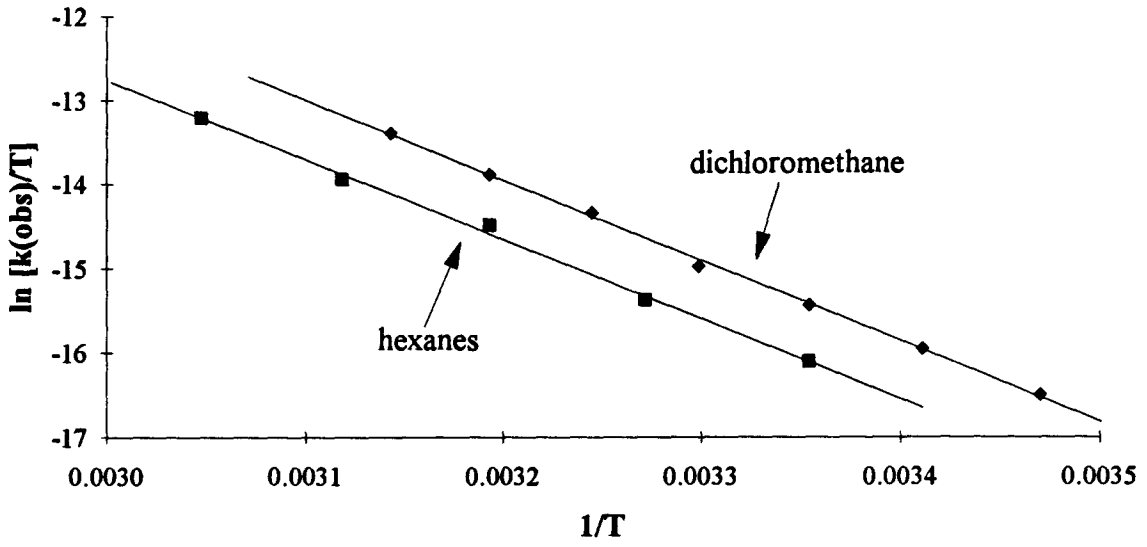

Figure 5.12 Representative Eyring plots for the conversion of $CpMo(NO)(CD_2CMe_3)_2$ (**5.1**-d_4) to $CpMo(NO)(=CDCMe_3)$ in hexanes and CH_2Cl_2

Table 5.7 Activation Parameters Derived from Eyring Plots

runs	solvent	$\Delta H^{\ddagger}$ (kJ/mol)	$\Delta S^{\ddagger}$ (J/mol·K)	$\Delta G^{\ddagger}_{298}$ (kJ/mol)
7 - 13	CH_2Cl_2	+ 79.2	- 60.1 (-14.4 eu)	+ 97.1
14 - 18	Et_2O	+ 81.4	- 58.9 (-14.1 eu)	+ 99.0
19 - 23	hexanes	+ 78.5	- 68.1 (-16.3 eu)	+ 98.8
24 - 28	THF	+ 78.9	- 68.1 (-16.3 eu)	+ 99.2
29 - 33	mesitylene	+ 73.7	- 84.0 (-20.1 eu)	+ 98.7

Interpretation of the thermolysis data leads to several conclusions. Fisrt, in all cases the entropy of activation is negative, thereby implying a highly ordered transition state.[39] Second, since both $\Delta H^{\ddagger}$ and $\Delta S^{\ddagger}$ do not really vary with solvent, it is proposed that the intramolecular expulsion of neopentane in this reaction is not particularly affected by the solvent and that the transition state is not highly solvated.

5.3.4.3 Mechanistic Implications on the Formation of $[CpMo(NO)(CHCMe_3)]_2$

Since the formation of $CpMo(NO)(=CHCMe_3)$ is rate-determining, simple coupling of two molecules of $CpMo(NO)(=CHCMe_3)$ is not a mechanistic path to the asymmetric dimer **5.2**. Instead, the transient neopentylidene monomer in all likelihood forms an adduct with a second molecule of **5.1** which then eliminates neopentane and rearranges to produce **5.2**. Just why the dimer adopts such an asymmetric structure remains to be ascertained. A proposal for the mechanistic sequence of events from **5.1** to **5.2** is outlined in Scheme 5.1.

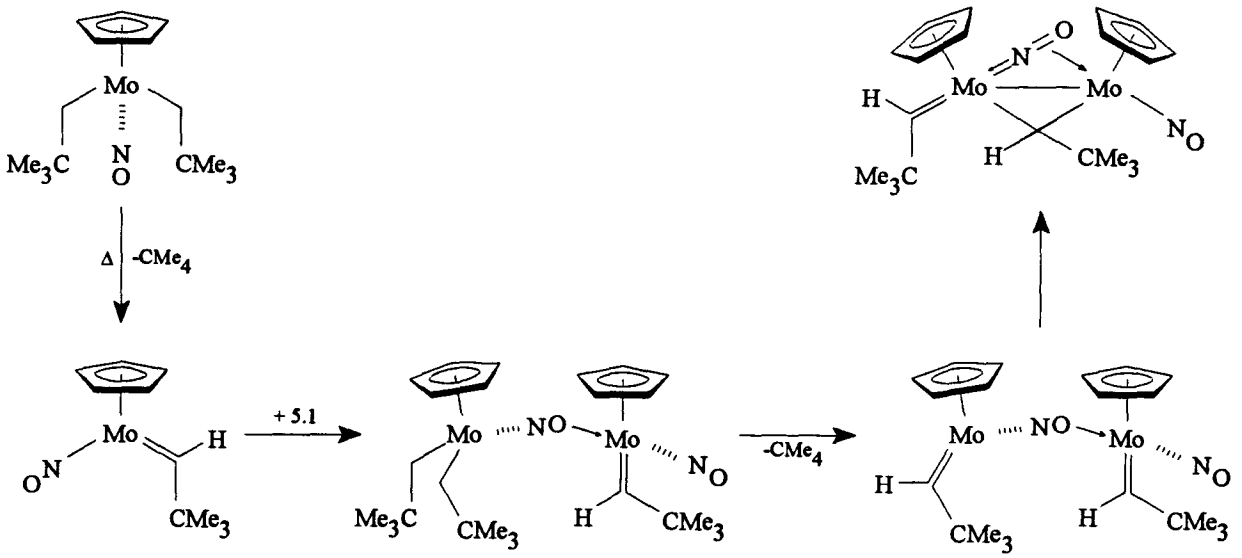

Scheme 5.1 Possible mechanism for the formation of $[CpMo(NO)](\mu\text{-}\eta^1\text{:}\eta^2\text{-}NO)(\mu\text{-}CHCMe_3)[CpMo(=CHCMe_3)]$ (**5.2**) from $CpMo(NO)(CH_2CMe_3)_2$ (**5.1**)

It is interesting that $CpMo(NO)(=CHCMe_3)(py)$ (**5.6**) thermally decomposes to complex **5.2**, albeit at a much slower rate than does complex **5.1**. It is likely that the mechanistic pathways to the dimer **5.2** from **5.1** and **5.6** are similar, but they clearly cannot be the same.

5.3.5 Further Chemistry of CpMo(NO)(=CHCMe$_3$): Trapping Reactions with Ligands Containing E-H bonds (E = N, O)

In order to learn more about the nature of the alkylidene ligand in the transient CpMo(NO)(=CHCMe$_3$) complex, two types of reactions were carried out. The N-H and O-H bonds of amines and alcohols can be added stereoselectively across the Mo=C double bond of CpMo(NO)(=CHCMe$_3$) yielding complexes of the general type CpMo(NO)(CH$_2$CMe$_3$)(ER').

5.3.5.1 Reactivity of CpMo(NO)(=CHCMe$_3$) With Amines

The reaction of CpMo(NO)(CH$_2$CMe$_3$)$_2$ with primary amines gives alkyl amide[40] complexes CpMo(NO)(CH$_2$CMe$_3$)(NHR) [R = CMe$_3$ (**5.9**), *p*-tolyl (**5.10**)] (eq 5.10).

(5.10)

In order to determine whether these products arise from protonolysis of the dialkyl complex or NH addition across the Mo=C double bond in CpMo(NO)(=CHCMe$_3$), a control experiment using the deuterated starting material was conducted. The reaction of CpMo(NO)(CD$_2$CMe$_3$)$_2$ with (*p*-tolyl)NH$_2$ affords CpMo(NO)(CHDCMe$_3$)(NH-*p*-tolyl) (**5.10**-d_1), thus confirming that the mechanism of the reaction proceeds via the alkylidene complex (Route **B**, Scheme 5.2) and not via direct protonolysis of an alkyl ligand (Route **A**, Scheme 5.2).

Route A

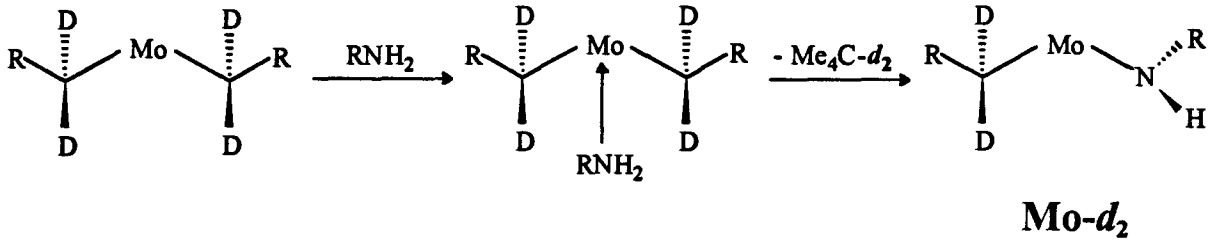

Mo-d_2

Route B

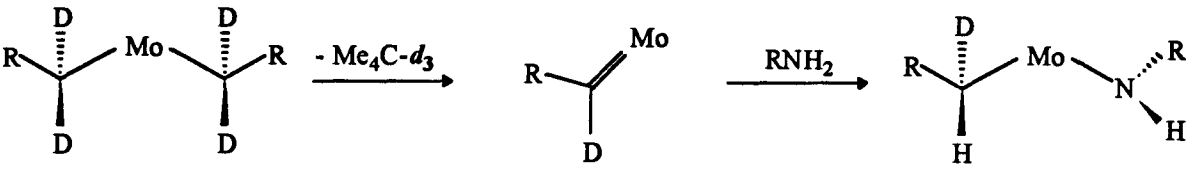

Mo-d_1

Scheme 5.2 Possible pathways for the reaction of $CpMo(NO)(CD_2CMe_3)_2$ with RNH_2

Additionally, this reaction of amine with $CpMo(NO)(=CDCMe_3)$ is stereoselective. There is only one ^2H NMR resonance and one ^1H NMR resonance attributable to the methylene protons of the newly created $CHDCMe_3$ group when $CpMo(NO)(CD_2CMe_3)_2$ is allowed to react with Me_3CNH_2.

An N-H addition across the Mo=C linkage is the only possible explanation for this experimental observation. This rules out prior coordination of the amine to the Mo center followed by proton transfer to the alkylidene carbon. Since only a single product is formed, we can assume that the transient alkylidene complex does not have C_s symmetry.

Curiously, when (*p*-tolyl)NH_2 is used in reaction 5.10, two diastereomeric products are isolated in a 1:1 ratio as evidenced by two sets of all resonances in the ^1H NMR spectra of **5.10** (Figure 5.13). It is left to future work to determine the nature of the two products, although it is most likely that the complexes are related by rotation about the Mo-amide bond (vide infra).

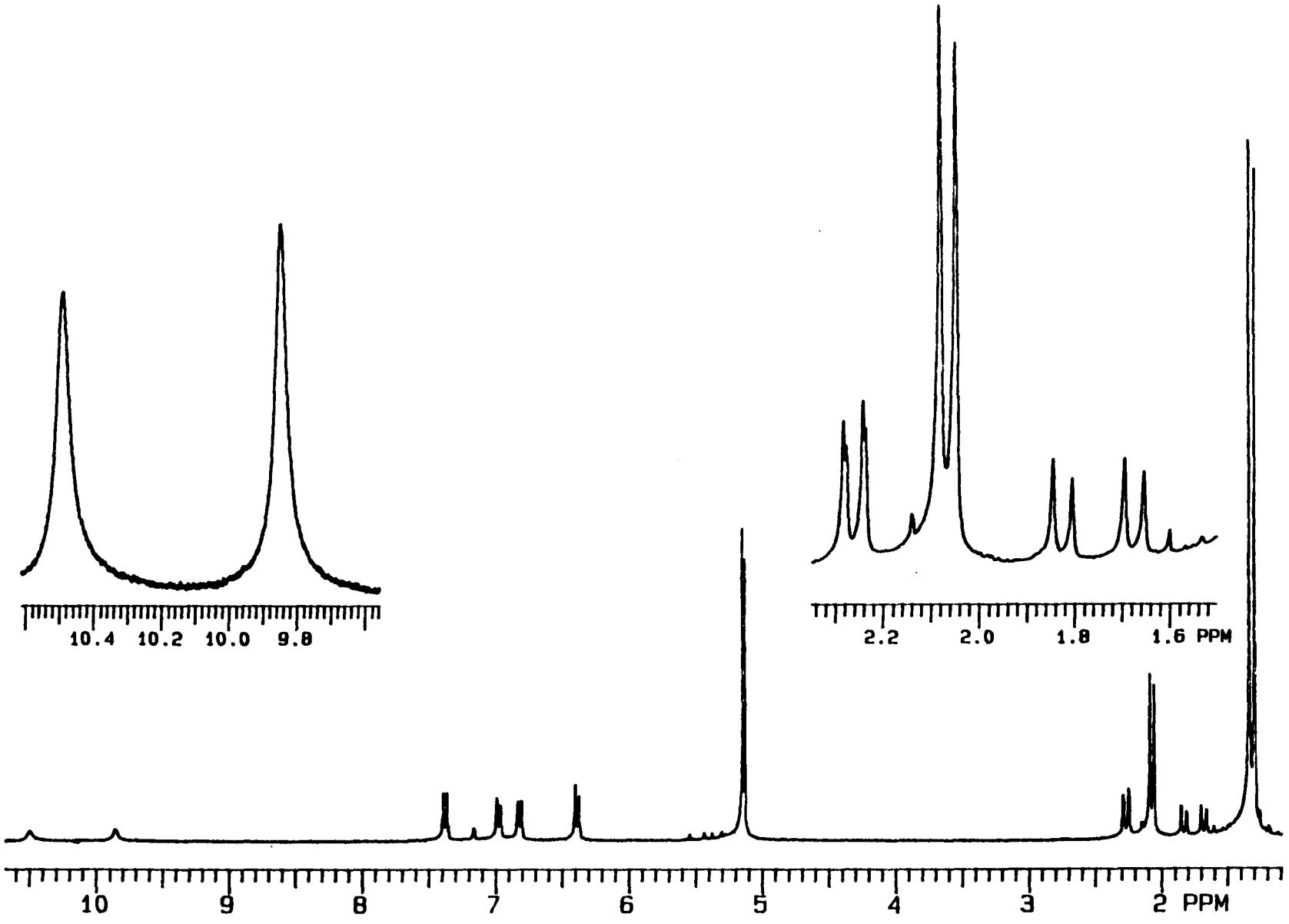

Figure 5.13 ^{1}H NMR spectrum of CpMo(NO)(CH_2CMe_3)(NH-*p*-tolyl) (**5.10**) in C_6D_6

5.3.5.2 X-ray Crystallographic Analysis of Complex 5.10

Due to the complicated nature of the NMR spectra of complex **5.10**, an X-ray crystallographic analysis of the compound seemed in order.[41] The molecular structure is shown in Figure 5.14, and the complex is indeed monomeric as suggested by its mass spectrum. The internal metrical parameters (Table 5.8) for the $CpMo(NO)(CH_2CMe_3)$ fragment resemble those found in $CpMo(NO)(CD_2CMe_3)_2$ (Section 5.3.1.1). The anilide hydrogen atom, H(20), lies in the plane defined by Mo-N(2)-C(11) (deviation from the plane = 0.003 (4) Å). The Mo-N(2) bond length of 1.955 (3) Å appears to be typical for a Mo-NHR linkage.[42] The large Mo-N(2)-C(11) bond angle of 137.1 (3)° indicates some degree of Mo-N multiple bonding is present in this molecule. However, the most obvious difference between this structure and its parent dineopentyl complex (**5.1**) is within the angles in the legs of the piano-stool. A comparison of projections down the Cp-centroid-Mo axis is shown in Figure 5.15.

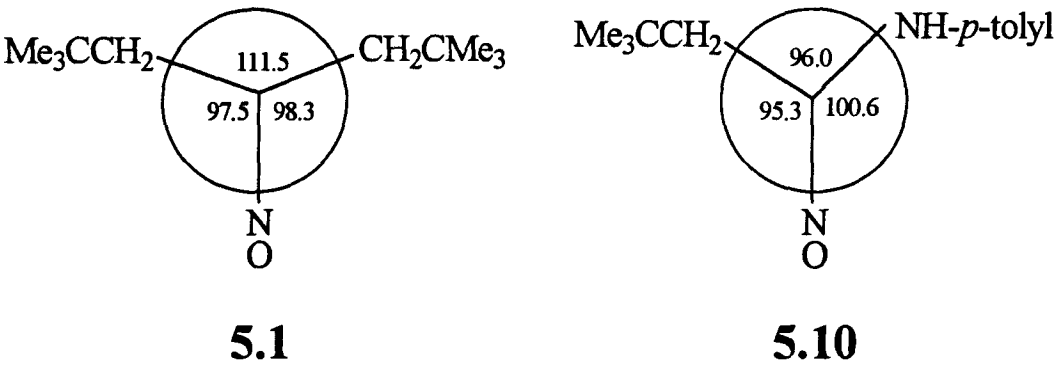

5.1 **5.10**

Figure 5.15 Comparison of the angles about Mo in complexes **5.1** and **5.10**

As discussed in Chapter 3 the bond angles about the metal centers in 16-electron alkyl and aryl complexes, $Cp'M(NO)R_2$ are substantially different (for complex **5.1** these angles are 97.5, 98.3 and 111.5°). In the structure of complex **5.10** the analogous angles are very similar (95.3, 100.6, 96.0°). Clearly, the ability of the amide ligand to donate extra electron density to the Mo center satiates some of the electron deficiency inherent in $CpMo(NO)(CH_2CMe_3)_2$ and effectively negates any open coordination position between the alkyl and amide linkages. Thus, the angle between the two neopentyl groups in **5.1** is 111.5°, and the angle between the neopentyl and

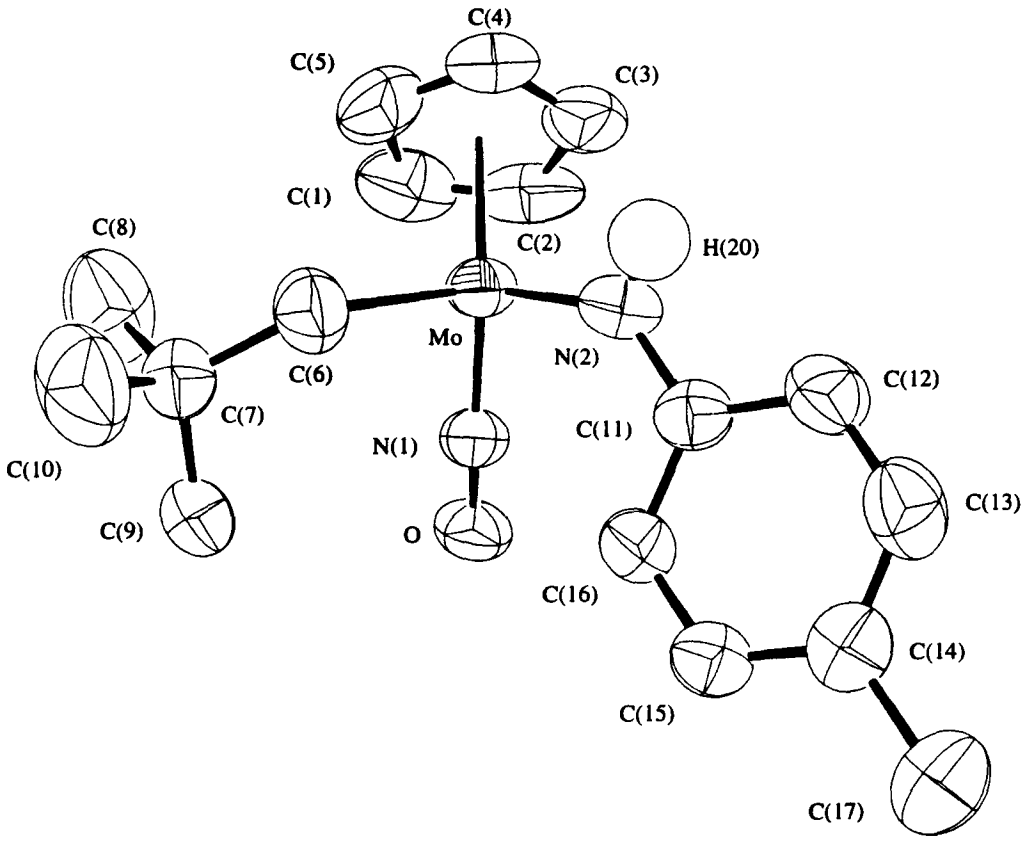

Figure 5.14 ORTEP diagram of $CpMo(NO)(CH_2CMe_3)(NH\text{-}p\text{-tolyl})$ **(5.10)**. 50% probability ellipsoids are shown for the non-hydrogen atoms. Hydrogen atoms other than H(20) have been omitted for clarity

Table 5.8 Representative bond lengths and angles for complex **5.10**

bond lengths (Å) (esd)		**bond angles (°) (esd)**	
N2-H20	0.76 (4)	C6-Mo-N1	95.3 (5)
Mo-C6	2.190[a]	N1-Mo-N2	100.6 (1)
Mo-N1	1.751 (3)	N2-Mo-C6	96.0 (5)
Mo-N2	1.955 (3)	Mo-C6-C7	130.4[a]
N1-O	1.221 (3)	Mo-N2-H20	113.3 (32)
		Mo-N2-C11	137.1 (3)
		Mo-N1-O	170.2 (3)

[a] Parameter restrained during refinement.

anilide groups in **5.10** is only 96.0°, a significant drop of 15.5°. Consistent with these structural observations are the IR spectra of both **5.1** and **5.10**. The observed values of ν_{NO} for these materials are 1623 and 1548 cm^{-1}, respectively, i.e. the spatially constricted complex (**5.10**) is the weaker Lewis acid by a substantial margin. The above evidence would indicate that the amide ligand can donate significant amounts of π-electron density to the Mo atom. Multiple-bond character in the Mo-N linkage likely accounts for the two rotational isomers of the complex observed in the room temperature NMR spectra of complex **5.10** (vide supra).

5.3.5.3 Reactivity of $CpMo(NO)(=CHCMe_3)$ with Phenol

Addition of the O-H bond of PhOH across the Mo=C double bond of $CpMo(NO)(=CHCMe_3)$ gives the alkyl alkoxide complex $CpMo(NO)(CH_2CMe_3)(OPh)$ (**5.11**) (eq 5.11). The complex is a red oil at room temperature, but may be purified by precipitation from hexanes at low temperatures.

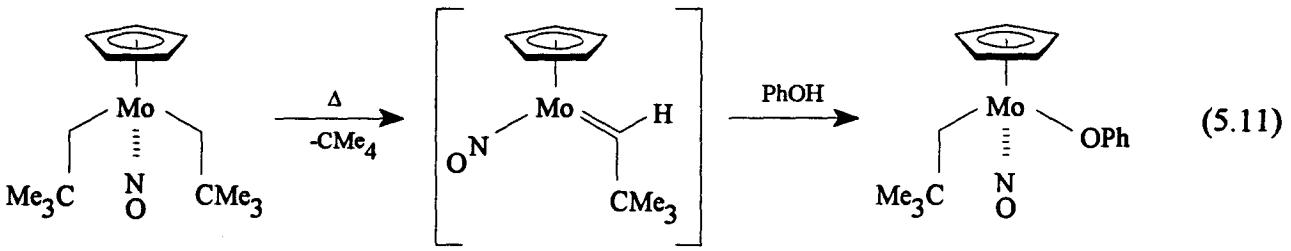

(5.11)

The fact that **5.11** is thermally stable implies that previously unsuccessful attempts[43] to synthesize $CpMo(NO)(R)(OR')$ complexes were more a function of the metathesis methodology employed and not the inherent instability of the product complexes.

5.4 Epilogue and Future Work

The original metathesis method (Chapter 1) leading to $Cp'M(NO)R_2$ complexes was conducted at room temperature. Clearly, this is the reason previous workers were unable to synthesize $CpMo(NO)(CH_2CMe_3)_2$. It is interesting that this complex, the most thermally

sensitive, yet isolable $Cp'M(NO)R_2$ complex, displays the cleanest thermolysis chemistry. The work described in this chapter has shown that $CpMo(NO)(CH_2CMe_3)_2$ decomposes via a first-order process to the transient 16-electron neopentylidene complex, $CpMo(NO)(=CHCMe_3)$.

The characteristic chemistry of $CpMo(NO)(=CHCMe_3)$ investigated to date has shown that it can be trapped either with 2-electron donor ligands or with heteroatom-hydrogen bonds which readily add across the Mo=C bond. Since the pyridine complex, $CpMo(NO)(=CHCMe_3)(py)$, serves as a stable source of the transient $CpMo(NO)(=CHCMe_3)$ complex, all future research should begin with this synthetic precursor. The characteristic reactivity of the transient $CpMo(NO)(=CHCMe_3)$ fragment with other E-H bonds than those described at the end of this chapter, such as primary phosphines and thiols, should reveal the entire manifold of CpMo(NO)(R)(ER') complexes that are synthesizable. Additionally, unsaturated organic entities capable of coupling with the alkylidene ligand should also be investigated.[44]

Preliminary investigations into the thermal behaviour of other $CpMo(NO)R_2$ complexes and $CpW(NO)(CH_2CMe_3)_2$ have shown some promise, but more work is required to fine tune the conditions under which alkylidene complexes are best generated.

5.5 References and Notes

(1) Fischer E. O.; Maasböl, A *Angew. Chem., Int. Ed. Engl.* **1964**, *3*, 580.

(2) Gallop, M. A.; Roper, W. R. *Adv. Organomet. Chem.* **1986**, *25*, 121.

(3) Schrock, R. R. *J. Am. Chem. Soc.* **1974**, *96*, 6796.

(4) Schrock, R. R. *Acc. Chem. Res.* **1979**, *12*, 98.

(5) This is only a very general comparison. Many complexes of both types have been found to be amphiphilic. For example, see the chemistry of (a) $CpRe(CO)_2(=CHR)$ in Casey, C.; Vosejpka, P. C.; Askham, F. R. *J. Am. Chem. Soc.* **1990**, *112*, 3713 or (b) $(CO)_2(Ph_3P)_2Ru(=CF_2)$ in Clark, G. R.; Hoskins, S. V.; Jones, T. C.; Roper, W. R. *J. Chem. Soc., Chem. Commun.* **1983**, 719.

(6) Collman, J. P.; Hegedus, L. S.; Norton, J. R.; Finke, R. G. *Principles and Applications of Organotransition Metal Chemistry*; University Science Books: Mill Valley, CA, 1987.

(7) Carter, E. A.; Goddard, W. A. *J. Am. Chem. Soc.* **1986**, *108*, 4746.

(8) Legzdins. P.; Rettig, S. J.; Veltheer, J. E. *J. Am. Chem. Soc.* **1992**, *114*, 6922.

(9) Perrin, D. D.; Armarego, W. L. F.; Perrin, D. R. *Purification of Laboratory Chemicals*, 3rd ed.; Pergamon Press: Oxford, U.K., 1988.

(10) This preparation is derived from that found in the literature for Me_3CCD_2MgBr, see Caulton, K. G.; Chisholm, M. H.; Streib, W. E.; Xue, Z. *J. Am. Chem. Soc.* **1991**, *113*, 6082.

(11) The darkening of this solution is consistent with the dimerization of CpH to $(CpH)_2$. Additionally, the crystallizing solution had the characteristic odor of dicyclopentadiene.

(12) Legzdins, P.; Rettig, S. J.; Sánchez, L.; Bursten, B. E.; Gatter, M. G. *Organometallics* **1988**, *7*, 2394. Dryden, N. H.; Legzdins, P.; Rettig, S. J.; Veltheer, J. E. *Organometallics* **1992**, *11*, 2583.

(13) (a) For Mo see: Legzdins, P.; Rettig, S. J.; Sánchez, L.; Bursten, B. E.; Gatter, M. G. *J. Am. Chem. Soc.* **1985**, *107*, 1411. (b) For W see: Bursten, B. E.; Cayton, R. H. *Organometallics* **1987**, *6*, 2004.

(14) Brouwer, E. B.; Debad, J. D.; Legzdins, P.; Ross, K. J.; Veltheer, J. E. unpublished observations.

(15) Crystals of **5.1**-d_4 are monoclinic of space group $P2_1/n$; a = 5.9781 (6) Å, b = 20.065 (4) Å, c = 13.6355 (17) Å; β = 95.520 (10)°; Z = 4. Drs. Ray Batchelor and Fred Einstein solved the structure using the Patterson method and full-matrix least-squares refinement procedures to R = 0.025, R_w = 0.032 for 2494 reflections with $I_o \geq 2.5\sigma(I_o)$.

(16) The red solid turns brown and exhibits two nitrosyl-stretching frequencies at 1597 and 1578 cm^{-1} in its Nujol mull IR spectrum. A ^1H NMR spectrum of the solid in C_6D_6 displays two major Cp resonances at δ 5.43 and 5.34 ppm in a 1:2 ratio as well as two CMe_3 peaks at δ

1.35 and 1.29 ppm in a 2:1 ratio. Numerous other smaller resonances are also observed. As more spectra are recorded signals due to numerous products appear and/or disappear. There is no evidence for the existence of complex **5.2** evident in these spectra.

(17) Crystals of **5.2** are orthorhombic of space group *Pcab*; a = 17.836 (2) Å, b = 18.265 (2) Å, c = 13.198 (2) Å; Z = 8. Dr. Steve Rettig solved the structure using the Patterson method and full-matrix least-squares refinement procedures to $R = 0.027$, $R_w = 0.026$ for 3406 reflections with $I \geq 3\sigma(I)$.

(18) Examples of complexes being associated symmetrically via two bridging alkylidene ligands,[16a] two conventionally bridging nitrosyl ligands,[16b] or multiple metal-metal bonds,[16c] are well known. For instance, see (a) Holton, J.; Lappert, M. F.; Pearce, R.; Yarrow, P. I. W. *Chem. Rev.* **1983**, *83*, 135. (b) Calderón, J. L.; Fontana, S.; Frauendorfer, E.; Day, V. W.; Iske, S. D. *J. Organomet. Chem.* **1974**, *64*, C10 and C16. (c) Toreki, R.; Schrock, R. R.; Vale, M. G. *J. Am. Chem. Soc.* **1991**, *113*, 3610 and references therein.

(19) For comparison, other long N-O bonds are: (a) 1.247 (5) Å for the μ_3-NO of $Cp_3Mn_3(NO)_4$: Elder, R. C. *Inorg. Chem.* **1974**, *13*, 1037; (b) 1.271 (7) Å for the μ_4-η^2-NO of a mixed Co/Mo cluster: Kyba, E. P.; Kerby, M. C.; Kashyap, R. P.; Mountzouris, J. A.; Davis, R. E. *J. Am. Chem. Soc.* **1990**, *112*, 905; and (c) 1.47 (1) Å for $CpRe(PPh_3)(SiMe_2Cl)(NO\text{-}BCl_3)$: Lee, K. E.; Arif, A. M.; Gladysz, J. A. *Inorg. Chem.* **1990**, *29*, 2885.

(20) Other long Mo-Mo single bonds have been reported: (a) 3.056(1) Å for $[CpMo(CO)_2]_2$-(μ-$NCNMe_2$): Chisholm, M. H.; Cotton, F. A.; Extine, M. W.; Rankel, L. A. *J. Am. Chem. Soc.* **1978**, *100*, 807. (b) 3.117(1) Å for $[CpMo(CO)_2]_2$-(μ-allene): Bailey, W. I.; Chisholm, M. H.; Cotton, F. A.; Murillo, C. A.; Rankel, L. A. *J. Am. Chem. Soc.* **1978**, *100*, 802.

(21) Richter-Addo, G. B.; Legzdins, P. *Metal Nitrosyls*; Oxford University Press: New York, 1992; Chapter 2 and references therein.

(22) Reference 21, p 64.

(23) Examples of μ_2-η^1:η^2-CO ligands have been documented; see, (a) Horwitz, C. P.; Shriver, D. F. *Adv. Organomet. Chem.* **1984**, *23*, 219 and references therein. (b) Marsella, J. A.; Huffman, J. C.; Caulton, K. G.; Longato, B.; Norton, J. R. *J. Am. Chem. Soc.* **1982**, *104*, 6360.

(24) Simpson, C. Q.; Hall, M. B. *J. Am. Chem. Soc.* **1992**, *114*, 1641.

(25) Reference 6, p 126 states that CPh_2 groups are electrophilic and thus best considered as Fischer carbenes.

(26) Herrmann, W. A.; Hubbard, J. L.; Bernal, I.; Korp, J. D.; Haymore, B. L.; Hillhouse, G. L. *Inorg. Chem.* **1984**, *23*, 2978.

(27) Fischer, E. O. *Pure Appl. Chem.* **1970**, *24*, 407.

(28) Nugent, W. A.; Mayer, J. M. *Metal-Ligand Multiple Bonds*, John-Wiley and Sons Ltd., NY, 1988, Chapter 4.

(29) Crystals of **5.3** are monoclinic of space group $P2_1/n$; a = 9.328 (2) Å, b = 15.516 (3) Å, c = 15.188 (2) Å, ß = 93.72 (1)°; Z = 4. Dr. Steve Rettig solved the structure using the Patterson method and full-matrix least-squares refinement procedures to R = 0.042, R_w = 0.037 for 4081 reflections with $I_o \geq 3\sigma(I_o)$.

(30) Kiel, W. A.; Lin, G-Y.; Constable, A. G.; McCormick, F. B.; Strouse, C. E.; Eisenstein, O.; Gladysz, J. A. *J. Am. Chem. Soc.* **1982**, *104*, 4865.

(31) Reference 28, p 132

(32) Schultz, A. J.; Williams, J. M.; Schrock, R. R.; Rupprecht, G. A.; Fellmann, J. D. *J. Am. Chem. Soc.* **1979**, *101*, 1593.

(33) For the purposes of this comparison formal oxidation state is determined assuming alkylidene ligands to be CHR^{2-} groups and not neutral dative donor ligands.

(34) Reference 28, p 187.

(35) Christensen, N. J.; Hunter, A. D.; Legzdins, P.; Sánchez, L. *Inorg. Chem.* **1987**, *26*, 3344.

(36) Durfee, L. D.; Rothwell, I. P. *Chem. Rev.* **1988**, *88*, 1059.

(37) Three attempts were made to determine the kinetic isotope effect for this system, but difficulty in handling samples of the non-deuterated dialkyl complex gave unreliable and non-reproducible measurements. The 3 values of k_H/k_D that were determined were 4, 7 and 11.

(38) Ebsworth, E. A. V.; Rankin, D. W. H.; Cradock, S. *Structural Methods in Inorganic Chemistry*, Blackwell Scientific, Oxford, U.K., 1987, p 276.

(39) Wood, C. D.; McLain, S. J.; Schrock, R. R. *J. Am. Chem. Soc.* **1979**, *101*, 3210

(40) Related Cp^*-containing alkyl amide complexes have been prepared by methathesis reactions of Li(amide) and $Cp^*M(NO)(R)Cl$. Legzdins, P; Rettig, S. J.; Ross, K. *Organometallics*, in press.

(41) Crystals of **5.10** are monoclinic of space group $P2_1/c$; a = 11.243 (2) Å, b = 9.632 (2) Å, c = 16.845 (3) Å, ß = 99.74 (1)°; Z = 4. Drs. Ray Batchelor and Fred Einstein solved the structure using the Patterson method and full-matrix least-squares refinement procedures to R_F = 0.031 for 2213 data with $I_o \geq 2.5\sigma(I_o)$.

(42) For example, the average Mo-amide bond length in (a) $Mo_2(OCMe_3)_4(PhNH)_2(PhNH_2)_2$ is 1.97 Å, see: Chisholm, M. H.; Parkin, I. P.; Streib, W. E.; Folting, K. S. *Polyhedron* 1991, **10**, 2309 and (b) $[HB(Me_2pz)_3]Mo(NH\text{-}n\text{-}Bu)_2$ is 1.94 Å, see: Obaidi, N. A.; Hamor, T. A.; Jones, C. J., McCleverty, J. A.; Paxton, K. *J. Chem. Soc., Dalton Trans.* **1986**, 1525.

(43) Lundmark, P. J., Ph.D. Dissertation, The University of British Columbia, 1993.

(44) For recent examples of this type of chemistry, see: Garrett, K. E.; Sheridan, J. B.; Pourreau, D. B.; Feng, W. C.; Geoffroy, G. L.; Staley, D. L.; Rheingold, A. L. *J. Am. Chem. Soc.* **1989**, *111*, 8383 and references therein.